Investigations into altered cellular glycosylation associated with metastatic competence in breast cancer cell lines

Ellie-May Beaman

A thesis submitted in partial fulfilment of the requirements of Oxford Brookes University for the degree of Doctor of Philosophy

March 2017

For Mum, Dad,
Grandma & Grandad

Abstract

Metastasis is the main cause of cancer patient death owing to the fact that metastatic disease is difficult to treat. Aberrant glycosylation is characteristic of cancer and plays a role in metastatic mechanisms. HPA, a lectin from the Roman snail *Helix pomatia*, recognises glycans terminating in α-GalNAc, and is associated with aggressive biological behaviour, poor patient prognosis and metastasis in breast and other cancers.

Three breast cancer cell lines characterised to stably synthesise an array of GalNAc-glycans were employed in the work reported here (MCF7, ZR751 and BT474). HPA lectin labelling and quantification were optimised and it revealed a more complex HPA-binding profile than previously reported. It was observed that HPA-positive cells were rounded, reminiscent of epithelial cells, and HPA-negative cells were elongated, and reminiscent of mesenchymal cells. One of the aberrant glycans that HPA reportedly binds is the initial O-glycan Tn structure which is commonly exposed in cancer. qPCR was performed to assess the gene expression levels of O-linked glycosylation initiation enzymes, GALNTs as well as C1GalT and its molecular chaperone *COSMC*. This analysis revealed that there is no clear association between aberrant glycosylation recognised by HPA-binding, although down-regulation of C1GalT and *COSMC* may result in failed normal chain extension.

A method of isolating cells based on their HPA-binding profile was developed. Cells were separated and grown on post-separation for 3 days. It was observed that the glycosylation profiles of the HPA-positive cell population and the HPA-negative cell population reverted to a mixed population over time that was similar to the unseparated lectin labelling proportions. The cell morphologies also reverted. The plasticity observed was reminiscent of EMT. Microarray analysis revealed that several EMT-associated genes were differentially expressed between the HPA-positive and HPA-negative isolated cell populations.

Using a Matrigel invasion assay it was observed that HPA-negative cells were significantly more invasive than HPA-positive cells. While in a static adhesion assay HPA-positive cells were significantly more adhesive to endothelial cell monolayers than HPA-negative cells. HPA-binding glycans were demonstrated to be functionally involved in HPA-positive cells adhesion to the endothelial cell monolayer as their adhesion was inhibited when HPA-binding glycans were masked. Furthermore, using conditioned medium transfer experiments it was observed that cell-cell signalling was occurring between the HPA-positive and HPA-negative cells and altering their adhesive characteristics.

To conclude the work reported here demonstrates that cells can modulate their glycosylation profiles and their subsequent morphologies and that this plasticity is important in cancer metastasis.

Acknowledgements

Thank you to Oxford Brookes biological and biomedical sciences department for the opportunity to perform my research and for their help in funding my project.

Thank you also to my supervisors Professor Susan Brooks and Dr Dave Carter for their support and guidance.

Thank you to Dr Ryan Pink, Dr Alison Forhead and Dr Louise Hughes for their help and expertise with different aspects of this project.

Thank you to Professor Munira Kadhim and Dr Miriam Dwek for help with cells and reagents.

Thank you also to Dr Priya Samuel for going through this journey with me.

Finally, thank you to Professor John Runions – this is all your fault!

Abbreviations

ΔΔCt	delta delta cycle threshold
°C	degrees Celsius
µg	microgram
µl	microlitre
µm	micrometre
2D	two-dimensional
3D	three-dimensional
+RT	plus reverse transcriptase
-RT	minus reverse transcriptase
ACTB	beta-actin
ActR-IIB	activin receptor type IIB
Asn	asparagine
BDKRB1	bradykinin receptor B1
BM	basement membrane
BME	basement membrane extracts
BMP7	bone morphogenetic protein 7
bp	base pair
BRCA1	breast cancer associated gene 1
BSA	bovine serum albumin
C1GalT	core 1 beta 1,3-galactosyltransferase
C1GALT1C1	core 1 beta 1,3-galactosyltransferase-specific molecular chaperone
C1S	complement component 1, S subcomponent
C2	complement component 2
C5AR1	complement component 5a receptor 1
Ca^{2+}	calcium
$CaCl_2$	calcium chloride

CAM	cell adhesion molecule
CCL21/6Ckine	C-C motif chemokine ligand 21
CCR7	C-C motif chemokine receptor 7
CD55	CD55 molecule (Cromer blood group)
CDH1	E-cadherin
cDNA	complementary deoxyribonucleic acid
CFH	complement factor H
CLDN2	claudin 2
CLDN8	claudin 8
CLDN9	claudin 9
CO_2	carbon dioxide
CODIS	combined deoxyribonucleic acid index system
COL5A2	collagen type V alpha 2 chain
Con A	Concanavalin A lectin
COSMC	core 1 Beta 1,3-galactosyltransferase-specific molecular chaperone
Ct	cycle threshold
CTCs	circulating tumour cells
CXCL10	C-X-C motif chemokine ligand 10
CXCL12	C-X-C motif chemokine ligand 12
CXCL12/SDF-1α	C-X-C motif chemokine ligand 12/stromal-cell derived factor-1alpha
CXCR4	C-X-C motif chemokine receptor 4
Da	Dalton
DAB	3,3'-diaminobenzadine
DAVID	the database for annotation, visualisation and integrated discovery
DMSO	dimethyl sulphoxide
DNA	deoxyribonucleic acid
DNASE1L2	deoxyribonuclease 1-like 2
Dol	dolichol

dsDNA	double-stranded deoxyribonucleic acid
ECACC	European collection of authenticated cell cultures
ECM	extracellular matrix
EDTA	ethylenediaminetetraacetic acid
EGF	epidermal growth factor
EGFR	epidermal growth factor receptor
ELF3	E74-like factor 3 (Ets domain transcription factor, epithelial-specific)
EMT	epithelial mesenchymal transition
ENO1	enolase 1
ER	endoplasmic reticulum
ER	oestrogen receptor
ERK	extracellular signal–regulated kinase
ETV5	Ets variant 5
FACS	fluorescence activated cell sorting
FBLN1	fibulin 1
FBLN5	fibulin 5
FBN2	Fibrillin 2
FC	fold change
FCS	foetal calf serum
FGB	fibrinogen beta chain
FGG	fibrinogen gamma chain
FLJ12691	UDP-N-α-D-galactosamine:polypeptide N-acetylgalactosaminyltransferase 16
Fuc	fucose
g	g-force
GABA	gamma-Aminobutyric acid
GAD1	glutamate decarboxylase 1
Gal	galactose
GalNAc	N-acetylgalactosamine

GALNT1	UDP-N-α-D-galactosamine:polypeptide N-acetylgalactosaminyltransferase 1
GALNT10	UDP-N-α-D-galactosamine:polypeptide N-acetylgalactosaminyltransferase 10
GALNT11	UDP-N-α-D-galactosamine:polypeptide N-acetylgalactosaminyltransferase 11
GALNT12	UDP-N-α-D-galactosamine:polypeptide N-acetylgalactosaminyltransferase 12
GALNT13	UDP-N-α-D-galactosamine:polypeptide N-acetylgalactosaminyltransferase 13
GALNT14	UDP-N-α-D-galactosamine:polypeptide N-acetylgalactosaminyltransferase 14
GALNT15	UDP-N-α-D-galactosamine:polypeptide N-acetylgalactosaminyltransferase 15
GALNT16	UDP-N-α-D-galactosamine:polypeptide N-acetylgalactosaminyltransferase 16
GALNT17	UDP-N-α-D-galactosamine:polypeptide N-acetylgalactosaminyltransferase 17
GALNT18	UDP-N-α-D-galactosamine:polypeptide N-acetylgalactosaminyltransferase 18
GALNT19	UDP-N-α-D-galactosamine:polypeptide N-acetylgalactosaminyltransferase 19
GALNT2	UDP-N-α-D-galactosamine:polypeptide N-acetylgalactosaminyltransferase 2
GALNT20	UDP-N-α-D-galactosamine:polypeptide N-acetylgalactosaminyltransferase 20
GALNT3	UDP-N-α-D-galactosamine:polypeptide N-acetylgalactosaminyltransferase 3
GALNT4	UDP-N-α-D-galactosamine:polypeptide N-acetylgalactosaminyltransferase 4
GALNT5	UDP-N-α-D-galactosamine:polypeptide N-acetylgalactosaminyltransferase 5
GALNT6	UDP-N-α-D-galactosamine:polypeptide N-acetylgalactosaminyltransferase 6
GALNT7	UDP-N-α-D-galactosamine:polypeptide N-acetylgalactosaminyltransferase 7
GALNT8	UDP-N-α-D-galactosamine:polypeptide N-acetylgalactosaminyltransferase 8
GALNT9	UDP-N-α-D-galactosamine:polypeptide N-acetylgalactosaminyltransferase 9
GALNTL1	UDP-N-α-D-galactosamine:polypeptide N-acetylgalactosaminyltransferase 16
GALNTL2	UDP-N-α-D-galactosamine:polypeptide N-acetylgalactosaminyltransferase 15
GALNTL3	UDP-N-α-D-galactosamine:polypeptide N-acetylgalactosaminyltransferase 19
GALNTL4	UDP-N-α-D-galactosamine:polypeptide N-acetylgalactosaminyltransferase 18
GALNTL5	UDP-N-α-D-galactosamine:polypeptide N-acetylgalactosaminyltransferase 20
GALNTL6	UDP-N-α-D-galactosamine:polypeptide N-acetylgalactosaminyltransferase 17
gDNA	genomic deoxyribonucleic acid
GDP	guanine diphosphate

GF	growth factor
Glc	glucose
GlcNAc	N-acetylglucosamine
GRHL2	grainyhead like transcription factor 2
GUSB	glucuronidase-beta
H_2O	water
H_2O_2	hydrogen peroxide
HBP	hexosamine biosynthetic pathway
HCl	hydrochloric acid
hEGF	human epidermal growth factor
HER2/neu	Erb-B2 receptor tyrosine kinase 2
hFGF-B	human fibroblast derived growth factor-B
HGF	hepatocyte growth factor
HIF-1	hypoxia inducible factor 1
HnRNPA2/B1	heterogeneous nuclear ribonucleoprotein A2/B1
HnRNPD-like	heterogeneous nuclear ribonucleoprotein D-like
HnRNPH1	heterogeneous nuclear ribonucleoprotein H1
HPA	*Helix pomatia* agglutinin lectin
HPAgly1	*Helix pomatia* agglutinin glycan 1
hPSCs	human pluripotent stem cells
hr	hour
HRE	hypoxia response element
Hsp27	heat shock protein 27
HSP90	heat shock protein 90
HUVEC	human umbilical vein endothelial cells
ICAM-1	intracellular adhesion molecule-1
IFNB1	interferon beta 1
IgSF	immunoglobulin superfamily

IMS	industrial methylated spirits
IRF7	interferon regulatory factor 7
JAM2	junctional adhesion molecule 2
kb	kilobase
kDa	kilo Dalton
KEGG	Kyoto encyclopaedia of genes and genomes
KIAA1130	UDP-N-α-D-galactosamine:polypeptide N-acetylgalactosaminyltransferase 16
KIRREL	kin of IRRE like
LEF	lymphoid enhancer binding factor 1
LFA-1	lymphocyte function-assisted antigen 1
LN	lymph node
LOXL2	lysyl oxidase like 2
M	molar
MACS	magnetic activated cell sorting
Man	mannose
MAPK	mitogen-activated protein kinase
MAPK10	mitogen-activated protein kinase 10
MAPK6	mitogen-activated protein kinase 6
MET	mesenchymal epithelial transition
mg	milligram
MGC71806	UDP-N-α-D-galactosamine:polypeptide N-acetylgalactosaminyltransferase 18
$MgCl_2$	magnesium chloride
Min	minute
MIQE	minimal information for publications of quantitative real-time PCR experiments
mirRNA	micro ribonucleic acid
ml	millilitre
mm	millimetre

mM	millimolar
MMPs	matrix metalloproteinases
mRNA	messenger ribonucleic acid
MUC1	mucin 1
NC	negative control
NFH_2O	nuclease-free water
ng	nanogram
NID1	nidogen 1
nm	nanometre
NRT	no reverse transcriptase
NTC	no template control
OGA	O-GlcNAcase
OST	oligosacchayltransferase enzyme complex
P	phosphate
p	p-value
PBS	phosphate buffered saline
PCR	polymerase chain reaction
PDGF	platelet derived growth factor
PDGFRL	platelet derived growth factor receptor like
PET	polyethylene terephthalate
PFA	paraformaldehyde
PHA	*Phaseolus vulgaris* antigen lectin
P_i	phosphate
PI3K	phosphoinositide-3-kinase
PIK3R3	phosphoinositide-3-kinase regulatory subunit 3
PIPES	piperazine-N,N'-bis-(2-ethanesulfonic acid)
PLAU	plasminogen activator, urokinase
PLTP	phospholipid transfer protein

pm	picometre
POC1B	proteome of centriole protein 1B
PTS	8-hydroxypyrenetrisulphonic acid
PXN	paxillin
qPCR	quantitative polymerase chain reaction
qRT-PCR	quantitative real-time polymerase chain reaction
R3-IGF-1	R3-insulin derived growth factor-1
RAPGEF3	rap guanine nucleotide exchange factor 3
RAS	rat sarcoma oncogene
RB	retinoblastoma-associated oncogene
RER	rough endoplasmic reticulum
RFT1	requiring fifty-three 1 homolog
RHOA	RAS homolog family member A
RHOH	RAS homolog family member H
RIN	ribonucleic acid integrity number
RNA	ribonucleic acid
RNAi	ribonucleic acid interference
RNF212	Rich finger protein 212
ROS	reactive oxygen species
SA	sialic acids/ neuraminic acids
SCID	severe combined immunodeficient mice
SDS-PAGE	sodium dodecyl sulfate polyacrylamide gel electrophoresis
SEM	scanning electron microscopy
Ser	serine
SERPING1	serpin family G member 1
Sez-6	seizure-related gene 6
SF	serum-free
SGCG	sarcoglycan, gamma (34kDa dystrophin-associated glycoprotein)

shRNA	short hairpin ribonucleic acid
SIPA1	signal-induced proliferation-associated 1
siRNA	small interfering ribonucleic acid
SIX1	sine oculis homeobox 1
SLC27A6	solute carrier family 27 (fatty acid transported), member 6
SLUG	snail family transcriptional repressor 2
SMAD2	mothers against decapentaplegic homolog 2
SNAI	snail family transcriptional repressor 1
SPARC	secreted protein acidic and cysteine rich
SPP1	secreted phosphoprotein 1
Src	SRC proto-oncogene, non-receptor tyrosine kinase
SRP	signal recognition particle
sTF	sialyl-Thomsen-Friedenreich antigen
sTn	sialyl-Thomsen nouvelle antigen
STR	short tandem repeat
TβR1	transforming growth factor beta receptor 1
TBS	tris buffered saline
TF	transcription factor
TF/T	Thomsen-Friedenreich antigen
TFPI2	tissue factor pathway inhibitor 2
TGFβ	transforming growth factor beta
Thr	threonine
TLR2	toll like receptor 2
TLR6	toll like receptor 6
Tm	melting temperature
Tn	Thomsen nouvelle antigen
TNF-α	tumour necrosis factor alpha
TRAP-1	tumour necrosis factor type 1 receptor-associated protein

TTRs	tetratricopeptide repeats
TWIST1	twist family BHLH transcription factor 1
U	units
UDP	uridine diphosphate
v/v	volume per volume
v	volts
VEGF	vascular endothelial growth factor
VEGFR-1	vascular endothelial growth factor receptor 1
VEGFR-2	vascular endothelial growth factor receptor 2
VIM	vimentin
VVA	*Vicia villosa* antigen lectin
w/v	weight per volume
WBSCR17	UDP-N-α-D-galactosamine:polypeptide N-acetylgalactosaminyltransferase 20
WNT2B	wnt family member 2B
ZEB1	zinc finger E-box binding homeobox 1

Contents

List of figures

List of tables

Chapter 1

Introduction

1.0 Introduction

1.1 Cancer

Cancer is a disease which develops from dynamic changes in the genome which cause abnormal regulation of molecular control of cell growth (Weinberg, 2014). The majority of genetic changes found in human cancer can be considered as either activation of proto-oncogenes and/or inactivation of tumour-suppressor genes (reviewed by Lee and Muller, 2010). Epidermal growth factor receptor (EGFR) is an example of a proto-oncogene. Overexpression or mutation of EGFR results in ligand-independent constitutive signalling which causes uncontrolled cell growth. An example of a tumour-suppressor gene is breast cancer associated gene 1 (BRCA1), germline mutations in this gene predispose women to breast and ovarian cancers. BRCA1 is extensively involved in cell cycle checkpoints and inactivation results in genetic instability (reviewed by Deng, 2006).

Hanahan and Weinberg (2000) proposed a set of novel acquired capabilities shared by most cancer types – alterations in cell physiology – that represent successful over coming of anti-cancer defence mechanisms (normal cellular growth). These "hallmarks of cancer" signify a system to rationalise the complexities of cancer as a disease and include (as described below and illustrated in Figure 1.1): 1. Sustaining proliferative signalling, 2. Evading growth suppressors, 3. Activating invasion and metastasis, 4. Enabling replicative immortality, 5. Inducing angiogenesis and 6. Resisting cell death.

1. **Sustaining proliferative signalling**

Tissues normally remain in a state of homeostasis where mitogenic signalling and therefore their growth is tightly controlled, ensuring that normal tissue architecture is maintained. However, the elementary characteristic of cancer is the capacity to sustain chronic proliferation thereby disrupting typical tissue organisation. Cancer cells can acquire the ability to sustain proliferative signalling by a number of methods for example, some cancers acquire the ability to produce growth factors (GFs) to which they are responsive in a process termed autocrine stimulation (Fedi et al., 1997). Alternatively, some cancers promote tumour associated stroma to produce GFs to which cancer cells are responsive (Skobe and Fusenig, 1998). Furthermore, upregulation in the number of GF receptors present on the cancer cell surface can cause hyperresponsiveness to diminutive amount of GFs that would not normally instigate a response (Fedi et al., 1997). Ligand-independent signalling can also be achieved through mutations arising in the GF receptors resulting in truncated versions which consequently fire constitutively (Fedi et al., 1997).

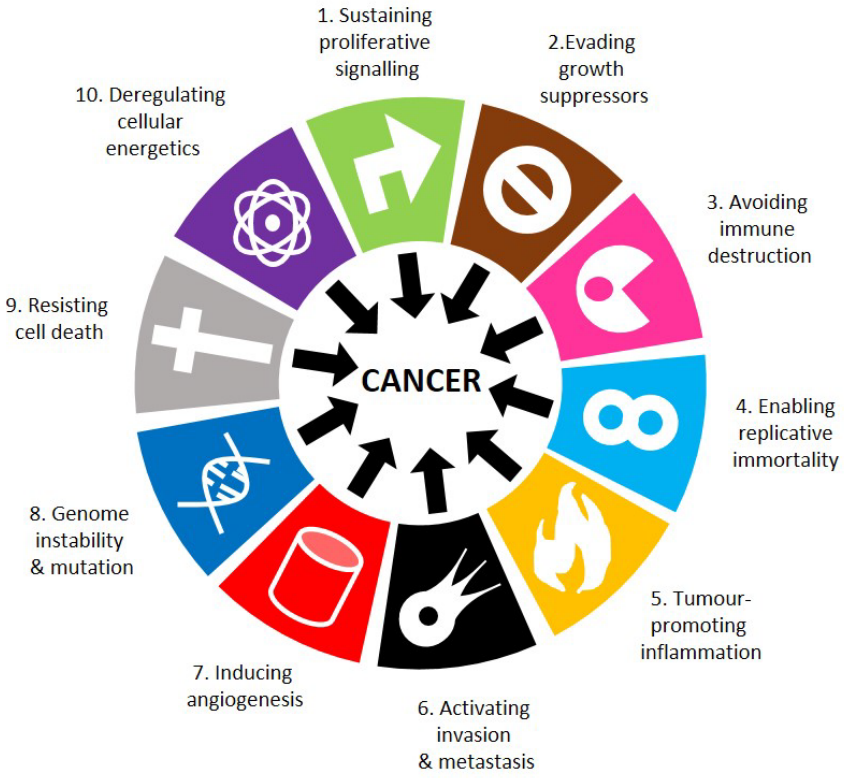

Figure 1.1 *The hallmarks of cancer as proposed by Hanahan and Weinberg (2011). Figure adapted from Hanahan and Weinberg (2011).*

2. Evading growth suppressors

In opposition to activating proliferation-inducing signals cancer cells can must also evade negative regulators of cell growth, these include removal from the cell cycle to quiescence or entering post-meiotic states becoming differentiated. The tumour-suppressor gene retinoblastoma-associated (RB) is a critical gatekeeper of cell cycle progression, therefore loss of function of RB results in continual cell growth (reviewed by Burkhart and Sage, 2008).

3. Activating invasion and metastasis

The multi-step process of invasion and metastasis is a culmination of several discrete steps which together results in spread of cancer cells to secondary sites ad is extensively discussed in Section 1.2.

4. Enabling replicative immortality

Immortalisation of cancer cells allows them to proliferate indefinitely. Telomere – repeats on the end of DNA which protect chromosomal DNA – length is a measure of cells replicative lifetime and determines when cell senescence and apoptosis will occur (Blasco, 2005). Telomerase, the enzyme which adds

telomere repeats is almost absent in non-immortal cells, however is highly expressed in immortal cells, which therefore bestows resistance to senescence and apoptosis (Shay and Wright, 2000).

5. Inducing angiogenesis

Like normal tissues tumours need to absorb nutrients and oxygen as well as eliminate metabolic waste and carbon dioxide, this is accomplished in a process termed tumour angiogenesis and is discussed in Section 1.2.1.

6. Resisting cell death

Programmed cell death by apoptosis is elicited in response to physiological stresses for example, DNA damage associated with hyperproliferation (Adams and Cory, 2007). Cancer avoids cell death by deregulation of proapoptotic processes and upregulation of antiapoptotic factors (Junttila and Evan, 2009).

Hanahan and Weinberg (2011) later elaborated on the six core hallmarks by adding four new categories (described below), which included two enabling hallmarks that promote/accelerate the core hallmarks - 7. Genome instability and mutation and 8. Tumour-promoting inflammation – and two emerging hallmarks that encompass general cancer characteristics – 9. Deregulating cellular energetics and 10. Avoiding immune destruction. Furthermore, the stroma and normal cells surrounding the tumour termed the "tumour microenvironment" also facilitate the initiation and continuation of the hallmarks (reviewed by Schauer et al., 2011).

7. Genome instability and mutation (enabling characteristic)

Procurement of the above mentioned hallmarks depends on a succession of alterations in the genome of cancer cells in a process reminiscent of Darwinian evolution. Specific mutations bestow selective advantage on sub-clones in a population which enables their survival and the persistence of favourable phenotypes (Hanahan and Weinberg, 2011). In addition to heritable phenotypes, initiation of the hallmarks can also be achieved through epigenetic mechanisms e.g. DNA methylation and histone modification (Berdasco and Esteller, 2010).

8. Tumour-promoting inflammation (enabling characteristic)

Inflammation can promote several hallmarks by imparting effector molecules to the tumour microenvironment for example, GFs which sustain proliferative signalling, survival factors which negate cell death, and proangiogenic factors (Karnoub and Weinberg, 2006-2007). Furthermore, inflammatory cells can release substances such as reactive oxygen species (ROS) that are mutagenic and therefore accelerate the genetic instability of the cancer cells (Grivennikov et al., 2010).

9. Deregulating cellular energetics (emerging characteristic)

Cancer cells often have altered energy metabolisms, using predominantly glycolysis in a process termed "aerobic glycolysis" (Warburg, 1930; Warburg, 1956a; Warburg 1956b). To compensate for the lower efficiency of this method cancer cells frequently have increased number of glucose transporters (Jones and Thompson, 2009). This type of metabolism is reported in rapidly dividing embryonic tissues, therefore suggesting a role of aerobic glycolysis for sustaining large-scale biosynthetic programs that are needed for cell proliferation (Vander Heiden et al., 2009).

10. Avoiding immune destruction (emerging characteristic)

Cancer cells are highly immunogenic, it is thought that they evade immune destruction by disabling components of the immune system that have been sent to kill them, by for example secreting immunosuppressive factors (Yang et al., 2010) or by recruiting immunosuppressive cells (Mougiakakos et al., 2010).

1.1.1 Breast cancer

The breast is composed of ducts which branch out and connect to milk producing lobules, which together can also be called terminal ductal-lobular units (see Figure 1.2). The lobules and ducts are located throughout the connective tissue and adipose tissues that comprise the mass of the breast (Russo and Russo, 2004). During pregnancy, lobules grow in response to increased levels of oestrogen and progesterone to prepare the breast for milk secretion (Vonderhaar, 1988). Post-parturition, the breast becomes insensitive to oestrogen-dependant regulation of growth and post-weaning pre-pregnancy state is resumed (Hansen and Bissell, 2000).

The majority of breast cancers are epithelial (95%), originating from cells that line either the ducts (80%) or the lobules (15%) (Cancer Research U.K., 2016). Non-epithelial cancers arising from the breast stroma and connective tissue occur less frequently (Dimri et al., 2005). Breast cancer is the most common malignancy in the U.K. with around 53,400 women and 340 men being diagnosed in 2014 (Cancer Research U.K., 2016). Breast cancer at stage I is described as a tumour greater than 2 cm at its greatest dimension whilst, breast cancer at stage IV has metastasised to internal mammary lymph nodes (Singletary et al., 2002). When diagnosed at stage I 99% of women survive their disease for 5 years and this reduces drastically to around 15% for women who are diagnosed with advanced stage IV metastatic breast cancer (Cancer Research U.K., 2016).

An independent review of the benefits and harms of breast cancer screening performed by Marmot et al. (2012) reported that earlier diagnosis through breast cancer screening every 3 years for women aged

between 50-70 years, has reduced breast cancer mortality by ~20% compared to not screening. Although 19% of breast cancer cases diagnosed by screening would not have caused any difficulty if left undiagnosed or untreated, the benefit of reduced mortality rates that result from early detection outweigh the harm caused by over diagnosis of cases (Marmot et al., 2012). Furthermore, improved treatments such as tamoxifen for oestrogen positive tumours and trastuzumab (Herceptin®) the monoclonal antibody treatment for HER2/neu positive tumours which is administered with conventional chemotherapy, have helped to improve survival rates (Howell and Wardley, 2005). For example, transtuzumab treatment for patients with HER2 positive tumours has improved the event-free survival (over 3 years) for breast cancer by 71% (Gianni et al., 2010).

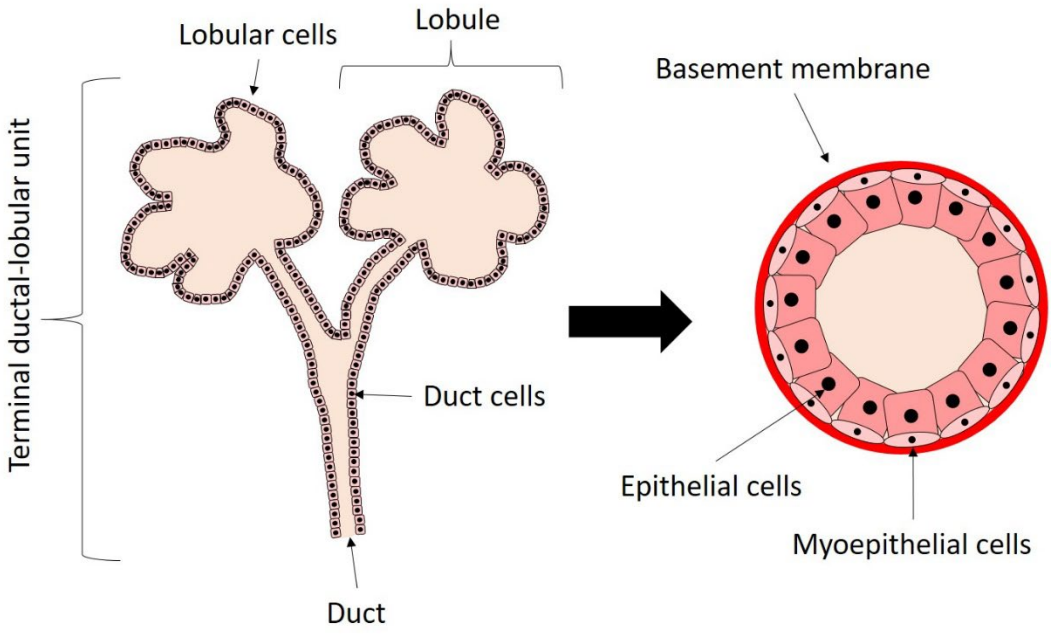

Figure 1.2 *Terminal ductal-lobular unit of normal breast. Ducts branch out to milk producing lobules. Both ducts and lobules are comprised of myoepithelial cells lined with epithelial cells and surrounded by basement membrane. Most breast cancers arise, from the epithelial cells lining the ducts and lobules.*

1.2 Metastasis

Metastasis is the dissemination of cancer cells from a primary tumour mass forming secondary lesions at distant anatomical sites. Metastasis is a significant cause of cancer mortality accounting for about 90% of cancer patient deaths (Sporn, 1996; Germanov et al., 2006). This is because it is often not detected until the secondary tumours have manifested clinically, at which point the disease is often well progressed, poorly responsive to chemotherapeutic drugs and is often difficult to excise surgically (Sun et al., 2011). Metastasis is believed to occur as a result of a cascade of events, although the exact order in which these events must proceed for metastasis to occur is not fully understood. However, all steps must be completed for successful secondary growths to form (Pantel and Brankenhoff, 2004). The metastatic cascade is discussed below and illustrated in Figure 1.3. Mina and Sledge (2011) proposed that the metastatic cascade has several targetable steps for therapy, although not all treatments are ready clinically. These include: 1. The tumour microenvironment of both primary and secondary cancers, 2. Regulation of metastatic suppressor and promoter genes, 3. Angiogenesis at both initial and secondary site, 4. Immune axis as a site of chronic inflammation providing a metastatic niche, 5. Cancer cell dormancy within vasculature and extravasation and, 6. Cancer stem cells which are often unresponsive to traditional chemotherapies. Therefore, it is important that further research into the metastatic cascade to aid understanding of the targetable metastatic processes is performed.

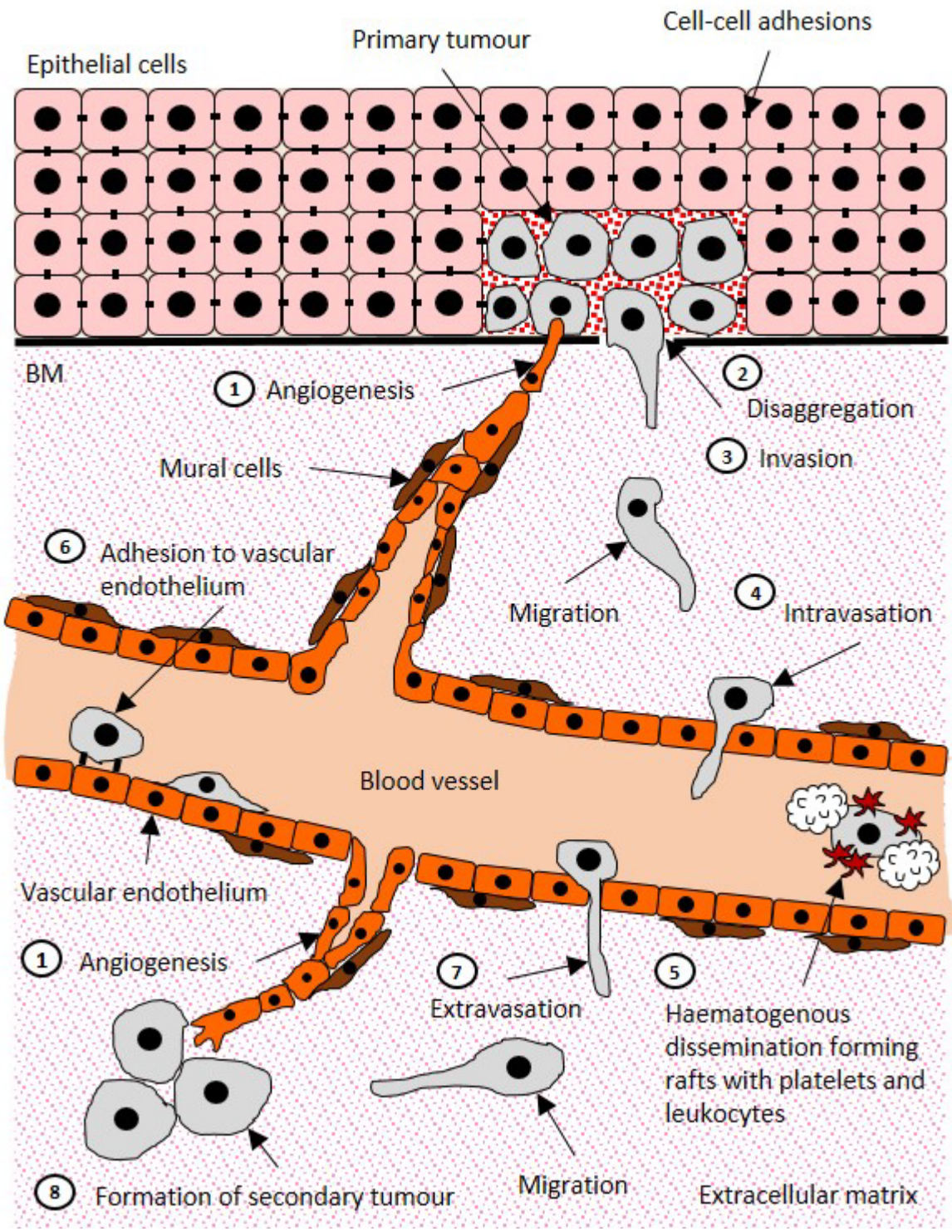

Figure 1.3 *The metastatic cascade, detailing the distinct "steps" that must be all successfully completed for cancer spread to occur. (1) Angiogenesis, development of a tumoural blood supply. (2) Disaggregation of cancer cells from the primary tumour mass, followed by (3) invasion of surrounding basement membrane (BM) and extracellular matrix (ECM). (4) Intravasation of the ECM and BM of the local vasculature, where (5) haematogenous dissemination can occur. Cancer cells arrest at a certain point in the circulation, (6) adhere to the vascular endothelium and (7) extravasate through the BM and ECM of the blood vessel to form a secondary tumour at a new site.*

1.2.1 Tumour angiogenesis

Tumours will remain dormant and not grow any larger than 2mm in diameter unless a blood supply, providing oxygen and nutrients, is formed (Duffy, 1996). Without neo-vasculature, primary tumours and micrometastases remain in a state of quiescence where numbers of proliferating cells are balanced against apoptotic cells (Naumov, et al. 2006). Hypoxia (low oxygen levels) is the primary physiological regulator of the angiogenic switch (induction of tumoural neovasculature) (Bergers and Benjamin, 2003). Hypoxia results from increased metabolic activity and oxygen requirements as a result of rapidly proliferating cells, leading to an increase in local pH and oxidative stress (Liao and Johnson, 2007). The master regulator of hypoxic response is the transcription factor hypoxia inducible factor 1 (HIF-1) (reviewed by Semenza, 2001). Loss of HIF-1 causes an inhibition of tumour vascularisation (Tang et al., 2004). Among other roles, HIF-1 can induce the expression of vascular endothelial growth factor (VEGF) by direct binding of hypoxia response element (HRE) within the promoter region of VEGF (Manalo et al., 2005). VEGF is a homodimeric glycoprotein, existing as five isoforms which have different biological activities (Zhang et al., 2003a) and are key mediators in angiogenesis (reviewed by Carmeliet, 2005). VEGF is released from the cell surface, and then binds to its tyrosine kinase-receptors VEGFR-1 and VEGFR-2 which are expressed on vascular endothelial cells (Kopparapu et al., 2013). In normal tissues, VEGF promotes angiogenesis in embryonic development (reviewed by Breier, 2000) and wound healing (reviewed by DiPietro, 2016).

Several mechanisms of tumoural angiogenesis exist, with the most well studied being (1) sprouting angiogenesis; the formation of new capillary vessels from pre-existing vasculature. This type of vasculature is often incomplete and is “fenestrated” (Ribatti, 2006; Ribatti and Crivellato, 2012), (2) intussusceptive or splitting angiogenesis; which is the formation of neo-vasculature by dividing a vessel in two by the formation of an intraluminal tissue pillar (Gianni-Barrera et al., 2014), (3) vasculogenic mimicry; the construction of tube-like formations from tumour cells autonomous from angiogenesis (Maniotis et al., 1999; Folberg et al., 2000; Hendrix et al., 2003). As illustrated in Figure 1.4, sprouting angiogenesis is initiated through hypoxic signals which stimulate endothelial cells of existing capillaries to form a dynamic and invasive “tip cell” phenotype (Eilken and Adams, 2010). Tip cells sprout towards an increased concentration of growth factors, such as VEGF guiding the angiogenic sprout, whilst degrading ECM (Gerhardt et al., 2003). The “stalk cells” that trail behind are more proliferative than the tip cells, therefore driving growth of the nascent sprout (Adams and Alitalo, 2007). To form new vasculature networks, tip cells must form connections with other endothelial cells (Francavilla et al., 2009). Lumenisation of the vessel occurs through pinocytosis (cell-drinking) and vacuole formation, subsequently allowing blood-flow to occur. Stabilisation of immature vessels is established through recruitment of mural cells, which generate ECM (Hillen and Griffioen, 2007).

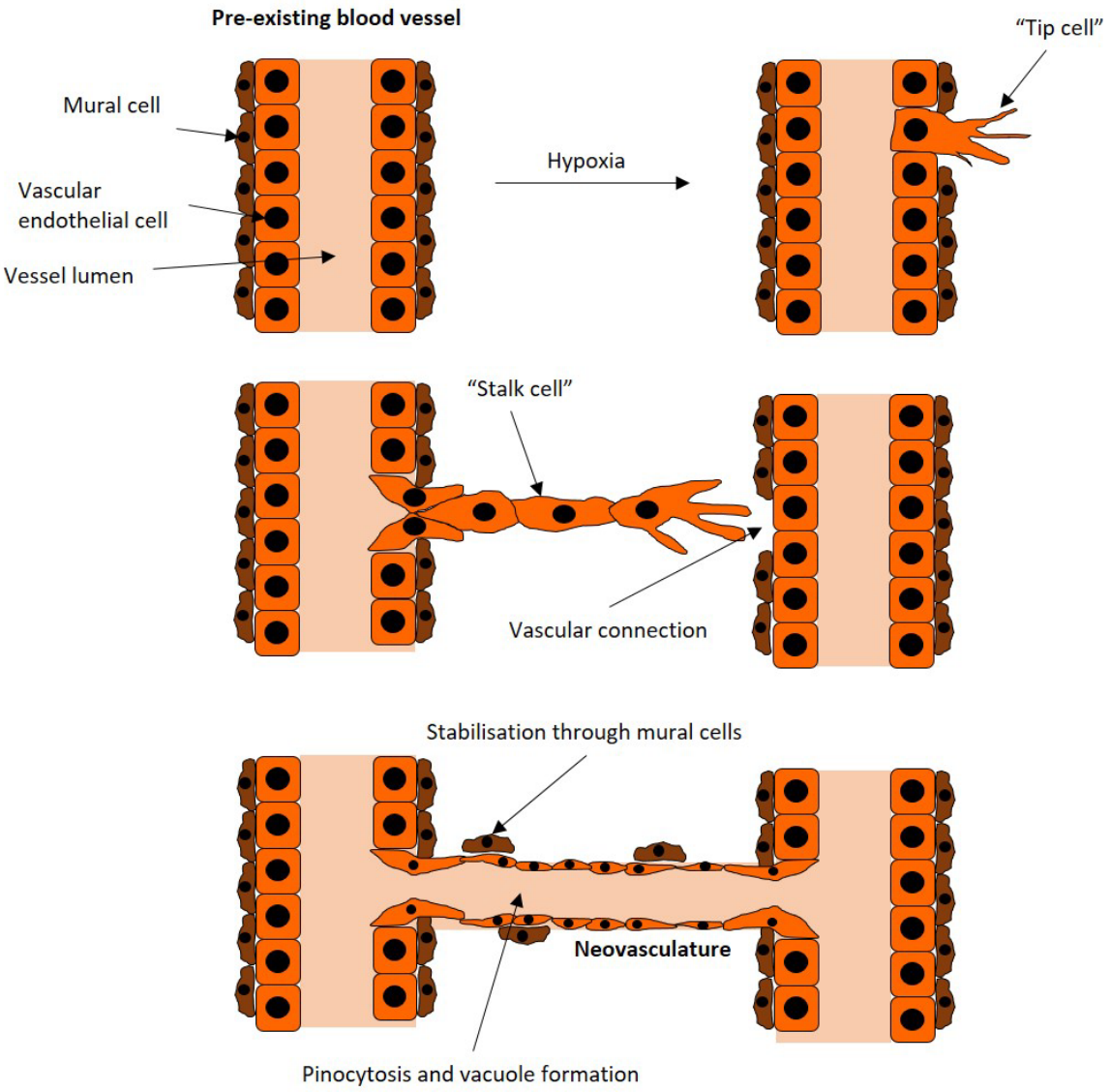

Figure 1.4 *Sprouting angiogenesis, the growth of new capillaries from pre-existing vasculature. Sprouting angiogenesis is initiated through hypoxia, where the tip cell is stimulated to form from vascular endothelial cells. Stalk cells act as the driver of the sprout, whilst the tip cell directs growth through chemotaxis. Upon encountering other vasculature, endothelial cells form connections and join together. Lumenisation occurs through pinocytosis and vacuole formation allowing blood to flow. Mural cells stabilise the neovasculature and secrete ECM.*

1.2.2 Disaggregation from primary tumour

The next step in the cascade after a tumoural blood supply has been established is cancer cell dissemination from the primary tumour mass. For this to occur cancer cells must reduce or lose cell-cell, cell-basement membrane (BM) and ECM adhesion through changes in expression of cell adhesion molecules (CAMs), such as cadherins, catenins, integrins and selectins (Beyers et al., 1995). One hypothesised scenario for cancer cells to be able to detach from a primary tumour and invade the surrounding basement membrane is the reactivation of the developmental program termed epithelial-mesenchymal transition (EMT) (Micalizzi et al., 2010a), discussed below and illustrated in Figure 1.5.

1.2.2.i Epithelial-mesenchymal transition (EMT)

EMT is the transdifferentiation of polarised, basement membrane bound epithelial cells to migratory and invasive mesenchymal cells (Hay, 1995). Epithelial cells typically possess tissue-specific functions, while mesenchymal cells in such a tissue provide a supportive role (Kalluri and Weinberg, 2009). An epithelium is a uniform sheet of cells usually one cell thick. Epithelial cells have regularly spaced cell-cell junctions and adhesions that provides the cell-cell organisation necessary for maintaining the integrity of multicellular organisms, but also meaning that epithelial cells are held tightly together and that individual cells are inhibited from movement away from the epithelial sheet. Mesenchymal cells have neither controlled structure nor regular shape or density. Mesenchymal cells have reduced cell adhesion in comparison to epithelial cells which permits migratory capacity (Lee et al., 2006a). The epithelium is polarised meaning that the apical and basal surfaces are often visually different and adhere to different substrates or possess different functions (Lee et al., 2006a). During EMT, epithelial cells lose their apical-basal polarity through the dissolution of tight junctions which permits the fraternisation of apical and basolateral membrane components resulting in anterior-posterior leading-edge polarity associated with mesenchymal cells (Greenburg and Hay, 1982). Cell adhesion structures such as gap junctions and adherens junctions are eliminated removing the structural integrity of epithelial cells (Shtutman et al., 2006). Unlike epithelium the irregular structure of mesenchyme does not allow for the rigid topological specialisation (Lee et al., 2006a). CAMs such as E-cadherin and epithelial-specific integrins that mediate cell-cell and cell-BM connections, respectively, are replaced with N-cadherin and extracellular-specific integrins which impart a more transient adhesion (Nakajima et al., 2004). The reduced adhesion that mesenchymal cell possess facilitates their migratory capacity (Lee et al., 2006a). In the process of becoming mesenchymal, the cell gains resistance to anoikis where epithelial cells which lose cell-cell adhesion are normally terminated (Frisch et al., 2013). The actin cytoskeleton of epithelial cells is re-structured and substituted with stress fibres, whilst cytokeratin intermediate filaments are exchanged for vimentin (Micalizzi et al., 2010a). These cytoskeletal changes result in a morphological revision from cuboidal to spindle-shaped cells (Boyer et al., 1989). Finally, the BM is degraded by the secretion of

proteases and the mesenchymal cells with acquired motility can now invade the ECM and surrounding stroma (Savagner, 2001). Mesenchymal migration is mechanically different from epithelial movement as epithelial cells migrate as a connected sheet whilst mesenchymal movement is dynamic (Lee et al., 2006a). EMT was first reported experimentally by Greenburg and Hay (1982) as "epithelio-mesenchymal transformation", as in the conversion of a cell from epithelial to mesenchymal. However, later this term was changed to epithelial-mesenchymal transition, which reflected the plasticity of EMT and its reciprocal process mesenchymal-epithelial transition (MET) (Kalluri and Neilson, 2003; Kalluri and Weinberg, 2009).

EMT can be categorised into three different types as proposed by Kalluri and Weinberg (2009), these are: 1. EMT associated with embryonic development, 2. EMT initiated by injury and 3. oncogenic EMT, all of which are discussed below.

During development, EMT is involved in a range of tissue remodelling events, including, for example, gastrulation (Kimelman, 2006), neural crest formation (Duband et al., 1995), development of the heart valve (Person et al., 2005), development of the craniofacial structures (Cordero et al., 2011) and secondary palate formation (Fitchett and Hay, 1989). MET is also observed in development, for example in formation of kidney tubules (Davies, 1996). In the adult tissue, EMT occurs in wound healing, fibrosis (Stone et al., 2016) and in the initiation and metastasis of cancer (Meng and Wu, 2012; De Craene and Berx, 2013). Transitioned cells are thought to form the invasive front of a primary tumour, therefore allowing disaggregation and subsequent invasion and dissemination. MET is also involved in cancer metastasis, as MET allows for colonisation of cancer cells at a secondary site (Chao et al., 2010; Gunasinghe et al., 2012). EMT/MET is difficult to observe in human tumours *in vivo*, and although EMT/MET in cancer has been reported repeatedly in *in vitro* models, some authors have cast doubts as to whether the processes actually occurs in tumour progression (Diepenbruck and Christofori, 2016). The main reason there is uncertainty surrounding EMT-METs involvement in cancer progression is that EMT-MET is thought to be partially formed in cancer cells, that is, cancer cells possess characteristics of both epithelial and mesenchymal cells and are termed "metastable" (Lee et al., 2006a; Tam and Weinberg, 2013). Such cells benefit from the use of both epithelial and mesenchymal traits and are therefore less constrained than either epithelial or mesenchymal cells.

EMT is thought to be initiated in the primary tumour microenvironment by autocrine/paracrine secretion of a number of growth factors, cytokines and ECM proteins (Tse and Kalluri, 2007; Martin et al., 2010; Jing et al., 2011) produced as a result of hypoxia (Jiang et al., 2011) and inflammation (López-Novoa and Nieto, 2009; Zhou et al., 2012). EMT-inducing signals derive from the tumour microenvironment, and include hepatocyte growth factor (HGF) (Nagai et al., 2011), epidermal growth factor (EGR) (Ackland et al., 2003), platelet derived growth factor (PDGF) (Kong et al., 2008) and transforming growth factor beta (TGFβ) (Willis et al., 2005). These signals are responsible for the

stimulation of EMT-inducing transcription factors (TFs) such as Snail (Cano et al., 2000), Slug (Savagner et al., 1997), ZEB1 (Xiong et al., 2012), and Twist (Lo et al., 2007). Once these TFs have been expressed and activated, each TF can act pleiotropically to orchestrate the EMT process (reviewed by Sáchez-Tilló et al., 2012). The implementation of the EMT program depends on a series of intracellular signalling networks involving signal transduction proteins, including: ERK, MAPK, PI3K, Smad, β-catenin, Lef and Ras (reviewed by Thiery, 2002; Thiery and Sleeman, 2006; Polyak and Weinberg, 2009; Lamouille et al., 2014; Heerboth et al., 2015; Nieto et al., 2016). MicroRNAs – small non-coding RNAs that can silence target genes by specific-binding to cleave mRNA or inhibit translation (Bartel, 2004) – have been reported as mediators of EMT by affecting both TFs and by directly regulating expression of cell surface molecules such as E-cadherin (Burk et al., 2008; Bullock et al., 2012).

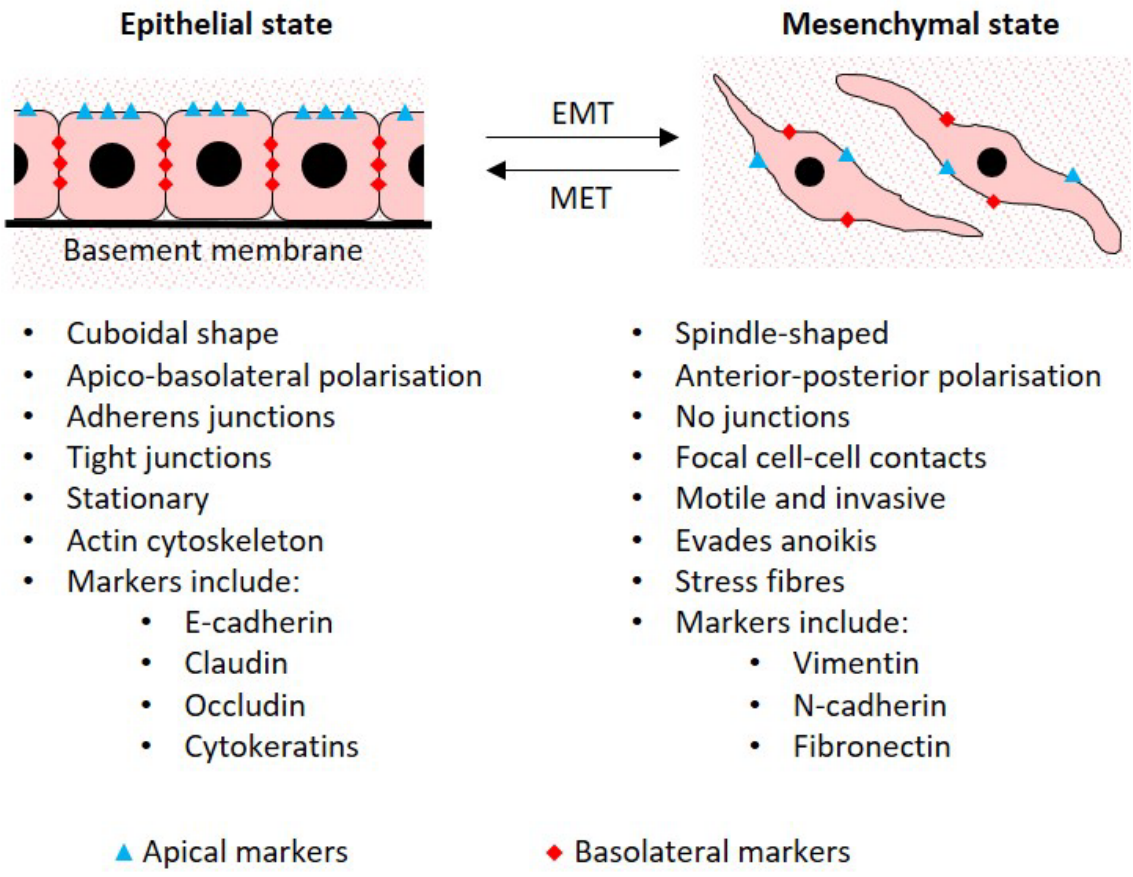

Figure 1.5 *Epithelial-mesenchymal transition (EMT) is the process by which epithelial cells transdifferentiate into mesenchymal cells. During EMT, epithelial cells down-regulate cell-cell adhesion structures. Epithelial-specific cell adhesion molecule (CAM) E-cadherin and integrins are replaced by extracellular-specific N-cadherin and integrins. Loss of cell-cell adhesion alters the cell polarity from apico-basal to end-end changing the cell morphology from cuboidal to spindle-shaped. This change in cell polarity allows apical and basolateral membrane components to merge. The actin cytoskeleton is transformed into stress fibres which accumulate at cell protrusions. Epithelial intermediate filaments, the cytokeratins, are replaced by vimentin which is specific to mesenchymal cells. The basement membrane (BM) is dissolved allowing newly formed mesenchymal cells to invade the surrounding stroma.*

1.2.3 Invasion of basement membrane (BM)

Once cancer cells have disaggregated from the primary tumour mass they must degrade and invade the local BM. BM acts as an impermeable layer of ECM, functioning to separate tissues from their stroma (reviewed by Liotta, 1984). The BM is normally only permeable in situations such as tissue development and repair and during the normal inflammatory response (reviewed by Liotta, 1986; Liotta and Stetler-Stevenson, 1991). Matrix metalloproteinases (MMPs) are a family of endopeptidases which have the ability to degrade almost all of the BM and ECM components (reviewed by Stamenkovic, 2003). MMPs are often upregulated in cancer, and have been shown to promote tumour cell migration (Sabeh et al., 2009). ECM provides both the substrate for, and acts as a barrier to, cell migration (reviewed by Friedl and Wolf, 2003). In order to migrate, cells must modify their shape and rigidity to be able to interact with their changing surroundings (Zhang et al., 2002). There are a range of migration and invasion mechanisms that occur in normal physiological processes, including embryonic morphogenesis (Young et al., 2004), wound healing (Maini et al., 2004) and immune cell trafficking (Klonowski et al., 2004). The five steps of cell migration (illustrated in Figure 1.6), as determined by Lauffenburger and Horwitz (1996), are as follows: 1. Protrusion of the leading edge, 2. Cell-matrix interactions and formation of focal contacts, 3. Recruitment of surface proteases resulting in focalised proteolysis, 4. Cell contraction by actomyosin and 5. Detachment of the trailing edge. These five steps are continuously cycled to produce movement. For cell protrusions to form, the cell must first become polarised and elongate. Cell protrusions can be diverse in shape and function, the most common occurring being pseudopodia or invadopodia (invasive foot processes) (Linder, 2009). These are F-actin rich membrane protrusions that protrude and retract and act to localise matrix-degradation and facilitate cancer cell migration through adhesion and chemotaxis (Alblazi and Siar, 2015). The modes of cell migration are categorised as either individual or collective. Individual cell migration can be either amoeboid, which is a fast, “crawling” type movement that is produced from transient and weak interactions with substrate and imitates features of the amoeba *Dictyostelium discoideum*, or mesenchymal which accomplishes the five steps of migration (mentioned above) (reviewed by Friedl and Wolf, 2003). Cells that maintain cell-cell junctions move collectively either as a multicellular connected strand or as a sheet (Matsubayashi et al., 2004). Each cell type employs a preferential pre-specified migration mode. For example, leukocytes prefer single-cell amoeboid migration, stromal cells prefer single-cell mesenchymal migration and epithelial cells prefer collective sheet migration (Friedl, 2004). However, changes in cell environment and cellular properties can result in revision of the mode of cell migration. For example, down-regulation of cell-cell junctions in collective cell migration can lead to amoeboid migration, whilst conversely, cell-cell junctions can re-form and collective cell migration resume presenting a plasticity that can benefits metastasis (Friedl and Gilmour, 2009; Friedl and Wolf, 2009).

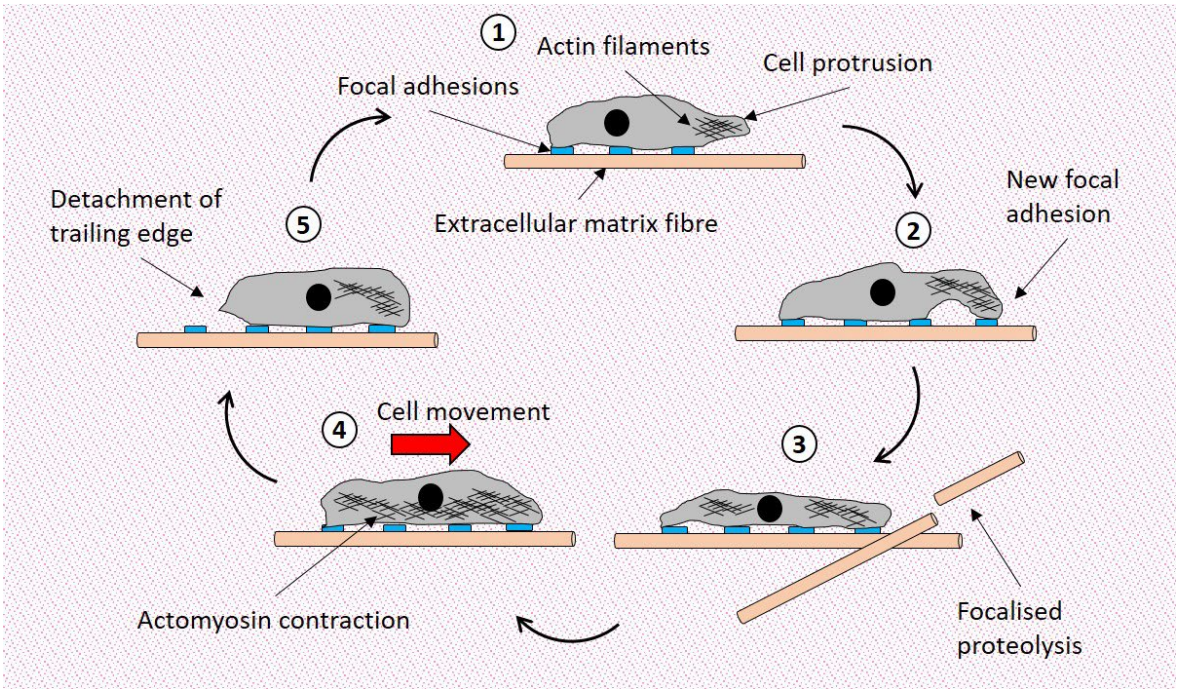

Figure 1.6 *Five steps of cell migration as described by Lauffenburger and Horwitz (1996). 1. Protrusion of the leading edge, 2. Cell-matrix interactions and formation of focal contacts, 3. Recruitment of surface proteases resulting in focalised proteolysis, 4. Cell contraction by actomyosin and 5. Detachment of trailing edge. These five steps are continuously cycled to produce movement.*

1.2.4 Intravasation of blood vessels and haematogenous dissemination

Intravasation is the process of cancer cells entering the blood vessels. This is accomplished by adhesion to, and degradation of, the vascular BM followed by invasion of blood vessels and haematogenous dissemination (Wyckoff et al., 2000). This process is aided by the flawed construction of the tumour-induced microvasculature as the fenestrations allow for ease of access (see Section 1.2.1). Upon negotiating their way through the BM, cancer cells are able to interact with the vascular endothelial cells, which withdraw allowing the cancer cells to pass into the vessel lumen (Blood and Zetter, 1990). Alternatively, uncontrolled focal growth of a tumour can impact on fragile tumour neovasculature and lead to passive shedding of cancer cells into circulation (Bockhorn et al., 2007). These cancer cells are often non-viable and apoptotic, perhaps due to anoikis or as a result of hypoxia (Méhes et al., 2001). Once inside the systemic circulation, the cancer cells come into contact with and aggregate with, platelets and leukocytes to form “rafts” which allows the cancer cells to be shielded from immune response as well as from the shear force of blood flow (Nash et al., 2002; Wyckoff et al., 2007). Circulating tumour cell (CTCs) can present with cell surface markers of epithelial cell, mesenchymal cell or both epithelial and mesenchymal cell type (Armstrong et al., 2011). CTCs with both types of markers,

or mesenchymal alone, have been reported to more frequently result in successful metastases (Wu et al., 2015).

1.2.5 Attachment to vascular endothelium and extravasation

In 1889, Stephen Paget first proposed the "seed and soil" hypothesis on the non-random distributions of cancer metastasis. Paget (1889) examined post-mortem data from 735 women with breast cancer and noted that the organ distribution of the metastases in the patients was non-random. Paget (1889) remarked that the metastases were not a result of chance events, but instead suggested that some tumours ("seeds") grew preferentially in the microenvironment ("soil") of certain organs, and that metastasis only occurred when the suitable "seed" was rooted in the appropriate "soil" (reviewed by Fidler, 2003). Pagets (1889) concept that the microenvironment is essential for the regulation and growth of metastases is supported by several studies. For example, Greene and Harvey (1964) demonstrated that the adhesive interactions between cancer cells and the luminal surface of microvascular endothelium may be responsible for determining metastasis localisation. Auerbach et al. (1987) supported Green's work by demonstrating that cancer cells preferentially bind to the microvasculature of their respective target organ. Some examples of the organ specificity of cancer metastases include, primary pancreatic cancer to liver and primary prostate cancer to bone (Hess et al., 2006). A further hypothesis for the non-random spread of cancer is that CTCs respond to chemokine gradients, in a process similar to leukocyte trafficking (Balkwill and Mantovani, 2001). For example, breast cancer cells highly express chemokine receptors CXCR4 and CCR7, while their ligands CXCL12/SDF-1α and CCL21/6Ckine are expressed on the cells of characteristic breast cancer metastasis destinations such as lung and liver (Müller et al., 2001).

An alternative hypothesis to explain the patterns of cancer metastasis proposed by Ewing in 1928 is the idea of "mechanical entrapment", where CTCs become lodged in the first capillary bed they come across (Glinskii et al., 2005). Glinskii et al. (2005) reported that mechanical entrapment alone is insufficient for successful extravasation, and adhesive interaction to the vascular endothelium is essential, similar to leukocyte-endothelial cell adhesion seen in inflammation, as illustrated in Figure 1.7 (as reviewed in Kannagi et al., 2004; Miles et al., 2008; Strell and Entschladen, 2008; Brooks et al., 2010). Pro-inflammatory cytokines are released at sites of inflammation, when bound to their subsequent ligands on ECM, endothelial cells, leukocytes or platelets a transcriptional up-regulation of selectin, immunoglobulin superfamily (IgSF) and integrins occurs (reviewed by Balkwill and Mantovani, 2001). Cytokines act in a site-specific manner to direct leukocyte recruitment to site of inflammation. At inflamed site, leukocytes adhere to the vascular endothelium in a loose tethering adhesion mediated by selectins and their ligands. Leukocytes are carried along (rolling on) the endothelium by blood flow until up-regulation of integrins and members of the IgSF stabilise leukocyte "firm adhesion" to the vascular

endothelium, followed by subsequent extravasation (reviewed by Bendas and Borsi, 2012; Kanada et al., 2014).

Although tumour cells mimic mechanisms used by leukocytes to bind to the vascular endothelium and extravasate, the adhesion molecules and ligands employed by tumour cells are different (Miles et al., 2008). For example, Galectin-3 expressed on the surface of vascular endothelial cells binds to the cancer associated Thomsen-Friedenreich (TF) antigen (Galβ1-3GalNAc) which is present on most cancers including those of the breast and prostate (Glinsky et al., 2001). During cancer progression, epithelial cells can alter their expression of E-cadherin to N-cadherin (see Section 1.2.2.i). N-cadherin on the surface of vascular endothelial cells can bind N-cadherin on the surface of CTCs (Li et al., 2001). Leukocytes can facilitate contact between CTCs and endothelial cells by acting as a linker, for example, both CTCs and endothelial cells express intracellular adhesion molecule (ICAM)-1, whilst leukocytes express their binding ligand lymphocyte function-assisted antigen (LFA)-1 (Strell et al., 2007).

Leukocytes can extravasate via two different methods, either paracellular, where a leukocyte temporarily abrogates endothelial cell-cell binding and passes through a cell-cell junction, or transcellular, where the leukocyte passes through an endothelial cell (reviewed in Engelhardt and Wolburg, 2004). CTCs can also extravate using these two routes (Tremblay et al., 2008). However, CTCs can also extravasate by creating a permeant perforation in the vascular endothelium using reactive oxygen species (ROS) resulting in irreversible damage to the vascular endothelial cells (Offner et al., 1992). Leong et al. (2014) proposed that invadopodia are also crucial for cancer cell extravasation as they facilitate both motility and BM degradation.

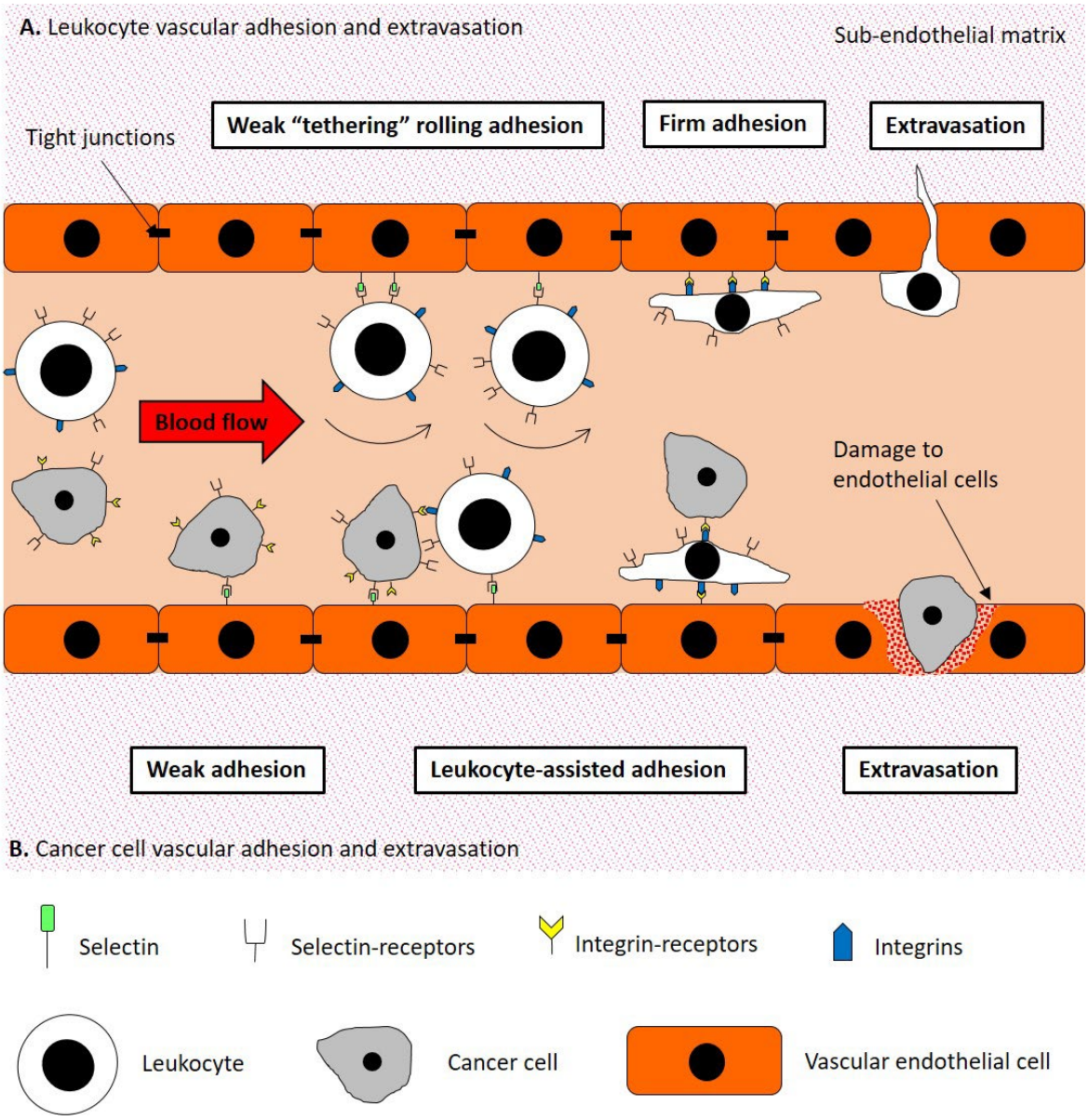

Figure 1.7 *Vascular adhesion and extravasation of A. leukocytes and B. cancer cells. A. Cytokines are released at site of inflammation and leukocytes migrate toward the site along chemokine gradients. Once at site of inflammation, leukocytes are captured on selectins producing weak tethering adhesion. Captured leukocytes are rolled along the vascular endothelium by the force of blood flow until firm adhesion is initiated by integrins. Leukocyte binding encourages endothelial cells to retract for extravasation to occur. B. Cancer cells in the circulation arrest on the vascular endothelium by cancer-associated ligands, and by attaching to leukocytes. Extravasation of cancer cells causes damage to the endothelial cells.*

1.2.6 Development of a secondary tumour

When a cancer cell has achieved extravasation at a secondary site, it is hypothesised that the cell undergoes a reversal of EMT. In a process termed mesenchymal-epithelial transition (MET), it regresses back to an epithelial cell (Yao et al., 2011). If the microenvironment of the secondary site is not suitable, the cancer cell may die immediately (Chambers et al., 2002), or may lie dormant until such conditions as to promote growth arise (Naumov, 2001; Almog, 2010).

1.3 Glycosylation of proteins

More than half of all proteins are glycosylated (Apweiler et al., 1999). Glycosylation is the addition of sugar moieties to proteins and lipids, and is functionally involved in many cell communication, adhesion and identification events (Varki, 1993; Zhao et al., 2008). Human glycans are synthesised from seven monosaccharides, these are: glucose (Glc), mannose (Man), galactose (Gal), N-acetylglucosamine (GlcNAc), N-acetylgalactosamine (GalNAc), fucose (Fuc), and sialic acids (SA) also called neuraminic acids (see Figure 1.8). Highly specific glycosyltransferases catalyse the sequential addition of these monosaccharide subunits to form glycans of varying length and complexity, which are most commonly branched structures, and with either α- or β-linkages between the component monosaccharides, giving rise to extensive structural heterogeneity (reviewed by Rudd and Dwek, 1997). Owing to this, carbohydrate structures have far greater structural diversity than proteins and this can make analysis of oligosaccharides technically challenging (Ghazarian et al., 2011). Unlike polypeptides, oligosaccharides are not direct gene products, instead they are assembled in rapid response to biological requirement (reviewed by Varki, 1993). Oligosaccharides can be either N- or O-linked to polypeptides, which will be discussed below.

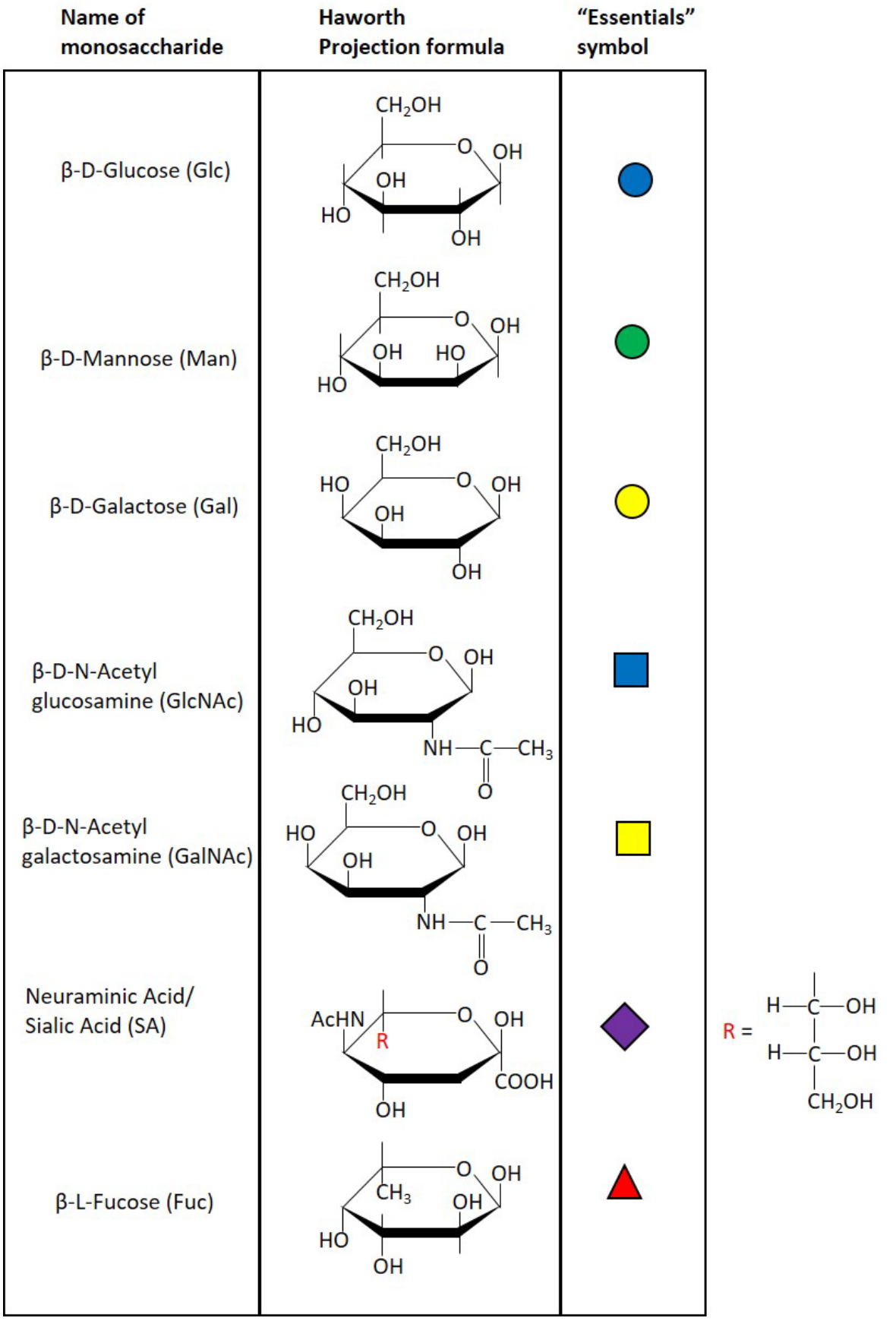

Figure 1.8 *Haworth projection formula and "Essentials" symbol system proposed by Varki et al. (2009) illustrating the seven monosaccharides used to create human glycans.*

1.3.1 N-linked protein glycosylation

N-linked protein glycosylation is reviewed by Brooks et al. (2002), Aebi (2013), Breitling and Aebi (2013) and Shrimal et al. (2015). A protein is N-linked to an oligosaccharide via a GlcNAc monosaccharide in a β-N-glycosidic bond to a nitrogen (hence N-linked) molecule of the amide group of an asparagine (Asn) amino acid of the polypeptide chain (see Figure 1.9). N-linked glycosylation is a co-translational event initiating during protein synthesis. As illustrated in Figure 1.10, for protein synthesis to occur, the gene that encodes the protein is activated and messenger RNA in (mRNA) is created and protein production initiates firstly on ribosomes in the cytoplasm and then, for membrane-bound proteins, the ribosome localises to the rough endoplasmic reticulum (RER). This is achieved through the binding of a signal recognition particle (SRP) on the nascent polypeptide chain to the SRP-receptor on the RER surface. Once the ribosome and the polypeptide chain are synthesising correctly on the ER membrane, the SRP dissociates and is recycled. Protein synthesis continues with the polypeptide chain inserting through a translocation channel in the ER membrane into the lumen of the ER, where N-linked glycosylation begins. N-linked oligosaccharide production continues as the protein is moved from ER to the Golgi apparatus and is concluded when the glycoprotein departs the trans-Golgi network. The enzymes of glycosylation needed for N-linked glycosylation are located throughout the ER and Golgi apparatus secretory pathway in the order in which they act.

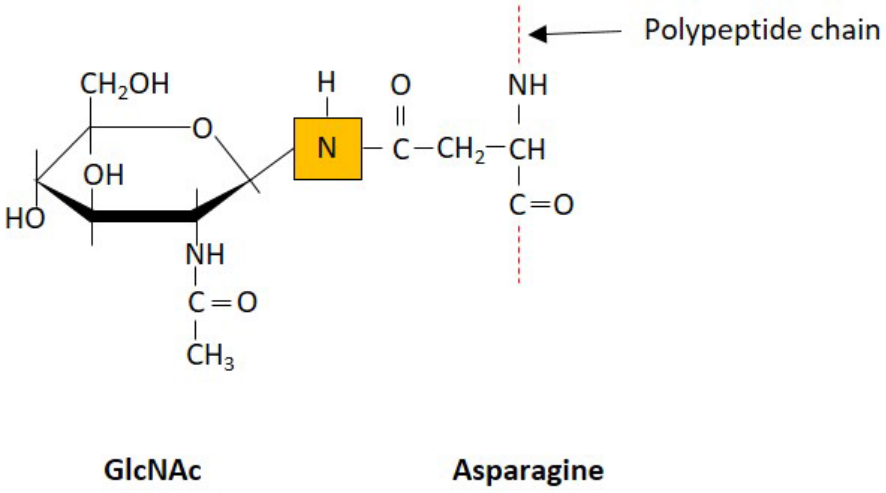

Figure 1.9 *N-linkage. In N-linked glycoproteins, the oligosaccharide is linked via a GlcNAc molecule in a β-N-glycosidic type bond to a nitrogen (orange) of the amide group of an asparagine amino acid residue on the polypeptide chain. Adapted from Brooks et al. (2002).*

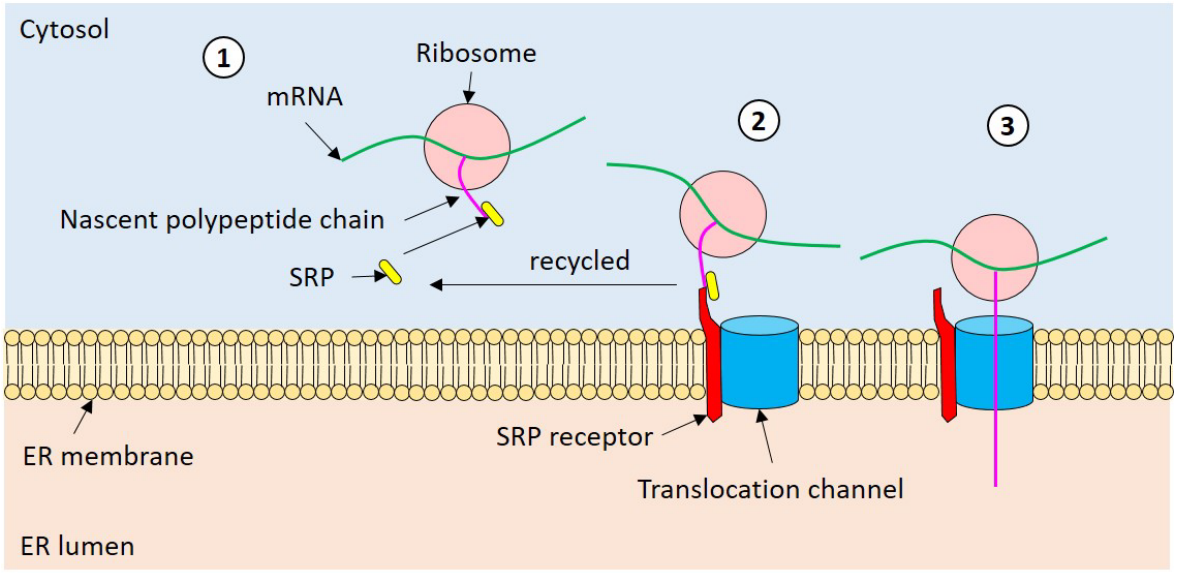

Figure 1.10 *Protein synthesis initiates on ribosomes in the cytoplasm. 1. A signal recognition particle (SRP) binds to the nascent polypeptide chain and 2. localises the ribosome and polypeptide chain to the endoplasmic reticulum (ER) membrane through binding to SRP-receptor. Once the ribosome and polypeptide chain are correctly positioned, the SRP dissociates and is recycled. 3. The nascent polypeptide chain inserts into the ER lumen through a translocation channel in the ER membrane and protein synthesis continues. Adapted from Brooks et al. (2002).*

The nascent polypeptide chain bears a consensus amino acid sequence -Asn-Xaa-Ser/Thr, where Xaa is any amino acid except for proline, and is a prerequisite for N-linked oligosaccharide synthesis. The consensus sequence may occur many times along the polypeptide chain, but not all potential glycosylation sites will be glycosylated. Potential glycosylation sites that are located within a loop or turn in a polypeptide chain are preferentially glycosylated. This is thought to be a function of the accessibility of these areas to glycosylation enzymes.

The initial step of N-linked oligosaccharide biosynthesis is to construct an oligosaccharide intermediate structure linked to a dolichol molecule. The dolichol phosphate (Dol-P) molecule is positioned between the layers of the ER membrane. As illustrated in Figure 1.11, an N-acetylglucosaminylphosphotransferase catalyses the addition of UDP-GlcNAc to Dol-P yielding GlcNAc-P-Dol + UMP. This structure is further extended by the action of an N-acetylglucosaminyltransferase to produce the structure GlcNAc(β1→4)GlcNAc-P-Dol, which is further elaborated by the action of mannosyltransferases I-V, generating $Man_5GlcNAc_2$-P-Dol. All reactions require sugar-donor molecules in the form of GDP-Man and UDP-GlcNAc. Once this structure is constructed in the cytoplasm, it is flipped into the ER lumen by RFT1, where it is further extended to yield the structure $Glc_3Man_9GlcNAc_2$-P-Dol (intermediate structure). The donor molecules for this (Dol-P-Man or Dol-P-Glc) are produced in

the cytoplasm and are flipped into the lumen of the ER. Secondly, the intermediate structure is transferred from Dol-P to a potential glycosylation site on the nascent polypeptide chain (see Figure 1.12). This handover is catalysed by the oligosacchayltransferase (OST) enzyme complex.

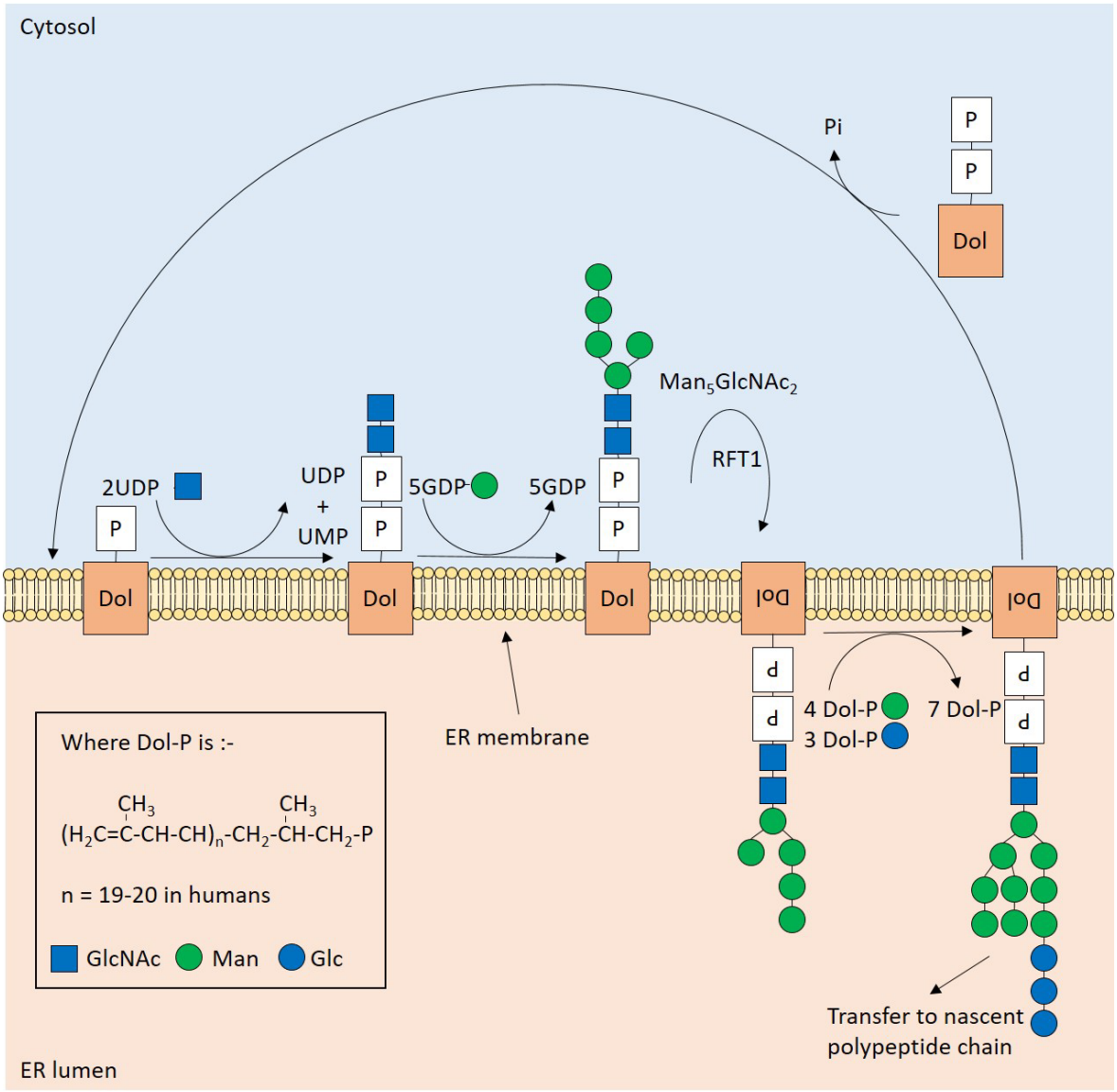

Figure 1.11 *The $Man_5GlcNAc_2$ molecule is constructed in the cytosol external to the ER on a lipid carrier which is embedded in the ER membrane. Once constructed the molecule is "flipped" across the lipid bilayer of the ER membrane so that it protrudes in the ER lumen where a further 4 Man and 3 Glc are added to the molecule yielding $Glc_3Man_9GlcNAc_2$ which is then transferred to the nascent polypeptide chain by OST complex to an asparagine residue. P = phosphate. Adapted from Brooks et al. (2002).*

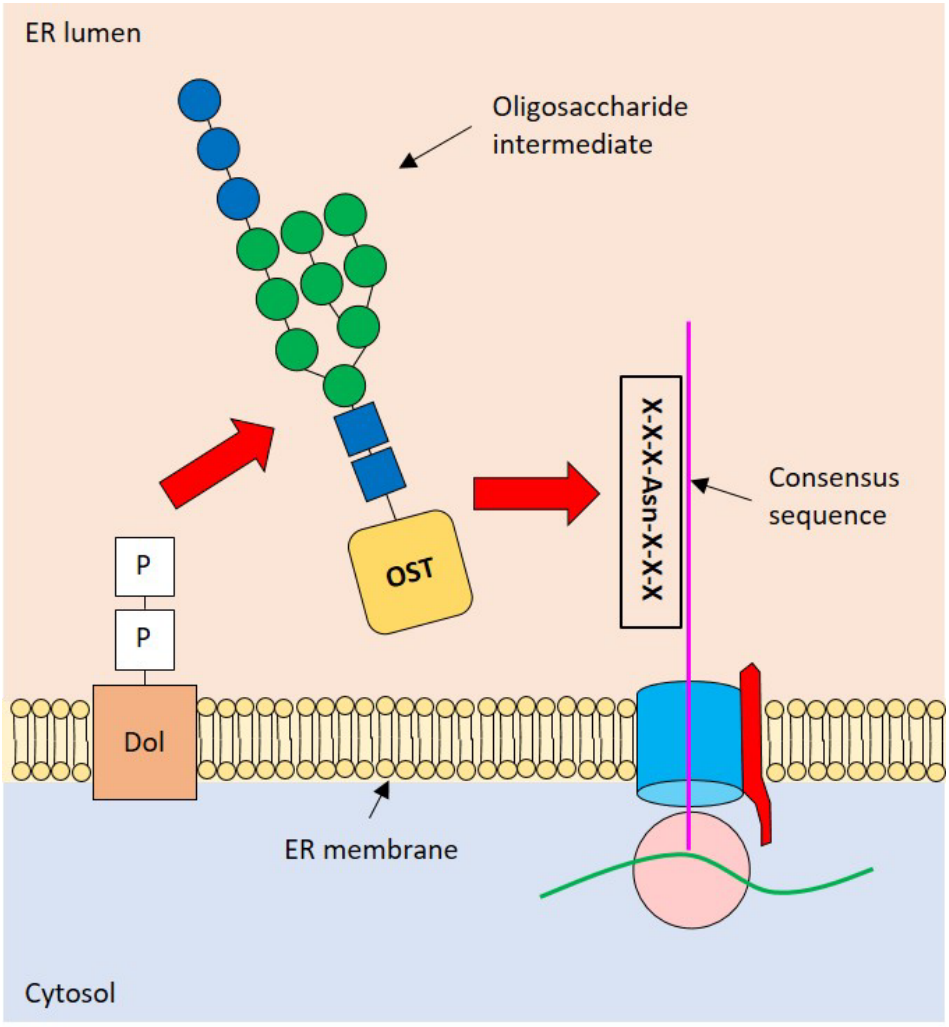

Figure 1.12 *The oligosaccharide intermediate is transferred from the dolichol-phosphate structure to an asparagine (Asn) residue of the consensus sequence on the nascent polypeptide chain by the enzyme complex oligosaccharyltransferase (OST). Adapted from Brooks et al. (2002).*

Once the oligosaccharide intermediate has been transferred to the nascent polypeptide, the structure is sequentially trimmed (see Figure 1.13). The trimming is important for protein folding. Firstly, while OST is still attached, α-glucosidase removes a Glc residue, which aids in the removal of OST from the growing polypeptide chain, yielding the structure $Glc_2Man_9GlcNAc_2$. Then α-glucosidase II removes a further two Glc residues, yielding $Man_9GlcNAc_2$. Finally, a Man residue is removed by α-mannosidase resulting in the structure $Man_8GlcNAc_2$. At this point if the glycoprotein is correctly folded, it leaves the ER and enters the cis-Golgi apparatus.

The Golgi apparatus comprises of the cis, medial and trans cisternae, each of which contain specific glycosidases or glycosyltransferases which either remove or add monosaccharides to yield the final N-linked oligosaccharide structure of the glycoprotein. All N-linked oligosaccharide structures share a

common trimannosyl core as illustrated in Figure 1.14, which comprises of two GlcNAc monosaccharides linked in a β1→4 configuration to which a Man is linked in a β1→4 configuration with two further Man residues linked in α1→3 and α1→6 configurations. The final structure can either be: (1) high mannose type, which have between 5 and 9 mannose residues attached to the inner GlcNAc of the trimannosyl core, (2) complex type which do not have any further Man residues than is in the trimannosyl core, but do have up to 4 oligosaccharide branches, in particular GlcNAc(β1→4)Gal branches, and (3) hybrid type which contain a mixture of both high mannose and complex type features. When the trimmed intermediate structure ($Man_8GlcNAc_2$) is further trimmed by α-mannosidase to yield $Man_5GlcNAc_2$, is not further acted upon by α-mannosidases, it will remain a high-mannose type oligosaccharide. As illustrated in Figure 1.15, the processing pathway for complex N-linked oligosaccharides in the Golgi apparatus starts with the addition of a (β1→4) GlcNAc to the (α1→3) Man branch catalysed by the enzyme GlcNAc-T I. This structure allows α1,3/α1,6 mannosidase to remove Man residues on the outer arm to yield $Man_3GlcNAc_2$, which can be further processed to yield either complex or hybrid type oligosaccharides.

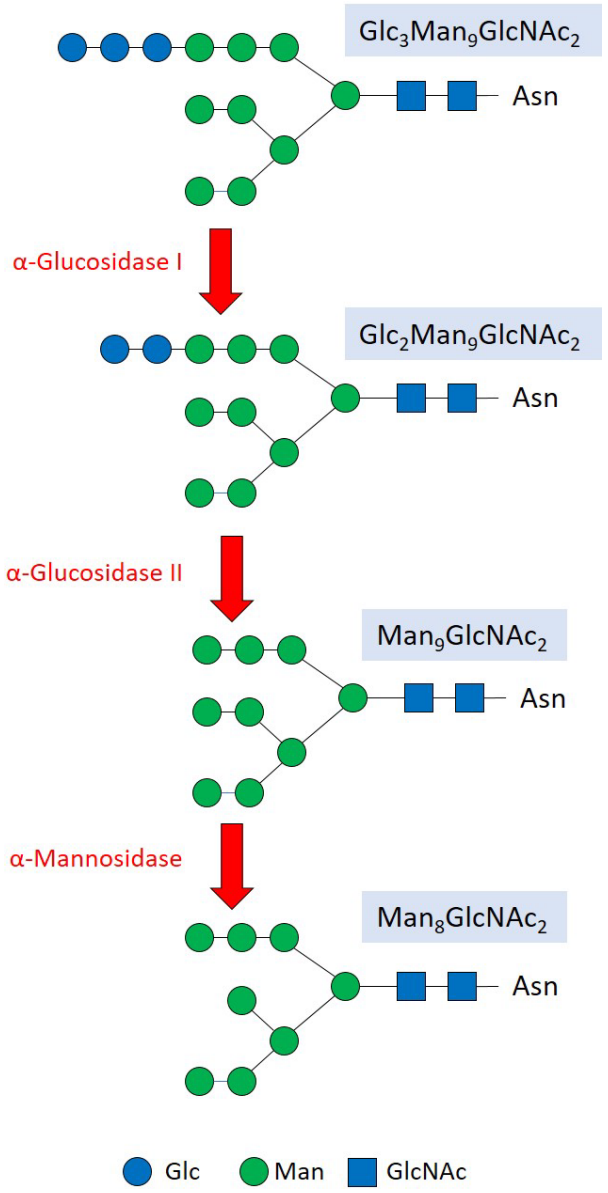

Figure 1.13 *Once the oligosaccharide intermediate ($Glc_3Man_9GlcNAc_2$) has been transferred to an asparagine residue (Asn) on the nascent polypeptide chain, the structure is trimmed. α-glucosidase I removes a glucose (Glc) residue, followed by the removal of two more Glc residues by α-glucosidase II and then a mannose (Man) residue by α-mannosidase. Adapted from Brooks et al. (2002).*

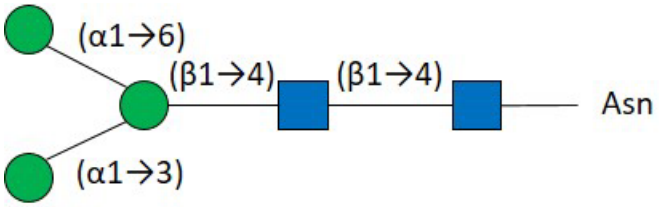

Figure 1.14 *Trimannosyl core comprising of 2 GlcNAc linked in a β1→4 configuration, with a Man linked in a β1→4 configuration with a further 2 Man attached in an α1→6 and an α1→3 configuration. This is the starting point for all N-linked structures. Adapted from Brooks et al. (2002).*

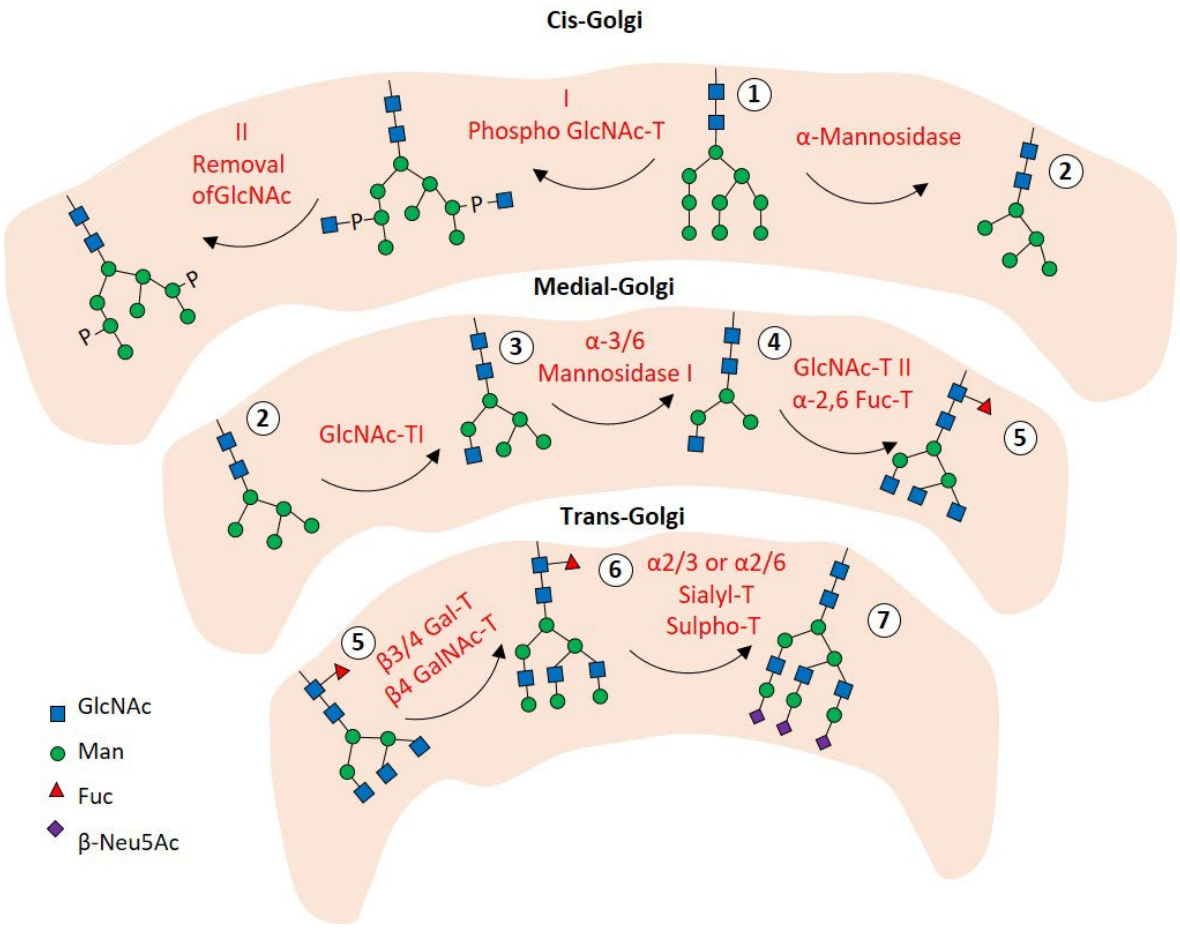

Figure 1.15 *The processing path for N-linked oligosaccharides. After entering the Golgi apparatus (step 1) the N-linked oligosaccharide either becomes a high-mannose type unless the enzyme GlcNAc-T I acts on the oligosaccharide then the structure will become a hybrid or complex type. The enzyme α-mannosidase removes mannose (steps 3-4), followed by the sequential actions of GlcNAc-T II (step 4), β1,3/4 Gal-T (step 5) and/or α2,3/2,6 ST or sulfotransferase (step 7). Steps shown as I or II illustrate the modification of the oligosaccharide by the enzymes phospho-GlcNAc-T and N-acetylglucosaminidase respectively, which is part of the protein degradation pathway. Adapted from Brooks et al. (2002).*

1.3.2 O-GlcNAc linked glycosylation of nuclear and cytosolic proteins

O-linked N-acetylglucosaminylation (O-GlcNAcylation) was discovered just over 30 years ago, by Torres and Hart (1984) when they used a galactosyltransferase isolated from bovine milk as an enzymatic probe for terminal GlcNAc residues on mouse immune cell plasma membrane proteins. O-GlcNAc glycosylation is a reversible post-translational event which unlike, N- and O-linked glycosylation, does not occur within the secretory pathway or extracellular compartment, but has a nucleocytoplasmic subcellular location (Holt and Hart, 1986). This type of glycosylation is not further extended and instead is thought to act as a molecular switch. Many nuclear and cytosolic proteins have been identified as being modified by O-

GlcNAc, including transcription factors, cytoskeletal components, metabolic enzymes, signalling components (reviewed by Wells et al., 2003), and modification of the C-terminal domain of RNA polymerase II (Kelly et al., 1993). O-GlcNAcylation also plays a role in important cellular events such as regulation of the cell cycle (Wang et al., 2010a).

The enzymes responsible for the addition (O-GlcNAc transferase, OGT) (Haltiwanger et al., 1990) and removal (O-GlcNAcase, OGA) (Gao et al., 2001) of O-GlcNAc act dynamically at serine and threonine residues on nuclear and cytoplasmic proteins (Hart et al., 2007). OGT is 110kDa polypeptide with an N-terminal protein-protein domain consisting of tetratricopeptide repeats (TTRs) and a catalytic C-terminal domain that transfers GlcNAc from UDP-GlcNAc to the hydroxyl group of serine or threonine residues in a β-configuration (Haltiwanger et al., 1990). The protein-protein domain has been reported to have several binding partners which may target OGT to specific subcellular locations (Iyer et al., 2003). OGA is a 130kDa polypeptide located preferentially to the cytoplasm and to a lesser extent the nucleus (Wells et al., 2002). All known proteins that are glycosylated by O-GlcNAc can also be phosphorylated, suggesting that dynamic modulation of O-GlcNAcylation is a regulatory modification that is closely linked with phosphorylation (reviewed by Butkinaree et al., 2010). O-GlcNAcylation of cytosolic and nuclear proteins by OGT is modulated by the availability of cell nutrients and in response to cellular stress (reviewed by Zachara and Hart, 2004). Hexosamine biosynthetic pathway (HBP) modulates O-GlcNAcylation, which in turn modulates cell behaviour by regulating cytosolic levels of glucose and other nutrients (reviewed in Zachara and Hart, 2004). As illustrated in Figure 1.16, glucose entering the cell is directed to the HBP where fructose-6-phosphate is converted to glucosamine-6-phosphate by glutamine:fructose-6-phosphate amidotransferase (GFAT). UDP-GlcNAc is generated and used by OGT as a substrate to add GlcNAc to serine or threonine residues of target proteins. O-GlcNAc is removed from O-GlcNAcylated proteins by OGA (Hanover et al., 2010). Not surprisingly, mis-regulation of OGT has been reported to be involved in diseases such as diabetes (Ma and Hart, 2010), neurodegeneration (Lazarus et al., 2009), cardiovascular disease (Laczy et al., 2009) and several different types of cancer (Slawson and Hart, 2011; Fardini et al., 2013) including breast (Slawson et al., 2001), lung, colon (Mi et al., 2011), liver (Zhou et al., 2012) and prostate (Lynch et al., 2012) cancers.

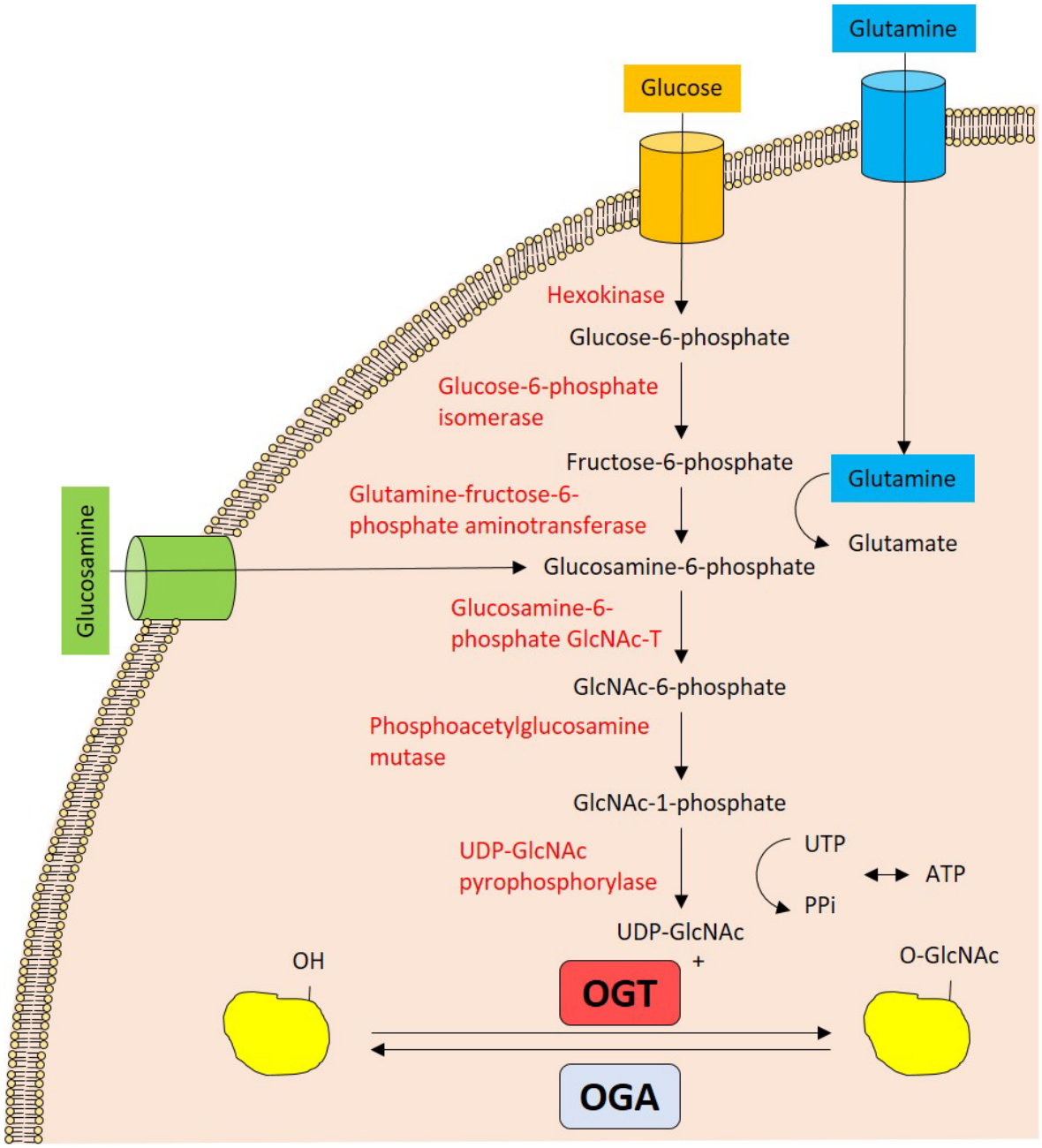

Figure 1.16 *The hexosamine biosynthetic pathway leading to O-GlcNAc cycling. The enzymes involved in the synthesis and use of UDP-GlcNAc from nutrient precursors are shown. Adapted from Hanover et al. (2010).*

1.3.3 O-linked (mucin type) protein glycosylation

Mucin-type O-linked glycosylation, so called as it is commonly found on mucins (a mucopolysaccharide that is the principal component of mucus) is a post-translational event which occurs in the Golgi apparatus once the polypeptide has been formed and folded into its tertiary structure (reviewed by Van der Steen et al., 1998). Initiation of O-linked glycosylation happens in the cis-Golgi whilst elongation and termination occurs in the trans-Golgi (Roth, 1984). As illustrated in Figure 1.17, the most commonly occurring initial structure made in this type of glycosylation is the Thomsen nouvelle (Tn) antigen (α-GalNAc-O-Ser/Thr) where N-acetylgalactosamine (GalNAc) is attached via an α-O-glycosidic bond to an oxygen molecule (hence O-linked) on serine (Ser) or threonine (Thr) residues of a polypeptide (Freire and Osinaga, 2003). This attachment is catalysed by a family of glycosyltransferases called the UDP-GalNAc:polypeptide N-acetylgalactosaminyltransferases (GalNAc-Ts) which are discussed in Section 1.3.4. The simplest finished glycan that can be built on Tn is sialyl-Tn (STn) (NeuAc-α6-GalNAc-α-Ser/Thr), where a sialic acid (SA) monosaccharide is attached in an α-2,6-linkaged to Tn; this reaction is catalysed by the sialyltransferase ST6GalNAc 1 (as illustrated in Figure 1.17 A). Sialyation here, as in the case of other glycan structures, terminates chain extension. Tn is always further elaborated in normal adult tissues and therefore not ordinarily present. STn is only weakly detectable in foetal and normal adult tissue (Yonezawa et al., 1992). Both, however, are frequently detected in cancers (Ju et al., 2008a; Julien et al., 2012). Typically, Tn is elaborated to form 7 core structures (see Figure 1.19). The most commonly occurring of which is core 1, also called the Thomsen–Friedenreich (TF or T) antigen, (Galβ1-3GalNAcα-O-Ser/Thr), where a Gal monosaccharide is attached through a β1-3 linkage to the GalNAc of Tn by the glycosyltransferase core 1 β1,3Gal-T. In humans, this requires the molecular chaperone, Cosmc (C1GALT1L1) (Ju and Cummings, 2002) which is located in the ER (Ju et al., 2008a). TF antigen is frequently detectable in cancers (Campbell et al., 1995). TF can be terminated with SA to yield STF as illustrated in Figure 1.18 B. TF can also be further extended to yield core 2 by the addition of a GlcNAc monosaccharide in a β1-6 linkage to GalNAc. This reaction is catalysed by the glycosyltransferase core 2 β1,6GlcNAc-T.

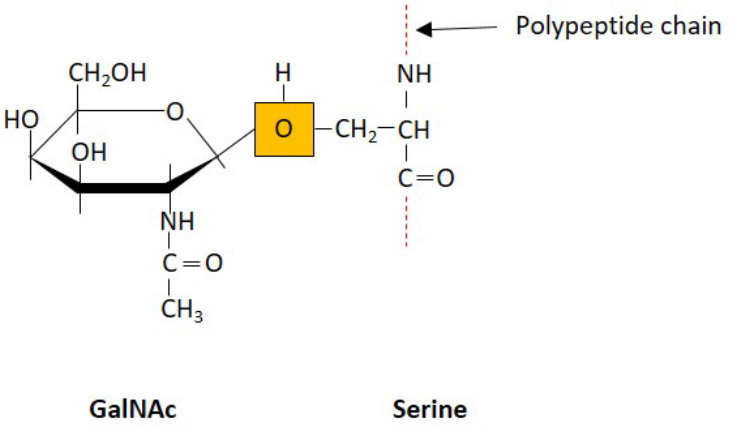

Figure 1.17 *O-linkage. In O-linked glycoproteins, the oligosaccharide is linked via a GalNAc molecule in a α-O-glycosidic type bond to an oxygen (orange) of a serine or threonine amino acid residue on the polypeptide chain. Adapted from Brooks et al. (2002).*

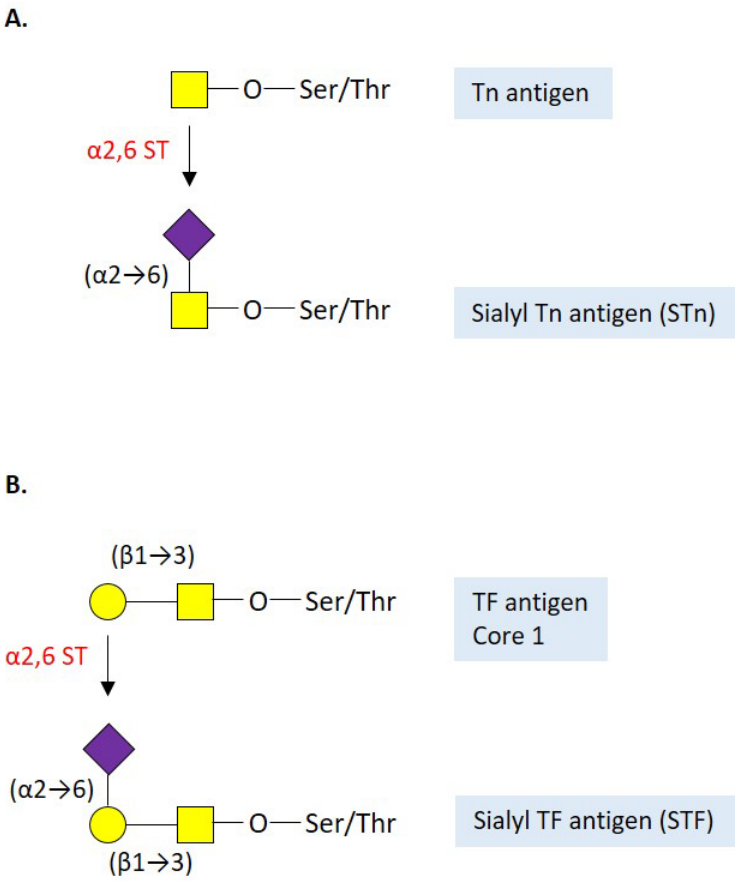

Figure 1.18 *Elaboration of Tn antigen and TF antigen (core 1). A. The Thomsen nouvelle (Tn) antigen GalNAcα→1Ser/Thr can be terminated by adding a β-D-Neu5Ac to yield sialyl Tn (STn), NeuAc(α2→6)GalNAcα1→Ser/Thr. B. The Thomsen Friedenreich (TF or T) antigen or core 1, Gal(β1→3)GalNAcα1→Ser/Thr can be terminated by adding a β-D-Neu5Ac to yield sialyl TF antigen NeuAc(α2→6)Gal(β1→3)GalNAcα1→Ser/Thr.*

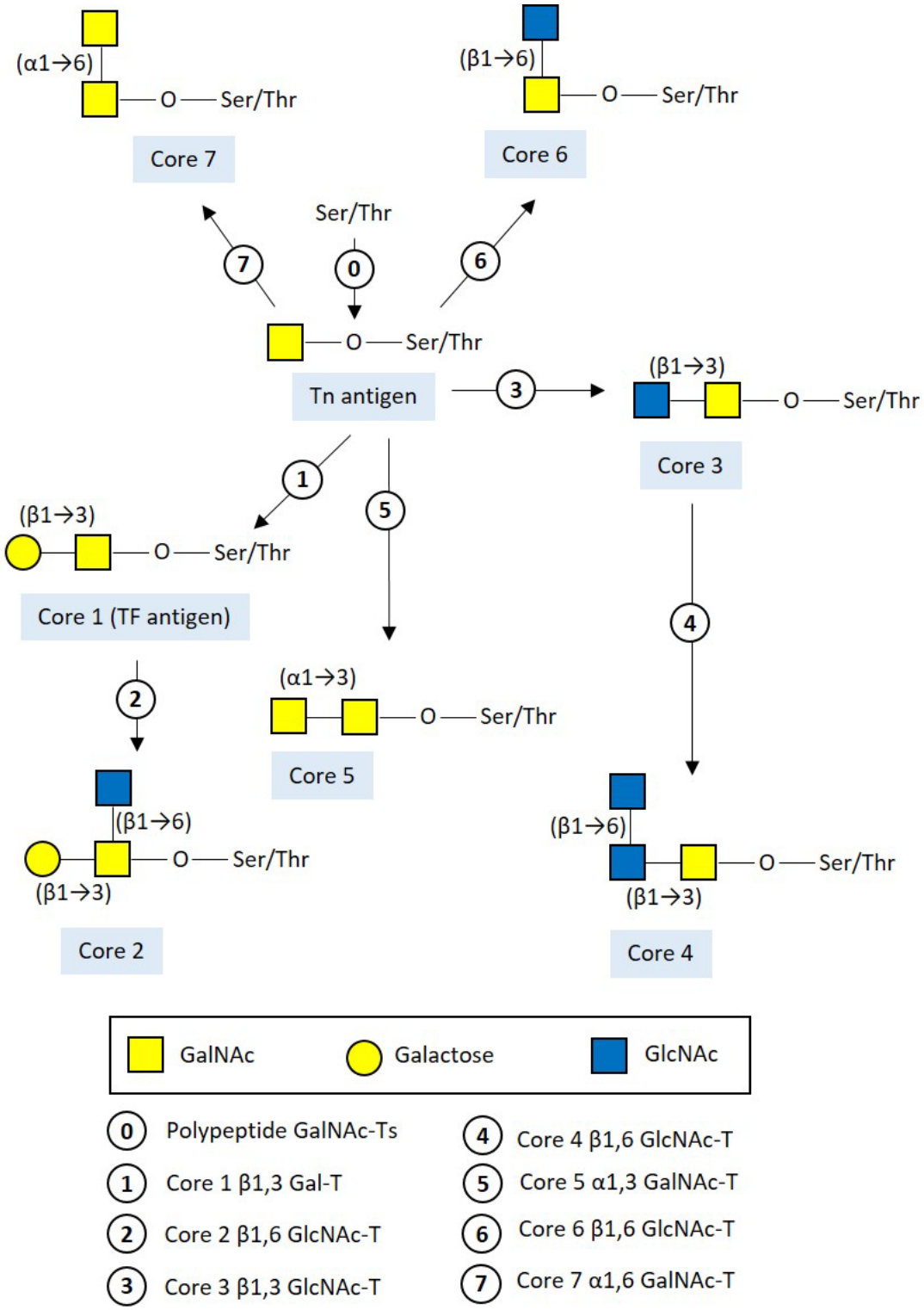

Figure 1.19 *Synthesis of O-linked core structures 1-7. Enzymes responsible for catalysing the addition of monosaccharides are detailed. Adapted from Brooks et al. (2002).*

Core 3 GlcNAc(β1→3)GalNAc→Ser/Thr is synthesised by the addition of a GlcNAc monosaccharide to Tn in a β1-3 linkage by β1,3 GlcNAc-T and can be further extended by the addition of a further GlcNAc in a β1-6 linkage catalysed by β1-6 GlcNAc-T to yield core 4 GlcNAc(β1→6)[GlcNAc(β1→3)]GalNAcα-Ser/Thr. The most commonly occurring O-linked core structures are 1-4, however other less common structures have been described. These include, Core 5 GalNAc(α1→3)GalNAcα-Ser/Thr, which is Tn with an α1-3 linked GalNAc monosaccharide and is catalysed by α1,3 GalNAc-T. Tn with the addition of a GlcNAc monosaccharide in a β1-6 linkage by β1,6 GlcNAc-T yields core 6 GlcNAc(β1→6)GalNAcα-Ser/Thr. Core 7 GalNAc(α1→6)GalNAcα-Ser/Thr is Tn with the addition of GalNAc in an α1-6 link by α1,6 GalNAc-T. Core 8 Gal(α1→3)GalNAcα-Ser/Thr is synthesised by the addition of a Gal monosaccharide in an α1-3 linkage to Tn, catalysed by the α1,3 Gal-T. The enzymes which catalyse the formation of the core structures are highly regulated and are only expressed in specific cells or tissues. Core structures that terminate in GlcNAc monosaccharide can be extended by either type 1 chain (Gal with a β1-3 linkage) or type 2 chain (Gal with β1-4 linkage) as illustrated in Figure 1.20 A. Core structures which terminate in a Gal monosaccharide can be elongated by the addition of GlcNAc to yield a range of structures as illustrated in Figure 1.20 B. Both type 1 and type 2 chains can be terminated by the addition of either a Fuc or SA monosaccharide (as illustrated in Figure 1.21) to yield a number of different structures.

O-glycan synthesis is thought to be regulated by a number of influencing factors such as, the levels of expression of glycosyltransferases, availability of nucleotide sugar donors and acceptor substrates as well as subcellular organisation, activity and specificity of the glycosyltransferases. Competition between the glycosyltransferases for the available substrates is another means of regulation of O-glycan synthesis. For example, as illustrated in Figure 1.22 Tn has three glycosyltransferases competing for it and core 1 has five.

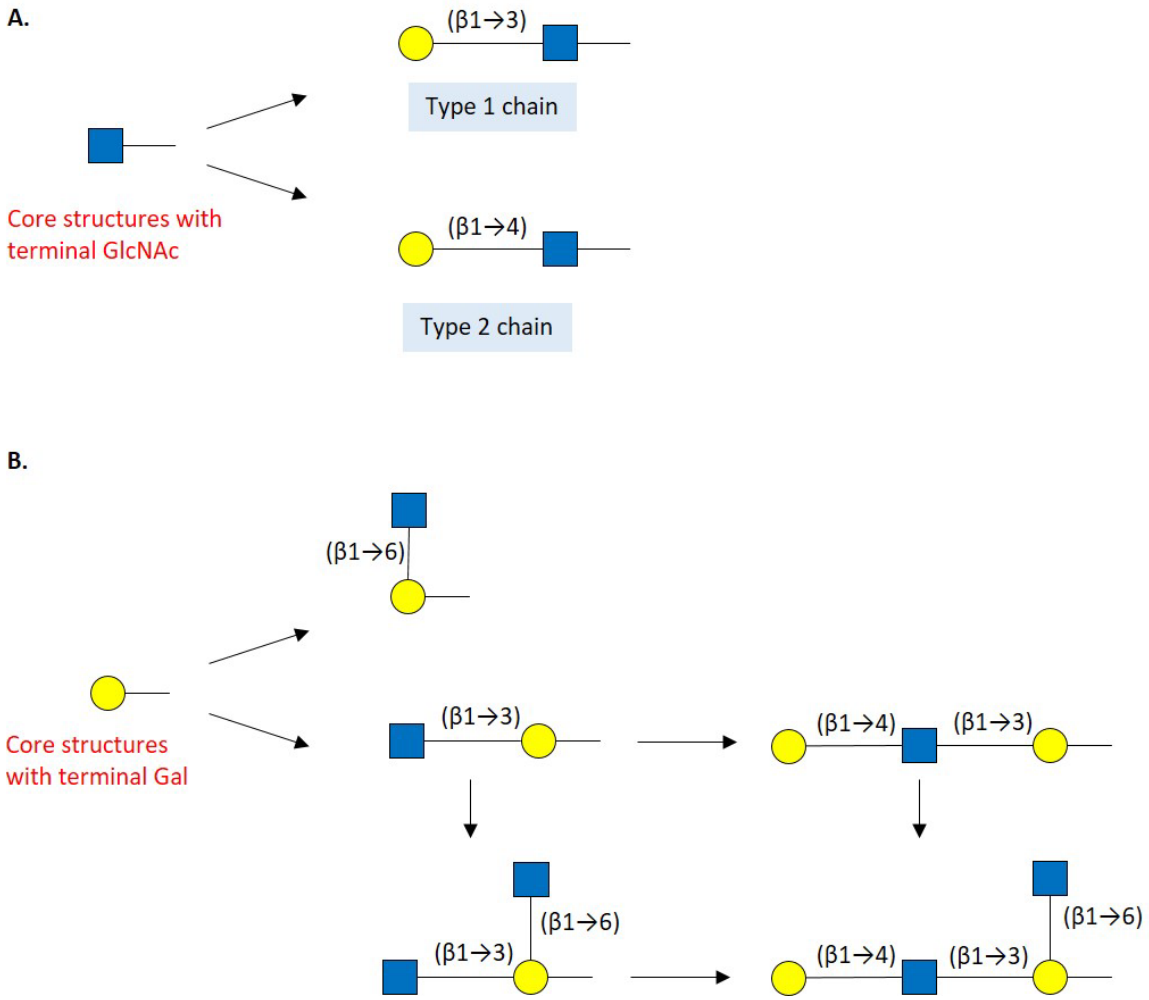

Figure 1.20 *Elongation pathways of core structures ending in either GlcNAc or Gal. A. Core structures that terminate in GlcNAc can be extended by the addition of a Gal monosaccharide in either a β1→3 configuration yielding a type 1 chain or in a β1→4 orientation yielding a type 2 chain. B. Core structures which terminate in Gal can be further extended by the monosaccharide GlcNAc to yield a variety of structures.*

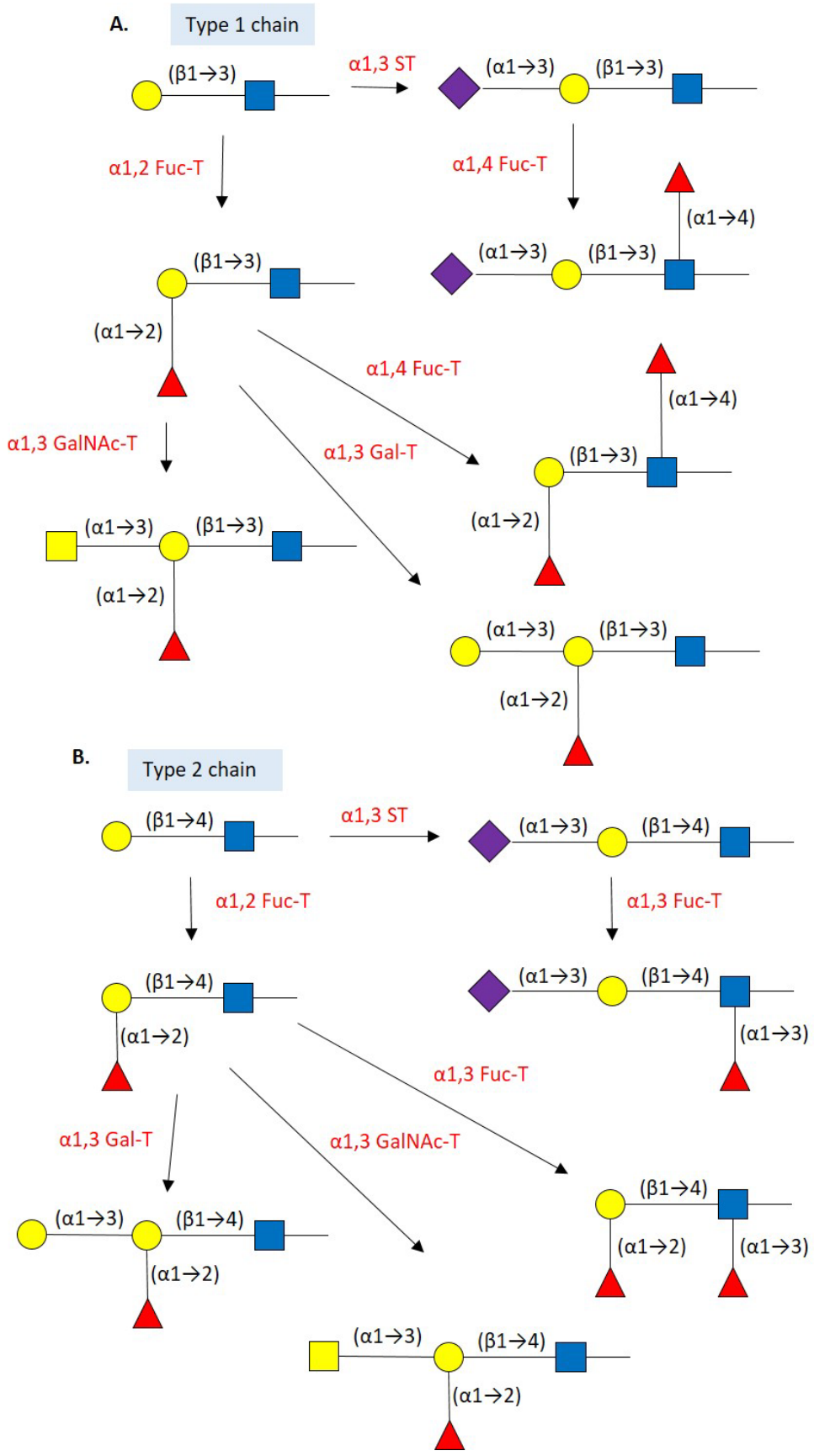

Figure 1.21 *Termination of type 1 (A) and type 2 (B) chains with either fucosylation or sialylation. Adapted from Brooks et al. (2002).*

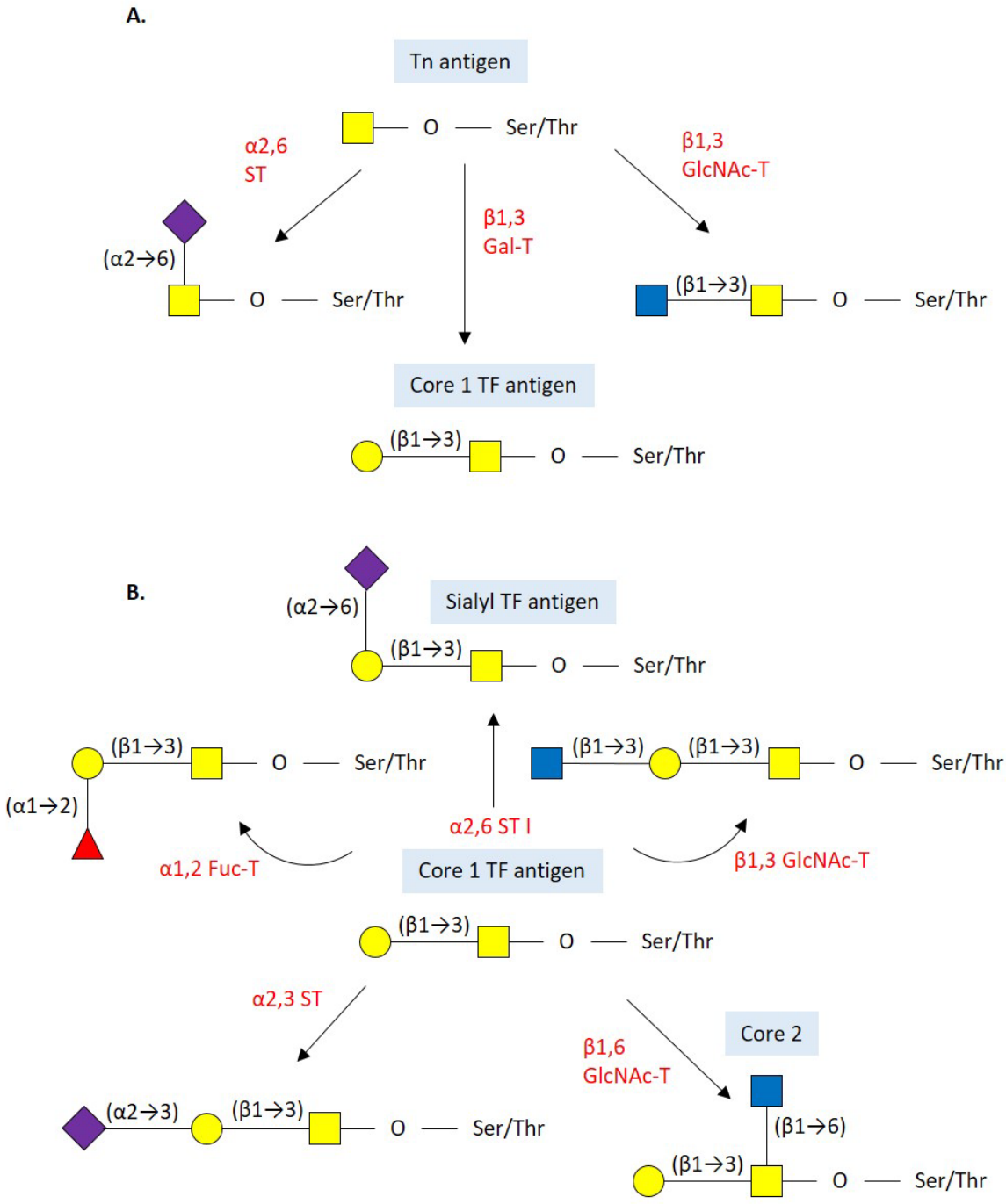

Figure 1.22 *O-glycan synthesis is thought to be in part regulated by the availability, activity and specificity of glycosyltransferases which compete for available substrates. A. Three glycosyltransferase compete for Tn antigen. B. Five glycosyltransferases compete for core 1.*

1.3.4 GALNTs

A family of 20 isoenzymes, UDP-N-α-D-galactosamine:polypeptide N-acetylgalactosaminyltransferases (GALNTs) catalyse the addition of the first N-acetylgalactosamine (GalNAc) monosaccharide to serine (Ser) or threonine (Thr) residues of polypeptides at the initiation of O-linked glycosylation (see Table 1.1 for an overview of the enzyme nomenclature and gene location). It is thought that all of the GALNT gene family, except for GALNT4, arose from an ancestral GALNT gene and throughout evolution various paralogs formed. Figure 1.23 illustrates the proposed phylogenetic tree for the GALNT gene family based upon subfamily clusters (reviewed by Bennett et al., 2012). GALNTs are designated GALNT1 to –T20 in accordance with when they were described. GALNTs are located throughout the Golgi apparatus (Röttger et al., 1998). All of the GALNTs except for GALNT20 share a type II membrane structure composed of a short N-terminal cytoplasmic tail (Smith and Lupashin, 2008), a hydrophobic membrane spanning domain, a stem region (90 amino acids, GALNT1, GALNT13, GALNT16, 170 amino acids GALNT3, GALNT8, GALNT15 and 470 amino acids GALNT5) (Bennett et al., 2012), a luminal catalytic domain (~230 amino acids long) (Paulson and Colley, 1989) and, unique to the GALNTs, a C-terminal ricin-like lectin domain (~120 amino acids in length) which has a binding specificity for α-GalNAc monosaccharides (Hazes, 1996; Imberty et al., 1997). This common structure is illustrated in Figure 1.24. GALNT10 has an additional binding-pocket in its catalytic domain (Kubota et al., 2006). GALNT20 does not have the lectin domain but does share the other structural components of this family (Bennett et al., 2012).

Why so many GALNTs are required for initiation of O-glycosylation is not understood. However GALNTs show different, albeit partly overlapping, substrate specificities and catalytic activities, as well as being expressed in a tissue-specific manner. Some GALNTs will only glycosylate proteins which have already had GalNAc added (Bennett et al., 2012). GALNT1 and -T2 are ubiquitously expressed in all human tissues and are thought to be housekeeping enzymes (Homa et al., 1993; White et al., 1995), whilst GALNT4 (Bennett et al., 1998), -T5, -T7 (Bennett et al., 1999a), -T8 (White et al., 2000), -T10 (Cheng et al., 2002), -T14 (Wang et al., 2003), -T15 (Cheng et al., 2004) and –T18 (Raman et al., 2012) are widely expressed but are not considered to be housekeeping enzymes. Expression of the remaining GALNTs are highly regulated (Hang and Bertozzi, 2005) and they have only been detected in specific locations. For example, -T3 in pancreas and testis (Bennet et al., 1996), -T6 in placenta and trachea (Bennett et al., 1999b), -T9 in brain and the spinal cord (Toba et al., 2000), -T11 in kidneys (Schwientek et al., 2002), -T12 in digestive organs (Guo et al., 2002), -T13 in neurons (Zhang et al., 2003b), -T16 in heart (Peng et al., 2010), -T17 in brain and testis (Raman et al., 2012), -T19 in cerebellum and cerebral cortex (Nakamura et al., 2005) and -T20 in testis (Raman et al, 2012).

Li et al. (2012) reported a sub-family within the GALNTs designated the Y subfamily genes, which are only expressed in vertebrates. These are GALNT8, -T9, -T17 and -T18, which all share a mutation in the

catalytic domain from YDX_5WGGENXE to LDX_5YGGENXE. The remaining 16 GALNTs are termed the W subfamily. This mutation observed in the Y subfamily affects the catalytic activity of the GALNT allowing the Y subfamily to act as molecular chaperones to the W subfamily which accords with another level of regulation of O-glycosylation (Li et al., 2012). Altered levels of expression of GALNTs has been reported in a number of cancers including; colorectal (Kohsaki et al., 2000; Shibao et al., 2002; Guo et al., 2004; Koyanagi et al., 2008 Guda et al., 2009; Gray-McGuire et al., 2010; Abuli et al., 2011; Clarke et al., 2012), gastric (Onitsuka et al., 2003; Gao et al., 2013), breast (Cavallo et al., 2005; Berois et al., 2006a; Freire et al., 2006; Patani et al., 2008; Wu et al., 2010), neuroblastoma (Berois et al., 2006b; Berois et al., 2013), pancreatic (Li et al., 2011), gallbladder (Miyahara et al., 2004), prostate (Landers et al., 2005), bladder (Ding et al., 2012a), lung adenocarcinoma (Gu et al., 2004), oesophageal cancer (Ishikawa et al., 2005) and lymphoma (Gibson et al., 2012). Furthermore, dysregulation of GALNTs in a number of epithelial cancers has been shown to be important at different stages of the metastatic cascade, as reviewed by Beaman and Brooks (2014) (see Appendix 3).

Table 1.1 *Members of the human GALNT family, which add the first GalNAc monosaccharide in O-linked glycosylation. Taken from Beaman and Brooks (2014).*

GALNT	Alternative names	Accession number (human)	Chromosome locus	Reference (human)
1		X85018	18q12.1	White et al., 1995
2		X85019	1q41-q42	White et al., 1995
3		X92689	2q24-q31	Bennett et al., 1996
4	POC1B	Y08564	12q21.33	Bennett et al., 1998
5		AJ245539	2q24.1	Bennett et al., 1999b
6		Y08565	12q13	Bennett et al., 1999a
7		AJ002744	4q34.1	Bennett et al., 1999b
8		AJ271385	12p13.3	White et al., 2000
9		AB040672	12q24.33	Toba et al., 2000
10		AJ505950	5q33.2	Cheng et al., 2002
11		Y12434	7q36.1	Schwientek et al., 2002
12		AJ32365	9q22.33	Guo et al., 2002
13		AJ505991	2q24.1	Zhang et al., 2003b
14	FLJ12691	Y09324	2q23.1	Wang et al., 2003
15	GALNTL2, GALNT13, GALNT7, PIH5	NM_054110	3q25.1	Cheng et al., 2004
16	GLANTL1, KIAA1130	AJ505951	14q24.1	Peng et al., 2010
17	GALNTL6, GALNT20	AJ626725	4q34.1	Raman et al., 2011
18	GALNTL4, GALNT15, MGC71806	AJ626724	11p15.3	Raman et al., 2011
19	GALNTL3, GALNT16, GALNT20, WBSCR17	AJ626726	7q11.23	Nakamura et al., 2005
20	GALNTL5, GALNT15, WBSCR17	NM_145292	7p36.1	Raman et al., 2011

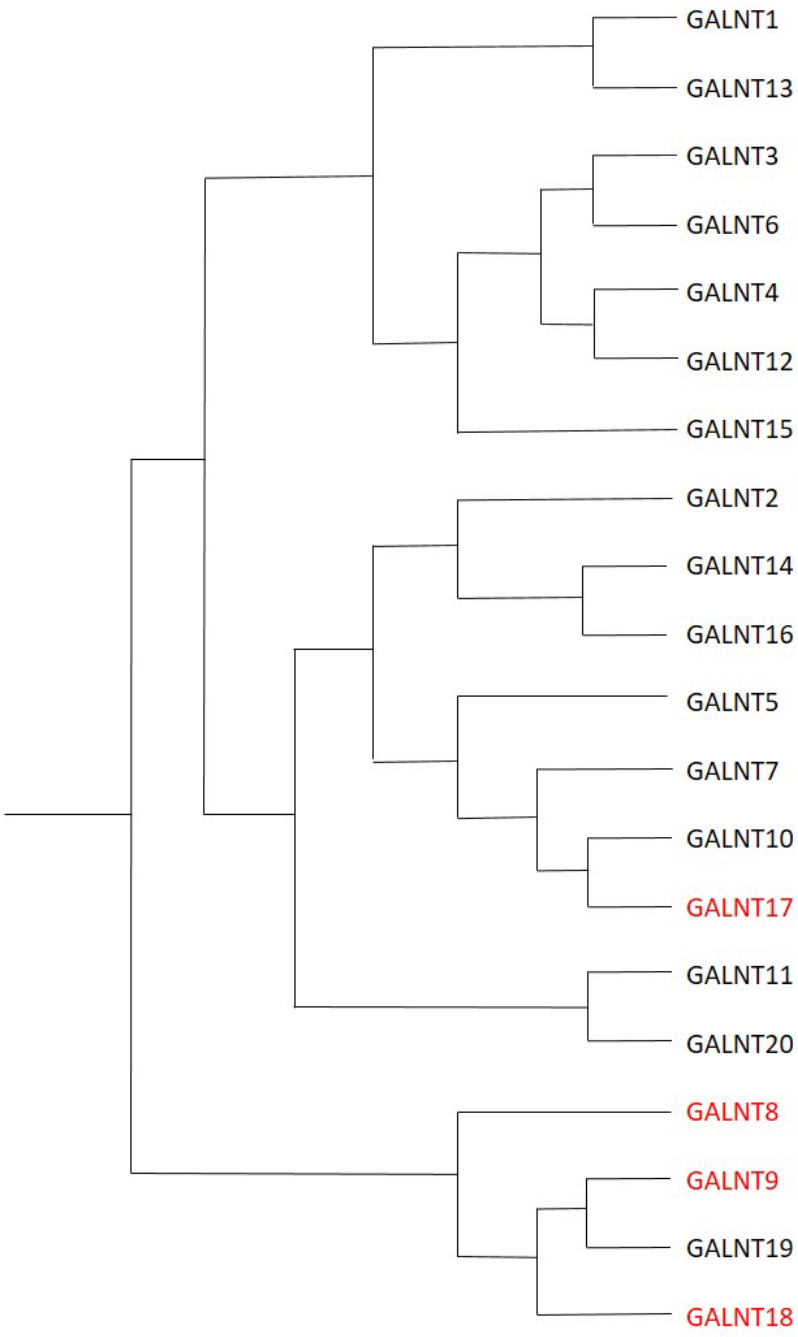

Figure 1.23 *Phylogenetic tree depicting the evolutionary divergence of the GALNT family from the hypothesised ancestral GALNT gene. GALNTs highlighted in red are termed sub-family Y and act as chaperones for the other GALNT family members. Adapted from Bennett et al. (2012).*

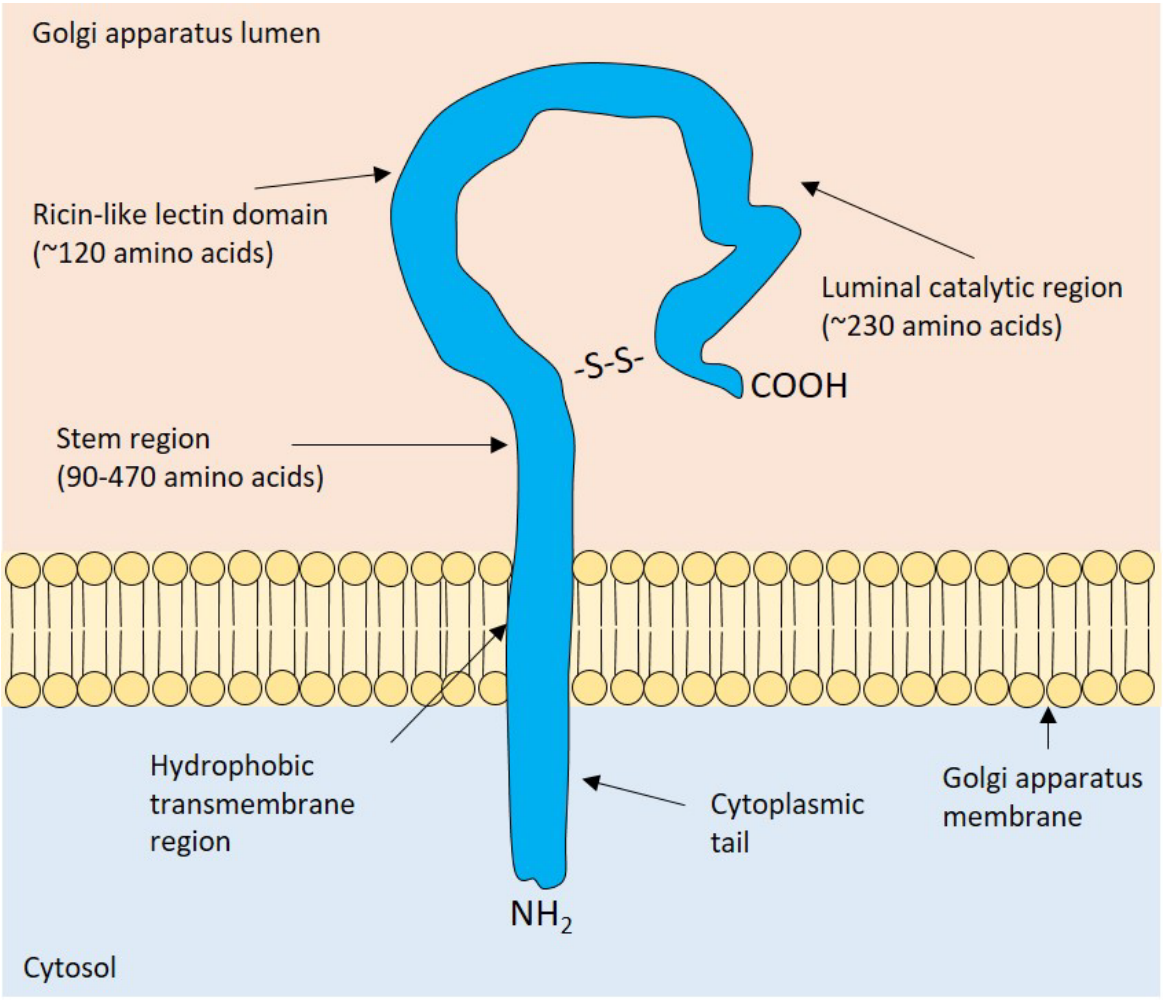

Figure 1.24 *Schematic representation of the shared type II membrane structure of the GALNTs, located in the Golgi apparatus. The luminal portion consists of a catalytic domain, a ricin-like lectin domain and a variable length stem region. They are held in place by a hydrophobic transmembrane domain followed by a short N-terminal tail. Adapted from Beaman and Brooks (2014).*

1.4 HPA as a prognostic marker of aggressive cancer

Leathem and Brooks (1987) first reported a lectin a "protein or glycoprotein of non-immune origin, not an enzyme, that binds to carbohydrates and agglutinates cells" (Goldstein et al., 1980) from the albumin gland of the Roman snail, *Helix pomatia* agglutinin (HPA), to be useful as an analytical tool for predicting aggressive biological behaviour, metastasis and poor patient prognosis in breast cancer. In the 25-year retrospective study, paraffin blocks of 179 primary cancers were labelled for HPA using an immunoperoxidase method. Labelling was recorded and compared with clinical progress, including disease free survival and time until death. It was found that there were significant differences between the groups with and without altered glycosylation as detected by HPA-labelling for time to first

recurrence and survival time, determined using Kaplan-Meier life-tables. Survival at 5-years post-diagnosis was 90% for patients with tumours without altered glycosylation as detected by HPA-labelling and only 40% for patients whose tumours had the altered glycosylation. At 10-years post-diagnosis, the respective percentages were 75% and 35%. Later, in an extension of the previous retrospective study, Brooks and Leathem (1991) reported that there was a significant difference in survival rates between patients with HPA-positive (293 patients) and HPA-negative (80 patients) tumours (p=<0.00001). At 5-years post-diagnosis, 85% of patients with HPA-positive tumours were alive, whilst only 55% of patients with HPA-negative tumours were alive. At 10-years post-diagnosis the respective figures were 65% and 30%. Brooks and Leathem (1991) also reported that there was a significant association between axillary lymph node (LN) metastases and HPA binding to the cells of the primary tumour.

In assessment of cancer stage, LN spread is the "gold standard" of prognostic markers, as it is a physical indication that a tumour has the ability to migrate and establish away from its primary site. The study used 373 primary breast cancers, which were labelled for HPA-binding. Labelling was recorded alongside lymph node involvement, tumour size, S-phase fraction, histological grade and patient age at diagnosis. Variables were cross-examined using a proportional hazards regression (Cox model), which explored the relationship between survival time/time to first relapse and other possible prognostic factors. Initially, a univariate analysis was used to assess the independent prognostic importance of each variable, then a forward step-wise process was used where a variable was added to the regression equation at a time to assess the variables "goodness of fit" in the model. Of the 373 samples, 79% were reported to label positively with HPA, of these 68% had lymph node involvement, whilst 90% of the HPA-negatively labelled samples were lymph node negative. Therefore, indicating a strong association between HPA staining and lymph node involvement, which was confirmed in the regression model. The association of HPA-binding and poor patient prognosis were subsequently confirmed in breast cancer by Fenlon et al. (1987), Fukutomi et al. (1989), Alam et al. (1990), Fukutomi et al. (1991), Thomas et al. (1993), Noguchi et al. (1993a), Brooks et al. (1993), Brooks et al. (1996) and Brooks and Wilkison (2003). This correlation was also reported in other cancers including those of prostate (Shiraishi et al., 1992), colorectum (Ikeda et al., 1994; Schumacher et al., 1994a; Schumacher et al., 1994b), stomach (Kakeji et al., 1991; Kakeji et al., 1994), oesophagus (Yoshida et al., 1993; Takahashi et al., 1994), bladder (Langkilde et al., 1992), lung (Kawai et al., 1991) and thyroid (Parameswaran et al., 2011). HPA therefore identifies a biological marker associated with metastasis and aggressive biological behaviour in breast and other cancers.

HPA is a constituent of perivitelline fluid, which, acting as part of the innate immune system, protects the fertilised egg of the snail from bacteria (Sanchez et al., 2006). HPA is a hexamer with a total molecular mass of 79kDa and has 6 carbohydrate binding sites (Sanchez et al., 2006). Markiv et al. (2010) revealed that the native HPA has two forms, HPAI and HPAII, which share a sequence identity of 45% and are

consistent with GalNAc-binding lectins of the H-type, therefore demonstrating the heterogeneity of the native lectin.

Lectins bind with carbohydrates non-covalently and usually reversibly in a highly specific manner (Ambrosi et al., 2005). The binding specificity of a lectin is usually quoted as the monosaccharide or more complex sugar that most effectively inhibits binding to its naturally occurring ligand. HPA has a nominal monosaccharide binding specificity for GalNAcα1,3GalNAc > α-GalNAc > α-GlcNAc » α-Gal (Goldstein and Poretz, 1986). HPA also has a binding specificity to the following glycoforms: the tumour associated Tn antigen (GalNAcα1-3-O-Ser/Thr) (Springer 1989; Ju et al., 2011), Cad antigen (NeuAcα2-3(GalNAcβ1-R) (Piller et al., 1990), Forssman antigen (GalNAcα1-3-GalNAc) (Baker et al., 1983; Lescar et al., 2007), blood group A substance (GalNAcα1-3Galβ1-4GlcNAcβ1-Fucα1-2) (Mourali et al., 1980; Matsui et al., 2001) GlcNAc (Wu and Suggi, 1991; Rambaruth et al., 2012) and sialic acid (Dwek et al., 2001). Brooks et al. (1994) reported that the prognostic significance of HPA binding in cancers is through recognition of a heterogeneous range of glycoproteins glycosylated by GalNAc-glycans including, but not exclusively, Tn. In this study, an anti-blood group A monoclonal antibody and an anti-Tn monoclonal antibody were used alongside HPA in immune- and lectin histochemistry of paraffin wax-embedded sections from 87 primary breast cancers. There were distinct differences in labelling distribution between the antibodies and HPA. Labelling for Tn was limited in distribution, whilst HPA had the broadest labelling profile. Interestingly, many samples that did not label for the presence of Tn, did label for α-GalNAc glycoproteins detectable by HPA, therefore demonstrating that HPA binds a wider range of GalNAc-glycans. These results were confirmed with use of SDS-PAGE and western blotting. These findings were confirmed by Mitchell et al. (1995).

Recently, there have been reports that HPA also recognises an array of glycosylated cancer-associated glycoproteins involved in cell migration and signalling, which further underpins HPA's importance as a tool for identifying metastatic cancers. A study by Fry et al. (2013) identified cadherin-5 from HPA-binding breast cancer serum proteins to be associated with recurrent disease with a specificity of 90%. This was later confirmed by Fry et al. (2016) in a breast cancer study and revealed that the ratio of cadherin-5 and HPA binding significantly ($p=0.007$) distinguished patients with metastatic disease compared to cadherin-5-binding alone ($p=0.028$), in patients with oestrogen receptor positive tumours and vascular invasion. In a proteomic study of colorectal cancer cells HPA-binding partners were found to include a number of cell-signalling and cell migration glycoproteins including integrin alphav/alpha6 and annexin A2/A4 complexed with cytoskeletal components (microfilament proteins alpha and beta tubulin, actin and cytokeratin 8 and 18), as well as HSP90, TRAP-1 and tumour rejection factor 1 (Saint-Guirons et al., 2007). Peiris et al. (2015) demonstrated in colon cancer cells that there is a significant association between the labelling score of annexin-4 and HPA ($p=0.0002$) and time until recurrence, than annexin-4 ($p=0.0007$) or HPA ($p=0.0026$) independently. Rambaruth et al. (2012) used a breast cancer

cell model to demonstrate that HPA-binding correlated with levels of HnRNPH1, HnRNPD-like, HnRNPA2/B1 as well as Hsp27 and ENO1, which were not observed in HPA-negatively labelled non-metastatic breast cancer cell lines. Furthermore, binding of HPA to HnRNPs, Hsp27 and ENO1 demonstrated that HPA-binding recognises O-GlcNAcylated transcription factors (Rambaruth et al., 2012). Additionally, the Functional Glycomics Gateway glycan-array analysis suggests numerous binding epitopes for HPA (Consortium for Functional Glycomics).

Brooks et al. (2001) reported on several human breast cancer cell lines which consistently synthesise a range of HPA binding glycoproteins identical to those observed in clinical tumours, therefore validating the use of these cell lines for work to carried out with HPA binding *in vitro*. In this study, 7 breast cancer cell lines were chosen to represent a range of phenotypes from normal breast epithelium (HMT3522), primary breast cancer (BT474, MDA MB 435) to malignant and metastatic (MDA MB 468, ZR751) and highly tumorigenic/metastatic (MCF7, DU 4475). These were labelled for binding with HPA. HPA binding was almost undetectable in the normal breast cell line (HMT3522), weak in cells derived from primary breast cancer (BT474) and strong in the highly tumorigenic and metastatic cell lines. HPA binding was further studied using flow cytometry and confocal microscopy, and these approaches also demonstrated that cells derived from primary breast cancer label weakly for HPA, whilst highly tumourigenic and metastatic cell lines label strongly for HPA. Analysis of HPA-binding glycoproteins of both the tumour samples and the breast cancer cell lines, was further investigated using SDS-PAGE and HPA lectin blotting, which revealed 11 major glycoprotein bands, between 20 to 200 kDa, shared between the tumour samples and the cell lines. The number of bands observed per tumour sample or cell line concurred with their HPA binding profile. For example, there were fewer bands in the less malignant cell lines and more in the metastatic cell lines, whilst the tumour samples which labelled weakly with HPA had the fewest bands and those which labelled strongly had the most. These findings validate the use of these cell lines for *in vitro* study of HPA-binding and metastasis.

Dwek et al. (2001) further validated the use of MCF7 by identifying an oligosaccharide (HPAgly1) common to both primary breast cancer sample and MCF7. Whilst Valentiner et al. (2005) reported transplanting several breast cancer cell lines into SCID mice to investigate the relationship between their metastatic potential and their glycosylation as revealed by HPA-binding. MDA MB 468 and ZR751 did not engraft, whilst strongly HPA-binding, DU 4475, MCF7, MDA MB 231, MDA MB 435 produced primary tumours and metastatic deposits in the lung. It was confirmed that HPA binding is a marker of metastatic potential in this SCID mouse model.

Since HPA labelling of primary cancers was associated with metastatic competence in human clinical studies, as described previously (e.g. Brooks and Leathem, 1987; Fenlon et al., 1987; Fukutomi et al., 1989; Alam et al., 1990; Brooks and Leathem, 1991; Fukutomi et al., 1991; Kakeji et al., 1991; Kawai et al., 1991; Langkilde et al., 1992; Shiraishi et al., 1992; Thomas et al., 1993; Noguchi et al., 1993; Brooks

et al., 1993; Yoshida et al., 1993; Ikeda et al., 1994; Kakeji et al., 1994; Schumacher et al., 1994a; Schumacher et al., 1994b; Takahashi et al., 1994; Brooks et al., 1996; Brooks and Wilkison, 2003; Parameswaran et al., 2011), it would be reasonable to hypothesise that the metastases themselves would also be 100% HPA-positive. However, work carried out by Schumacher et al. (1992) revealed that this hypothesis was mistaken. The study examined 16 samples of brain metastases arising from HPA-positive primary breast cancers which were labelled for HPA-binding. 13 (81%) were found to be HPA-positive, whilst unexpectedly 3 (19%) were HPA-negative. These finding were confirmed by Brooks and Leathem (1989) and Brooks and Leathem (1999) in breast cancer metastases to an array of different sites. The studies found that 20% of metastases were HPA-negative. Furthermore, at metastatic locations where multiple discrete metastatic deposits were found they were a distribution of both HPA-positive and HPA-negative tumours. Brooks and Leathem (1999) explained the presence of HPA-negative metastases arising from HPA-positive primary tumours possibly being a result of the natural progression of cancer resulting in alterations of glycosylation over time leading to emergence of HPA-negative clones.

Some research has been performed aimed at understanding how HPA-binding glycans function in metastatic mechanisms. For example, Brooks and Hall (2002) used the 7 breast cancer cell lines which were reported by Brooks et al. (2001) to stably synthesise α-GalNAc-glycans consistent with those observed in clinical tumours (HMT3522, BT474, MDA MB 435, MDA MB 468, ZR751, MCF7, DU 4475) and examined their behaviour in a Matrigel invasion assay. They found that HPA-binding glycans were not involved in adhesion to, and invasion through, basement membrane components during metastasis. Bapu et al. (2016) reported that HPA-binding glycans are involved in the adhesion to vascular endothelium under conditions of sweeping flow. This study reported, however, that MCF7 (highly HPA-positive) and ZR751 (moderately HPA-positive) breast cancer cell lines adhered greatly to endothelial cell monolayers under sweeping flow and that adhesion was significantly ($p=<0.001$) inhibited when GalNAc-glycans were masked. This effect was not observed in weakly HPA-positive and therefore poorly GalNAc-glycan exhibiting BT474 breast cancer cells.

1.5 Project aims

HPA identifies a biological marker associated with aggressive biological behaviour, poor patient prognosis and metastasis of breast and other cancers. HPA has been reported to bind to an array of α-GalNAc glycosylated glycans, including the cancer-associated marker Tn (α-GalNAc-O-Ser/Thr). Tn is not normally exposed in adult tissues, however it is frequently detectable in cancers. Tn exposure in cancers could result from either increased GALNT expression (the family of enzymes to catalyse the addition of GalNAc to Ser/Thr residues to form the initial structure in O-linked glycosylation), or a failure in normal chain extension resulting from a reduced expression of either C1GalT (the enzyme that catalyses the addition of Gal to Tn forming most commonly occurring core structure, core 1) or its molecular chaperone *COSMC*. Little is known about the role of HPA-binding glycans in metastatic mechanisms, although it has been observed that HPA-positivity is associated with adhesion to endothelial cell monolayer under conditions of sweeping flow. Therefore, the aims of the project described in this report are to:

i. Develop a method for comprehensively documenting the aberrant GalNAc glycosylation profiles of a range of breast cancer cell lines (BT474, ZR751 and MCF7).
ii. Determine whether differentially expressed GALNTs, responsible for initiation of O-linked glycosylation, or C1GalT and *COSMC*, responsible for chain extension are responsible for aberrant GalNAc-glycosylation.
iii. Develop a method to isolate the HPA-positive and HPA-negative cell populations and monitor their glycosylation profiles over time.
iv. Identify transcriptomic differences between HPA-positive and HPA-negative isolated cell populations.
v. Ascertain the functional role of HPA-binding glycans in cell invasion as well as adhesion to endothelial cell monolayers.

Chapter 2

General methods

2.0 General methods

2.1 Cell lines and routine culturing

2.1.1 Cell lines

Breast cancer cell lines

The breast cancer cell lines used in this study (see Table 2.1 and Figure 2.1) were chosen to represent a range of breast cancer phenotypes from primary, non-metastatic cancer (BT474) to more biologically aggressive and metastatic cancers (ZR751 and MCF7). The cell lines have been previously characterised within our group and by our collaborators (Schumacher et al., 1995; Schumacher and Adam 1997; Brooks et al., 2001) and stably synthesise a heterogeneous profile of HPA-binding glycoproteins identical to those synthesised by clinical tumour samples, therefore validating their use as a model in these investigations. Figure 2.3, illustrates HPA-binding of MCF7, ZR751 and BT474 cell lines as reported by Brooks et al. (2001). All breast-cancer cell lines were obtained from European Collection of Authenticated Cell Cultures (ECACC).

Table 2.1 *Characteristics of all breast-cancer cell lines validated for use in this work, in order of ascending aggressiveness. Adapted from Brooks et al. (2001).*

	BT474	**ZR751**	**MCF7**
Derived from	Invasive ductal cancer.	Metastatic, malignant ascites from invasive primary ductal breast cancer.	Metastatic, malignant pleural effusion from invasive primary ductal breast cancer.
Age of patient (years)	60	63	69
Evidence of metastasis in SCID mice	Poorly tumourigenic in SCID mice (Valentiner et al., 2005; Iorns et al., 2012).	Tumourigenic in SCID mice (Yin et al., 2003; Valentiner et al., 2005).	Highly tumourigenic in SCID mice (Schumacher and Adam, 1997; Valentiner et al., 2005).
ER status	- (Engel and Young, 1978)	+ (Engel et al., 1978)	+ (Brooks et al., 1973)
HPA lectin labelling characteristics as reported by Brooks et al. (2001)	+	+++	++++
Derived by	Lasfargues et al. (1978)	Engel et al. (1978)	Soule et al. (1973)

Endothelial cells

Human umbilical vein endothelial cells (HUVECs) (see Figure 2.2) are a primary cell line which were used in this project as detailed in Section 6 for the static adhesion assay. HUVECs were obtained from Lonza, Slough UK.

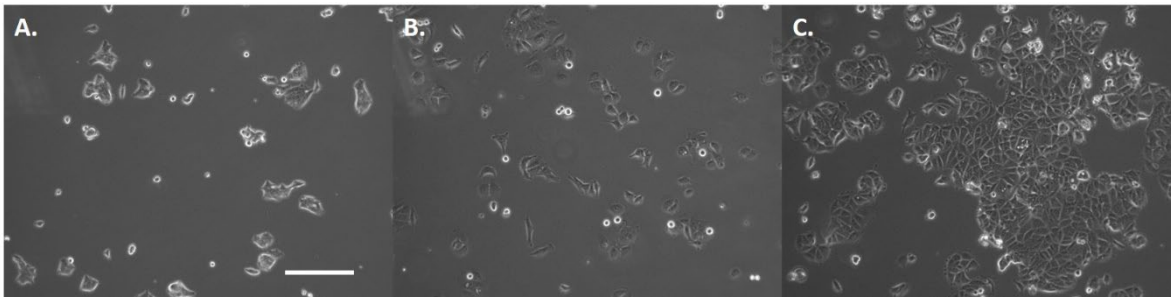

Figure 2.1 *Phase contrast images of (A) BT474, (B) ZR751 and (C) MCF7 cells 24hrs post seeding under routine cell culture procedures. Scale bar = 100µm.*

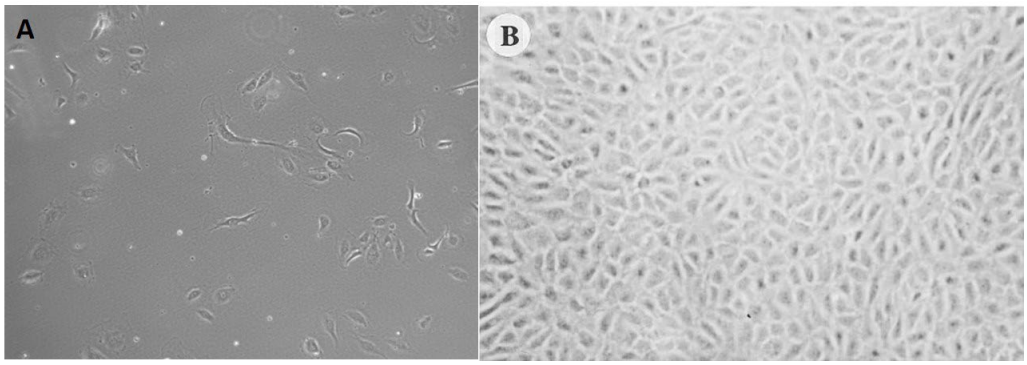

Figure 2.2 *(A) Phase contrast image of HUVEC cells 24hrs post seeding under routine cell culture procedures. (B) Confluent monolayer of HUVEC cells, taken from Mason et al. (1997).*

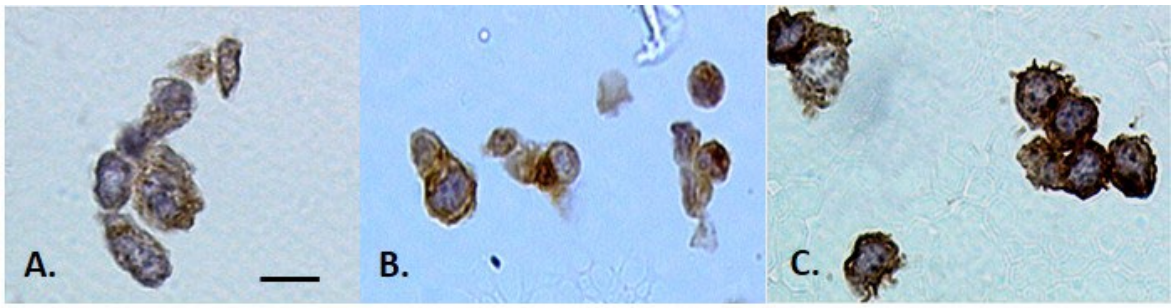

Figure 2.3 *HPA labelling of (A.) BT474, (B.) ZR751 and, (C.) MCF7 cells analysed at the light microscope level, from weak to intense HPA labelling (brown colour). Nuclear counterstain haematoxylin (blue). Taken from Brooks et al. (2001). Scale bar =15µm*

2.1.2 Routine cell culture procedures

Retrieval of cells from liquid nitrogen storage

A T-25 cell culture flask and 15ml centrifuge tube were each prepared with 5ml of warmed (37°C) preferred growth medium (see Table 2.2) and placed in a humidified tissue culture incubator, 37°C, 5% CO_2 atmosphere until required. A 1.2ml cryovial containing frozen cell suspension was retrieved from long-term storage in liquid nitrogen. The cell suspension was gently thawed by rolling in the palm of the hand until only a crystal of ice could be observed. The 15ml centrifuge tube was retrieved from the tissue culture incubator and the thawed cell suspension was quickly aspirated from the cryovial and dispensed into the 15ml centrifuge tube. The cell suspension was centrifuged at 1,100 x g for 3min to pellet. The supernatant was discarded and the cell pellet re-suspended in 1ml of warmed (37°C) preferred growth medium. The T-25 cell culture flask was retrieved from the tissue culture incubator. The cell suspension was aspirated from the 15ml centrifuge tube and dispensed into the prepared T-25 cell culture flask. The cells were placed in a humidified tissue culture incubator, 37°C, 5% CO_2 atmosphere for 24hr after which point the spent medium was aspirated and discarded and replenished with 5ml of warmed (37°C) preferred growth medium. The cells were allowed to grow to confluence and were passaged as described below.

Table 2.2 *Details of growth medium and supplements for cell lines used within this project.*

Cell line	Basal medium	Supplements
MCF7	DMEM:F-12 (Lonza)	• Heat inactivated foetal calf serum (FCS) 10% v/v (Gibco™) • L-Glutamine 2mM (Gibco™)
ZR751	RPMI-1640 (Gibco™)	• Heat inactivated FCS 10% v/v (Gibco™) • L-Glutamine 2mM (Gibco™) • Sodium pyruvate 1mM (Sigma-Aldrich®)
BT474	RPMI-1640 (Gibco™)	• Heat inactivated FCS 10% v/v (Gibco™) • L-Glutamine 2mM (Gibco™) • Insulin 2% v/v (Sigma-Aldrich®)
HUVEC	EBM-2 (Lonza)	• Hydrocortisone 0.4% v/v (Lonza) • Human fibroblast derived growth factor-B (hFGF-B) 0.1% v/v (Lonza) • Vascular endothelial growth factor (VEGF) 0.1% v/v (Lonza) • R3-insulin derived growth factor-1 (R3-IGF-1) 0.1% v/v (Lonza) • Ascorbic acid 0.1% v/v (Lonza) • Human epidermal growth factor (hEGF) 0.1% v/v (Lonza) • Foetal bovine serum 2% v/v (Lonza) • Gentamycin and amphotericin (GA-1000) 0.1% v/v (Lonza)

Maintenance of cell cultures

Cells were routinely cultured in T-75 cell culture flasks. Cell culture medium was changed every 48-72hr by aspirating spent medium and replenishing with 10ml warmed (37°C) preferred growth medium (see Table 2.2) until 70% confluence was achieved, at which point the cells were passaged as detailed below.

Passaging of cell cultures

Cells were passaged when 70% confluence was achieved. This was done by aspirating spent medium and washing the cells 3x with warmed (37°C) phosphate buffered saline (PBS, pH 7.2-7.4) (Fisher Scientific). PBS was aspirated, discarded and replaced with 5ml of 0.05% w/v trypsin/EDTA (Gibco™) diluted 1:9 with PBS. The flask was placed in a humidified tissue culture incubator, 37°C, 5% CO_2 atmosphere until cells detached from the culture surface (~5-8min depending on cell line). During this time, a 15ml centrifuge tube was prepared with 5ml of warmed (37°C) preferred growth medium (see Table 2.2). The flask was retrieved from the tissue culture incubator and the cells checked under an inverted microscope to ensure that the cells had detached. The cell suspension was aspirated from the flask and dispensed into the prepared 15ml centrifuge tube to deactivate the trypsin. Cells were centrifuged at 1100 x g for 3min to pellet. During this time, T-75 cell culture flasks were prepared with 10ml of warmed (37°C) preferred growth medium. The supernatant was discarded and the cell pellet re-suspended in 3ml of warmed (37°C) preferred growth medium. Cells were seeded into T-75 cell culture flasks at a ratio of 1:2 or 1:5, depending upon the downstream application. Cells were used for a maximum of 10 passages before being discarded and replaced with a new frozen stock to ensure minimal phenotypic drift.

Preparation of cell line stocks

Before any experimental work was carried out, a number of cell stocks were created which were employed in all subsequent experiments. Cells were allowed to grow to 100% confluency and then trypsinised and pelleted as described above. The supernatant was discarded and the cell pellet re-suspended in 2ml of 1:9 solution of dimethyl sulphoxide (DMSO) in preferred growth medium (see Table 2.2). 1ml of the cell suspension was added per 1.2ml cryovial. The cryovials were placed in a freezing container (Nalgene®) at -80°C overnight and then transferred to liquid nitrogen for long-term storage.

Routine mycoplasma testing

Cells were routinely tested for mycoplasma contamination using the e-Myco™ Mycoplasma PCR Detection Kit, according to manufacturers' instructions (iNtRON Biotechnology).

2.2 HPA lectin labelling

As detailed in Section 1.4, HPA lectin binding is a useful prognostic tool for assessing metastatic competence and poor patient prognosis in a range of cancers as the presence of HPA-binding glycoproteins on cancer cells, although largely uncharacterised, are associated with cancer progression. A considerable number of histochemical studies have used HPA lectin labelling on both histological specimens and cancer cell lines. The HPA lectin labelling procedure was optimised as detailed in Section 3.2.1 to give results consistent with published studies and what is reported here is that optimised method. For HPA lectin labelling protocol overview see Figure 2.4.

Preparation of cells on coverslips

T-75 cell culture flasks of cancer cells were prepared and allowed to grow to 80% confluence. 13mm diameter 70% IMS (industrial methylated spirits) sterilised coverslips were placed into a 24-well cell culture plate and left to air dry in a class II cell culture hood. Cells were scraped from their flask, dissociated by gentle pipetting and then counted. A suspension of 40,000 cells/ml in warmed (37°C) preferred cell culture medium (see Section 2.1.2) was prepared and 500µl of cell suspension was added per well, swirled once and placed in a humidified tissue culture incubator, 37°C, 5% CO_2 atmosphere for 24hr to allow sufficient attachment to the coverslips.

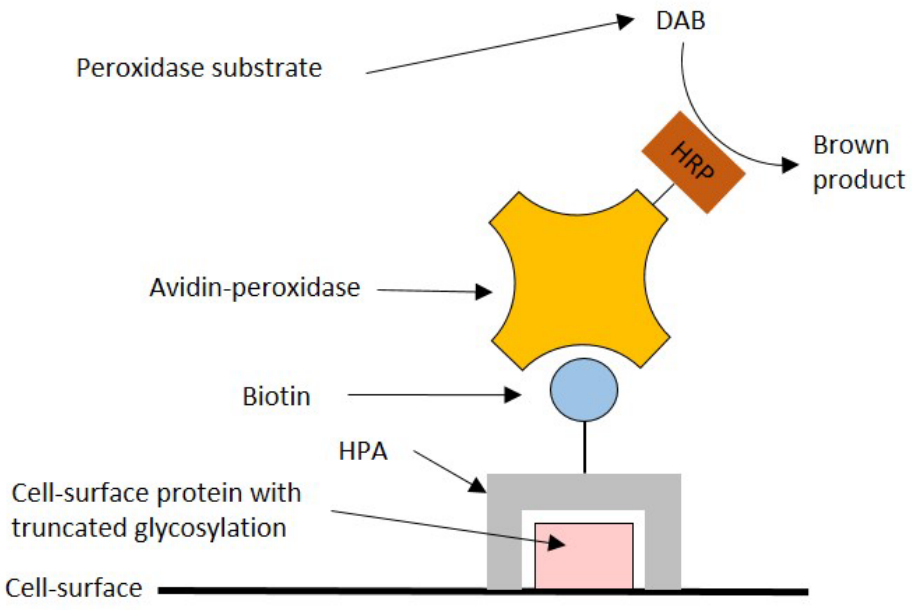

Figure 2.4 *HPA lectin labelling protocol. Truncated cell-surface glycoproteins with terminal GalNAc are recognised by biotinylated-HPA lectin which is then incubated with avidin-peroxidase (HRP = horseradish peroxidase) and its chromogenic substrate 3,3'-diaminobenzedine (DAB)/hydrogen peroxide (H_2O_2) to produce the brown product.*

Fixation, HPA lectin labelling and mounting

Cell culture medium was aspirated and the cells washed 3x with FCS-free preferred growth medium and then fixed with cold (4°C) 4% v/v paraformaldehyde (PFA) in 0.1M piperazine-N,N'-bis-(2-ethanesulfonic acid) (PIPES) buffer, pH 6.9, for 30min at 4°C. Cells were then washed 3x with PIPES buffer and then permeabilised with 0.1% v/v Triton X-100 in PIPES buffer for 10min. Cells were washed 3x with PIPES buffer and then endogenous peroxidases were blocked by incubating with 3% v/v hydrogen peroxide in methanol for 20min. Cells were washed 3x with lectin buffer (lectin buffer: 50mM Tris, 100mM NaCl, 2mM $MgCl_2$, 1mM $CaCl_2$), pH 7.6, and then incubated with 10µg/ml biotinylated-HPA (Sigma-Aldrich®) in lectin buffer/BSA (lectin buffer/BSA: 3% w/v bovine serum albumin (BSA) in lectin buffer), for 5min. Cells were washed 3x with lectin buffer and then incubated with 5µg/ml avidin-peroxidase (Sigma-Aldrich®) in lectin buffer/BSA, for 30min. Cells were washed 3x in lectin buffer and then incubated with the peroxidase substrate 3,3-diaminobenzidine tetrahydrochloride (DAB)/ H_2O_2 prepared according to manufacturers' instructions (Vector Labs) for 2min. Cells were washed 3x in distilled water and then counterstained with Harris' haematoxylin (Sigma-Aldrich®) for 30sec and then "blued" in running tap water for approximately 2min. Coverslips were removed from their wells and were dehydrated by passing through 70% v/v IMS in distilled water, then 2 changes of 100% IMS and then cleared in xylene. Coverslips were inverted and mounted onto slides with Depex mounting medium (Sigma-Aldrich®).

Negative and specificity of HPA-labelling controls

Slides were viewed using a light microscope (Zeiss Axioplan microscope fitted with a JENOPTIK ProgResC3 colour camera). Labelling was considered good if controls were as expected.

1. Negative controls: omission of HPA lectin from the labelling procedure should completely abolish labelling. This ensures that there is no avidin-peroxidase binding non-specifically to endogenous biotin. Omission of both HPA lectin and avidin-peroxidase from the labelling procedure should completely abolish labelling. This ensures that endogenous peroxidases were sufficiently blocked.
2. Specificity control: by adding 0.1M αGalNAc (*N*-acetylgalactosamine) – the monosaccharide to which HPA has the greatest affinity - in lectin buffer/BSA, to the lectin solution for 30min prior to incubation with the cells should completely abolish labelling through competitive inhibition of HPA binding.

2.3 Isolation of viable glycosylation-specific cell populations for further *in vitro* analysis using lectin-coated magnetic beads (cell-separation)

The method described here, when performed under sterile conditions, can be used to separate cells into different populations based on their glycosylation profiles. These can then be sub-cultured for further assays or analysis. Maintaining sterility is, however, not necessary if cells are to be used for immediate analysis post-separation, for example genetic profiling. Development of the method described here resulted in publication (Beaman et al., 2017, see Appendix 3).

The technique, illustrated in Figure 2.5, employs magnetic beads bearing streptavidin (DynaBeads®) to which biotinylated-HPA lectin is immobilised. Once the lectin is immobilised on the beads, they are very gently – to minimise physical trauma to the cells – mixed with a suspension of cells. The mixing step is kept brief so that it can be conveniently carried out on the bench-top, rather than in a 37°C / CO_2 incubator, without being detrimental to cell viability. During the mixing step, cells that exhibit cell surface glycosylation profiles recognised by the immobilised lectin will bind to the beads; those that do not will remain free in suspension. Once the lectin-binding cells are attached to the beads, the beads can be very easily removed using a magnet. This leaves behind the cells with glycosylation profiles not recognised by the lectin. Thorough washing of the bead-lectin bound cells is then necessary to remove any contaminating non-lectin bound cells. These cells are pooled with the non-lectin bound cells in the original suspension, thus giving two separated populations (see Figure 2.6) for further analysis.

Once cells have bound to the beads, it is not necessary to release / dissociate the cells. The presence of cell-bound beads (see Figure 2.6) does not adversely affect cell viability and during subsequent culture the presence of beads naturally diminishes. However, when separated cells have been subjected to further lectin cytochemistry, using the same lectin that was employed to separate them in order to assess their glycosylation profiles post-separation, the presence of cell-bound beads does reduce their ability to label. This could be a result of either steric hindrance due to the physical presence of the beads, or to unavailability of lectin-binding sites as they are occupied by binding to lectin immobilised on the beads. If this is an issue, it is possible to dissociate the beads from the separated cells. This can be achieved using competitive inhibition in a solution of the simple sugar for which the lectin shows greatest specificity (i.e. for HPA, α-GalNAc), or by using EDTA/trypsin.

Preparation of cells

T75 cell culture flasks were prepared and allowed to grow to 80% confluence as detailed in Section 2.1.2. Cells were washed 3x in warmed (37°C) FCS-free preferred cell culture medium. Washing medium was aspirated and discarded and replaced with 2ml of warmed (37°C) FCS-free preferred cell culture medium (see Table 2.1) into which the cells were scraped from the culture flask using a rubber scraper. The cell suspension was sieved through a 70µm cell-strainer and then a 40µm cell-strainer (Fisher Scientific) to

yield a single-cell suspension. Cells were counted and 1 x 10^6 cells were used. Cells were pelleted by centrifugation at 1,100 x g for 3min and the supernatant discarded.

Preparation of lectin and streptavidin-coupled magnetic beads

500µl of 10µg/ml of biotinylated-HPA (Sigma-Aldrich®) in 3% w/v BSA in TBS, pH 7.6 (BSA/TBS), was prepared and added to 500µl of 5µg/ml of streptavidin-DynaBeads® (Sigma-Aldrich®) in BSA/TBS, and placed on an end-over-end mixer for 30min. After this time, the beads were pooled using a magnet and unbound-lectin/buffer was aspirated and discarded. The beads were washed 3x with BSA/TBS, to remove any unbound-lectin. The magnet was removed and the lectin-bound magnetic-beads were re-suspended in 1ml of BSA/TBS.

Combining cell and lectin streptavidin-coupled magnetic-bead preparations

All reagents were warmed (37°C) and all procedures with cells at room temperature were performed swiftly to reduce stress upon cells. The cell pellet was re-suspended in the lectin-bound bead preparation and placed on an end-over-end mixer for 5min at room temperature.

Isolation of glycosylation-specific cell populations

A magnet was placed on the side of the tube containing the cell/lectin/bead mixture for 2min at room temperature in order to trap the cells conjugated to the beads at one side of the tube. Holding the magnet in place, unbound cells, and supernatant were gently aspirated into a new tube (this is the negative population i.e. the population of cells without the selected glycosylation profile). Holding the magnet in place, the positive population (i.e. the population of cells with the selected glycosylation profile) was washed 3x with BSA/TBS to ensure that only cells bound to the lectin/beads remain. The wash solution was aspirated and added to the negative population. The washing of the bound beads was repeated twice more. The positive population was pelleted by centrifugation at 1,100 x g for 3min, and the supernatant discarded. The positive population was re-suspended in 1 ml of complete culture medium, counted and sub-cultured. The negative population was further purified by holding a magnet to the side of the tube for 2min to trap any contaminating positive cell/beads that remained. The remaining pure population of free, unbound cells and solution was aspirated into a new tube (this is the negative population) and the tube containing any contaminating positive cells/beads was discarded. This purification step was repeated twice more. The negative population was pelleted by centrifugation at 1,100 x g for 3min, and the supernatant was discarded. The negative population was re-suspended in 1 ml of complete culture medium, the cells were counted and sub-cultured.

Dissociation of cells from beads using competitive inhibition of lectin-binding

Instead of re-suspending in complete culture medium, the positive population was re-suspended in 1 ml of 0.1M α-GalNAc (Sigma-Aldrich®) in BSA/TBS and placed on an end-over-end mixer for 5min at room temperature. A magnet was placed on the tube for 2min to pool the beads and dissociated cells were aspirated into a new tube. This pooling and aspiration was repeated twice more. The negative population was re-suspended in 1ml of BSA/TBS, and placed on an end-over-end mixer as a "mock dissociation" step.

"Mock cell separation" control

To ensure that the separation protocol itself does not affect the cells a "mock separation" was performed, where cells were incubated with streptavidin-beads that had not been conjugated to biotinylated-HPA and therefore remain unseparated.

"Mixed population" control

Again, to ensure that the separation protocol, and, in particular, incubation with biotinylated-HPA does not affect the cells, a "mixed population" control was performed. Cells were separated as detailed previously and then the HPA-positive and HPA-negative populations were mixed back together in the proportions which they are reported to exist as an unseparated population; for example MCF7 are reported as being 90% HPA-positive (Brooks et al., 2001) and so are a mixture of 90% HPA-positive and 10% HPA-negative. These were then placed on an end-over-end mixer for 10min before use.

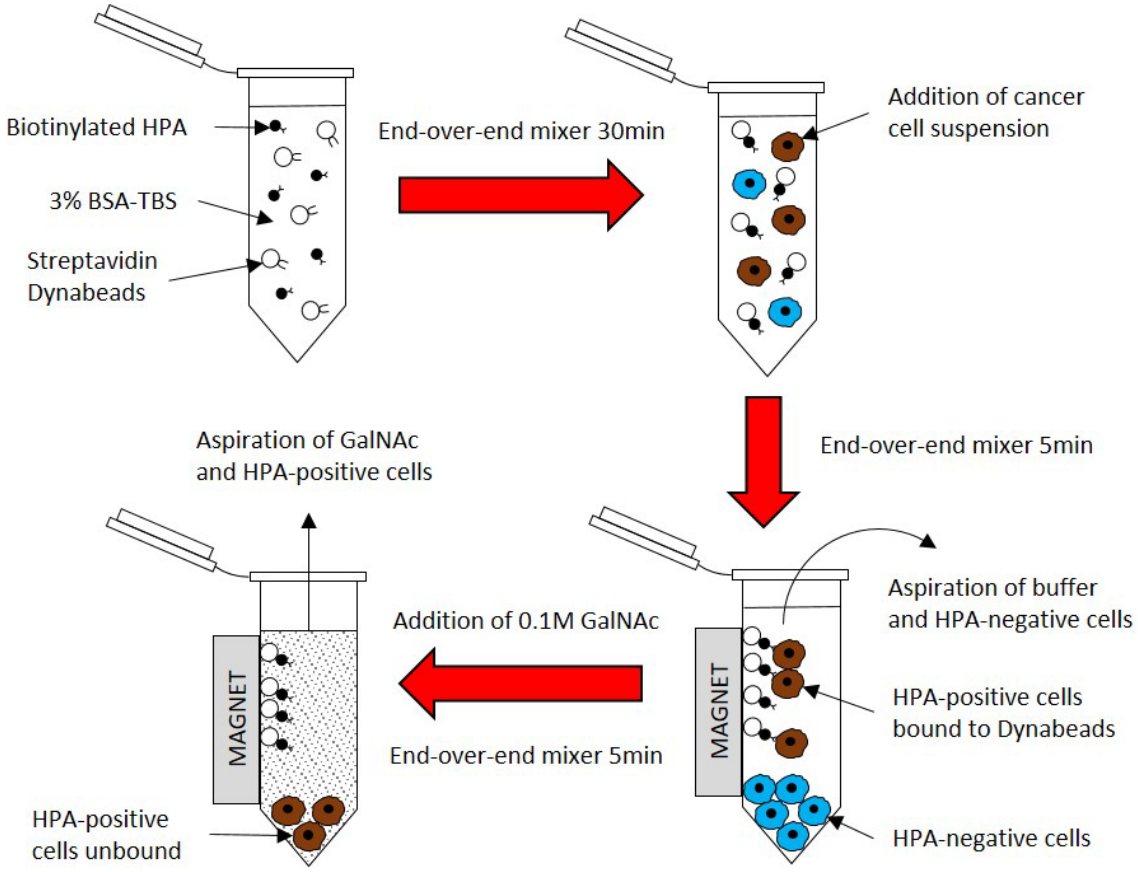

Figure 2.5 *Isolation of viable glycosylation-specific cell populations for further in vitro analysis using lectin-coated magnetic beads. Biotinylated-HPA lectin is immobilised on streptavidin-coated magnetic beads by mixing 10µg/ml biotinylated-HPA and 5µg/ml streptavidin-DynaBeads® in 3% BSA-TBS on an end-over-end mixer for 30min. The HPA-bound DynaBeads® are then incubated with a cell suspension for 5min on an end-over-end mixer. Cells with terminal GalNAc bind to the HPA-bound DynaBeads® and a magnet is used to pool the DynaBeads®. Non-bound cells can be aspirated and bound-cells are re-suspended in 0.1M GalNAc to elute HPA-bound DynaBeads® leaving an HPA-positive and HPA-negative population.*

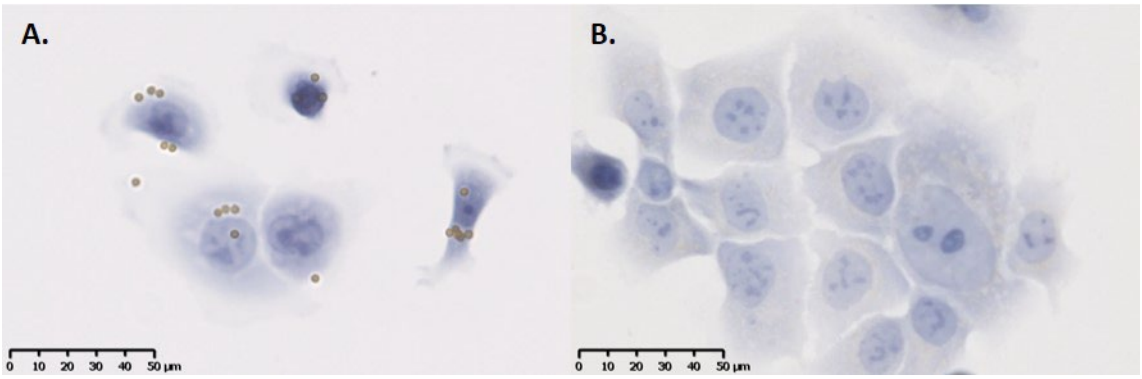

Figure 2.6 *Isolated populations using cell separation procedure. A. HPA-positive population with magnetic beads still bound to their surface. B. HPA-negative population. Scale bar = 50µm.*

2.4 Extraction of genomic DNA

Extraction of genomic DNA (gDNA) was performed using an Invitrogen™ PureLink™ Genomic DNA Mini kit, according to manufacturers' instructions (Invitrogen™). Tan and Yiap (2009) reported that the process of extracting gDNA using spin columns is more efficient and cleaner than traditional phenol-based processes. The method employs the use of chaotropic salts to disrupt hydrogen bonds and hydrophobic interactions. These changes destabilise the protein and assist the transfer of the DNA to the silica of the spin column; the addition of alcohol also aids this.

Sample preparation

T-25 cell culture flasks were prepared with cells and allowed to grow to 80% confluence as detailed in Section 2.1.2. Cells were scraped from their flask and counted. No more than $5x10^6$ cells were used per preparation. Cells were pelleted by centrifugation at 1,100 x g for 3min, the supernatant was discarded and the cell pellet re-suspended in 200µl PBS (Fisher Scientific). The cell suspension was transferred to a 1.5ml microcentrifuge tube and then 20µl of proteinase K (Invitrogen™, 20mg/ml in storage buffer) added to remove DNases that may be present. To this 20µl of RNase A (Invitrogen™, 20mg/ml in 50mM Tris-HCl, pH 8.0, 10mM EDTA) was added, mixed by brief vortexing and incubated at room temperature for 2min to remove any RNA from the sample. After this time, 200µl of PureLink™ genomic lysis/binding buffer (Invitrogen™) was added to the sample and mixed well by vortexing. This was then incubated at 55^oC for 10min to aid protein digestion.

gDNA isolation

The gDNA was precipitated from the sample by the addition of 200µl of 100% ethanol to the lysate. The gDNA was purified by adding the sample (~640µl) to a PureLink™ spin column (Invitrogen™) in a collection tube. This was then centrifuged at 10,000 x g for 1min to bind the DNA to the column. The collection tube was discarded and the spin column was placed into a fresh collection tube. To remove impurities from the DNA, such as proteins and salts, the sample was washed twice, firstly by adding 500µl of wash buffer 1 (Invitrogen™) to the spin column and then centrifuged at 10,000 x g for 1 min. The collection tube was discarded and replaced with a fresh tube. Secondly, 500µl of wash buffer 2 (Invitrogen™) was added to the spin column and centrifuged at 20,000 x g for 3min. The collection tube was discarded and replaced with a 1.5ml microcentrifuge tube. To elute the DNA from the spin column, 200µl of PureLink™ genomic elution buffer (Invitrogen™) was added to the spin column and incubated at room temperature for 1 min for maximum yield of sample and then centrifuged at 20,000 x g for 1min. The DNA was quantified using a spectrophotometer with UV absorbance at 260nm and the concentration adjusted to 50ng/µl using nuclease-free H_2O (NFH_2O).

2.5 Isolation of RNA

TRI Reagent® is a monophasic solution of phenol and guanidinium isothiocyanate that is used for simultaneous isolation of RNA, DNA and protein (Chomczynski, 1993). This procedure is an improvement on the single-step method reported by Chomczynski and Sacchi (1987) for total RNA isolation. TRI Reagent® is the most effective method for isolation of total RNA of all types from 0.1-15kb in length. The resulting RNA is intact with little or no contaminating DNA or protein (Chomczynski, 1993).

Homogenising sample

T-75 cell culture flasks of cells were prepared and allowed to grow to 80% confluence as detailed in Section 2.1.2. Cells were scraped from their flask and counted and $5x10^6$ cells were used per extraction. Cells were pelleted and growth medium aspirated and discarded. 1ml of TRI Reagent® (Sigma-Aldrich®) was added to the cell pellet and was mixed to produce a homogenous lysate, then left to stand for 5min to ensure complete dissolution of nucleoprotein complexes.

Phase separation

0.2ml of chloroform was added to the lysate and mixed well for 15sec then allowed to stand for 15min. The sample was centrifuged at 12,000 x g for 15min at 4°C to separate into 3 phases: a red organic layer containing protein, an interphase containing DNA, and a colourless upper aqueous layer containing RNA. The colourless upper aqueous layer was carefully aspirated and transferred to a new tube. 0.5ml of 2-propanol was added and mixed then allowed to stand for 10min. The sample was centrifuged at 12,000 x g for 10min at 4°C. The supernatant was carefully aspirated and 1ml of 75% ethanol was added to wash the pellet. The sample was mixed and then centrifuged at 7,500 x g for 5min at 4°C. The supernatant was carefully aspirated and the pellet left to air-dry for 10min. The pellet was re-suspended in 10µl of NFH_2O. The RNA was quantified using a spectrophotometer with UV absorbance at 260nm and the concentration adjusted to 50ng/µl using NFH_2O.

2.6 DNase I treatment of RNA

DNase I is an endonuclease isolated from bovine pancreas that digests double- and single-stranded DNA. It has been purified to remove RNase activity, therefore making it suitable for removing DNA from RNA preparations. It is important when using RNA for quantitative polymerase chain reaction (qPCR) that the sample is digested with DNase I, as PCR can detect even a single molecule of DNA. Parallel reactions should also be run without adding reverse transcriptase to check for amplification of contaminating DNA. This is especially important if primers that do not span an intron are to be used (Huang et al., 1996).

Preparation of RNA for reverse transcription

To duplicate tubes (i.e. for +RT and -RT reactions) 1µl of RNA prepared as described in Section 2.5 was added to 5µl of NFH_2O, 1µl of 10x reaction buffer (1ml of 200mM Tris-HCl, pH 8.3 and 20mM $MgCl_2$) and 1µl of DNase I (Sigma-Aldrich®, 1 unit/µl in 50% glycerol, 10mM Tris-HCl, pH 7.5, 10mM $CaCl_2$ and 10mM $MgCl_2$). The preparations were mixed gently by flicking the tube then incubated for 15min. 1µl of stop solution (50mM EDTA) to bind Ca^{2+} and Mg^{2+} ions and therefore inactivate DNase I was added per preparation, then heated at 70°C for 10min to denature both the DNase I and the RNA (Sanyal et al., 1997).

2.7 Reverse transcription

Reverse transcription was performed using a High-Capacity RNA-to-cDNA™ kit (Applied Biosystems™) according to manufacturers' instructions and as described here. Reverse transcription synthesises complementary DNA (cDNA) from an RNA template. The production of the first strand cDNA is achieved by reverse transcriptases (RTs) and a short primer complementary to the 3' end of the RNA. cDNA can be used directly as a template for the PCR. A minus reverse transcription control (-RT control) is run alongside to test for contaminating DNA that may be present in the RNA from previous steps. This control contains all the reaction components except for the RTs, therefore when used in PCR no amplification should be observed (Bustin, 2004).

RNA-to-cDNA reaction

A master mix was prepared on ice of the reagents detailed in Table 2.3 for the required number of reactions plus 10% to allow for pipetting error. To the tubes prepared as detailed in Section 2.6, 11µl of each master mix was added per +RT and -RT reaction and mixed. The tubes were heated to 37°C for 1hr and then the reaction was stopped by heating to 95°C for 5min. The preparations were stored at -20°C until required.

Table 2.3 *Reaction components for reverse transcription.*

Component	**Component volume/reaction (µl)**	
	+RT reaction	**-RT control**
2x RT buffer	10	10
20x Enzyme mix	1	-
NFH_2O	-	1
Total/reaction	11	11

2.8 qPCR

After the reverse transcription of RNA to cDNA (detailed in Section 2.7), qPCR is used to amplify and report in real-time the presence of PCR products. This requires a suitable detection chemistry to report the presence of PCR products, which can be either probe or non-probe based. The experimental work carried out here used iTaq™ SYBR® green supermix (Bio-Rad). This is a non-probe based detection method; SYBR green fluoresces when intercalated with double stranded DNA (dsDNA). In solution, the unbound dye emits little fluorescence; during the PCR assay, increasing amounts of dye bind to the nascent dsDNA. qPCRs are described as the point when amplification of a PCR product is first detected, termed the cycle threshold (*Ct*). The smaller the *Ct*, the larger the starting copy number of the nucleic acid target (Bustin and Mueller, 2005). Two types of control are performed in qPCR to ensure that there is no contaminating DNA: no template control (NTC) where cDNA is omitted from the reaction and -RT or no reverse transcriptase (NRT) control where the -RT template prepared as described in Section 2.7 is used instead of the +RT. In order to reduce errors, such as difference in starting amount of template, efficiency of amplification and correct for sample-to-sample variation, reference genes are used as an internal control to normalise *Ct* values against. The reference genes used in the experimental work carried out here are beta-actin (ACTB) and glucuronidase-beta (GUSB), which are commonly used reference genes that should theoretically be expressed at a constant level (Arya et al., 2005). Ideally a range of reference genes would have been trialled to ensure that those genes with stable expression across all three cell lines were chosen, however due to time constraints commonly used reference genes were utilised. There are two types of quantification used in qPCR; these are absolute and relative. Absolute quantification relates the signal detected (*Ct*) to copy number of the amplicon using a calibration curve, whilst relative quantification is based on the expression level of the target gene versus the reference gene (Bustin, 2004). In the experimental work carried out here, relative quantification was used. Relative quantification or the comparative threshold method ($2^{-\Delta\Delta Ct}$) calculates the relative expression levels of the target gene relative to a reference control. The amount of target in the sample normalised to an endogenous reference gene and relative to a normal calibrator (for example, an untreated sample versus a treated sample) is then given by $2^{-\Delta\Delta Ct}$, where ΔΔCt = ΔCt (sample) - ΔCt (calibrator) and ΔCt is the Ct of the target gene subtracted from the Ct of the reference gene (Arya et al., 2005). Relative quantification was used for the work reported here due to the higher cost of using absolute quantification resulting from the high number of samples and genes being tested. Bustin et al. (2009) proposed a set of guidelines, termed MIQE (minimal information for publications of quantitative real-time PCR experiments), to provide consistency to the manner in which qPCR data are reported.

Reaction mix preparation and thermal cycling profile

A master mix was prepared on ice of the reagents detailed in Table 2.4 for the required number of reactions plus 10% to allow for pipetting error. 19µl of master mix was added per reaction well on a 96-

well plate. To this, 1µl of cDNA prepared as described in Section 2.7 was added and mixed per reaction or 1µl of -RT for NRT controls or 1µl of NFH_2O for NTCs. The plate was spun briefly by centrifugation to remove any air bubbles and then placed in a CFX96 Touch™ thermal-cycler on a 2-step amplification protocol (detailed in Table 2.5) with melt curve analysis.

Table 2.4 *qPCR reaction setup.*

Component	**Volume (µl)**
iTaq™ universal SYBR® green supermix (2x)	10
Forward primer	0.2
Reverse primer	0.2
NFH_2O	8.6
Total reaction mix volume	19

Table 2.5 *Thermal cycling profile, 2-step amplification with melt curve.*

	Temperature (°C)	**Time (sec)**	**Cycles**
Denaturation	95	5	40
Annealing/extension	60	30	
Melt curve	65-95, 0.5 increments	5	-

Chapter 3

Characterisation of model cell lines

3.0 Characterisation of model cell lines

3.1 Background

Leathem and Brooks (1987) first reported that binding of a lectin from the albumin gland of the Roman snail, *Helix pomatia* agglutinin (HPA), was a useful analytical tool for predicting aggressive biological behaviour, metastasis and poor patient prognosis in breast cancer. Since then, HPA labelling has been repeatedly reported to be associated with long-term poor patient prognosis and reduced survival in a range of cancers, including breast cancer (reviewed by Mitchell and Schumacher, 1999; Brooks, 2000). HPA primarily binds glycans terminating in the monosaccharide GalNAc, however its prognostic significance is through recognition of a heterogeneous range of glycoproteins glycosylated by GalNAc-glycans, most notably Tn (Brooks et al., 1994). Brooks and Carter (2001) reported that over production of GalNAc bearing moieties is not a result of failed sialylation (addition of SA, a common chain terminator), as proposed by Fenlon et al. (1987). Instead, they suggested, it is most likely to be a result of failed normal chain-extension, possibly through up-regulation of GALNTs, therefore overwhelming downstream transferases and leading to an abundance of exposed Tn (Brooks and Carter, 2001). This is supported by numerous publications in the literature reporting that aberrant expression of GALNTs is a useful indicator of metastatic disease in cancers including colorectal (Kohsaki et al. 2000; Shibao et al. 2002; Guo et al. 2004; Koyanagi et al. 2008; Guda et al. 2009; Gray-McGuire et al. 2010; Abuli et al. 2011; Clarke et al. 2012), gastric (Onitsuka et al. 2003; Gao et al. 2013), breast (Cavallo et al. 2005; Berois et al. 2006a; Freire et al. 2006; Patani et al. 2008; Wu et al. 2010), neuroblastoma (Berois et al. 2006b; Berois et al. 2013), pancreatic (Li et al. 2011), gallbladder (Miyahara et al. 2004), prostate (Landers et al. 2005), bladder (Ding et al. 2012a), lung adenocarcinoma (Gu et al. 2004), oesophageal cancer (Ishikawa et al. 2005) and lymphoma (Gibson et al. 2012). Alternatively, alterations in the highly organised and compartmentalised secretory pathway have been reported in the literature to be the cause of the appearance of Tn/TF antigens on a number of cancers (reviewed by Chia et al., 2016). Neo-proteins passing through the secretory-pathway encounter enzymes in a specific order of action in a kinetically constrained manner (reviewed by Bard and Chia, 2016). Gill et al. (2012) reported that the overexpression of Src by growth factor stimulation led to the relocation of GALNT2 from the Golgi apparatus to the ER in human fibroblast cells, therefore exposing protein substrates to GALNTs sooner and for a longer period, thus leading to increased O-glycosylation and potentially a greater amount of truncated glycans, such as Tn and TF, that are seen in cancers.

MCF7, ZR751 and BT474 breast cancer cell lines have been previously characterised within our group and by others and stably synthesise a heterogeneous profile of HPA-binding glycoproteins (see Section 2.1.1 and Figure 2.3) identical to those synthesized by clinical tumour samples (Schumacher et al., 1995;

Schumacher and Adam, 1997; Brooks et al., 2001). 98.66% of MCF7 cells are reported by Brooks et al. (2001) to label for HPA binding with an intensity of +++, 73.56% of ZR751 cells labelling ++ and 31% of BT474 cells labelling +/-. In this study, as others in the literature, HPA labelling was estimated subjectively by eye. In order to validate their use as a model in the investigations reported here, HPA-labelling profiles of the cells used in the studies needed be comparable to those reported previously, and therefore optimisation of the HPA lectin labelling procedure was required. Cell lines and routine culturing are described in Section 2.1.1. Optimisation of HPA lectin labelling of cultured cells is described here and the optimised procedure, then employed in investigations throughout this thesis, is detailed in Section 2.2. Optimisation was carried out based on a "standard" HPA lectin labelling procedure reported by Brooks and Hall (2002). Once optimal conditions were created, methods of quantifying the labelling were also developed. Previously, in studies of clinical tumours and of cell lines (as described above and in Section 1.4), HPA lectin labelling was recorded as a combination of approximate percentage of labelled cells alongside an estimate of intensity of labelling (+/-, +, ++, +++, ++++) on a subjective scale; for example, "80% ++" or "30% +++" (Leathem and Brooks, 1987; Fenlon et al., 1987; Fukutomi et al., 1989; Alam et al., 1990). In some studies, a simpler classification of "stainers" and "non-stainers" irrespective of HPA labelling intensity was employed, as it was observed that there was no relationship between extent of HPA positivity and prognosis in clinical studies, only with presence or absence of HPA labelling. "Stainers" were classified as >5% of cells clearly labelled (+) or >50% labelled (+/-). "Non-stainers" were classified as <5% of cell labelled (+) or <50% labelled (+/-) (e.g. Brooks and Leathem, 1991; Gusterson et al., 1993; Noguchi et al., 1993a; Noguchi et al., 1993b; Thomas et al., 1993; Scumacher et al., 1994a; Noguchi et al., 1994a; Noguchi et al., 1994b Dwek et al., 2001). By further exploring and extending the more complex initial quantification of HPA lectin labelling in cell lines, it is hoped that new insight into the GalNAc-glycosylation of the cancer cells and the analytical use of HPA labelling will be determined.

As aberrant expression of GALNTs are reported to be useful as a prognostic marker of metastatic disease in a number of cancers, described previously, and as it has been proposed that the aberrant GalNAc-glycosylation associated with poor prognosis may result from dysregulation in GALNTs (Brooks and Carter, 2001), also described above, the expression profiles of GALNTs were established for the model cell lines. It was necessary to identify which of the 20 known GALNT genes would be considered within this study. GALNT2 was included as it is considered a "house-keeping" gene and is reported to be expressed ubiquitously (Homa et al., 1993; White et al., 1995). GALNT3 and GALNT6 were reported by Brooks et al. (2007) as being abundantly detectable by immunocytochemistry in aggressive, malignant breast cell lines (ZR751, T47D, MCF7 and DU4475), which also label strongly with HPA, whilst being weakly or undetectable in cell lines (HMT3522 and BT474) where HPA labelling is weak or negative. GALNT14 was chosen as several studies have shown that GALNT14 is implicated in metastasis (Wang et al., 2013; Huanna et al., 2015). GALNT20 or WBSCR17 was included as it is a rarely studied GALNT that

shares a family with GALNT11; both genes have been reported to be involved in cell motility (Nakayama et al., 2012; Takasaki et al., 2014). C1GalT is the most common transferase to build upon the Tn structure (see Section1.3.3) and it has been hypothesised that the abundance of truncated glycosylation in cancers results from reduced expression of C1GalT (Barrow et al., 2013; Hofmann et al., 2015) or its molecular chaperone *COSMC* (Beatson et al., 2015), not upregulation of the GALNTs, and so for completeness C1GalT and *COSMC* were also included in this study.

Aims and objectives

The aims of the experiments described in this chapter were to optimise the HPA lectin labelling procedure and quantification, as well as establishing GALNT/C1GalT/*COSMC* gene expression profiles for the model breast cancer cell lines BT474, ZR751 and MCF7. Therefore, the objectives of this chapter are to:

I. Optimise the HPA lectin labelling procedure for MCF7, ZR751 and BT474 cell lines to ensure that HPA-labelling profiles are consistent with previous reports.
II. Optimise HPA lectin labelling quantification methods to assess in more detail than previously reported the range of aberrant GalNAc-glycosylation in MCF7, ZR751 and BT474 cells.
III. Investigate gene expression levels of a number of GALNT genes as well as C1GalT and *COSMC* in MCF7, ZR751 and BT474 cells to seek mechanisms underlying HPA-binding GalNAc-glycosylation.

3.2 Methods

3.2.1 HPA lectin labelling optimisation

The “standard” HPA lectin labelling procedure (for example, as described by Brooks and Hall, 2012) was originally developed from protocols used to label fixed, paraffin wax embedded histology section with antibodies. HPA lectin labelling of cultured cells is considerably different from labelling prepared histology sections; for example, formalin fixation and processing for paraffin wax embedding is chemically harsh and can mask antigens (Cerio and MacDonald, 1986). Furthermore, antibody binding to an antigen and lectin binding to a carbohydrate have different dynamics (MacCallum et al., 1996; Sanchez et al., 2006). The critical steps, as far as sensitivity and specificity are concerned, of the procedure are the lectin concentration and incubation period. HPA lectin labelling was optimised for MCF7, ZR751 and BT474 breast cancer cell lines. The “standard” procedure (Brooks and Hall, 2012) uses a concentration of 10 µg/ml biotinylated HPA, incubated at room temperature for 1 hour. Using the

"standard" as a starting point, a "checkerboard of conditions" was trialled, testing a range of HPA concentrations and incubation times as illustrated in Figure 3.1 (suppliers of reagents are as listed in Section 2.2). Cells were fixed with 4% v/v PFA in 0.1M PIPES buffer, pH 6.9, for 30min at 4°C. Cells were then washed 3x with PIPES buffer and cells were permeabilised with 0.1% v/v Triton X-100 in PIPES buffer for 10min. Cells were washed 3x with 0.1M PIPES buffer and endogenous peroxidases were blocked with 3% v/v hydrogen peroxide in methanol for 20min. Cells were washed 3x with lectin buffer and then incubated with either 2.5, 5 or 10 µg/ml biotinylated-HPA in 3% w/v BSA in lectin buffer for either 5, 15, 30 or 60 minutes. Cells were washed 3x with lectin buffer and then incubated with 5µg/ml avidin-peroxidase in 3% w/v BSA in lectin buffer for 30min. Cells were washed 3x in lectin buffer and then incubated with DAB-H_2O_2 for 2min. Cells were washed 3x in distilled water and then the cells were counterstained with Harris' haematoxylin for 30sec. Haematoxylin was blued in running tap water for 2min. The cells were dehydrated through an alcohol series, cleared in xylene and mounted using Depex. Three replicates per condition were prepared and all 3 cell lines were trialled. To ensure that the labelling was specific, several controls where included: a positive, a negative and a specificity control, as detailed in Section 2.2, with 3 replicates per control prepared. Slides were observed using a light microscope and HPA lectin labelling intensity and percentage were discerned by eye. This was achieved through an estimation of the intensity of the brown colouration (HPA labelling) of the cells and estimating the percentage of the cells which are labelled; for example cells are either highly labelled (+++), moderately labelled (++), weakly labelled (+) or negative (-) plus an estimate of the percentage of cells labelling positive, from 0-100% as described by Leathem and Brooks (1987).

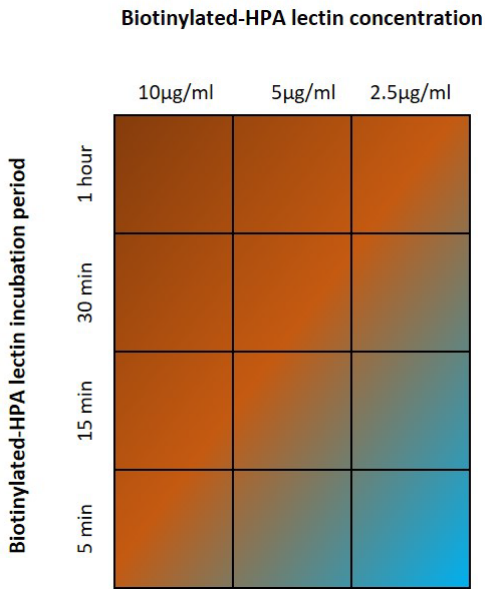

Figure 3.1 *A checkerboard of conditions, testing a range of concentrations of biotinylated-HPA (10 µg/ml, 5 µg/ml and 2.5 µg/ml) and a range of incubation times (1 hour, 30 minutes, 15 minutes and 5 minutes).*

3.2.2 A different quantification method of HPA lectin labelling

A different, more comprehensive quantification method of HPA lectin labelling than was employed in Section 3.2.1 was then developed. This involved physically counting HPA-positive and HPA-negative cells in selected fields of view, rather than their subjective estimation. 6 slides per cell line were HPA lectin labelled using the method optimised in Section 3.2.1 (described in Section 2.2). Starting from the centre of the slide and working outward in an anti-clockwise spiral, 10 discrete fields of view were captured (illustrated in Figure 3.2) using a Zeiss Axioplan microscope fitted with a JENOPTIK ProgResC3 colour camera. Figure 3.3 shows a field of view used for counting. All cells in the field of view were counted unless cells were rounded up, did not contain a visibly labelled nucleus or straddled the edge of the field of view. If the majority of cells in a field of view were un-countable then the next field of view was taken in its place. HPA positive cells were considered as any cells which had brown cytoplasmic labelling of any degree of intensity (+, ++, +++, or ++++) and HPA-negative cells were cells which had a blue cytoplasm (-) as indicated in Figure 3.3.

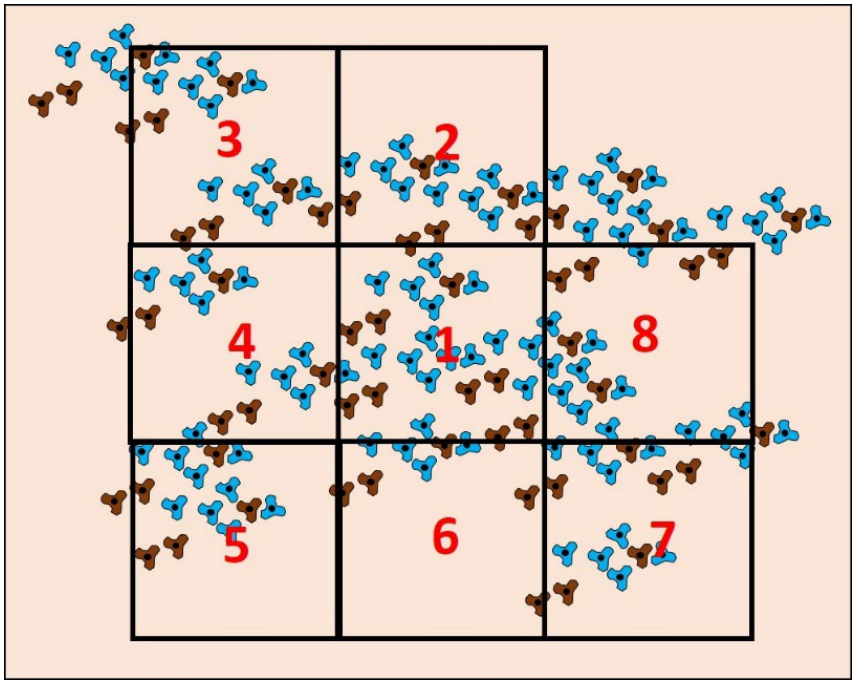

Figure 3.2 *Representation of how images were captured. Images were captured by starting in the middle of the sample and then moving out in an anti-clockwise spiral. 10 discrete fields of view were captured per slide.*

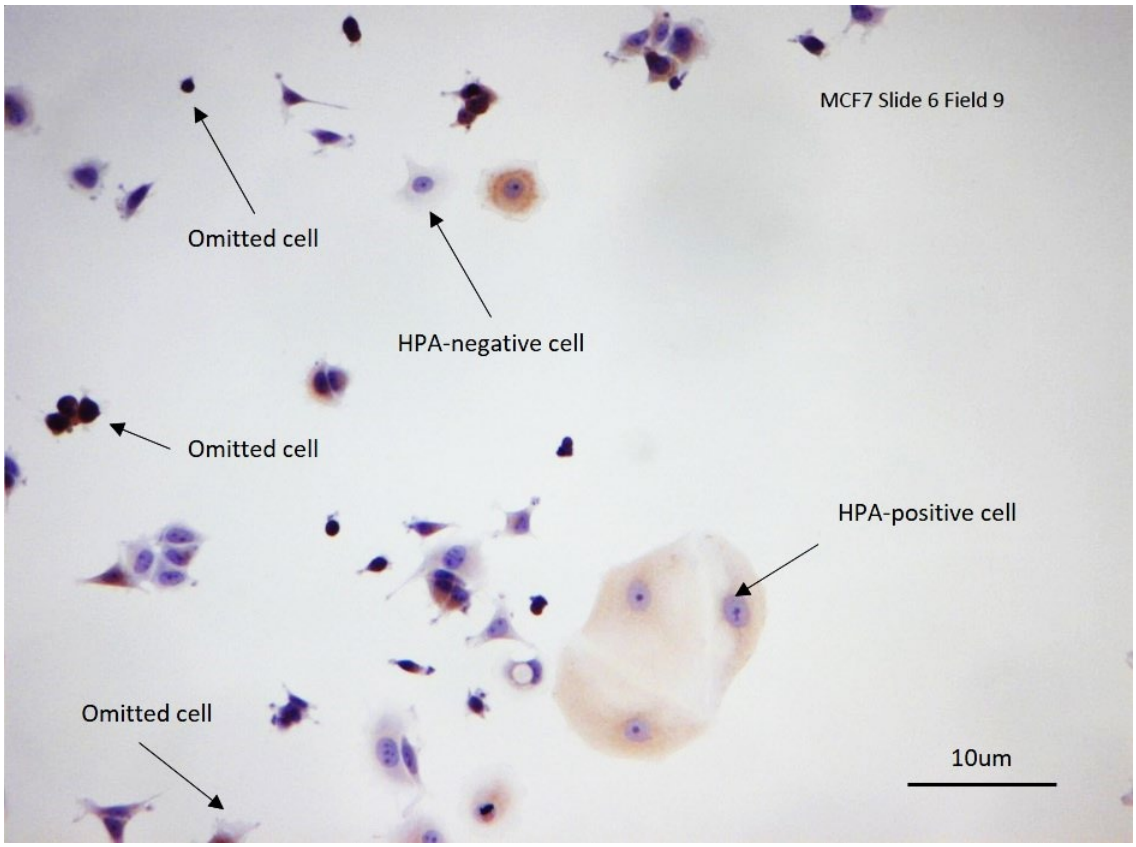

Figure 3.3 *Example field of view of slides prepared for counting HPA-positivity. HPA positive cells were considered as any cells which had brown cytoplasmic labelling as indicated. HPA-negative cells were cells which had a blue cytoplasm as indicated. Cells which were rounded up, did not contain a visibly labelled nucleus or straddled the edge of the field of view were omitted as indicated. Images captured with a Zeiss Axioplan microscope fitted with a JENOPTIK ProgResC3 colour camera. Scale bar = 10µm.*

3.2.3 NanoZoom quantification of HPA lectin labelling and morphology assessment

In order to analyse the glycosylation of the cells, as revealed by HPA labelling, in even greater detail and using an approach that eliminates observer bias to an even greater extent, slides prepared as described in section 3.2.2 were converted into a digital image using a Hamamatsu NanoZoomer 2.0-HT Digital Slide Scanner: C9600 by Dr Alison Forhead at Cambridge University. These images were then imported into a program called NewCast where it was possible to take the complete coverslip as the area to be counted and set up parameters for random zones within the coverslip area to be selected. This was achieved by indicating the number zones required within NewCast, which then randomly generated the desired number of zones, thus removing any potential human bias as to the fields selected for analysis. These zones where then analysed using a program called NDP.viewer, which was then used for all subsequent data collection. For all NanoZoom data collected, the same 20 random zones were used. Of the 20 random zones identified, the first 10 random zones that were suitable for analysis were used for

collecting data. If the zone was out of focus, contained no cells or contained damage from slide processing it was not used and the next random zone was used in its place. Similarly, when counting cells within a selected zone, the same rules applied as detailed in Section 3.2.2 and Figure 3.3 where cells that were rounded-up or did not contain a visibly labelled nucleus, as well as cells straddling the border, were omitted. HPA labelling intensity was classified as: negative (-), slightly positive (+), moderately positive (++), highly positive (+++) or ambiguous (which weren't counted), as illustrated in Figure 3.4. This refinement in assessing labelling provides a more accurate and detailed account of the data collected from section 3.2.2 which merely described the labelling seen within the cell lines as present or absent and also removed observer bias in selection of zones of the slide to be scored. One feature of the software was that cell morphology measurements could easily be taken, an approach that was not possible in the analysis described in Section 3.2.1. As well as HPA labelling intensity, therefore, measurements of the longest (X) and shortest (Y) aspects of a cell were recorded, as illustrated in Figure 3.5. A ratio of the X and Y measurements >2:1 was taken to indicate an elongated morphology and anything under this was termed a rounded morphology.

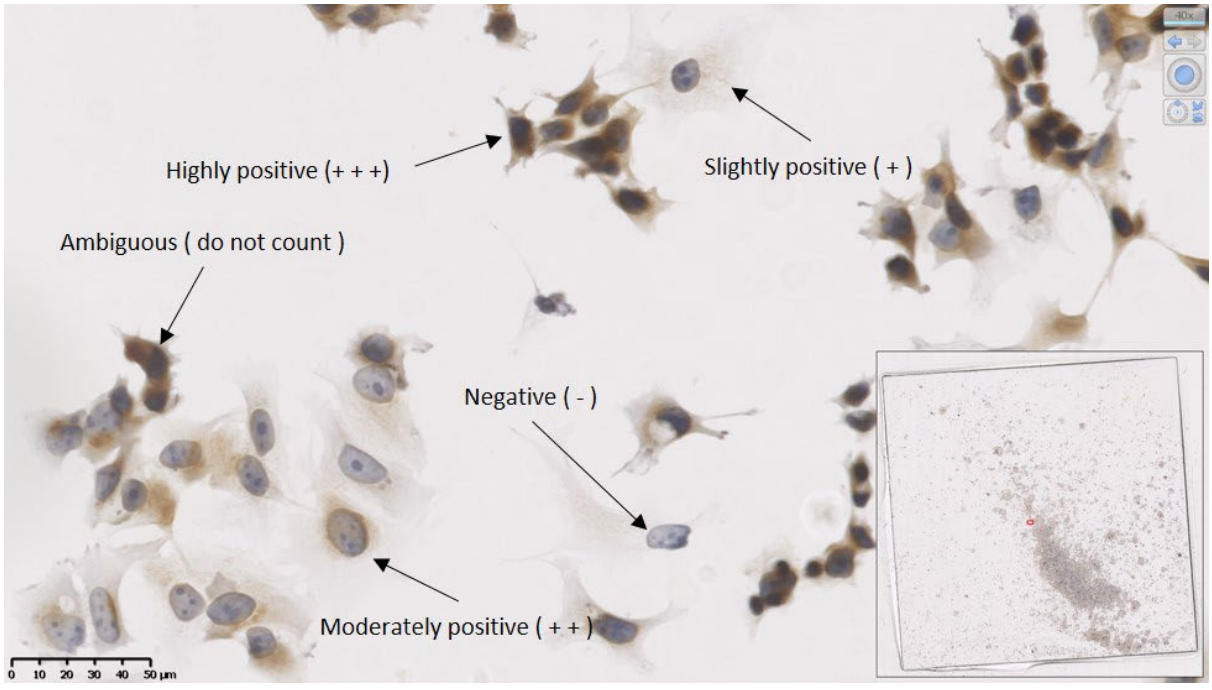

Figure 3.4 *Print screen of a zone in NDP.viewer illustrating cells which are: (-) negative for HPA-labelling, (+) slightly positive, (++) moderately positive, (+++) highly positive and ambiguous, which wasn't counted. Screen shown in bottom right of figure is a view of complete coverslip area, with the small red box indicating where in the coverslip the field of view originates. Scale bar = 50µm.*

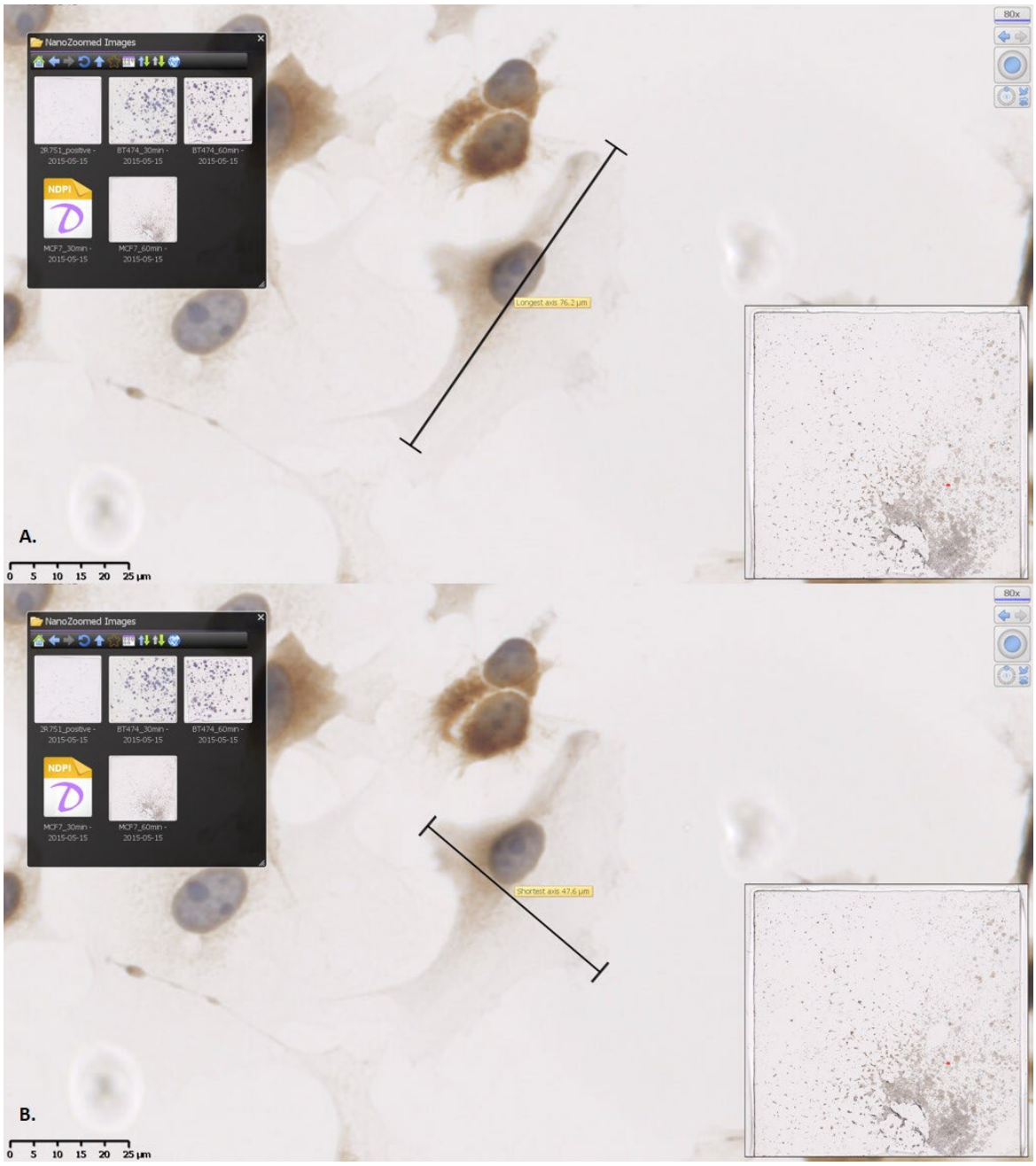

Figure 3.5 *Print screens of a zone in NDP.viewer illustrating how measurements of the longest axis X (A) and the shortest axis y (B) were taken. In this example an MCF7 moderately positive (++) cell measures X = 76.2µm by Y = 47.6µm and so would have an X:Y ratio of 1.6:1 indicating a rounded morphology. Screen shown in bottom right of figures is a view of complete coverslip area, with the small red box indicating where in the coverslip the field of view originates. Screen show in top left of figures is NDP.viewer menu. Scale bar = 25µm.*

3.2.4 Expression levels of GALNTs

Primer pairs were designed and optimised for use with both DNA and RNA (see Table 3.1). RNA was extracted from the cell lines (see Section 2.5 and 2.6) and converted to cDNA (see Section 2.7), which was used in qRT-PCR (see Section 2.8). ACTB and GUSB were the two reference genes chosen to normalise the data to as they were reported to be in the top five most stably expressed reference genes in breast cancer by Gur-Dedeoglu et al. (2009). Data were compiled from 3 biological repeats per cell line as well as minus reverse transcriptase (-RT) and no template control (NTC) controls. Samples were normalised using the delta-delta Ct method where samples were normalised to either ACTB or GUSB and then to MCF7. Normalised data were compared against one another using a 2-tailed t-test, error bars were created from the standard deviation of the mean.

Table 3.1 *Primer pair sequences, and melting temperature (Tm) for genes of interest and reference genes, designed and optimised for use with both DNA and RNA.*

Primer name	**Primer sequence**	**Tm (°C)**
ACTB	(F) 5'-AATGTCACGCACGATTTCCC-3' (R) 5'-CTATCCCTGTACGCCTCTGG-3'	59.2 59.0
GUSB	(F) 5'-AAACCCTGCAATCGTTTCTG-3' (R) 5'-GGCTCCGTATGTGGATGTG-3'	64.3 64.6
GALNT2	(F) 5'-GGTTCCAGACCATCAGGATA-3' (R) 5'-CCCAGCATTGTGACATTCAT-3'	61.8 63.9
GALNT3	(F) 5'-CTCATGATCAGGAAGCGACTC-3' (R) 5'-TGAGAACTACACGGCTGTCG-3'	64.3 64.5
GALNT6	(F) 5'-ATTCCCATTCCTCGTCCTTG-3' (R) 5'-CGCAAAGCAGCTGTGTCTAC-3'	65.4 64.2
GALNT14	(F) 5'-ACTCTCCCGCTGGTTGAAAG-3' (R) 5'-ACCTGTGGGACCAGTTTGAT-3'	65.9 63.7
GALNT20	(F) 5'-TCCTCCCCTCCATTGACAAC-3' (R) 5'-CTGATGGGGAGAGAAGGGTC-3'	55.0 60.0
C1GalT	(F) 5'-GGGCTACATGAGTGGAGGAG-3' (R) 5'-GGCACAAAGGGATGAAAAGT-3'	64.1 63.2
COSMC	(F) 5'-ATCATCCCTCCCTGTTCAGG-3' (R) 5'-GCCCCACTACGTTTGCTATC-3'	58.5 58.7

3.3 Results

3.3.1 HPA lectin labelling optimisation

In order to determine the optimal HPA lectin labelling conditions for the model breast cancer cell lines used within this study, and in agreement with what has been reported previously (Schumacher et al., 1995; Brooks et al., 2001; Brooks and Hall, 2002), a checkerboard of HPA lectin concentration and incubation periods was tested for MCF7, ZR751 and BT474 cell lines. Figures 3.6-3.8, illustrate the HPA-lectin labelling results of all tested conditions for the cell lines. To ensure that HPA lectin labelling was specific, controls were included as detailed in Section 2.2. As illustrated in Figure 3.10, HPA lectin labelling for all three cell lines was specific as all negative controls were negative. Images were assessed for HPA labelling intensity by eye and an estimation of the percentage of HPA-positively labelled cells were given in each case (see Table 3.2). Figure 3.6 illustrates that MCF7 HPA labelling was seen very strongly at both 10µg/ml and 5µg/ml for all incubation periods and labelling was still apparent, but not as intensely, even at 2.5µg/ml and with only 5min incubation. ZR751 cells, illustrated in Figure 3.7, labelled very strongly at both 10µg/ml and 5µg/ml for incubation periods of 1hr to 15min and less so for 5min. For all the remaining options, labelling was moderate to weak with 2.5µg/ml for 15 min, and with 5min incubation not labelling at all. Figure 3.8 illustrates that BT474 HPA labelling was weak to negligible under all conditions. As illustrated in Figure 3.9, HPA concentration 10 µg/ml, incubated for 5 minutes was selected as providing the optimal labelling for all cell lines, as those conditions resulted in the same HPA labelling intensity and proportion of labelled cells consistent with that reported previously (Brooks et al., 2001), therefore, validating these conditions for use in this study.

Table 3.2 *Intensity and percentage of HPA lectin labelling from optimisation of HPA concentration and incubation period of all breast cancer cell lines. Optimised conditions of 10 µg/ml HPA lectin incubated for 5 minutes are highlighted.*

HPA incubation period	**HPA concentration**								
	10 µg/ml			**5 µg/ml**			**2.5 µg/ml**		
	MCF7	ZR751	BT474	MCF7	ZR751	BT474	MCF7	ZR751	BT474
1 hr	++++ (100%)	++++ (99%)	+ (50%)	+++ (100%)	++ (75%)	+ (30%)	+++ (90%)	+ (40%)	+ (10%)
30 min	+++ (100%)	+++ (80%)	+ (50%)	+++ (99%)	++ (75%)	+ (20%)	++ (80%)	+/- (10%)	+/- (5%)
15 min	+++ (100%)	+++ (80%)	+ (40%)	+++ (99%)	+/- (50%)	+/- (5%)	++ (80%)	- (0%)	- (0%)
5 min	**+++ (99%)**	**++ (75%)**	**+/- (30%)**	++ (85%)	+/- (45%)	- (0%)	+ (80%)	- (0%)	- (0%)

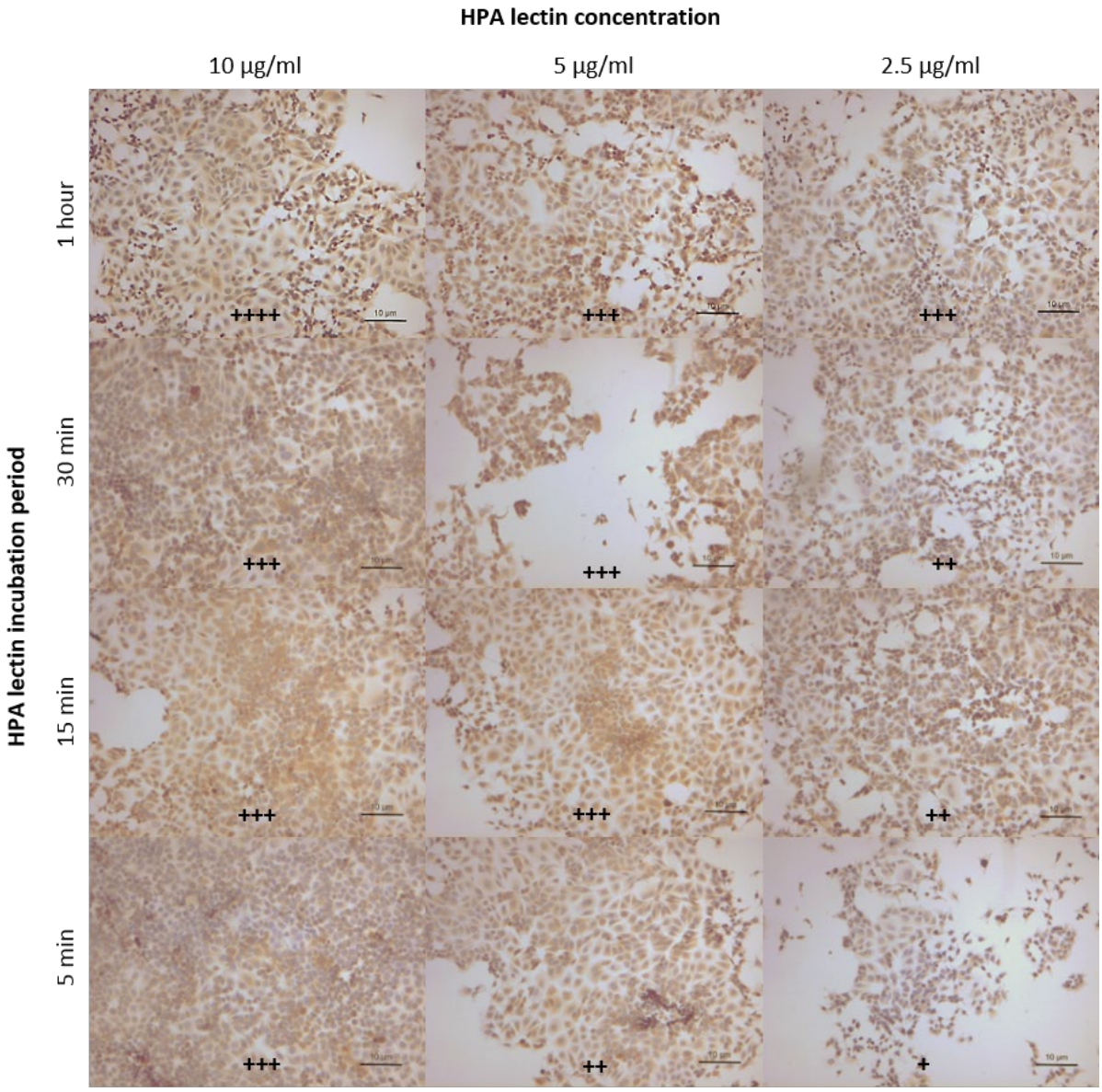

Figure 3.6 *Optimisation of HPA labelling of MCF7 breast cancer cell line. HPA labelling is the strongest (++++) with 10µg/ml biotinylated HPA incubated for 1 hour and gradually decreases in intensity to the weakest (+) labelling observed with 2.5µg/ml biotinylated HPA incubated for 5 minutes. Images representative of 3 biological replicates with 10 images captured per condition. Slides were imaged with a Zeiss Axioplan microscope fitted with a JENOPTIK ProgResC3 colour camera. Scale bar = 10 µm.*

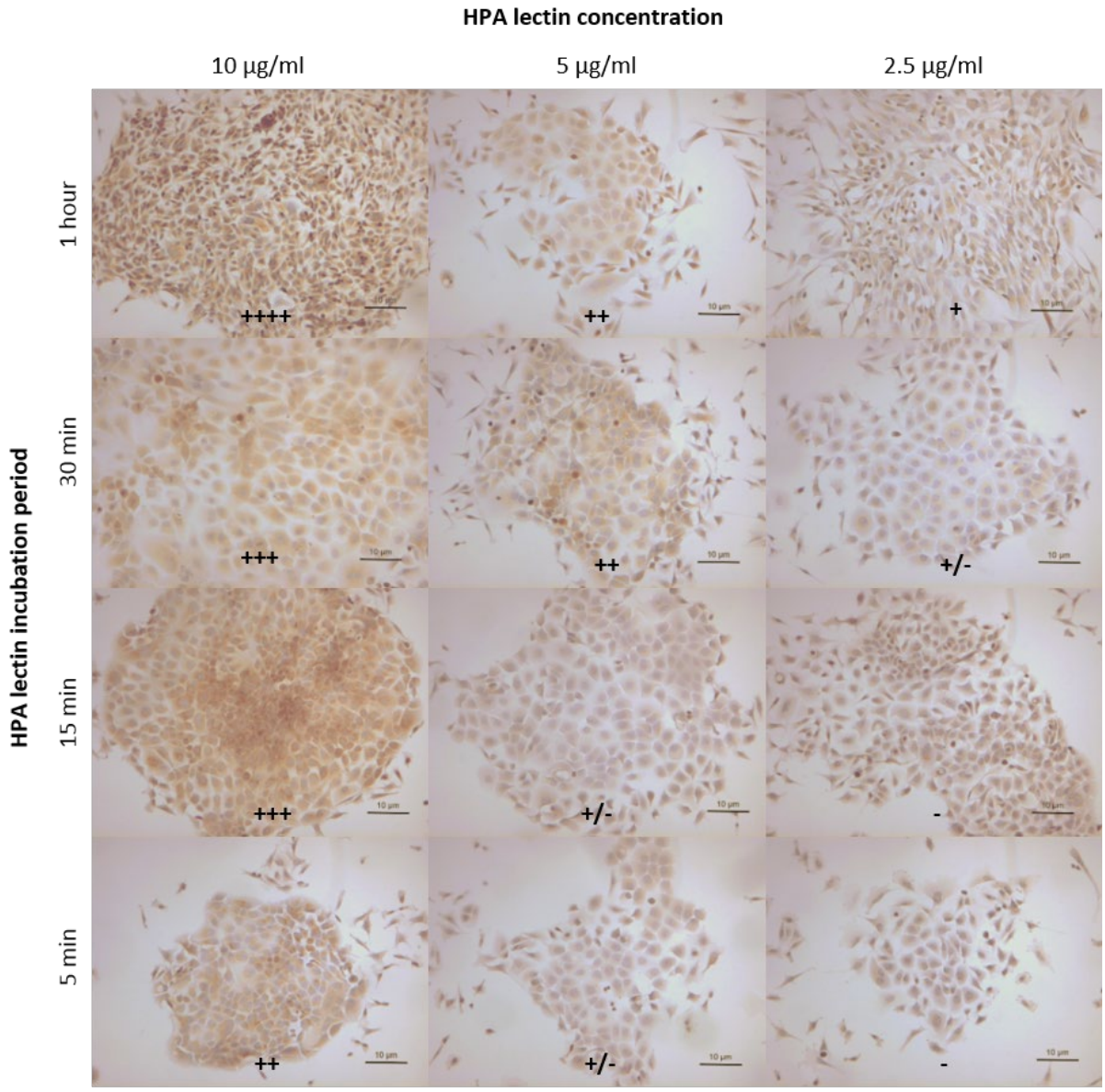

Figure 3.7 *Optimisation of HPA labelling of ZR751 breast cancer cell line. HPA labelling is the strongest (++++) with 10µg/ml biotinylated HPA incubated for 1 hour and gradually decreases in intensity to the weakest (-) labelling observed with 2.5µg/ml biotinylated HPA incubated for 15 and 5 minutes. Images representative of 3 biological replicates with 10 images captured per condition. Slides were imaged with a Zeiss Axioplan microscope fitted with a JENOPTIK ProgResC3 colour camera. Scale bar = 10 µm.*

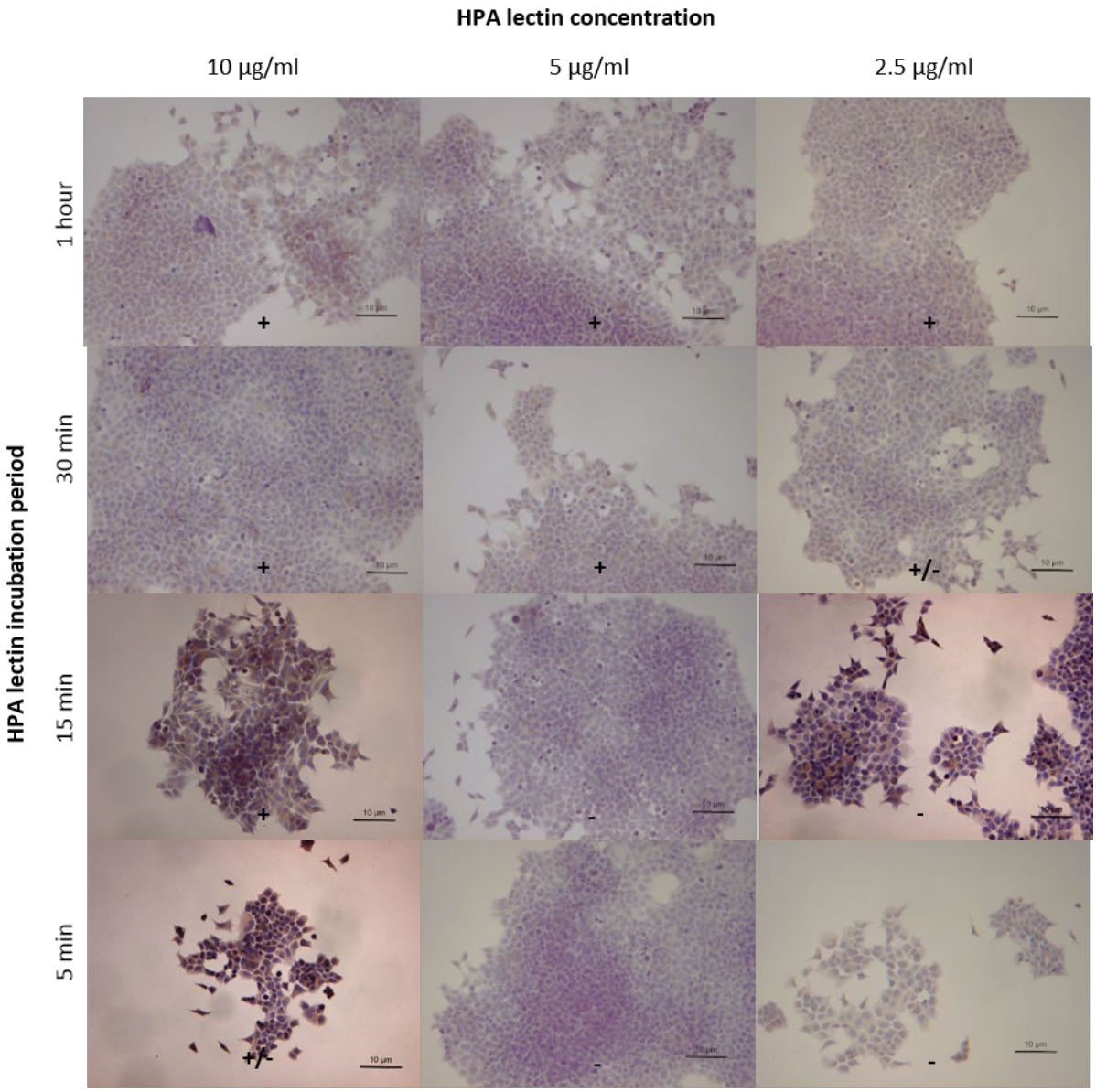

Figure 3.8 *Optimisation of HPA labelling of BT474 breast cancer cell line. HPA labelling is the strongest (+) with 10µg/ml biotinylated HPA incubated for 1 hour, 30 and 15 minutes also with 5µg/ml biotinylated HPA incubated for 1 hour and 30 minutes and with 2.5µg/ml biotinylated HPA incubated for 1 hour and gradually decreases in intensity to the weakest (-) labelling observed with 5µg/ml biotinylated HPA incubated for 15 and 5 minutes also with 2.5µg/ml biotinylated HPA incubated for 15 and 5 minutes. Images representative of 3 biological replicates with 10 images captured per condition. Slides were imaged with a Zeiss Axioplan microscope fitted with a JENOPTIK ProgResC3 colour camera. Scale bar = 10 µm.*

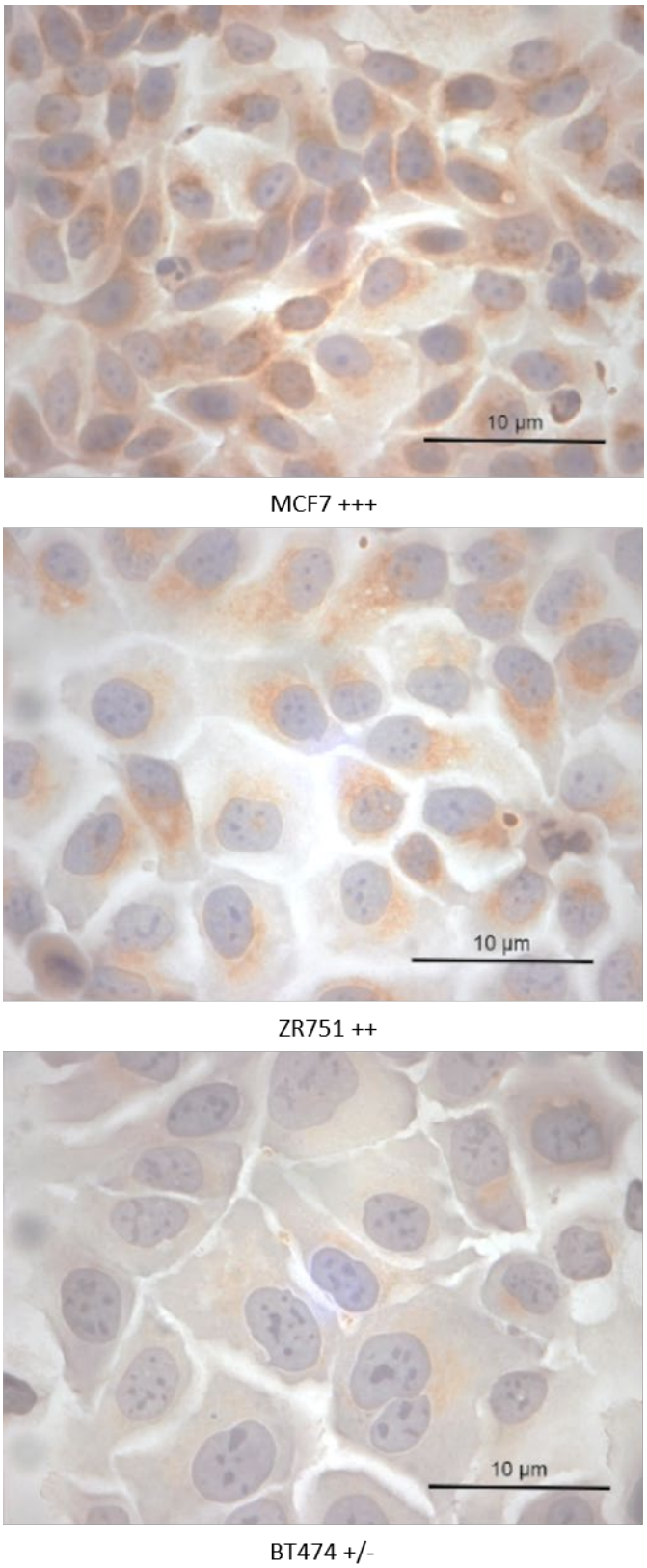

Figure 3.9 *Optimised HPA lectin labelling conditions of 10 µg/ml biotinylated HPA, incubated for 5 minutes. Breast cancer cell lines labelled as follows: MCF7 (+++), ZR751 (++) and BT474 (+/-). Images representative of 3 biological replicates with 10 technical replicates. Images captured with a Zeiss Axioplan microscope fitted with a JENOPTIK ProgResC3 colour camera. Scale bar = 10µm.*

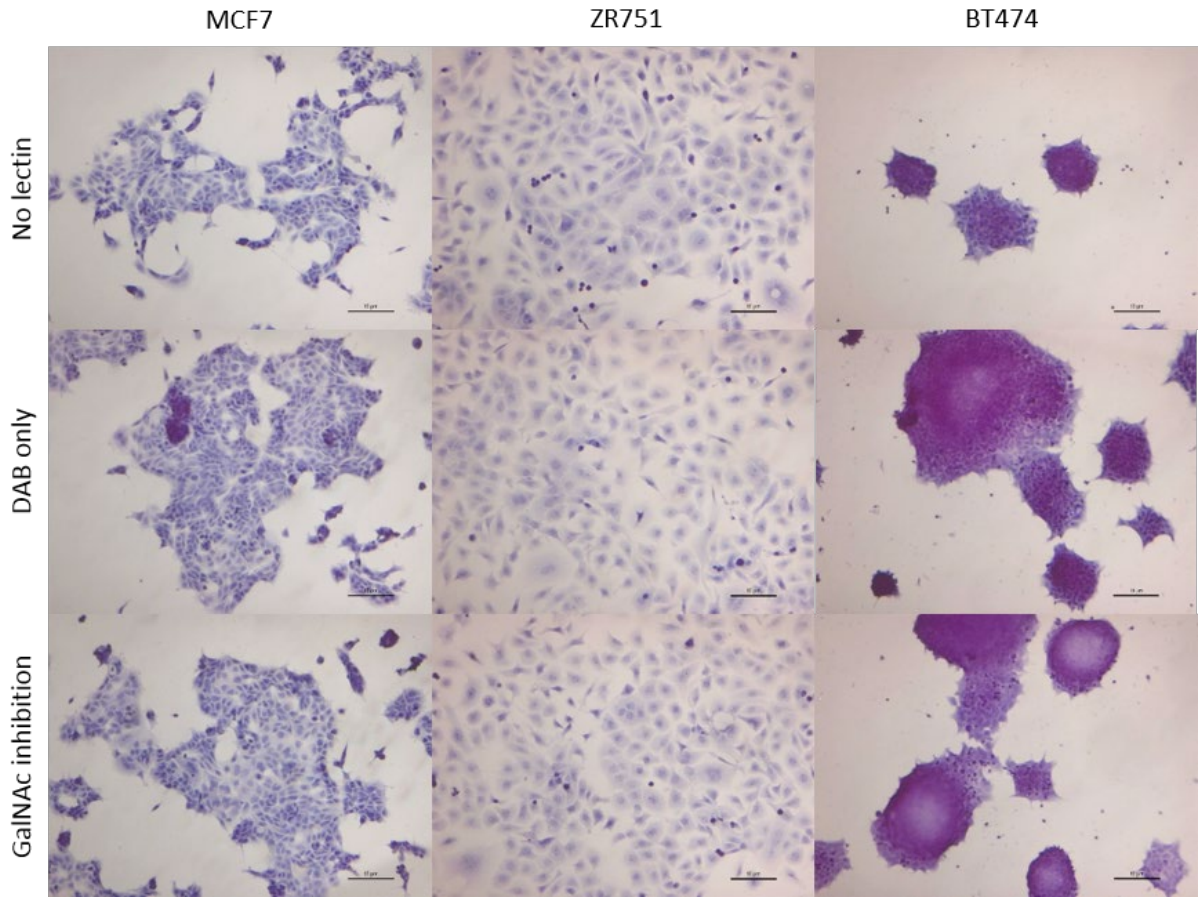

Figure 3.10 *Lectin labelling negative controls. All negative controls had abolished HPA labelling. Images representative of 3 biological replicates with 10 images captured per condition. Images captured with a Zeiss Axioplan microscope fitted with a JENOPTIK ProgResC3 colour camera. Scale bar = 10 µm.*

3.3.2 A different quantification method of HPA lectin labelling

In order to investigate the HPA positivity of the model cell lines further, a different and more detailed quantification method was devised. Previously, quantification of HPA-positive cells was discerned by visual estimation of the intensity of the HPA labelling and an estimate of the percentage of positively labelling cells. Here, cells were HPA labelled with the optimised procedure as described in Section 3.2.1 and 10 fields of view were captured. Cells within the fields of view were individually counted as either HPA-positive cells (of any intensity +++, ++ or +) and the number of negative cells (-). This was performed for each cell line, MCF7, ZR751 and BT474. See data Tables A1.1-A1.3. As illustrated in Figure 3.11, 93.8% of MCF7 cells were HPA-positive; 46.9% of ZR751 cells were HPA-positive; and only 6.44% of BT474 cells were HPA-positive. MCF7 HPA-positivity was significantly greater than both ZR751 ($p<0.001$) and BT474 ($p<0.001$), whilst ZR751 HPA-positivity was significantly greater than BT474 ($p<0.001$). These findings were in agreement with what was determined more subjectively in Section 3.3.1.

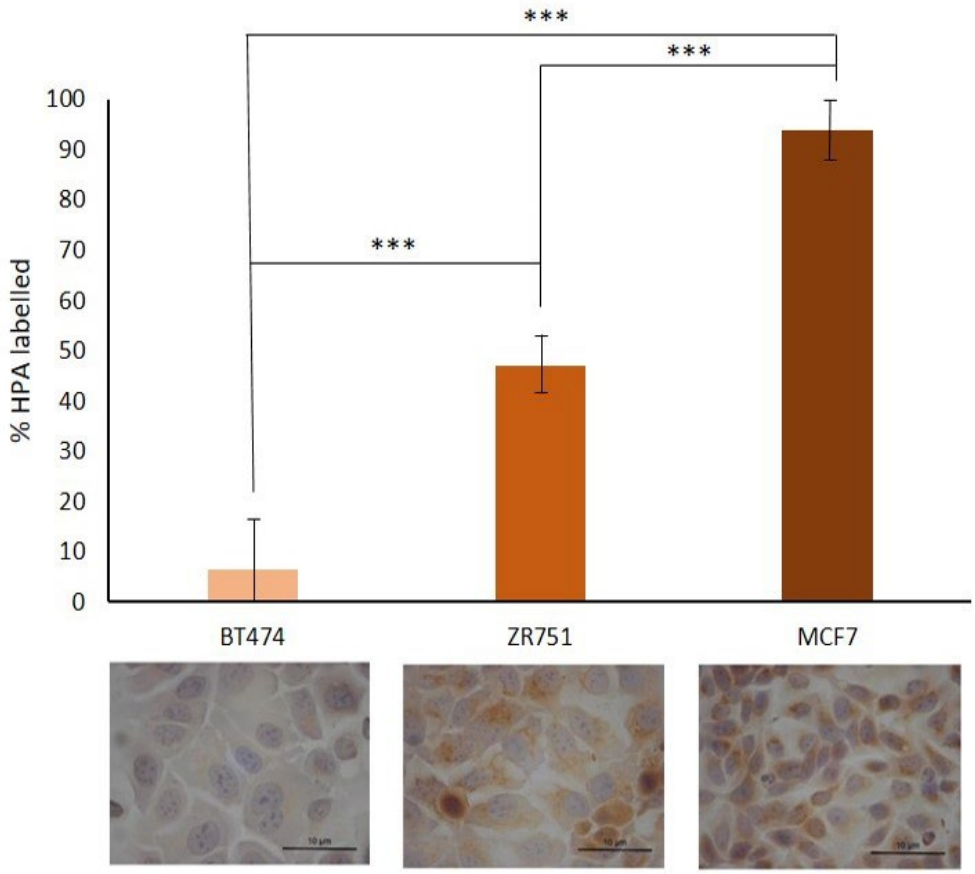

Figure 3.11 *Percentages of HPA-positivity for all three breast cancer cell lines. MCF7 cells labelled highly with HPA with 93.8%, whilst ZR751 cells labelled less with 46.9% of cells being HPA positive. BT474 cells were the least HPA positive with only 6.44% of cells labelling. Error bars are calculated from standard error of the mean. p values are calculated using a two-tailed t-test with unequal variance. Images captured with a Zeiss, Axioplan microscope fitted with a JENOPTIK ProgResC3 colour camera. Scale bar = 10µm.*

3.3.3 NanoZoom quantification of HPA lectin labelling and morphology assessment

In order to better understand the complexities of HPA lectin labelling of the cell lines, a more complex quantification method was employed where digital images of the slides were captured and all cells within randomly selected fields were classified as either negative (-), slightly positive (+), moderately positive (++), highly positive (+++). This allowed the detail of the cell line HPA-labelled identity to reflect not just a percentage of HPA-positive cells, but what proportional intensity of HPA labelling makes up the HPA-positivity. Moreover, the program NewCast randomly generated fields of view selected for analysis, thus removing an element of human bias. NDP.viewer facilitated data analysis. As illustrated in Figure 3.12, MCF7 cells presented as an overwhelmingly HPA-positive population with only 7.8% HPA negative cells, which is split roughly 90:10 between HPA +++ or HPA ++ (strongly HPA-positive) and HPA+ or HPA – (weakly HPA-positive). ZR751 cells were 84.4% HPA-positive, which comprised 27.6% HPA+++, 29.2% HPA++ (i.e. strongly HPA-positive) and 27.6% HPA+ (weakly HPA-positive). The majority of ZR751 cells were HPA++, however the populations were split roughly 50:50 between HPA +++ or HPA ++ (strongly HPA-positive) and HPA+ or HPA – (weakly HPA-positive). BT474 cells were 80.4% HPA-positive, but only 2.9% were HPA+++, and 14.3% HPA++ (strongly HPA-positive) and 63.2% HPA+ (weakly HPA-positive). BT474 cells were therefore predominantly very weakly HPA-positive (HPA+) or HPA-negative (HPA-) (82.8%), which was roughly split 10:90 between HPA +++ or HPA ++ (strongly HPA-positive) and HPA+ or HPA – (weakly HPA-positive). These finding illustrate that the glycosylation profile of a cell line is more complex than previously reported.

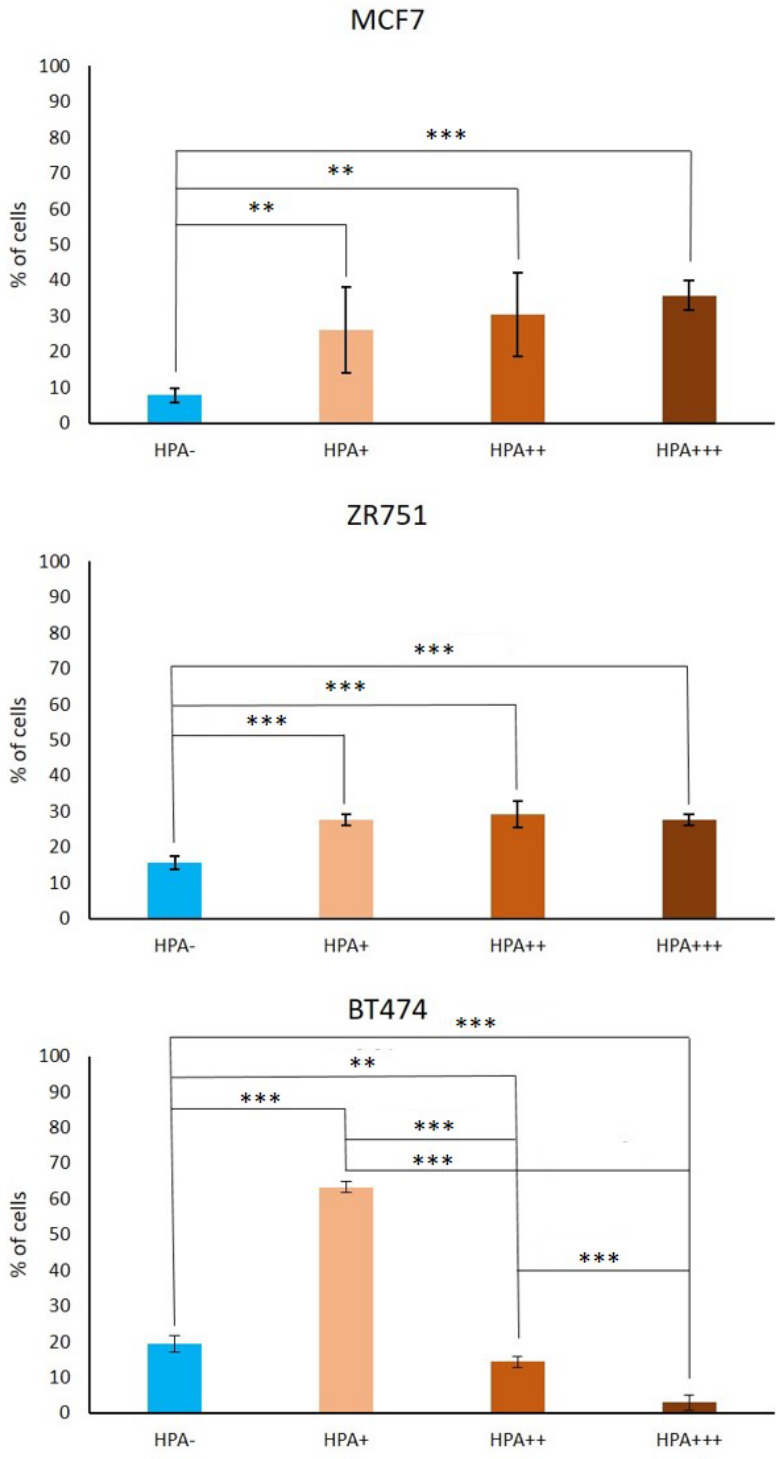

Figure 3.12 *HPA labelling intensities designated as negative (-), slightly positive (+), moderately positive (++) and highly positive (+++) as a percentage of the whole population for MCF7, ZR751 and BT474 cells. MCF7 cells are divided mostly between HPA++ and HPA+++, whilst ZR751 cells are mostly HPA+ and HPA++, and BT474 cells are predominantly HPA+. Data collected using NDP.viewer. Error bars are calculated from standard deviation of the mean and p values are calculated using a two-tailed t-test with unequal variance. Data collected from 3 biological replicates per cell lines with 10 technical replicates each.*

In order to investigate the morphology of cells in relation to their HPA positivity, the longest (X) and shortest (Y) aspects of the cells reported above were recorded against their HPA-labelling intensities. Table 3.3 details the average X:Y ratio as well as the percentage of cells within each HPA labelling intensity for all three cell lines. An X:Y ratio >2:1 was taken to indicate an elongated morphology. It became clear that the MCF7 cells had a rounded morphology across all HPA labelling intensities (as illustrated in Figure 3.13). ZR751 cells, however, displayed considerably greater morphological variation across HPA labelling categories than MCF7 cells. As illustrated in Figure 3.13 and Table 3.3, ZR751 HPA-negative cells were significantly more elongated (with an X:Y ratio of 2.34:1) than HPA + (X:Y ratio 1.96:1, $p<0.01$), HPA ++ (X:Y ratio 1.68:1, $p<0.001$) and HPA +++ (X:Y ratio 1.67:1, $p<0.001$) cells. The same was observed in BT474 cells where HPA-negative cells were significantly more elongated (with an X:Y ratio of 2.47:1) than HPA+ (X:Y ratio 1.73:1, $p<0.001$), than HPA++ (X:Y ratio 1.54:1, $p<0.001$) and HPA+++ (X:Y ratio 1.76:1, $p<0.001$) cells.

Table 3.3 *Average percentage HPA labelled, X:Y ratio and corresponding morphology against HPA labelling intensity for: MCF7, ZR751 and BT474 cells.*

	HPA-labelling intensity			
	HPA -	**HPA +**	**HPA ++**	**HPA +++**
MCF7				
% HPA labelled	7.76	26.12	30.35	35.76
Average X:Y ratio	1.99:1	2.00:1	1.93:1	2.00:1
Morphology	**Rounded**	**Rounded**	**Rounded**	**Rounded**
ZR751				
% HPA labelled	15.6	27.6	29.2	27.6
Average X:Y ratio	2.34:1	1.96:1	1.68:1	1.67:1
Morphology	**Elongated**	**Rounded**	**Rounded**	**Rounded**
BT474				
% HPA labelled	19.5	63.24	14.34	2.94
Average X:Y ratio	2.47:1	1.73:1	1.54:1	1.67:1
Morphology	**Elongated**	**Rounded**	**Rounded**	**Rounded**

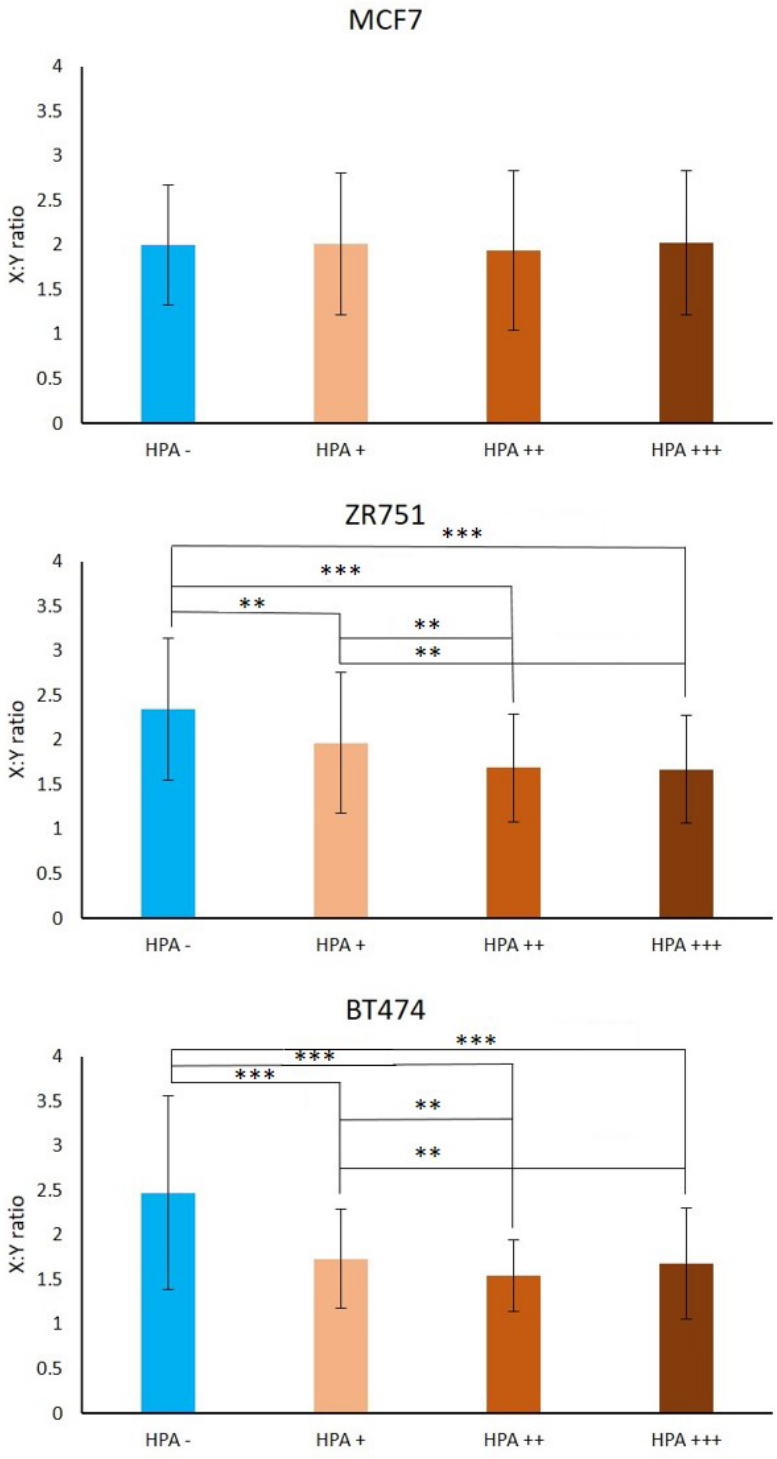

Figure 3.13 *Morphology (X:Y ratio) plotted against HPA labelling intensity for MCF7, ZR751 and BT474 cells. MCF7 cells do not appear to have any relationship between HPA labelling status and their morphology, whilst ZR751 and BT474 HPA-negative cells are significantly more elongated than HPA-positive cells irrespective of intensity. Data collected using NDP.viewer. Numbers (n) of Y axis are n:1. Error bars are calculated from standard deviation of the mean and p values are calculated using a two-tailed t-test with unequal variance. Data collected from 3 biological replicates per cell lines with 10 technical replicates each.*

3.3.4 Expression levels of GALNTs

In order to determine the expression levels of chosen GALNTs (GALNT2, GALNT3, GALNT6, GALNT14, GALNT20) as well as the transferase (C1GalT) and its chaperone (*COSMC*), qPCR was performed and the data analysed using the delta-delta Ct method. If aberrant expression of GALNTs results in greater exposure of terminal GalNAc-glycans recognised by HPA, we would expect that the MCF7 and ZR751 cells, which label highly and moderately, respectively, with HPA, would have a number of differentially expressed GALNTs. Conversely, BT474 cells which label weakly with HPA would have the least number of differentially expressed GALNTs. Similarly, it would be expected that C1GalT and *COSMC*, responsible for chain extension and therefore reduction in exposed Tn and consequent HPA-labelling, would be reduced in both MCF7 and ZR751 cells, and increased in BT474 cells. Figures 3.14 and 3.15 illustrate the mRNA expression levels of the chosen genes when normalised to MCF7 and either ACTB or GUSB, respectively.

When normalised using either ACTB or GUSB, ZR751 cells expressed significantly more ($p<0.01$ or $p<0.05$, respectively) GALNT2 than MCF7 cells. MCF7 cells normalised to ACTB expressed significantly more GALNT3 ($p<0.01$) than ZR751 cells. When normalised to GUSB, ZR751 cells expressed significantly more ($p<0.001$) GALNT20 than MCF7 cells. These findings are in opposition with what was expected, with MCF7 cells expressing significantly less GALNTs than weakly HPA-positive BT474 cells. When normalised to GUSB, MCF7 expressed significantly less C1GalT ($p<0.05$) than ZR751 cells. Also, when normalised to GUSB, MCF7 cells expressed significantly less C1GalT ($p<0.05$) than BT474 cells. When normalised either ACTB or GUSB, MCF7 cells expressed significantly less *COSMC* ($p<0.05$ or $p<0.01$, respectively) than ZR751 cells and BT474 cells ($p<0.01$ or $p<0.05$). Also, ZR751 cells expressed significantly more *COSMC* than BT474 cells ($p<0.05$). These data suggest that MCF7 cells, which label highly with HPA and therefore synthesise high levels of GalNAc-glycans, have a reduction in C1GalT and *COSMC* but there is no clear indication that aberrant GALNT expression is responsible for the synthesis of HPA-binding GalNAc-glycans in the three cell lines.

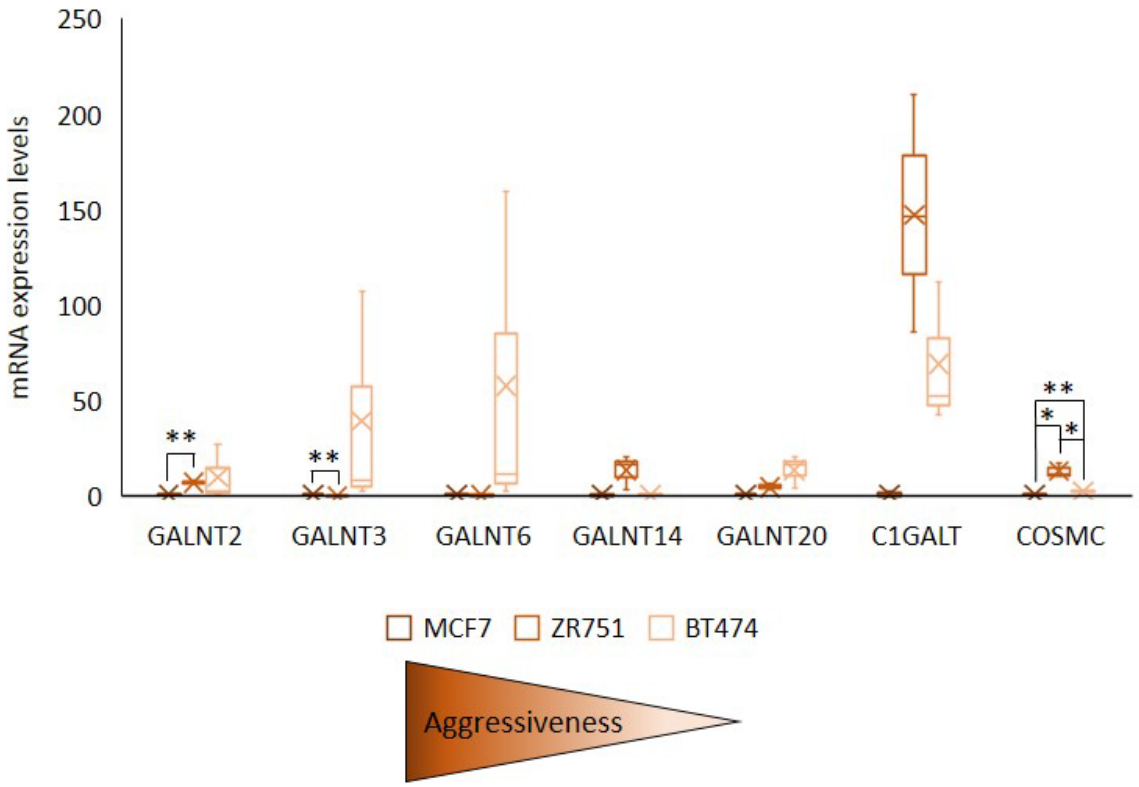

Figure 3.14 *mRNA expression levels of GALNT2, GALNT3, GALNT6, GALNT14, GALNT20, C1GalT and COSMC normalised using the ΔΔCt method to ACTB and MCF7. There is no apparent correlation between HPA labelling and GALNT expression, however MCF7 cells express significantly less COSMC than either ZR751 and BT474 cells suggesting a possible role of failed normal chain extension as a cause for the increased amount of terminal GalNAc residues. Data compiled from 3 biological replicates per cell line. Normalised data were compared against one another using a 2-tailed t-test. MCF7 cells are considered a more aggressive breast cancer cell line than ZR751 cells and BT474 cells are the least aggressive as they are poorly tumorigenic in animal models which is represented by the aggressiveness triangle.*

Table 3.4 *p values for Figure 3.13 mRNA expression levels of genes of interest normalised to reference gene ACTB. Significant p values have been highlighted.*

	MCF7/ZR751	MCF7/BT474	ZR751/BT474
GALNT2	**0.005923**	0.401299	0.767565
GALNT3	**0.005877**	0.377217	0.369164
GALNT6	0.130694	0.380387	0.376506
GALNT14	0.137391	0.611012	0.133093
GALNT20	0.055383	0.118425	0.198036
C1GalT	0.054934	0.088861	0.150655
COSMC	**0.03126**	**0.001403**	**0.041467**

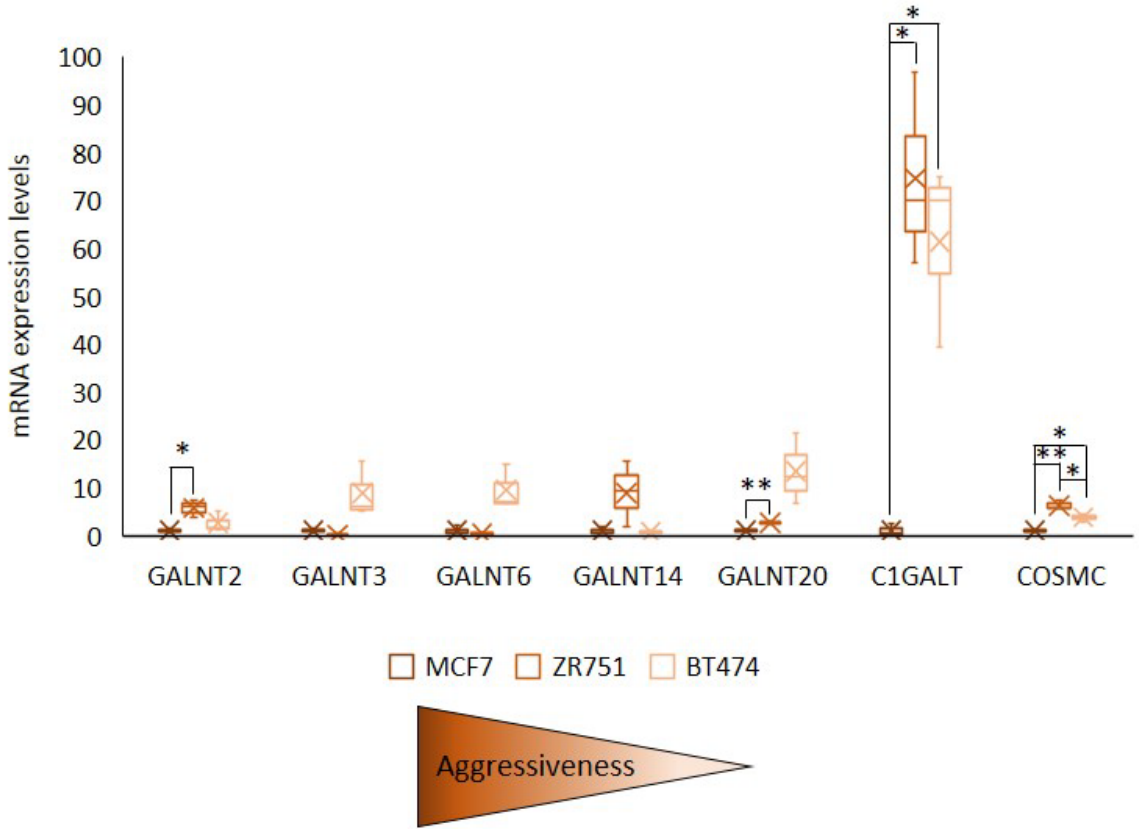

Figure 3.15 *mRNA expression levels of GALNT2, GALNT3, GALNT6, GALNT14, GALNT20, C1GalT and COSMC normalised using the ΔΔCt method to GUSB and MCF7. There is no apparent correlation between HPA labelling and GALNT expression, however MCF7 cells express significantly less C1GALT and COSMC than either ZR751 and BT474 cells suggesting a possible role of failed normal chain extension as a cause for the increased amount of terminal GalNAc residues. Data compiled from 3 biological replicates per cell line. Normalised data were compared against one another using a 2-tailed t-test. MCF7 cells are considered a more aggressive breast cancer cell line than ZR751 cells and BT474 cells are the least aggressive as they are poorly tumorigenic in animal models which is represented by the aggressiveness triangle.*

Table 3.5 *p values for Figure 3.14 mRNA expression levels of genes of interest normalised to reference gene GUSB. Significant p values have been highlighted.*

	MCF7/ZR751	MCF7/BT474	ZR751/BT474
GALNT2	**0.041356**	0.328203	0.128385
GALNT3	0.065442	0.141693	0.121132
GALNT6	0.271487	0.081629	0.074203
GALNT14	0.183998	0.601847	0.175699
GALNT20	**0.000771**	0.10208	0.129999
C1GalT	**0.024376**	**0.031813**	0.463765
COSMC	**0.008948**	**0.022911**	**0.03235**

3.4 Discussion

The work described in this chapter began by optimising an HPA lectin labelling method for use with cultured cells instead of paraffin wax embedded histology samples. This resulted in a labelling method in which the HPA incubation step was reduced from 1 hour to 5 minutes and which gave labelling entirely consistent with that previously reported in the literature (Brooks et al., 2001) for the cell lines under study (MCF7, ZR751 and BT474). Confirmation that HPA binding occurs effectively in less than 5 minutes may prove to be beneficial in other applications, including those described in other parts of this thesis. The "standard" labelling protocol reported by Brooks and Hall (2012) had originally been adapted from published protocols optimised for antibody labelling in immunohistochemistry and that equivalent lectin labelling could be achieved with such a reduced incubation time is consistent with the idea that lectins bind much more quickly than antibodies. In the case of endogenous human lectins, GALNTs of the Y subfamily (which include GALNT8, GALNT9, GALNT17 and GALNT18) have lectin binding sites which act as chaperones to other GALNTs (Raman et al., 2012). Here, having a rapid binding time would be beneficial physiologically as the Y subfamily modulate the kinetic properties of the remaining GALNTs (Wandall et al., 2007). The optimised HPA labelling protocol will be employed in further investigations reported in this thesis.

Using the optimised HPA labelling method, HPA lectin labelling was initially quantified by eye as a subjective estimate of percentage of the cells that were labelled alongside an estimation of the intensity of the HPA labelling, consistent with the assessment method employed in numerous published studies (e.g. Leathem and Brooks, 1987; Fenlon et al., 1987; Fukutomi et al., 1989; Alam et al., 1990; Fukutomi et al., 1991; Thomas et al., 1993; Noguchi et al., 1993; Brooks et al., 1993; Brookes et al., 1996; Brooks and Wilkison, 2003). This confirmed that HPA labelling of the cell lines achieved using the optimised method gave results consistent with that previously reported in the literature for these cell lines (Schumacher et al., 1995; Brooks et al., 2001). A different quantification method was then employed where defined fields of view were selected according to a pre-designed grid pattern and every individual cell counted as either HPA-negative or HPA-positive (with any degree of positivity). This approach reflected the practice of defining clinical tumour specimens as simply HPA "stainers" and "non-stainers" adopted by some authors (e.g. Brooks et al., 2001; Schumacher et al., 1994a), based on the observation that it was the presence or absence of the glycosylation pattern detected by HPA-labelling, and not its intensity that carried prognostic significance. It also gave a more precise count of HPA-labelling and non-labelling cells within the cell population. Results of this analysis revealed that 93.8% of MCF7 cells, 46.9% of ZR751 cells and 6.44% of BT474 cells were HPA-positive. These proportions are consistent with what was observed by eye in the previous analysis and with what was previously reported in the literature (Brooks and Leathem, 1991; Schumacher et al., 1995; Brooks et al., 2001), therefore confirming that these cell lines exhibit a stable HPA-binding profile over time and in different laboratories.

In order to provide more detailed information on the HPA lectin labelling profile of the cell lines, a more complex approach was employed, where digital images of HPA labelled slides were created, viewed in a program called NDP.viewer and fields of view selected using the software NewCast. This allowed for analysis of the entire slide, random selection of fields for analysis thereby removing an aspect of human bias, and in the analysis cells were scored as either highly positive (+++), moderately positive (++), slightly positive (+) or negative (-) for HPA labelling. Thus, a more detailed and complex profile of glycosylation revealed by HPA labelling than has been reported previously was determined. This, plus the earlier observation that the cell lines consistently exhibit different and stable profiles of HPA-labelling suggests that there is fine regulation of glycosylation occurring.

Little is known about how glycosylation is controlled, although the GALNT gene family, which initiates O-linked GalNAc glycosylation, plays a role in O-glycosylation regulation by interplay of their large family number (20 isoenzymes in humans) and in their acceptor peptide substrate specificities. There is not complete functional redundancy between them, as they have distinct acceptor peptide substrate specificities with some overlap. For example, it is theorised that some members of the family show preference for unmodified peptide sequences, or partially glycosylated peptide sequences (reviewed by Bennett et al., 2012). GALNT1s lectin and catalytic domains are closely associated, so is therefore thought to prefer acceptors in high O-glycan density regions (Fritz et al., 2004). GALNT2s lectin and catalytic domains show little interaction and so it is thought that they prefer low-density O-glycan or "naked" peptide acceptors (Fritz et al., 2006). Furthermore, some GALNTs show preference for glycosylating Ser or Thr residues; for example, GALNT2 prefers to glycosylate Thr versus Ser (Fritz et al., 2006). Also, the Y family of GALNTs do not have a functional catalytic domain and instead act as chaperones by binding GalNAc on partially glycosylated peptide sequences therefore increasing the activity of the other GALNTs members and adding a further layer of control (Li et al., 2011).

The heterogeneity of glycosylation profiles within cell population is intriguing and is consistent with what has been observed in clinical tumours (Brooks and Leathem, 1999) where a significant sub-population of cells within a tumour labelled ++ to +++ whilst the remaining tumour cells were negative for HPA labelling. The findings detailed in this chapter illustrate that the glycosylation profiles of the cell lines is more complex than previously reported and a more detailed classification of HPA labelling intensity, as reported here, may provide a clearer picture of glycosylation as a prognostic tool. Furthermore, it is clear that subtle control of glycosylation is at play for cell lines to display heterogeneous, yet consistently proportioned, HPA-binding glycosylation profiles, consistent with that observed in clinical tumours.

The NDP.viewer programme allowed for other aspects of the digital images of the cells to be conveniently assessed, and morphology of the cells was thus evaluated. The longest (X) and shortest (Y) axis of the cells was measured and recorded alongside their HPA labelling intensity. An X:Y ratio of >2:1

was taken to indicate an elongated morphology and anything below this was classified as a rounded morphology. Analysis revealed that for ZR751 and BT474 cells, unexpectedly, HPA-negative (–) cells had an elongated morphology whilst HPA-slightly positive (+), HPA-moderately positive (++) and HPA-highly positive (+++) cells had a rounded morphology. This association was not observed in MCF7 cells, which all exhibited a rounded morphology. A rounded morphology is associated with epithelial, non-invasive cells, whilst elongated morphology is associated with invasive mesenchymal cells (as reviewed by Yang and Weinberg, 2008). This unexpected association between HPA-positivity and an epithelial morphology and HPA-negativity with a mesenchymal morphology in cell populations within a cell population is intriguingly reminiscent of EMT, described in Section 1.2.2.i. This distinction may not have been observed if not for categorising HPA labelling intensity in the manner described in this chapter.

Schumacher et al. (1992) first reported in a SCID mouse model that in spite of the strong association between the HPA positivity of the primary tumour and its metastatic competence, HPA-positive tumours can give rise to both HPA-positive and HPA-negative metastases. This was later confirmed by Brooks and Leathem (1999) using clinical primary breast cancer samples and samples of metastases later taken at post mortem-examination. They reported that the primary tumours were all HPA-positive whilst only 79% of metastases were HPA-positive. They explained this observation by suggesting that further disruptions in the glycosylation pathways as tumours progressed resulted in the emergence of HPA-negative clones and HPA-negative metastases. The results of the work presented in this chapter suggest another, intriguing, possibility that populations of cells undergoing EMT, and the reverse process MET, might, as well as changing morphological characteristics, change their glycosylation.

In order to determine whether altered expression of GALNTs was responsible for exposure of the terminal GalNAc-glycans that HPA recognises, qPCR analysis was performed. Several GALNTs were chosen to be assessed for expression in MCF7, ZR751 and BT474 cell lines using qPCR. Previously, Brooks et al. (2007) reported GALNT3 and GALNT6 to be abundantly detectable by immunocytochemistry in the aggressive breast cancer cell lines ZR751, T47D, MCF7 and DU4475. These cell lines were also reported to label extensively with HPA lectin. GALNT3 and GALNT6 were not detectable in the less aggressive cell lines HMT3522 and BT474, which exhibit considerably less HPA labelling. These findings suggested that GALNT expression might correlate with HPA binding. When several GALNT genes were investigated for expression in MCF7, ZR751 and BT474 in the study reported here, no correlation between HPA labelling and GALNT (GALNT2, GALNT3, GALNT6, GALNT14, GALNT20) expression was discerned. This may be because GALNTs other than the ones studied here are also involved in this process. For example, some GALNTs act as molecular chaperones to other members of the family thereby increasing their capacity to catalyse O-linked reactions (Li et al., 2012). Alternatively, relocation of GALNTs to the ER from the Golgi apparatus could result in prolonged exposure to GALNTs without the need for increased expression levels (Gill et al., 2011). Gill et al. (2010) demonstrated that activation of Src kinase in the

Golgi apparatus by EGF and/or PDGF selectively re-distributes Golgi-localised GALNTs to the ER, which subsequently results in increased protein O-glycosylation density as well as increasing the truncated O-glycans that are frequently observed in cancers. In the study reported here, alongside the GALNTs, C1GalT and *COSMC* expression levels were investigated. C1GalT and its molecular chaperone *COSMC* build core 1, the next most commonly occurring O-linked glycan structure after Tn. Both C1GalT and *COSMC* were significantly downregulated in MCF7 cells compared to ZR751 and BT474. This is consistent with failure of normal chain extension (building of core 1) resulting in MCF7 cells being highly HPA labelled. Barrow et al. (2013) reported that knock-down of C1GalT in colon cancer cells resulted in an increase in the truncated O-linked glycans Tn, TF and sTn. *COSMC* is essential for expression of C1GalT, and must be present during C1GalT translation, or the enzyme is inactive (Narimatsu et al., 2011). Ju et al. (2008b) reported that knock-down of *COSMC* resulted in failure of formation of active C1GalT, which also increased the prevalence of Tn and sTn antigens in colorectal cancer cells, therefore demonstrating that both C1GalT and *COSMC* are essential for normal chain extension of O-linked protein glycosylation. Taken together, these finding suggest that there is no clear indication that aberrant GALNT expression is responsible for exposure of GalNAc-glycans recognised by HPA. However, the significant reduction in expression of C1GalT and *COSMC* in MCF7 cells compared to both ZR751 and BT474 suggests a possible role of lack of normal chain extension as being a cause for MCF7 cells labelling strongly for GalNAc-glycans.

3.5 Key findings

- The HPA lectin labelling procedure was optimised, which enabled the incubation period of HPA lectin to be reduced from 1 hour to 5 minutes.
- MCF7, ZR751 and BT474 cells exhibit a range of HPA labelling intensities, which demonstrates that their glycosylation profiles, as far as GalNAc-glycans are concerned, are more complex than previously reported.
- HPA-negative cells are significantly more elongated in morphology than HPA +, HPA ++ and HPA +++ cells in both ZR751 and BT474 cell lines, suggesting a potential link between GalNAc-glycosylation and EMT.
- No relationship was observed between GALNT expression and exposure of GalNAc-glycans detected by HPA lectin labelling. However, C1GalT and *COSMC* are significantly down-regulated in strongly HPA-binding MCF7 cells suggesting that a failure in normal chain extension may contribute to the exposure of truncated GalNAc-glycans.

Chapter 4

Isolation of viable glycosylation-specific cell populations for further *in vitro* analysis using lectin-coated magnetic beads.

4.0 Isolation of viable glycosylation-specific cell populations for further *in vitro* analysis using lectin-coated magnetic beads

4.1 Background

HPA binding profiles of the cell lines were characterised as described in Chapter 3.0, revealing a difference in morphology between the HPA-positive (+++/++/+) and HPA-negative (-) cells. It was observed that HPA-positive cells generally exhibited a round morphology whilst HPA-negative cells were more elongated. To explore this further, an assay was developed which enabled isolation of the two populations so that they could be studied independently from one another. Figure 4.1 illustrates the cell separation procedure, which is described in Section 2.3 and published (Beaman et al., 2017, see Appendix 3). Initially, streptavidin linked magnetic beads were mixed with biotinylated-HPA to immobilise the HPA on the surface of the beads. Then, cells were scraped from their culture flask and counted. The HPA-coated beads where mixed briefly with the prepared cells and then, HPA binding cells attached to the beads were isolated from the unbound population by using a magnet. To dissociate the HPA/beads from the HPA-positive cells, competitive inhibition was performed by the addition of the monosaccharide α-GalNAc. The freed beads were isolated using a magnet leaving free HPA-positive cells.

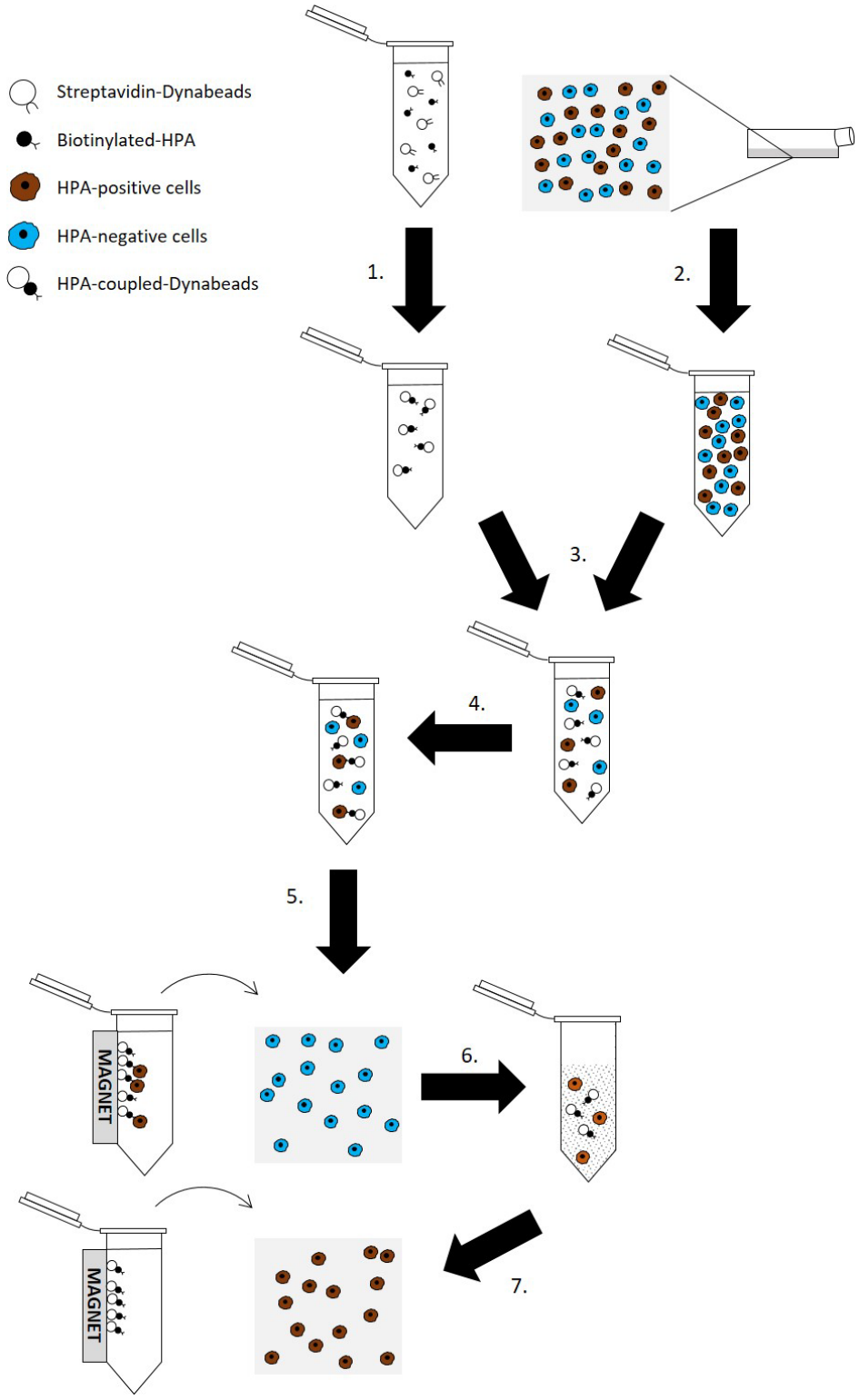

Figure 4.1 *Cell separation with HPA coated magnetic beads. 1. Biotinylated HPA and streptavidin magnetic beads are combined in an end-over-end mixer. 2. Cells are removed from their flask and (3.) added to the bound lectin/beads. 4. HPA-positive cells bind to lectin/beads, (5.) and are isolated with a magnet, allowing for HPA-negative, unbound cells to be removed. 6. HPA-positive cells are removed from the lectin/beads using competitive inhibition with 0.1M GalNAc and (7.) then the lectin/beads are pooled with a magnet and the HPA-positive cells removed.*

Isolation of distinct populations of cells from a heterogeneous population allows for the study of discrete cell types. Isolated cells are considered to be where "a population of cells is depleted of cells which share particular characteristics" (Sharpe, 1988). However, it is important to note that no separated cell population can be considered to be completely "pure", as a population of one cell type is not entirely homogeneous (Baguley and Leung, 2010). The efficiency of a cell separation technique can be determined by a combination of purity and "recovery". Recovery can be considered in two ways: 1. total recovery, where the number of separated cells as a percentage of the total cell count of the unseparated population, or 2. target recovery, where the number of separated cells are measured against the number of target cells in the original population. Total recovery is used in assessing whether cells have been lost during the procedure. However, perhaps, the more important of the two is target recovery as this is a measure of the number of target cells lost (Sharpe, 1988; Tomlinson et al., 2012). The most central concept when performing cell separation is the cell viability, as there is no point in separating cells with a high degree of purity if recovered cells are dead or altered as a result of the process. In order to maintain cell viability during cell separation procedures, the following needs to considered: firstly, cells need to be separated in conditions that are closest to optimal, for example, kept in growth medium and at 37^{o}C; secondly, the procedure must not contain any reagents that may damage or change the cells; and thirdly, physical stresses such as high g force during centrifugation must be kept to a minimum. Furthermore, it is imperative that the separation method itself is brief, again to minimise stresses incurred to the cells (Sharpe, 1988; Beaman et al., 2017). The degree of: purity, recovery and viability, of the separated cell population is a function of the assay used.

The choice of cell separation technique is made based on consideration of the following: the initial cell source, the characteristics of the cell type, and the required purity of the isolated population. There are four main categories of cell separation type (see Table 4.1), these are, 1. by adherence, 2. by density, 3. by antibody binding and 4. by lectin binding (Tomlinson et al., 2012).

Table 4.1 *Main categories of cell separation, their use and pros and cons. See text for source material.*

Cell separation type	Uses	Pros	Cons
Adherence	Isolating cells from tissue	Simple and inexpensive	Non-specific and relies on ability of cells to adhere and proliferate
Density	Tissues that contain many unwanted cells, for example, blood and bone marrow	Can be used for large-scale cell isolation	Non-specific
Antibody-binding	Isolation of cells with a known antigen	High-purity	Limited to antibody availability and presence of unique markers for cell type
Lectin-binding	Isolation of cells with specific glycosylation profile	Purity	Purity based on isolation of cells with an array of glycans

The method of cell isolation by adherence is used for isolating cells from whole tissues, for example, isolation of stromal cells from dental pulp (Gronthos et al., 2000), and although it is a simple technique and inexpensive, the process is non-specific and reliant on cells to adhere and proliferate. Adherence isolation is achieved by disrupting whole tissue by either enzymatic, mechanical or a combination of both methods. Then this is followed by subsequent filtration to remove clumps and produce a single cell suspension. This is then plated onto an adhesive surface, such as a cell culture flask, and cells are cultured until they have adhered. Non-adhered cells are eluted and either retained or discarded (Tomlinson et al., 2012).

Density-based isolation of cells uses centrifugation to separate cells based on cell density relative to a graduated separation medium. The most common tissue with which this method is clinically used is blood; for example, in processes such as aphaeresis, where mononuclear cells are isolated for treatment of conditions such as leukaemia (Buckner et al., 1969). Density-based cell isolation is limited; for example, if the densities of cells are similar, it is difficult to isolate a specific cell type.

Cell separation by antibody labelling can be categorised as either positive isolation, where an antibody binds to, and is used to then isolate target cells, or negative-isolation where an antibody binds to and isolates unwanted cells therefore leaving targets cells. Antibody-binding provides populations with high purity as isolation of target or unwanted cells is dependent on the presence of the particular antigen that the antibody is raised against. Antibodies can be bound to, for example, a fluorescent molecule or magnetic particles. Alternatively, antibodies can be immobilised on a substrate. Fluorescence activated cell sorting (FACS) is a commonly used cell separation technique (Herzenberg et al., 2002). It requires cells to be labelled with an antibody conjugated to a fluorescent molecule. Single cells are passed

through a laser, the excitation emission of the fluorophore bound to the cell is detected and determined to be either above or below the threshold value. By electrically charging the droplet, each cell is contained within, and then passes through, charge detector plates. Cells are deflected to designated collection tubes and are therefore sorted. FACS allows multiple fluorescent labels to be used to identify different cell types, and cells are analysed individually, therefore providing considerable information. However, viability of unlabelled cells post-sorting can be reduced due to high likelihood of bacterial contamination incurred through the process, and removal of antibodies from cells cannot be achieved. FACS is used, for example, in the isolation and sorting of circulating tumour cells (CTCs) of breast cancer patients and the subsequent characterisation of tumour-initiating cells from the sorted populations (Baccelli et al., 2012). Magnetic activated cell sorting (MACS) uses antibodies bound to magnetic particles (Šafařík and Šafaříková, 1999). Unwanted cells are labelled, and, when passed through a magnetic field, are retained whilst target un-labelled cells are collected. MACS does not allow for analysis of single cells in the way that FACS does, and only one label can be used (Tomlinson et al., 2012). MACS can be used for example, in enrichment of $CD34^+$ leukocytes for further characterisation and immunophenotyping (Kato and Radbruch, 1992). Antibodies conjugated to magnetic beads are also used for small-scale or batch cell separations. An example is, DynaBeads®, patented by Professor John Ugelstadv in 1976 (Olsvik et al., 1994). There are further techniques for cell separation that utilise antibody-binding, for example, antibodies immobilised to a polymer surface (Adams et al., 2008), antibodies immobilised on a column surface (Mahara and Yamaoka, 2010), cryo-gel-based affinity chromatography (Kumar and Srivastava, 2010) and aqueous-phase partitioning (Sousa et al., 2011).

Lectin-based cell separation was first reported by Li and Osgood (1949), where the lectin *Phaseolus vulgaris* agglutinin (PHA) from red kidney beans was used to agglutinate erythrocytes, making their density greater so that they could be pelleted out, and thereby isolating leukocytes. Agglutination is an historically used technique for cell separation by lectins (Sharon and Lis, 1989). Lectin-based cell separation is similar to antibody-based separation except that separation is based on lectin-identification cell surface sugars. Dodla et al. (2011) reported that the lectin *Vicia villosa* agglutinin (VVA) from the hairy vetch plant could be used for isolation of human neural progenitor cells. Wang et al. (2011) reported that lectins can be used for the isolation and identification of human pluripotent stem cells (hPSCs). They found that lectins that bound hPSCs and not non-pluripotent stem cells, and preferentially bound hPSC proteins, had a high affinity for glycans containing the monosaccharide GalNAc. HPA is an example of such a lectin.

The experiments reported in Chapter 3 revealed great heterogeneity of HPA lectin labelling intensity and cell morphology within a cell population. The HPA lectin labelling profiles, as characterised in Chapter 3, have also been well documented in the literature for MCF7, ZR741 and BT474 cells (reviewed by Brooks et al., 2001). Why such proportions of differentially glycosylated cells exist within in a cell

population is unknown and why these proportions remain constant within a cell line is also under question. Cellular glycosylation changes in response to events such as inflammation (Dewald et al., 2016) and hypoxia (Lehnus et al., 2013) have been observed, so it would be reasonable to assume that cells isolated based on their glycosylation profiles would have the ability to change their profile over-time in response to cell signalling.

Aims and objectives

The aims of the experiments in this chapter are to separate the HPA-positive and HPA-negative cell populations and investigate whether their glycosylation and morphology changes over time or remains constant. Therefore, the objectives of this chapter are to:

I. Isolate cells based on HPA-binding characteristics.
II. Assess the morphologies of the isolated populations, at time 0 and over a time course of up to 72 hours.
III. Assess glycosylation and morphological characteristics of isolated populations over time.
IV. Verify that the isolated HPA-positive and HPA-negative populations isolated from the parental cell lines are of the same origin.

4.2 Methods

4.2.1 Cell separation

The cell separation protocol is based around the optimised HPA lectin labelling protocol developed in the work described in Chapter 3 and detailed in Section 2.3. In summary, streptavidin-coupled M280 Dynabeads® (2.8 µm beads containing 17% iron to make them magnetic, with 650-900 pm of free biotin /mg of beads) were incubated with biotinylated-HPA for 30 minutes at room temperature on an end-over-end mixer. 1 µg of biotinylated HPA to 0.1 µg of streptavidin-coupled M280 Dynabeads® was used for the separation of 1 million cells. To minimise stress to the cells, the HPA-bead conjugate was incubated with the cells in suspension for 5 minutes at room temperature, also on an end-over-end mixer. By limiting the amount of time the cells are at less than optimal temperature and conditions, minimal stress was incurred by the cells. Cells which bound to the HPA-bead conjugate were pooled to the side of a microcentrifuge tube using a magnet (as the beads are magnetic) for 2 minutes and the HPA-negative (un-bound) cells collected at the bottom of the microcentrifuge tube and were aspirated leaving only the bound HPA-positive cells. The HPA-negative cells were placed into a new microcentrifuge tube and the magnet removed from the HPA-positive cells which were then re-

suspended. Henceforward, in this chapter, the HPA-negative cell population will be referred to as the "N-population" and the HPA-positive cell population as the "P-population".

ZR751 cells were used to optimise the procedure as this cell line has equal proportions of HPA-positive and HPA-negative cells as demonstrated previously (see Section 3.3.2). Three biological replicates of ZR751 cells were used for the cell-separations. The P- and N-populations were grown on separately and then lectin labelled and imaged as detailed in Section 2.2 over 72 hours post-separation. The ZR751 cells were lectin labelled and imaged at the time points 0, 24, 48 and 72 hours post-separation. This was then trialled with MCF7 and BT474 cells – also with 3 biological replicates each – with cells lectin labelled and imaged at 0 hours for MCF7 cell and 24 hours for BT474 then 72 hours post-separation for both cell lines. Ideally the BT474 cells would also have been images at 0 hours, however the cells were too rounded up to be able the discern HPA-labelling. To ensure that exposure to the Dynabeads® itself had no effect on the cell sample, a control was performed where cells were subjected to an identical sham procedure but without the addition of biotinylated HPA. Cells were imaged using a light microscope and observed for HPA-labelling changes over time as detailed in Section 3.2.2.

4.2.2 NanoZoom assessment of HPA lectin labelling and morphology of isolated populations over time

P- and N-populations derived from ZR751 cells, as detailed in Section 4.2.1, were converted to digital images by NanoZoomer 2.0-RS digital slide scanner (Hamamatsu Photonics, Welwyn, UK) which was performed by Dr Alison Forhead at Cambridge University. Cells were assessed for HPA-positivity and X:Y measurements as described in Section 3.2.3.

4.2.3 SEM analysis of isolated populations

MCF7, ZR751 and BT474 cell lines were separated based on their HPA binding status as summarised in Section 4.2.1 and described in detail in Section 2.3. Three biological replicates were prepared per cell line. 13mm diameter glass coverslips were sterilised in 70% IMS, placed in a cell culture 24-well plate and left to air-dry in a class II cell culture hood. A suspension of 40,000 separated cells/ml was prepared and 500µl of cell suspension was added per well. Plates were gently swirled once and then left to grow at 37°C with 5% CO_2 atmosphere for 24 hours. Then, media was aspirated from the wells and the cells fixed with 2% v/v glutaraldehyde in PIPES buffer, pH 7.4, for 30min at room temperature. Cells were then dehydrated through an ethanol series (10%, 20%, 30%, 50%, 70%, 90%, 95%, 100%) before 3x washes in absolute ethanol. The slides were critical point dried, sputter coated in gold and mounted on 13mm diameter stubs using carbon tabs and then imaged using a Hitachi S3400 scanning electron microscope. Critical point drying, sputter coating and training on the Hitachi S3400 scanning electron microscope was carried out by Dr Louise Hughes, Oxford Brookes University.

Images were captured of individual cells or small groups of cells, so that pseudopodia could be discerned. If an HPA-labelled Dynabead was adherent to a cell, it confirmed that the cell was HPA-positive. Pseudopodia were classified as projections from the main cell body. The HPA lectin labelling profile (HPA-positive or HPA-negative) and presence of pseudopodia were recorded for each cell captured per cell line.

4.2.4 CODIS STR analysis

Having identified a morphological difference between populations of cells isolated based on their HPA-binding profiles, it was necessary to ensure that the HPA-positive and HPA-negative populations were of the same cell line and were not a product of contamination. For this a comparative method of identification was used. Combined DNA Index System (CODIS) Short Tandem Repeat (STR) analysis was used to verify the cell lines used in this study. STRs are repetitive sequences of DNA, typified by a variable number of short sequences ~2-7bp in length (Ruitberg et al., 2001). They are highly polymorphic and are good genetic markers. In cell line authentication, 13 CODIS STR loci are employed all of which are (1) tetrameric repeat sequences, (2) located on separate chromosomes, (3) characterised in population genetics and (4) reproducible (Ruitberg et al., 2001). Of the 13 CODIS STR loci, the loci listed in Table 4.2, are generally used for cell line authentication and so where used in the work described here.

Table 4.2 *CODIS STR loci primer pair sequences as determined by Azari et al. (2007).*

STR Locus	**Chromosomal location**	**Primers**
Amelogenin	X,Y	(F) 5'-CCC TGG GCT CTG TAA AGA ATA GTG-3' (R) 5'-ATC AGA GCT TAA ACT GGG AAG CTG-3'
CSF1PO	5q	(F) 5'-AAC CTG AGT CTG CCA AGG ACT AGC-3' (R) 5'-TTC CAC ACA CCA CTG GCC ATC TTC-3'
D16S539	16q	(F) 5'-GGG GGT CTA AGA GCT TGT AAA AAG-3' (R) 5'-GTT TGT GTG TGC ATC TGT AAG CAT-3'
D5S818	5q	(F) 5'-GGT GAT TTT CCT CTT TGG TAT-3' (R) 5'-AGC CAC AGT TTA CAA CAT TTG TAT CC-3'
D7S820	7q	(F) 5'-ATG TTG GTC AGG CTG ACT ATG-3' (R) 5'-GAT TCC ACA TTT ATC CTC ATT GAC-3'
THO1	11p	(F) 5'-ATT CAA AGG GTA TCT GGG CTC TGG-3' (R) 5'-GTG GGC TGA AAA GCT CCC GAT TAT-3'
TPOX	2p	(F) 5'-ACT GGC ACA GAA CAG GCA CTT AGG-3' (R) 5'-GGA GGA ACT GGG AAC CAC ACA GGT TA-3'

Genomic DNA (gDNA) was extracted (as detailed in Section 2.4) from MCF7, ZR751 and BT474 unseparated parental cell lines as well as HPA-positive and HPA-negative isolated cell populations (cells separated as detailed in Section 2.3). A PCR was set up for each of the 7 primer pairs for the STR loci detailed in Table 4.2, for each sample, as well as a negative control which contained nuclease-free water

instead of gDNA template. PCR was performed using Taq PCR core kit (Qiagen). PCR components per reaction are detailed in Table 4.3. The thermocycler program used for the PCR is detailed in Table 4.4. The recipe detailed in Table 4.5 was sufficient to cast 2x 0.75mm 12% polyacrylamide gels, to which 10 µl of PCR product was added per well, as well as 10 µl of 103ng/µl MassRuler™ (Thermo Scientific) per gel. The gel was run for 3 hours at 50 volts and then stained using 10mg/ml ethidium bromide for 30 minutes. The gel was visualised under UV using a ChemiDoc™ XRS+ system with ImageLab™ and images were captured.

Table 4.3 *Volumes used per PCR reaction and per no temple control (NTC) for CODIS STR.*

Component	**Volume/reaction (µl)**	**Volume/NTC (µl)**
10x PCR buffer (Qiagen)	2	5
dNTP (10mM each)	0.4	1
Forward primer (0.5µM)	0.5	1
Reverse primer (0.5µM)	0.5	1
Taq DNA polymerase (5U/µl)	1	1
NFH_2O	10	11
gDNA (50ng/µl)	1	N/A
Total reaction volume	20	20

Table 4.4 *Thermal profile used for CODIS STR PCR reaction (Azari et al., 2007).*

Step		**Time (sec)**	**Temperature (°C)**
Initial denaturation		120	94
35 cycles	Denaturation	30	94
	Annealing	45	64
	Extension	45	72
Final extension		600	72
Hold		∞	4

Table 4.5 *12% polyacrylamide gel recipe sufficient for the casting of 2x 0.75mm gels.* *Tetramethylethylenediamine *was added last.*

Component	**Volume**
30% Bis-acrylamide (29:1) (Sigma Aldrich®)	4.8ml
H_2O	4.8ml
5x tris borate EDTA (Sigma Aldrich®)	2.4ml
10% ammonium persulphate (v/v) (Sigma Aldrich®)	200µl
Tetramethylethylenediamine* (Sigma Aldrich®)	10µl

4.3 Results

4.3.1 Cells separated based on their HPA-binding profile, revert to mixed HPA-binding populations over-time

In order to independently assess HPA-positive (P-population) and HPA-negative (N-population) cells, cells were separated using HPA conjugated to magnetic beads and cultured for 72 hours post-separation. The HPA-positivity of the isolated P- and N-populations were quantified at 0hrs, 24hrs, 48hr and 72hrs post-separation for the ZR751 cell line (illustrated in Figure 4.2) and at 0hr for MCF7 or 24hr for BT474 and 72hrs post-separation for both the MCF7 (illustrated in Figure 4.4) and BT474 cell lines (illustrated in Figure 4.5). To ensure that the Dynabeads did not bind non-specifically, the ZR751 cells were also subjected to a sham separation protocol involving non-HPA labelled beads. As illustrated in Figure 4.3, this resulted in no separation of the cells. Figure 4.6 A illustrates the changing HPA-positivity proportions over 72 hours post-separation for the ZR751 P- and N-populations. At 0hrs post-separation, the ZR751 P-population was 100% HPA +++, and the ZR751 N-population was 100% HPA –. By 24 hours post-separation, the ZR751 P-population had become a mixture of highly and moderately HPA-positive (61.3% HPA ++ and 38.7% HPA +++), whilst the ZR751 N-population had become a mixture of weakly HPA-positive and negative (60.8% HPA + and 39.2% HPA-) cells. By 48 hours post-separation, the ZR751 P-population had started to become a mixed population (2.15% HPA -, 11.8% HPA +, 58.1% HPA ++ and 28% HPA +++), whilst the ZR751 N-population had also started to become a mixed population (20.9% HPA -, 48.8% HPA +, 26.7% HPA ++ and 3.98% HPA +++). At 72 hours post-separation, the ZR751 P-population exhibited almost the same HPA labelling profiles as pre-separation (18.9% HPA +, 56.8% HPA ++ and 24.3% HPA +++), whilst the ZR751 N-population also exhibited HPA labelling proportions similar to those seen pre-separation (33.3% HPA +, 54.6% HPA ++ and 12% HPA +++). Both the P- and N- ZR751 populations had changed their HPA-positivity profile to almost obtain an unseparated proportion of HPA-positivity as illustrated in Figure 4.6 B. (pre-separation proportions are 15.6% HPA -, 27.6% HPA +, 29.2% HPA ++ and 27.6% HPA +++). It was impossible to distinguish HPA – cells in both P- and N-populations for 72 hours post-separation, as the haematoxylin counterstain did not work. The lack of HPA-negative cells at 72 hours post-separation are therefore considered an anomaly.

This reversion to pre-separated glycosylation profiles over time was also observed in the MCF7 P- and N-populations as illustrated in Figure 4.7 A. MCF7 P-population at 0 hours post separation were 2.3% HPA ++ and 97.7% HPA +++, whilst the MCF7 N-population were 100% HPA -. By 72 hours post-separation, the MCF7 P-population were mixed (2.6% HPA -, 14.06% HPA +, 33.33% HPA ++ and 50% HPA +++), whilst the MCF7 N-population was also mixed (3.7% HPA -, 10.55% HPA +, 45.76% HPA ++ and 40% HPA +++). Therefore, showing a reversion to nearly unseparated proportions as illustrated in Figure 4.7 B (pre-separation proportions are 7.76% HPA -, 26.12 HPA +, 30.35% HPA ++ and 35.76% HPA +++).

This reversion to pre-separated glycosylation profiles over time was also observed in the BT474 P- and N-populations, as illustrated in Figure 4.8 A. BT474 P-population 24 hours post-separation were 85.3% HPA ++ and 14.7% HPA +++. The BT474 N-population were 84.41% HPA – and 15.58% HPA +. Then, at 72 hours post-separation, the BT474 P-population were mixed (3.88% HPA -, 49.22% HPA +, 38.76% HPA ++ and 8.14% HPA +++), whilst the BT474 N-population 72 hours post-separation were also mixed (29.35% HPA -, 61.64% HPA + and 9% HPA ++). This again illustrates a reversion to nearly unseparated proportions (as illustrated in Figure 4.8 B pre-separation proportions are 19.5% HPA -, 63.24% HPA +, 14.34% HPA ++ and 2.94% HPA +++).

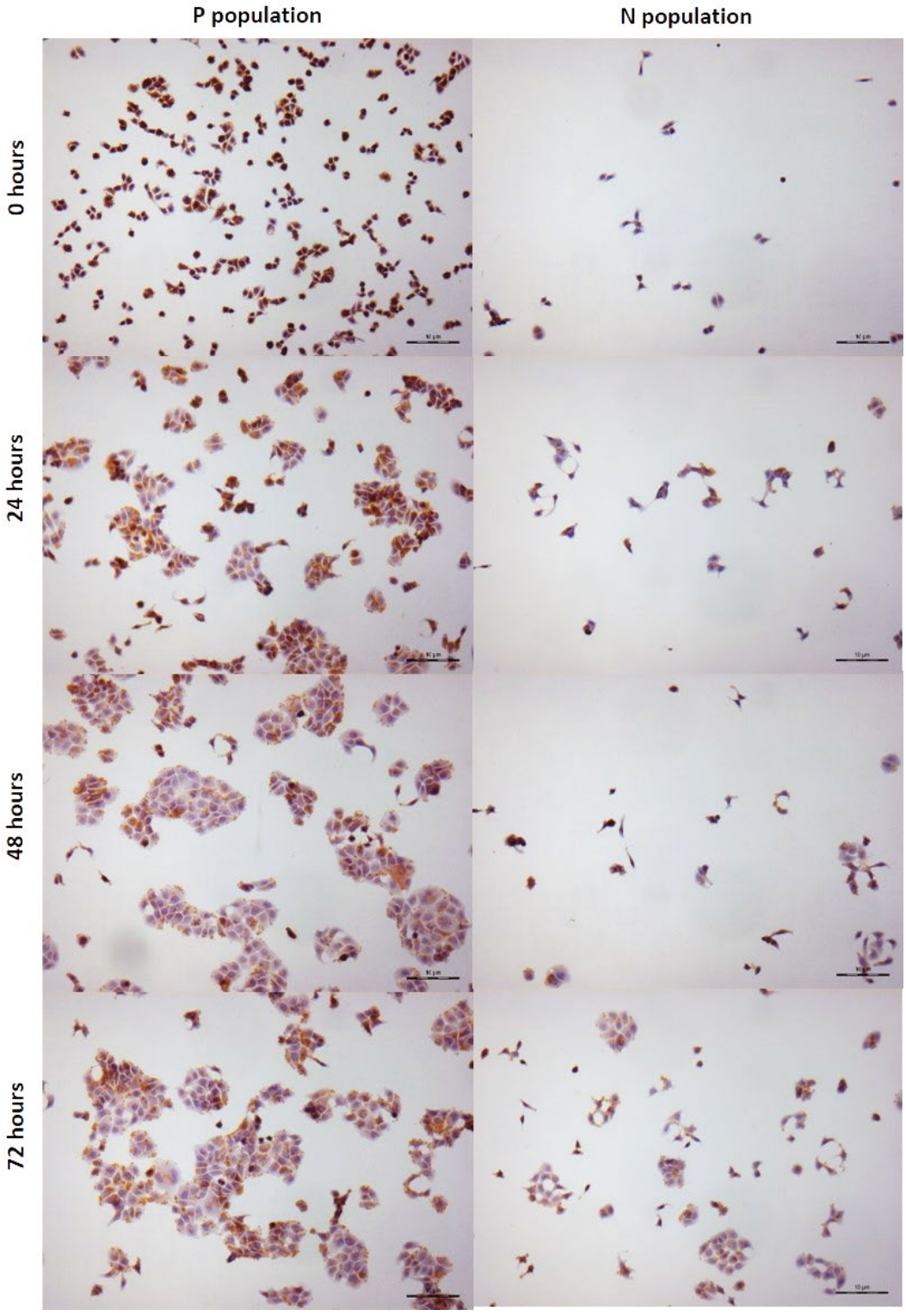

Figure 4.2 *ZR751 cells separated and populations cultured over 72 hours post-separation, labelled for HPA binding. At 0hrs post-separation the P-population was highly HPA-positive whilst the N-population was completely HPA-negative. Over time both the P- and N-populations become a mixture of HPA-positive and HPA-negative cells. Images here are representative of 3 biological replicates, with 10 images captured per replicate and per day. Images captured with a Zeiss Axioplan microscope fitted with a JENOPTIK ProgResC3 colour camera. Scale bar = 10 µm.*

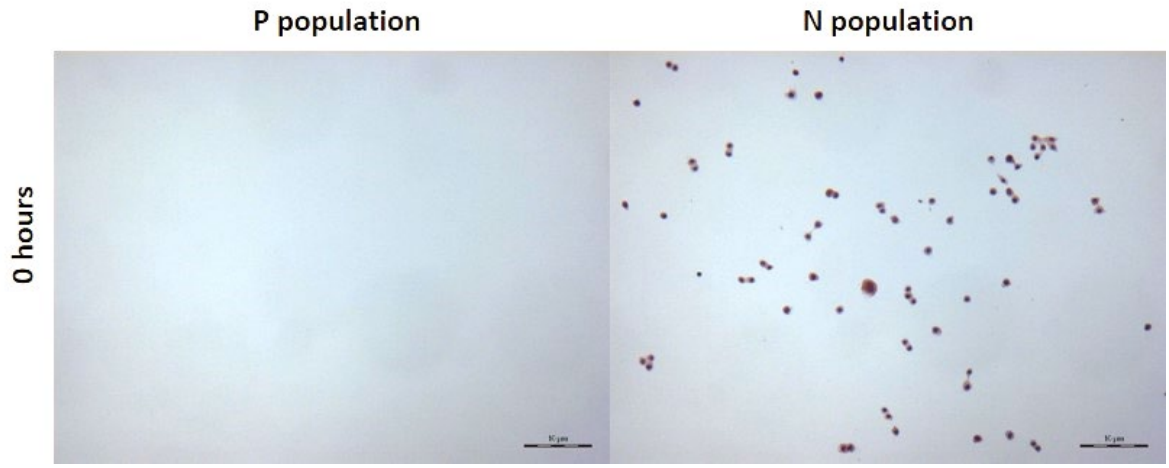

Figure 4.3 *Sham separation control. ZR751 cells were subjected to a sham separation protocol using non HPA-labelled beads to ensure that the beads themselves were not adhering to them non-specifically. Images captured with a Zeiss Axioplan microscope fitted with a JENOPTIK ProgResC3 colour camera. Scale bar = 10 µm.*

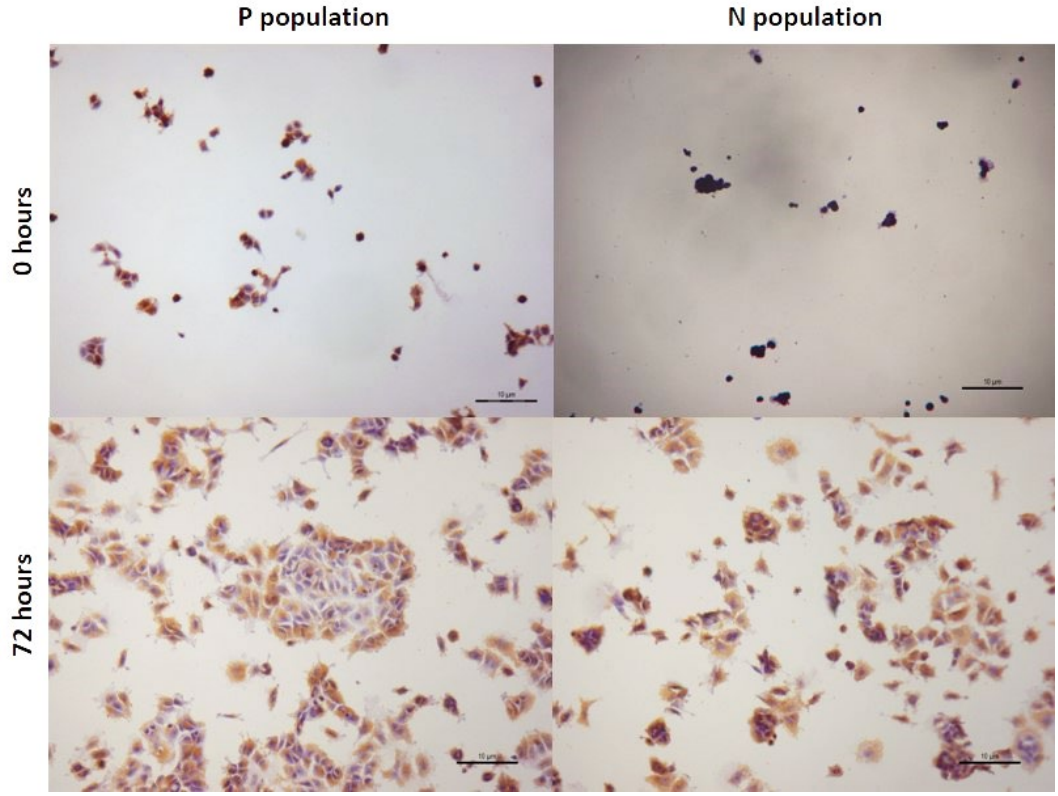

Figure 4.4 *MCF7 cells separated and cultured over 72 hours, labelled for HPA binding. At 0hrs post-separation the P-population was highly HPA-positive whilst the N-population was completely HPA-negative. At 72hrs post-separation both P- and N-populations were a mixture of HPA-positive and HPA-negative cells. Images here are representative of 3 biological replicates, with 10 images captured per replicate and per day. Images captured with a Zeiss Axioplan microscope fitted with a JENOPTIK ProgResC3 colour camera. Scale bar = 10µm.*

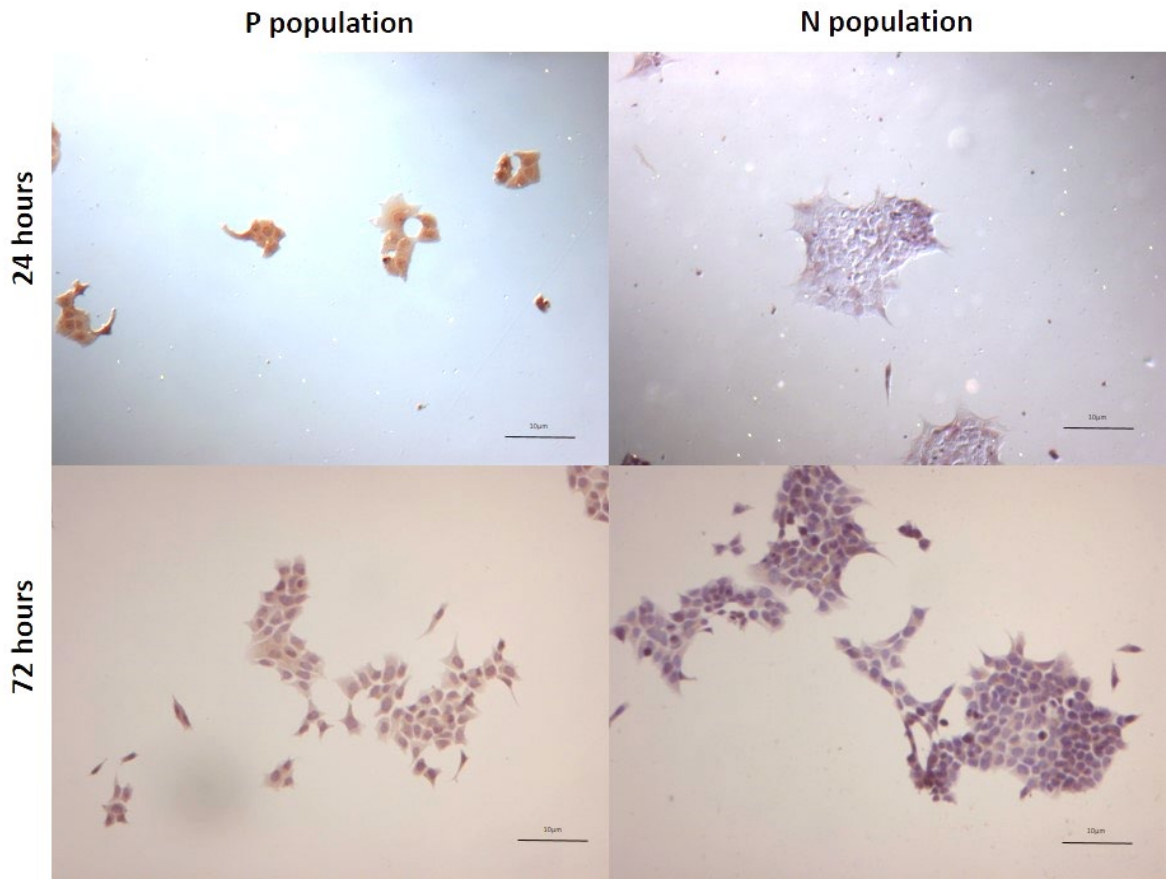

Figure 4.5 *BT474 cells separated and cultured over 72 hours, labelled for HPA binding. At 0hrs post-separation the P-population was highly HPA-positive whilst the N-population was completely HPA-negative. At 72hrs post-separation both P- and N-populations were a mixture of HPA-positive and HPA-negative cells. Images here are representative of 3 biological replicates, with 10 images captured per replicate and per day. As quantification of HPA-labelling was impossible for the BT474s at 0 hours post-separation, 24 hours was used instead. Images captured with a Zeiss Axioplan microscope fitted with a JENOPTIK ProgResC3 colour camera. Scale bar = 10µm.*

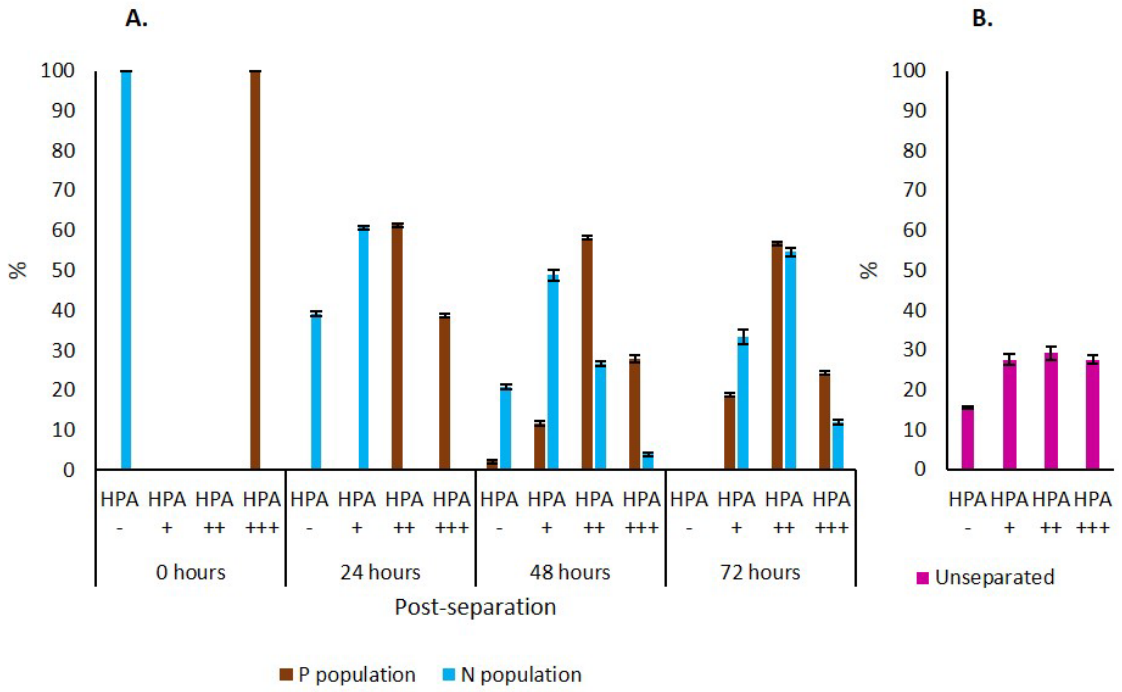

Figure 4.6 *A. ZR751 isolated P- (HPA-positive, brown bars) and N- (HPA-negative, blue bars) populations, percentage cells exhibiting different degrees of HPA-positivity over 72hrs post-separation. B. Unseparated ZR751 cells (pink bars), percentage cells exhibiting different degrees of HPA-positivity. Error bars showing standard error of the mean of 3 biological replicates. Initially P- and N-populations are completely HPA+++ or HPA-, respectively, however over 72hrs both P- and N-populations exhibit a similar HPA labelling profile as the unseparated parental population.*

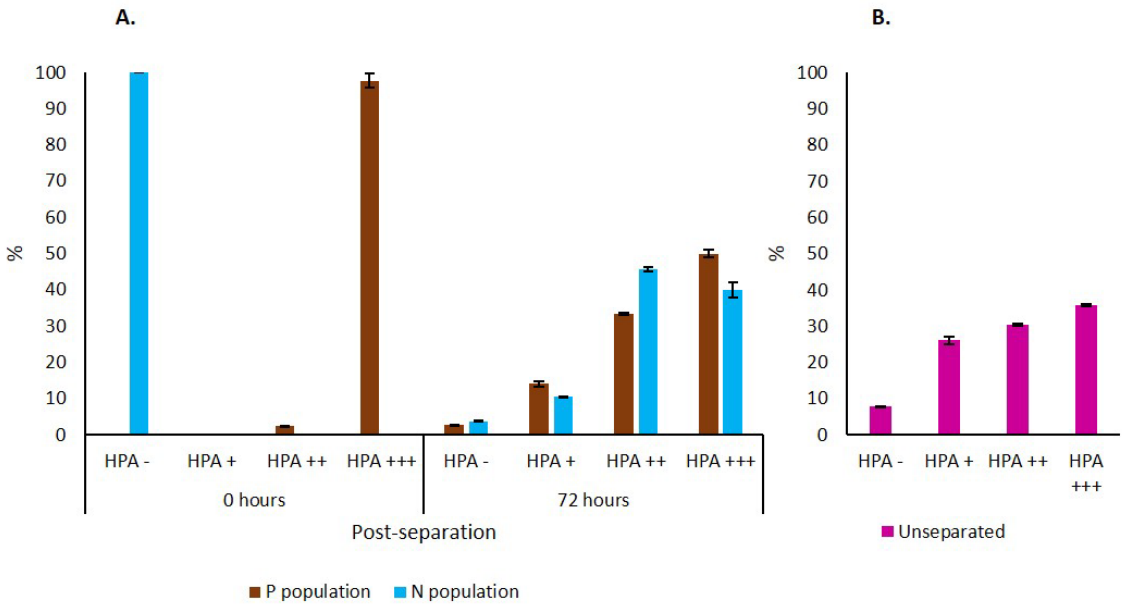

Figure 4.7 *A. MCF7 isolated P- (HPA-positive, brown bars) and N- (HPA-negative, blue bars) populations, percentage cells exhibiting different degrees of HPA-positivity at 0 and 72hrs post-separation. B. Unseparated MCF7 cells (pink bars), percentage cells exhibiting different degrees of HPA-positivity. Error bars calculated by standard error of the mean with 3 biological replicates. Initially P- and N-populations are completely HPA+++ or HPA-, respectively, however over 72hrs both P- and N-populations exhibit a similar HPA labelling profile as the unseparated parental population.*

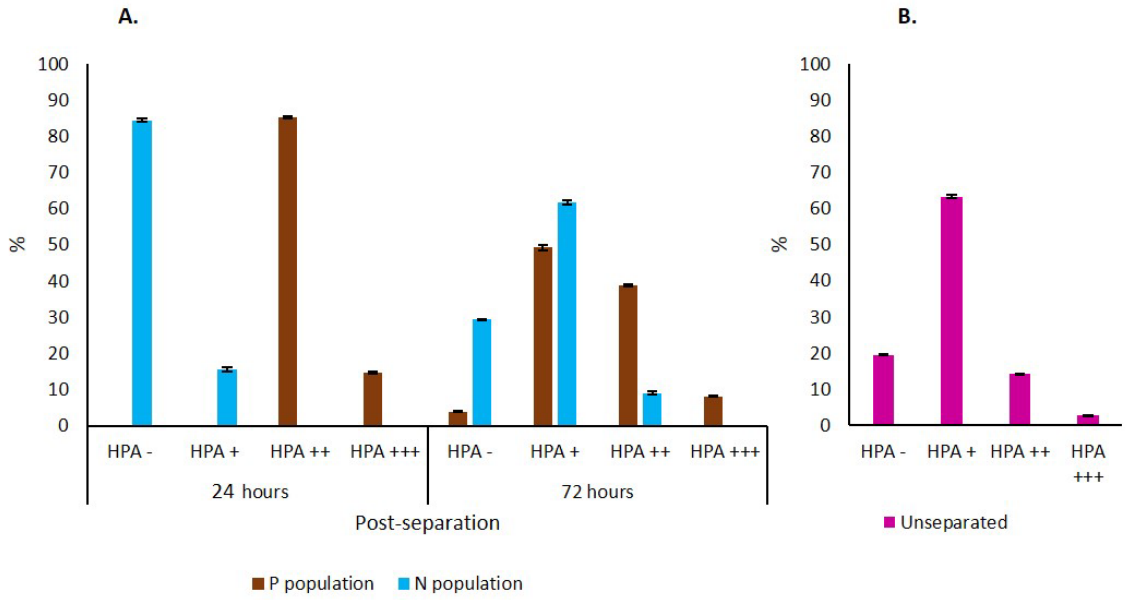

Figure 4.8 *A. BT474 isolated P- (HPA-positive, brown bars) and N- (HPA-negative, blue bars) populations, percentage cells exhibiting different degrees of HPA-positivity at 24 and 72hrs post-separation. B. Unseparated BT474 cells (pink bars), percentage cells exhibiting different degrees of HPA-positivity. Error bars calculated by standard error of the mean with 3 biological replicates. Initially P- and N-populations are completely HPA+++ or HPA-, respectively, however over 72hrs both P- and N-populations exhibit a similar HPA labelling profile as the unseparated parental population.*

4.3.2 HPA-negative cells are elongated, whilst HPA-positive cells are rounded

In order to independently assess the morphology of HPA-positive (P-population) and HPA-negative (N-population) populations over time, ZR751 cells were separated based on their HPA-binding profiles using HPA conjugated to magnetic beads and cultured post-separation for 72 hours. Populations were labelled for HPA binding at 0hr, 24hrs, 48hrs and 72hrs post-separation and then digital images of the preparations were captured by NanoZoom. The HPA-positivity and X and Y measurement of the cells were recorded. Figure 4.9 illustrates ZR751 P- and N-populations at 0hr, 24hrs, 48hrs and 72hrs post-separation. Both the ZR751 P- and N-populations at 0 hours post-separation are all rounded with an X:Y ratio of less than 2:1. Over 72 hours post-separation, the ZR751 P- and N-populations gradually reverted to mixed HPA labelled populations with distinct morphologies of the HPA-positive (rounded) and HPA-negative (elongated) cells within them. As illustrated in Figure 4.10 A, initially, the ZR751 P-population were 100% HPA +++ and rounded in morphology with an X:Y ratio of 1.06:1. The ZR751 N-population were 100% HPA – and also rounded in morphology with an X:Y ratio of 1.46:1. At 24 hours post-separation, the ZR751 P-population were split between HPA +++ and HPA ++ and were rounded with X:Y ratios of 1.13:1 and 1.04:1, respectively. The ZR751 N-population at 24 hours post-separation were split

between HPA – and HPA + cells and were markedly elongated with X:Y ratios of 3.28:1 and 3.08:1, respectively. At 48 hours post-separation, the ZR751 P-population consisted of a mixture of HPA labelling intensities. Cells that were HPA +++ (X:Y ratio of 1.21:1) were rounded, whilst cells that were HPA ++ (X:Y ratio of 2.06:1), HPA + (X:Y ratio of 2.97:1) or HPA – (X:Y ratio of 5.6:1) were elongated. The ZR751 N-population also consisted of a mixture of HPA labelling intensities. Again, HPA +++ (X:Y ratio of 1.67:1) and HPA ++ (X:Y ratio 1.99:1) were rounded, whilst HPA + (X:Y ratio of 2.6:1) and HPA – (X:Y ratio of 2.96:1) were elongated. At 72 hours post-separation, both ZR751 P- and N-populations displayed similar proportions of HPA positivity and corresponding morphology to that which was observed in unseparated ZR751 cells (as illustrated in Figure 4.10 B). These results illustrate that HPA-negative cells have an elongated morphology whilst HPA-positive cells have a rounded morphology and confirm that cells isolated based on their HPA-binding profile revert to an unseparated HPA-positivity and morphology profile over a time frame of 72 hours.

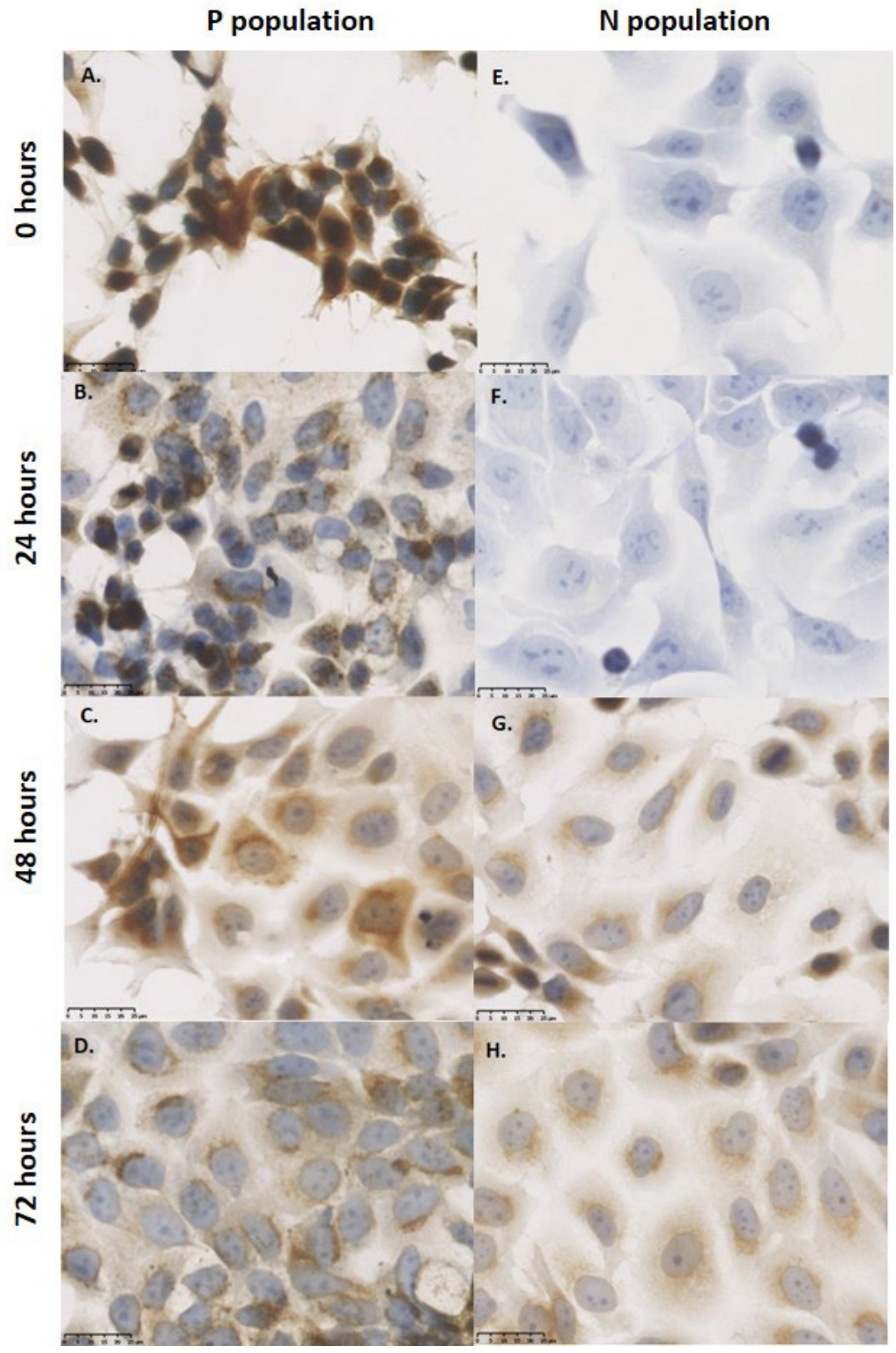

Figure 4.9 *ZR751 cells separated and populations captured over 72 hours, labelled for HPA binding. Initially P- and N-populations were either highly HPA-positive or HPA-negative, respectively. However, at 72hrs post-separation both the P- and N-populations exhibit similar HPA labelling profiles. Images here are representative of 3 biological replicates, with 10 images captured per replicate and per day. Images captured with a NanoZoomer 2.0-RS digital slide scanner (Hamamatsu Photonics, Welwyn, UK). Scale bar = 25 µm.*

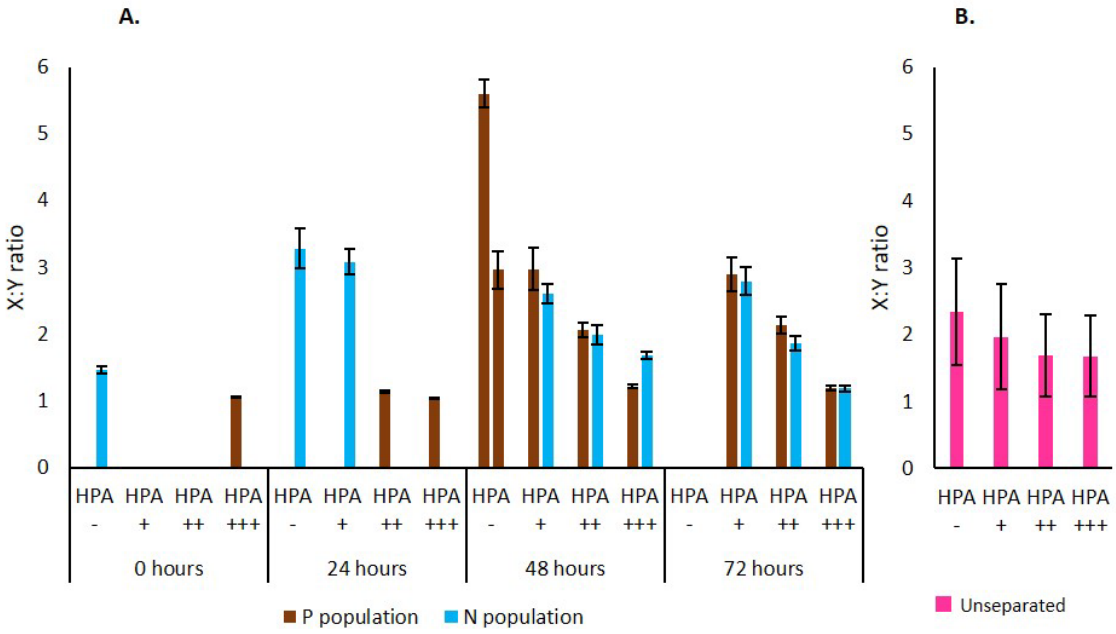

Figure 4.10 *A. ZR751 isolated P- (brown bars) and N- (blue bars) populations, average X:Y ratio against HPA-positivity over 72hrs post-separation. B. Unseparated ZR751 cells (pink bars), average X:Y ratio against HPA positivity. Error bars calculated by standard error of the mean with 3 biological replicates. In isolation as well as unseparated HPA-negative cells remain significantly more elongated than HPA-positive cells of any intensity.*

4.3.3 HPA-negative cells have significantly more pseudopodia than HPA-positive cells

In order to further assess the morphology of HPA-positive and HPA-negative cells, cells were isolated based on their HPA-binding profile using HPA conjugated magnetic beads and imaged using scanning electron microscopy (SEM). Single cells were assessed for HPA-positivity and presence of pseudopodia. Figure 4.11 illustrates a representative HPA-positive and a representative HPA-negative ZR751 cell. The HPA-positive cell is rounded in morphology and the HPA-negative cell is elongated and has many pseudopodia. This observation was consistent across the 146 images captured. As illustrated in Figure 4.12, HPA-negative cells have significantly (MCF7 $p<0.05$, ZR751 $p<0.001$, BT474 $p<0.001$) more pseudopodia than the HPA-positive cells. It was observed (as illustrated in Figure 4.13) that when HPA-positive cells do have pseudopodia, the HPA-binding site (signified by the presence of a Dynabead) is usually located opposite to the projection. HPA-negative cells have a more elongated and invasive morphology as determined by the incidence of pseudopodia, whilst HPA-positive cells have a round morphology and rarely possess pseudopodia.

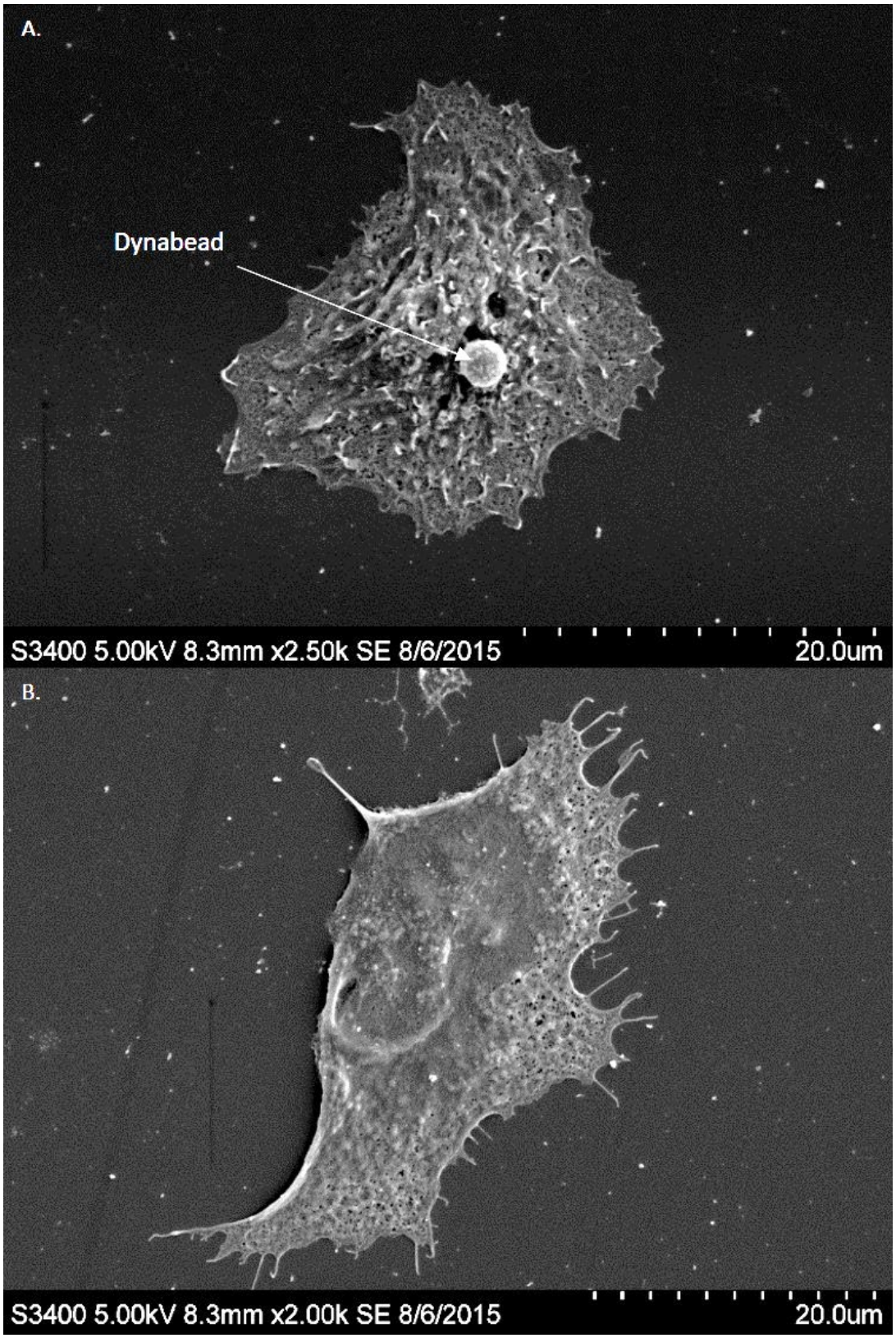

Figure 4.11 *ZR751 cells separated and imaged at 24hrs post-separation. A. HPA-positive cell, very rounded and no pseudopodia. B. HPA-negative cell, elongated and many pseudopodia. Images here are representative of 3 biological replicates, with 10 images captured per replicate. Images captured with SEM S3400 (Hitachi). Scale bar = 20µm.*

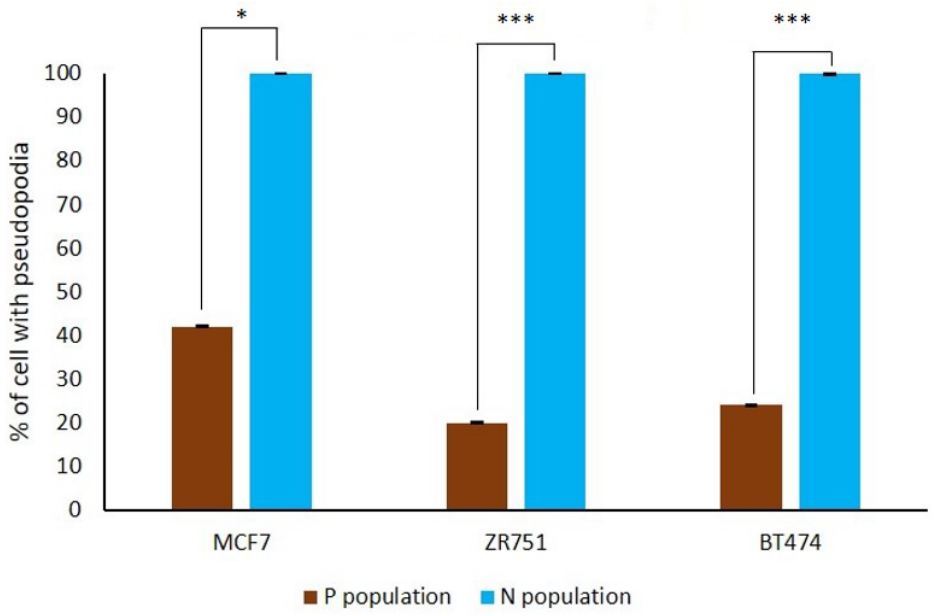

Figure 4.12 *A comparison of HPA-positive (brown bars) and HPA-negative (blue bars) cells across MCF7, ZR751 and BT474 cell lines with pseudopodia. For all cell lines HPA-negative cells are significantly more likely to have pseudopodia. Error bars represent standard error of the mean of three biological replicates per cell line.*

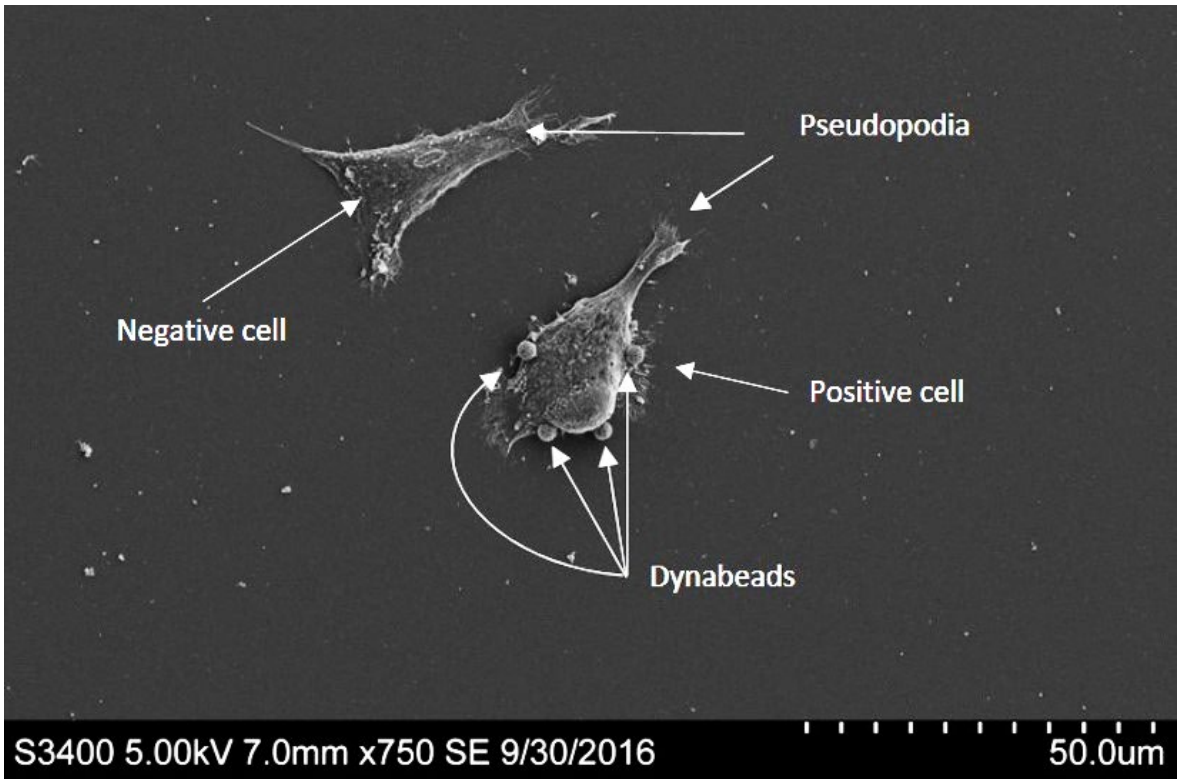

Figure 4.13 *SEM image of MCF7 cells, highlighting Dynabead position in opposition to pseudopodia formation. Images captured with SEM S3400 (Hitachi). Scale bar = 50µm.*

4.3.4 CODIS STR analysis

In order to determine whether the HPA-positive and HPA-negative isolated populations really represent different states of a single cell line, or the presence of two separate cell lines through contamination, CODIS STR analysis was performed. Every cell line has a characteristic STR profile in which a known number of repeats for the STR loci is expected (see Table 4.6). Expected sizes were determined from the STRbase (http://www.cstl.nist.gov/div831/strbase/str_fact.htm). As illustrated in Figures 4.14-4.16, the same sized bands are present in unseparated parental cell lines, and HPA-positive and HPA-negative populations for all cell lines (MCF7, ZR751 and BT474). Table 4.7 details the expected and observed band sizes for each cell line. Although, from this simple method of analysis the exact band sizes cannot be easily determined, bands sizes across unseparated, HPA-positive and HPA-negative populations are the same. Taken together this suggests that the isolated HPA-positive and HPA-negative populations are the same as the unseparated parent cell lines.

Table 4.6 *CODIS STR loci and alleles for cell lines with expected PCR product sizes as determined by STRbase http://www.cstl.nist.gov/div831/strbase/str_fact.htm. Number in brackets indicates expected allele repeat characteristic of the cell line.*

STR Locus	**MCF7 (allele) size bp**	**ZR751 (allele) size bp**	**BT474 (allele) size bp**
Amelogenin	(x) 106bp	(x) 106bp	(x) 106bp
CSF1PO	(10) 199bp	(10) 199bp (11) 203bp	(10) 199bp (11) 203bp
D16S539	(11) 288bp (12) 292bp	(11) 288bp	(9) 280bp (11) 288bp
D5S818	(11) 135bp (12) 139bp	(13) 143bp	(11) 135bp (13) 143bp
D7S820	(8) 223bp (9) 227bp	(10) 231bp (11) 235bp	(9) 227bp (12) 239bp
THO1	(6) 183bp	(7) 187bp (9) 195bp (3) 171bp	(7) 187bp
TPOX	(9) 236bp (12) 248bp	(8) 232bp	(8) 232bp

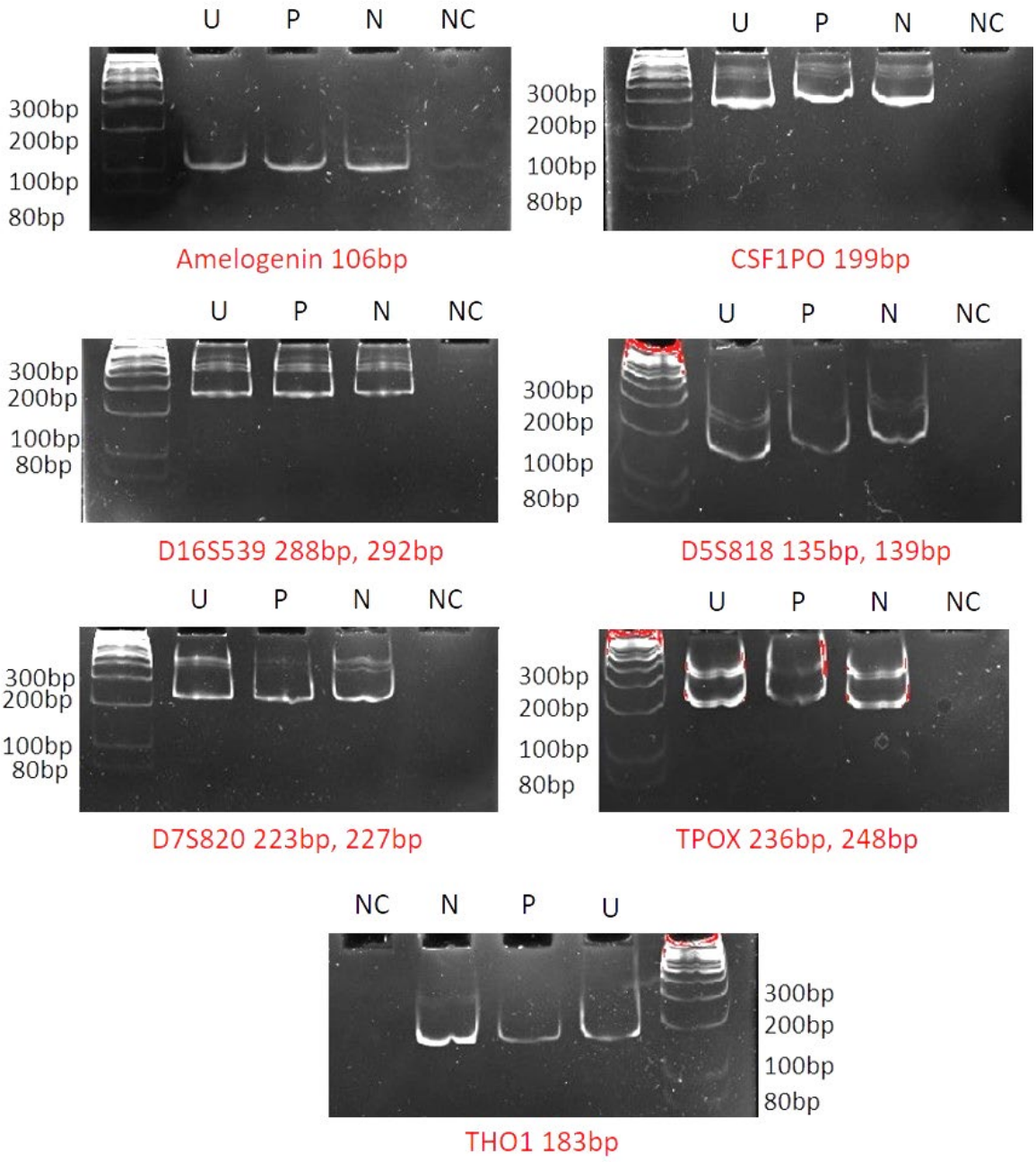

Figure 4.14 *MCF7 STR gels, detailing expected sizes (in red under each gel) of STR loci. U = unseparated, P = HPA-positive, N = HPA-negative and NC = negative control.*

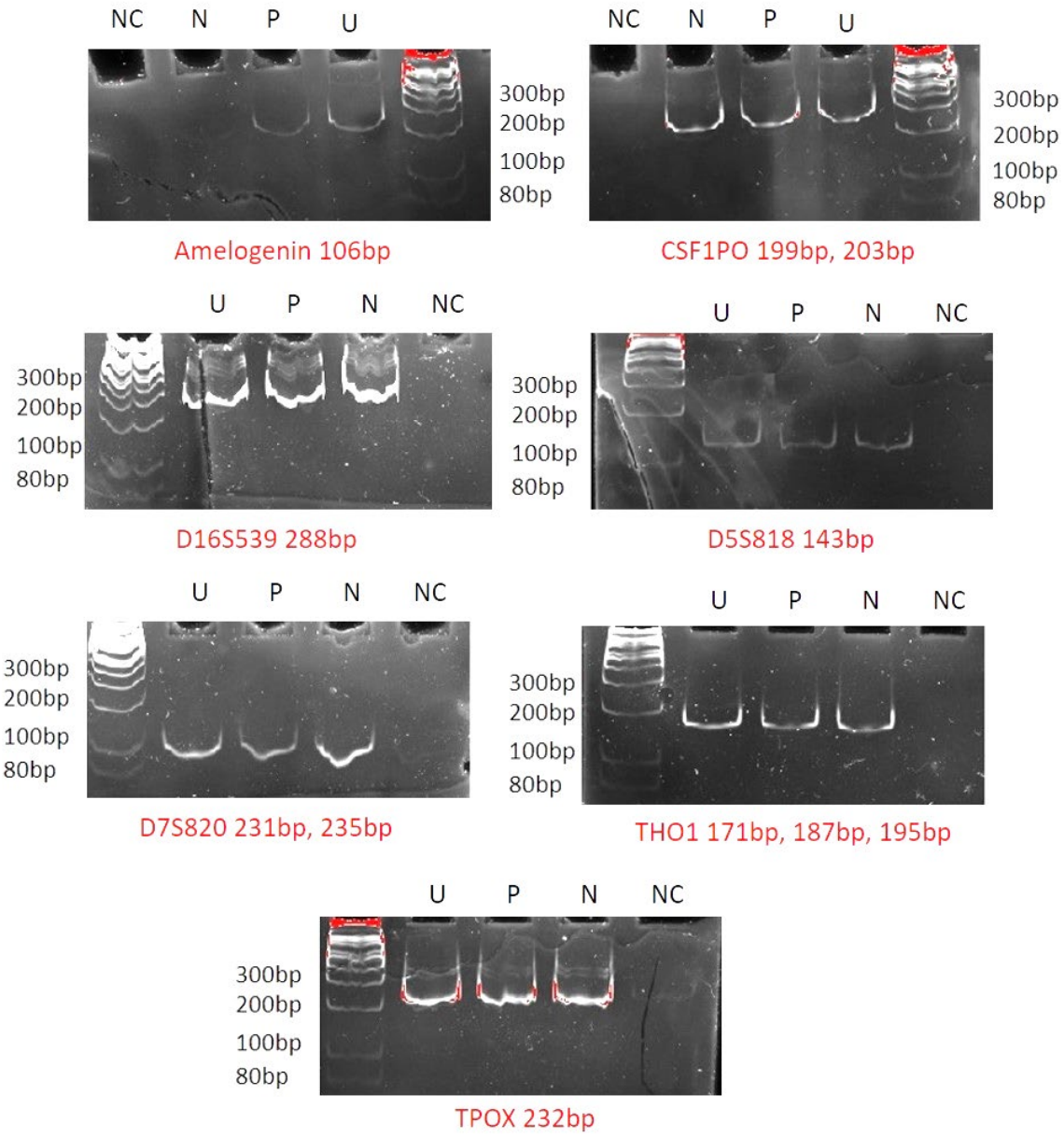

Figure 4.15 *ZR751 STR gels, detailing expected sizes (in red under each gel) of STR loci. U = unseparated, P = HPA-positive, N = HPA-negative and NC = negative control.*

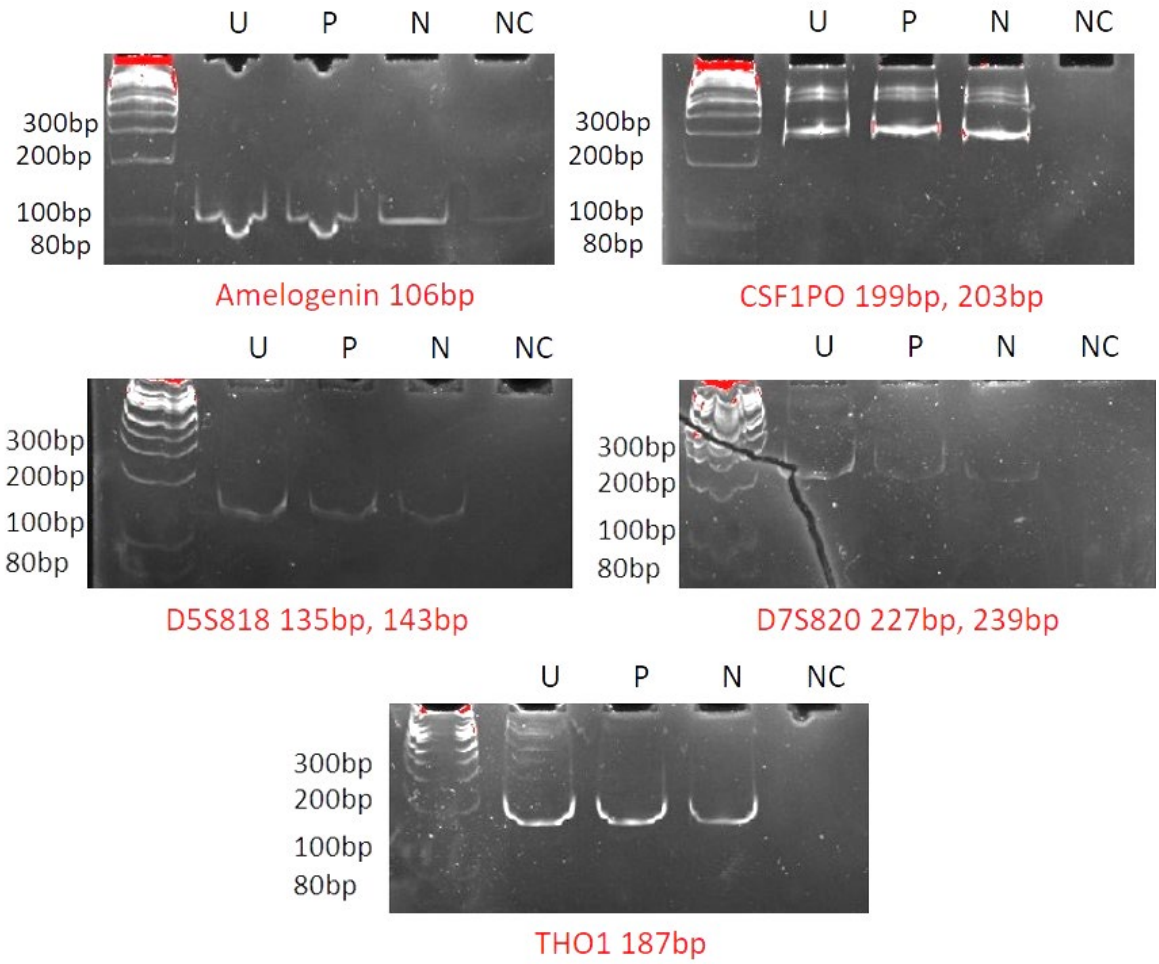

Figure 4.16 *BT474 STR gels, detailing expected sizes (in red under each gel) of STR loci. U = unseparated, P = HPA-positive, N = HPA-negative and NC = negative control.*

Table 4.7 *Expected (E) and observed values for STR loci for MCF7, ZR751 and BT474 for unseparated (U), HPA-positive (P) and HPA-negative (N) cell populations.*

STR locus	MCF7				ZR751				BT474			
	E	U	P	N	E	U	P	N	E	U	P	N
Amelogenin	106	~100	~100	~100	106	~200	~200	-	106	~100	~100	~100
CSF1PO	199	~200	~200	~200	199, 203	~300	~300	~300	199, 203	~200	~200	~200
D16S539	288, 292	~300	~300	~300	288	~300	~300	~300	280, 288	-	-	-
D5S818	135, 139	~150	~150	~150	143	~150	~150	~150	135, 143	~150	~150	~150
D7S820	223, 227	~200	~200	~200	231, 235	~100	~100	~100	227, 239	~250	~250	~250
THO1	183	~200	~200	~200	171, 187, 195	~200	~200	~200	187	~200	~200	~200
TPOX	236, 248	~200	~200	~200	232	~200	~200	~200	232	-	-	-

4.4 Discussion

4.4.1 The plasticity of glycosylation-specific populations and cell morphology – connection between glycosylation and EMT?

It was observed that when cells were separated based on their HPA-binding glycosylation profile and grown-on post-separation, the HPA-positive (P-population) and HPA-negative (N-population) populations revert to their unseparated glycosylation profile over a time course of 72 hours. If the isolated populations had been observed over a longer period of time than the 72 hours post-separation detailed here, exact unseparated HPA-positivity proportions would likely have been achieved. At 0 hours post-separation, both P- and N-populations had a rounded morphology, which was consistent with cells not having fully adhered to the coverslip, or due to cellular division. However, by 24 hours post-separation, the HPA-positive cells were observed to have a markedly rounded morphology reminiscent of epithelial cells, whilst the HPA-negative cells had an elongated morphology like mesenchymal cells (Kalluri and Weinberg, 2009). Interestingly, these glycosylation-related morphological characteristics persisted during isolation of the P- and N-populations and their reversion to an unseparated profile. Plasticity of the HPA-positive (rounded) and HPA-negative cells (elongated) could be viewed as being analogous to EMT-MET and MET-EMT, its reverse process (Tsai and Yang, 2013). That separated cells revert to their unseparated glycosylation profiles suggests some form of cell-cell communication underlying homeostasis of glycosylation profiles within the cell population. Gill et al. (2010) reported that translocation of GALNTs from the Golgi apparatus to the ER increased cell adhesion to the ECM and

cell invasiveness, as well as increasing the presence of Tn. They also reported that cell invasion is dependent on Tn-bearing proteins on lamellipodia (Gill et al., 2010). This may suggest that modification of protein glycosylation alters protein function in this case and therefore may have a role in controlling EMT-MET (Kurkon et al., 2015). Park et al. (2010) demonstrated that GALNT6 glycosylates and stabilises the oncogene MUC1. MUC1 is often up regulated in breast cancer, and over expression of MUC1 was reported by Gnemmi et al. (2014) as inducing EMT features including Snail (an EMT associated transcription factor) activation. Taken together, these data suggest a role for glycosylation initiation enzymes and glycosylation in control of EMT, consistent with the observations reported here. Freire-de-Lima et al. (2011) reported that TGFβ, an EMT inducer, promotes up-regulation of site specific O-glycosylation in the variable region of oncofoetal fibronectin, a major component of the EMC, involved in integrin binding and expressed by tumour cells. This demonstrates that O-glycosylation of proteins has control over EMT induction.

4.4.2 HPA-negative cells have an elongated morphology and pseudopodia – a more invasive phenotype?

Shankar et al. (2010) demonstrated that actin-dependant pseudopodia are critical in mesenchymal cell migration and together are determinants of EMT. This was achieved by knock-down of four pseudopod-specific proteins in human tumour cell lines, resulting in reduced actin cytoskeleton dynamics and induction of MET. In the work reported here, HPA-negative cells were significantly more likely to have pseudopodia than HPA-positive cells. This further suggests that HPA-negative cells have a mesenchymal-like phenotype and that the plasticity observed between HPA-positive and HPA-negative cells is EMT/MET-related. Appeddu and Shur (1994) reported that binding of cell-surface β1,4-galactosyltransferase (GalTase) to specific N-linked oligosaccharides on laminin mediates cell locomotion via pseudopodia. This further identifies glycosylation playing a role in cell migration and EMT. In the work reported here, it was observed that when a HPA-positive cell possessed pseudopodia, the projection was always opposite the location of the magnetic bead, which could possibly be due to steric hindrance caused by the bead binding or, intriguingly, perhaps suggesting that pseudopodia can only form where HPA-binding glycans are not present. Hidaka and Mitsui (2015) reported that N-glycosylation of seizure-related gene 6 (sez-6) regulates cell surface distribution, and therefore modulates the position of, filopodia-like protrusions. Furthermore, Nakayama et al. (2012) reported that knock-down of WBSCR17 (GALNT20) in HEK293T cells reduced lamellipodia formation. These findings suggest that pseudopodia formation and localisation can be a result of glycosylation modulation.

How the HPA-positive and HPA-negative isolated cell populations revert to a mixed population is a major question that is posed from the work reported here. One potential answer is epigenetic regulation of the GALNT genes. Gaziel-Sovran et al. (2011) reported that knock-down of mir-30d in melanoma cells up-regulated GALNT7 and alters the glycosylation status of the cells. Whilst up-regulation of mir-30d,

suppresses GALNT7 and enhances cell invasion. Alternatively, the reversion maybe orchestrated by EMT↔MET plasticity.

To conclude, the work described in this chapter suggests for the first time that GalNAc-glycosylation, detected by HPA-labelling, and morphology of cancer cells are interrelated, and plastic, and that cancer cells have the ability to regulate their glycosylation profile as a collective population. The ability to alter not only their glycosylation status but also their morphology is analogous to the reversible developmental program EMT, as discussed in Section 1.2.2.i, and therefore may be important in cancer cells ability to successfully metastasise.

4.4.3 Cell populations isolated based on their HPA-binging profile are from the same parental cell line

In order to determine whether the HPA-positive and HPA-negative isolated cell populations really were representing different states, CODIS STR analysis was performed. From these results it was clear that the isolated cell populations were not a result of the presence of two separate cell lines but were cells from the same cell line with different cell surface properties. It was not possible to determine the exact band sizes with the simple CODIS STR method reported here, however band sizes across the unseparated, HPA-positive and HPA-negative populations for each cell lines were the same, as illustrated in Table 4.6. Most of the observed band sizes were roughly the same as the expected band sizes (as illustrated in Figures 4.14-4.16). However, for ZR751 in particular Amelogenin was expected to be 106bp but was observed to be 200bp, CSF1PO was expected to be 199bp and 203bp and was observed to be 300bp, and D7S820 was expected to be 231bp and 235bp but was observed to be 100bp. These observed differences in ZR751 unseparated, HPA-positive and HPA-negative cells could potentially mean that the cell line is not correctly identified. Furthermore, some non-specific bands were present, for example as observed in MCF7 TPOX (see Figure 4.14). This is thought to be a result of technical issues with the PCR reaction. For example, as a result of the annealing time being too long or too much primer being added which increased the likelihood of non-specific binding. However, the same discrepancies are observed in both the unseparated parental cell line and isolated populations of each cell line, confirming that the isolated populations arise from a single parental cell line. If more time and resources were afforded to the project, it would be preferable to have the unseparated cell lines authenticated. Misidentification and cross-contamination of cell lines is a considerable problem which can compromise research (Geraghty et al., 2014). It has been reported that 18-36% of cell lines in use are incorrectly designated (reviewed by Lacroix, 2007). For example, Liscovitch and Ravid (2007) reported that multi-drug resistant breast cancer cell line MCF-7/AdrR were actually cells derived from the ovarian adenocarcinoma cell line OVCAR-8. Nelson-Rees and Flandermeyer (1976) demonstrated that a number of supposedly different cell lines were in fact all HeLa cells.

4.4 Key findings

- Cells that have been isolated based on their HPA-binding profile and subsequently cultured, revert to their unseparated glycosylation profile, as determined by HPA-labelling, over a time frame of approximately 72 hours.
- HPA-positive and HPA-negative cells isolated from the same cell lines have distinct morphologies, with the HPA-positive cells being rounded and the HPA-negative cells being elongated.
- The morphologies of the cells separated on the basis of their glycosylation profiles changes over a time frame of up to 72 hours consistent with their changing glycosylation.
- HPA-negative cells are significantly more likely to have pseudopodia and pseudopodia are more likely to form where HPA-binding glycans are absent.
- The separated HPA-positive and HPA-negative cell populations are the same as the unseparated cell lines, as determined by CODIS STR analysis.

Chapter 5

Molecular analysis of HPA-positive and HPA-negative populations

5.0 Molecular analysis of HPA-positive and HPA-negative populations

5.1 Background

The clear morphological differences between the HPA-positive and HPA-negative populations and their plasticity revealed by the work described in Chapter 4 suggested a potential transcriptomic difference between the two populations and so a microarray was performed to help identify any differentially expressed genes between the populations A microarray allows for the investigation of gene expression between two samples of thousands of genes at a time. This is achieved through fluorescently labelling sample cDNA which can then hybridise to DNA probes on the chip, un-bound cDNA is washed away and then detection and quantification of the bound fluorescent cDNA follows (Kurella et al., 2001).

As discussed in Section 1.2.2.i, activation of the developmental program EMT allows epithelial cancer cells to disaggregate from tightly structured epithelial cell monolayers, become motile, invade BM and ECM and disseminate to distant sites. Thiery (2002) proposed that once mesenchymal cancer cells have reached their secondary site, they undergo a reversion to epithelial cells, to form epithelial tumours through the process of MET. The plasticity of EMT↔MET in cancer cells may underlie the successful completion of metastasis. To understand the dynamics of EMT↔MET plasticity, first the molecular mechanisms underlying EMT must be considered. EMT effectors are proteins which identify cells as being either epithelial or mesenchymal, such as, E-cadherin, cytokeratin, vimentin and N-cadherin (as reviewed by Tsai and Yang, 2013). EMT core regulators are those transcription factors which regulate EMT effectors, and can be considered as three groups: (1) SNAI1 and SNAI2, (2) ZEB1 and ZEB2 and (3) TWIST1 and TWIST2. SNAI1 (Cano et al., 2000), SNAI2 (Bolós et al., 2016), ZEB1 (Eger et al., 2005), ZEB2 (Comijn et al., 2001) and TWIST1 (Vesuna et al., 2008) mediate EMT through repression of E-cadherin by binding to the promoter region. Casas et al. (2011), reported that TWIST1 and SNAI2 act co-ordinately to initiate EMT and that TWIST1 induces SNAI2 to repress E-cadherin. TWIST2 also initiates EMT through repression of E-cadherin, but does so through activation of STAT3 (Fang et al., 2011). EMT is thought to be generated in response to extracellular signals termed EMT inducers, which induce EMT core regulators (Yang and Weinberg, 2008). EMT inducers include, TGFβ (Zavadil and Böttinger, 2005), Wnt (Yook et al., 2005) and Notch (Wang et al., 2010b). However, TGFβ appears to be the principal regulator of EMT being able to induce EMT at transcriptional, translational and posttranslational levels (reviewed by Katsuno et al., 2013).

Several mechanisms of control of the core regulators have been reported in the literature, suggesting a greater level of control of the plasticity of the EMT↔MET program. One such example is the ZEB/miR-

200 double negative feed-back loop. ZEB factors repress miR-200 transcription through binding to the conserved recognition sequence in the promoter region, whilst miR-200 inhibits expression of ZEB by binding to sites within their 3' UTRs (Korpal et al., 2008; Park et al., 2008; Brabletz and Brabletz, 2010). A further double negative feed-back loop, SNAI/miR34, was reported by Siemens et al. (2011), which was also found to be interconnected to the ZEB/miR200 feed-back loop, which taken together pushes cell plasticity (Brabletz, 2012). SNAI represses miR200, whilst ZEB represses miR34. Lu et al. (2013) proposed that interconnection of the two negative feed-back loops helps to give rise to hybrid epithelial-mesenchymal phenotypes that are often seen in cancer cells. Yu et al. (2014) reported that miR-300 negatively regulates TWIST by binding to the 3' UTR region. A number of miRs have been reported to modulate EMT core regulators and are reviewed by Zheng and Kang (2014). miR control of EMT core regulators demonstrates a level of control over the EMT↔MET program that correlates with cellular plasticity in cancer metastasis.

Aims and objectives

The aims of the experiments in this chapter were to:

I. To assess the gene expression differences between the populations and highlight any potential pathways or processes that the differentially expressed genes may be involved in.

5.2 Methods

5.2.1 Microarray

A work-flowchart for the microarray is illustrated in Figure 5.1. Three cell separations were performed as detailed in Section 2.3 using MCF7 cells and the HPA-positive and HPA-negative populations were pelleted by centrifugation at 1,100 x g for 3min and snap-frozen. RNA was extracted from both populations using Tri Reagent as detailed in Section 2.5. The quality of the RNA was assessed using an ©Agilent 2100 Bioanalyser and if the RIN (RNA integrity number) value was ≥7 it was considered good quality. The cDNA was synthesised using a Pico 6000 RNA chip (©Aligent) and the quality checked again on an ©Agilent 2100 Bioanalyser. The array used had 12 sub arrays (24 samples) and 135,000 probes. A NimbleGen array slide (Roche) was scanned at 3µm on an InnoScan 700 Microarray Scanner for split channel Cy3 and Cy5 TIFF images using Mapix version 5.1 software. The TIFF images were aligned to their NimbleGen design files and converted into probe intensity values using the NimbleGen DEVA software. The data were LOESS normalised for within array variation of Cy3 and Cy5 dyes using the R statistical program. This was quintile normalised for across array variation using DNAstar (ArrayStar Inc.). The Log_2 intensity values were formatted using Excel. The RNA quality assessment, microarray,

normalisation processes, heatmap and scatter plot were performed by Dr Ryan Pink of Oxford Brookes University. The complete microarray data set was analysed with three different methods, these were: (1) with hierarchical clustering using Euclidean distances and centroid linkages to produce a heatmap using ArrayStar® software (DNASTAR, Inc), (2) as a pair-wise comparison using scatter plot of expression values (log_2) of MCF7 HPA-positive versus HPA-negative populations using ArrayStar® software (DNASTAR, Inc) and (3) with a volcano plot of expression values (log_2) against p values. The microarray data was also analysed for genes associated with EMT that had a >1.8-fold change differences between MCF7 HPA-positive and HPA-negative cell populations. Furthermore, for significantly altered gene expression levels of GALNTs, C1GalT and *COSMC*, which were investigated previously in the whole cell lines (see Section 3.3.4). As well as the top 10 most significantly altered genes.

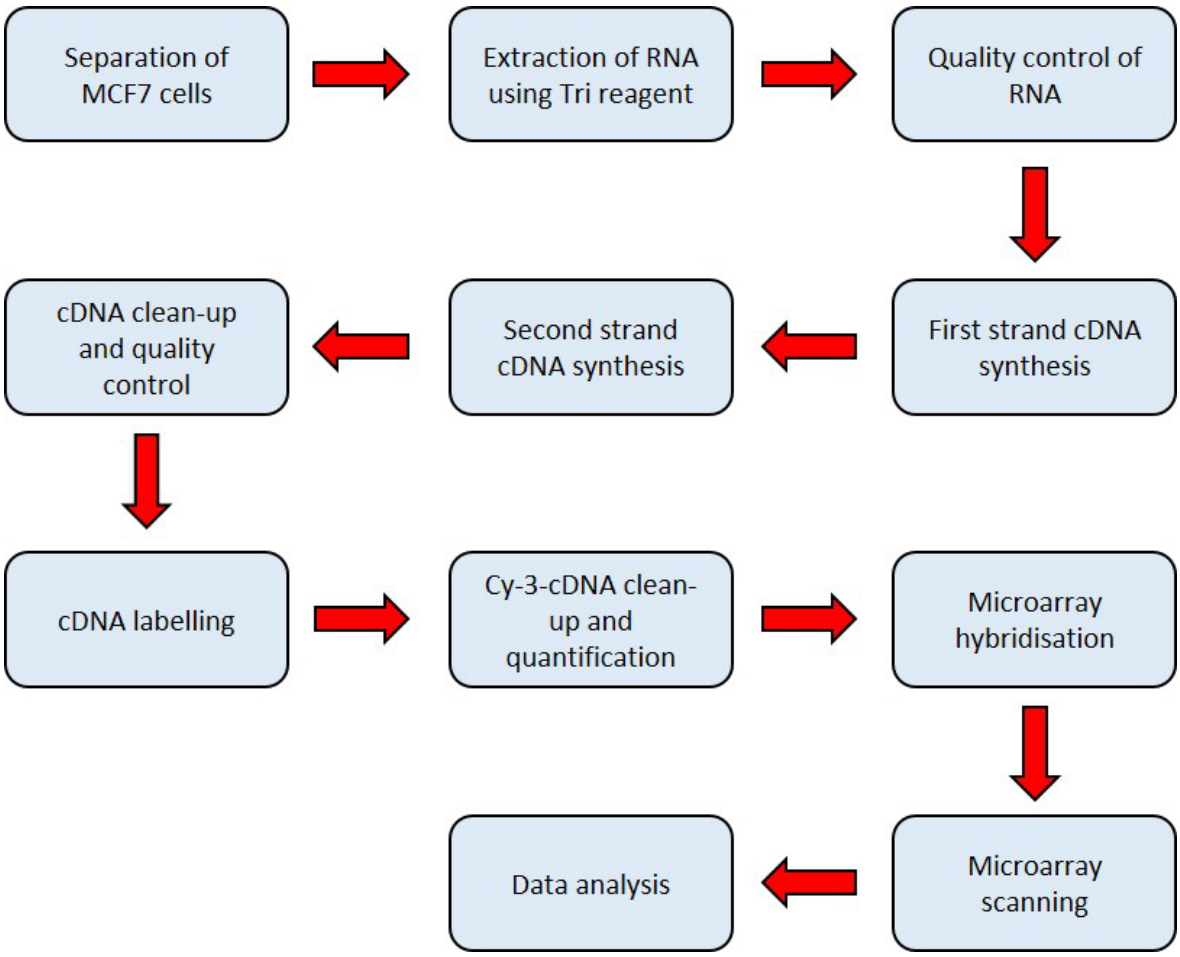

Figure 5.1 *Work-flowchart of microarray.*

5.2.2 DAVID KEGG pathway analysis

Analysis was performed on the microarray data so pathways that the differentially expressed genes are involved in could be identified. DAVID (The Database for Annotation, Visualization and Integrated Discovery, https://david.ncifcrf.gov/) is an online bioinformatics database for microarray data, which contains a number of resources to efficiently evaluate the data for example, Annotation Tool, GoCharts, KeggCharts and Domain Charts. KeggCharts produce an annotated illustration of a KEGG (Kyoto Encyclopaedia of Genes and Genomes) biochemical pathway that several of the differentially expressed genes are involved in (Dennis et al., 2003).

The microarray data were organised into those genes which displayed a 1.8-fold change, the minimum limit of detection before measurement noise influences results (Butte et al., 2001) and with <0.06 significance level between the HPA-positive and HPA-negative cells, in order to encompass those differences that are just outside of significant, which may have been reduced as a result of normalisation. The EntrezIDs for all the genes which corresponded to these criteria were used within DAVID, and KEGG pathway analysis was performed where genes were grouped based on biological systems they are known to be within.

5.2.3 qPCR to validate Microarray data

Eight genes were selected from the microarray results to have their expression within the HPA-positive and HPA-negative populations validated using qPCR. These were: CDH1, VIM, SMAD2, GALNT6, TFPI2, SPARC, FBLN1 and ZEB1. The genes were chosen as they were considerably differentially expressed between the HPA-positive and HPA-negative cell populations and have been reported in the literature to be implicated in EMT. Primers for these genes were designed and are detailed in Table 5.1. Three biological replicates each of MCF7, ZR751 and BT474 cells were separated as detailed in Section 2.3 and had their RNA extracted as detailed in Section 2.5. The RNA samples were DNase treated (see Section 2.6) and converted to cDNA (see Section 2.7). qPCRs were run and analysed as detailed in Section 2.8.

Table 5.1 *Primer pair sequences, and melting temperature (Tm) for genes of interest and reference genes, designed and optimised for use with both DNA and RNA.*

Primer name	Primer sequence	Tm (°C)
GUSB	(F) 5'-AAACCCTGCAATCGTTTCTG-3' (R) 5'-GGCTCCGTATGTGGATGTG-3'	64.3 64.6
CDH1	(F) 5'-CCCAAGTGCCTGCTTTTGAT-3' (R) 5'-CCTACCCCTCAACTAACCCC-3'	59.0 58.8
VIM	(F) 5'-GCTTCGCCAACTACATCGAC-3' (R) 5'-TTGTCGTTGGTTAGCTGGTC-3'	59.4 58.1
SMAD	(F) 5'-ACTCTCTGATAGTGGTAAGGGT-3' (R) 5'-CGTCTCCAGGTATCCCATCG-3'	57.4 59.4
GALNT6	(F) 5'-ATTCCCATTCCTCGTCCTTG-3' (R) 5'-CGCAAAGCAGCTGTGTCTAC-3'	65.4 64.2
TFPI2	(F) 5'-CAGAAGCCCATACAAGTAGCT-3' (R) 5'-CTGCAAGTGAGTGTGGACGA-3'	57.5 60.3
SPARC	(F) 5'-GTGAGATCCGACCATCCCAT-3' (R) 5'-GCTCTTCTCAGGGGCTCTAG-3'	59.0 59.0
FBLN1	(F) 5'-TTTGAGTATCAGTGCCCCGT-3' (R) 5'-TCCTCGTTGAGATGGTAGCC-3'	59.0 58.9
ZEB1	(F) 5'-CTCTTTCAGCATCACCAGGC-3' (R) 5'-CAGAACAACAGCTTGCACCA-3'	58.9 59.2

5.3 Results

5.3.1 Microarray

The complete microarray data set was analysed using three different methods to provide both a visual representation of the complex data and a method for measuring similarity between experiments (gene ratios), these were, (1) a heatmap, (2) a scatter plot and (3) a volcano plot. The heatmap illustrated in Figure 5.2 utilised hierarchical clustering of the genes using Euclidean distances and centroid linkages. Gene clusters which are expressed highly (red colour) in MCF7 HPA-positive (right side) are expressed lowly (blue colour) in HPA-negative (left side) population and *vice versa*. The scatter plot as illustrated in Figure 5.3 demonstrates the correlation between MCF7 HPA-positive and HPA-negative samples (r^2) and the number of genes present at specific fold changes between samples as calculated using a Student's t-test. For example, at 2-fold change there are 423 genes with a 95% confidence, at 4-fold change there are 32 genes with a 95% confidence and at 8-fold change there are 3 genes with a 95% confidence. The volcano plot illustrated in Figure 5.4 demonstrates the spread of the fold change ($\log_2$) between MCF7 HPA-positive and HPA-negative populations and indicates the number of genes which have a >1.8-fold change and <0.06 p value.

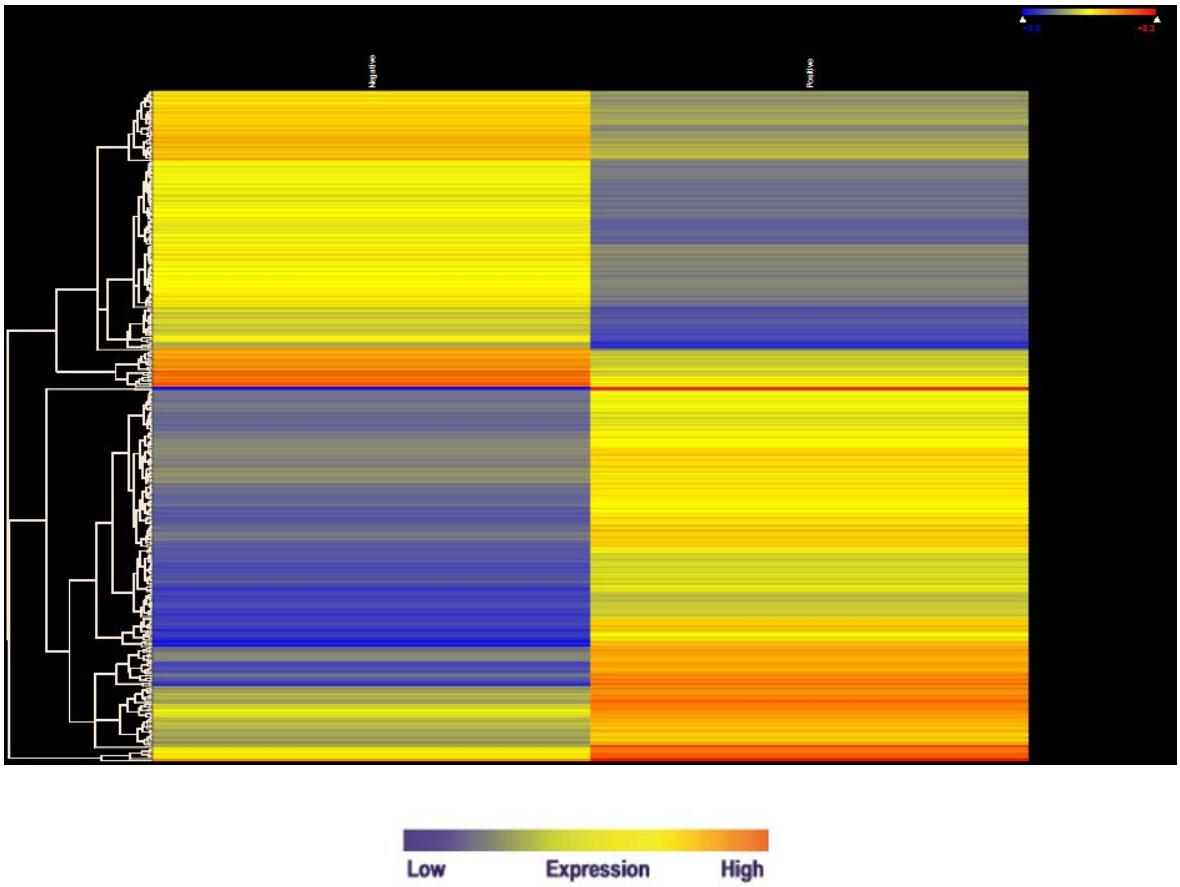

Figure 5.2 *Heatmap produced using ArrayStar® software (DNASTAR, Inc) of gene expression organised in to hierarchical clusters of MCF7 HPA-positive (right) versus HPA-negative populations (left). Blue colour indicates low gene expression level and red indicates high gene expression level.*

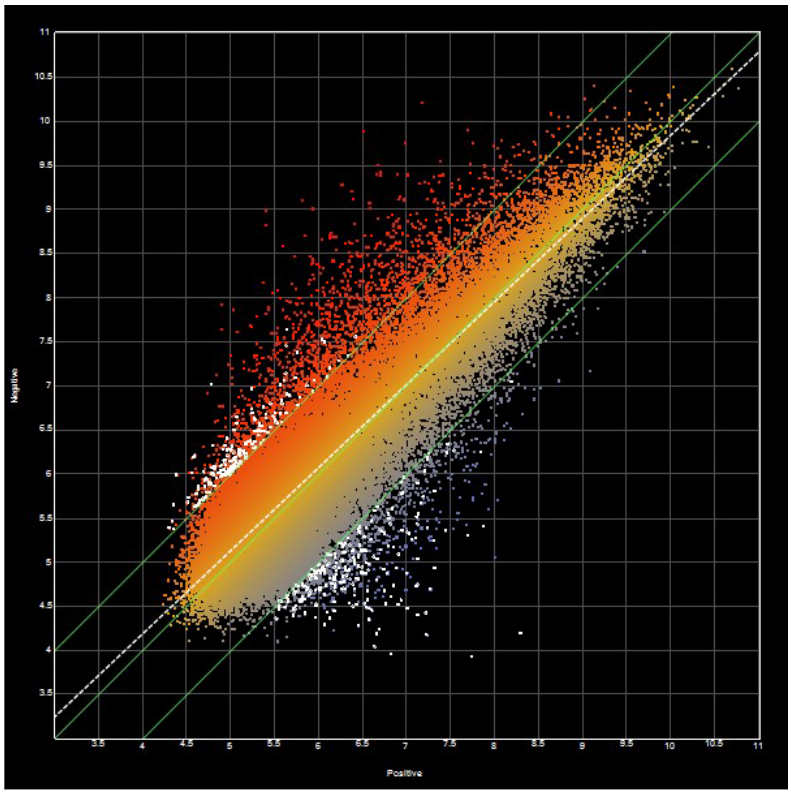

Figure 5.3 *Scatter plot produced using ArrayStar® software (DNASTAR, Inc) illustrating the correlation between samples (r^2 = 0.8002) and the number of genes present at specific fold changes (log_2) between MCF7 HPA-positive (x axis) and HPA-negative (y axis) populations.*

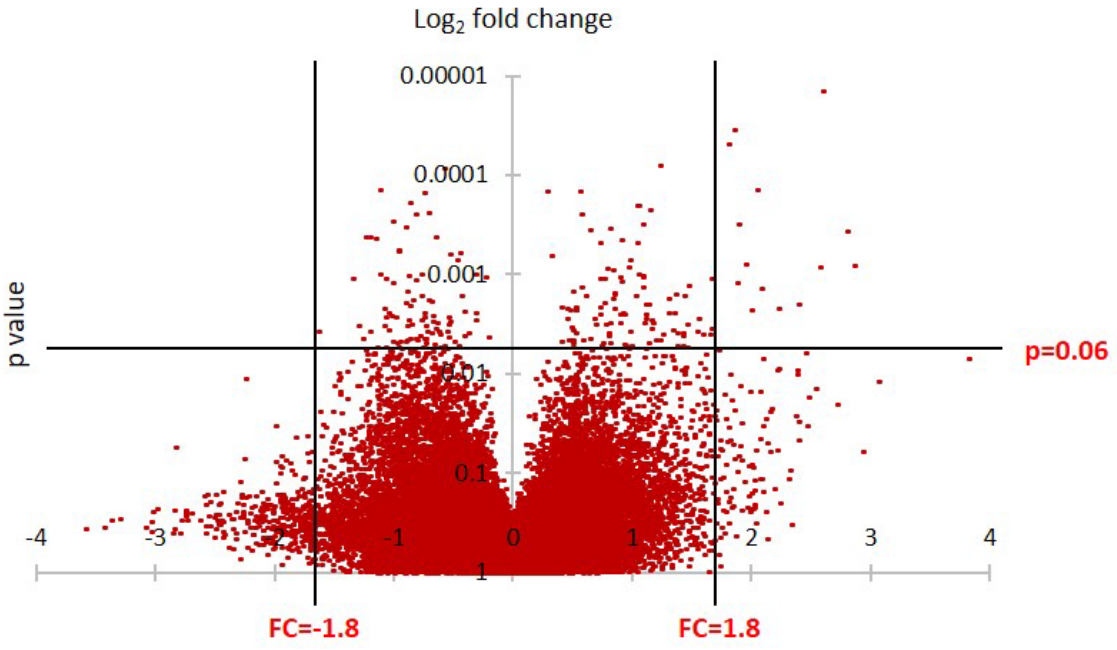

Figure 5.4 *Volcano plot illustrating the number of genes which have a p value (y axis) <0.06 and a fold change (log2) (x axis) >1.8 between MCF7 HPA-positive and HPA-negative populations.*

In order to investigate whether the gene expression patterns of the HPA-positive and HPA-negative populations are consistent with their suspected epithelial or mesenchymal phenotypes, MCF7 cells were separated based on their HPA-binding profiles, RNA was extracted and microarray was performed. Microarray analysis was carried out to investigate transcriptomic differences between HPA-positive and HPA-negative cell populations. There was found to be 911 significantly different genes between the HPA-positive and HPA-negative cell populations. The microarray dataset was examined for >1.8 fold changes in expression levels between HPA-positive and HPA-negative cells of genes known to be involved in EMT. As shown in Table 5.2, seventeen genes reported to be involved in EMT had a fold change of >1.8 between HPA-positive and HPA-negative cells, five of which were significantly different. These were: nidogen 1 (NID1) ($p<0.05$) up-regulated in HPA-negative cells, complement factor H (CFH) ($p<0.05$) up-regulated in HPA-negative cells, sine oculis homeobox 1 (SIX1) ($p<0.05$) up-regulated in HPA-negative cells, wnt family member 2B (WNT2B) ($p<0.05$) down-regulated in HPA-negative cells.

Table 5.2 *Genes reported to be involved in EMT with a fold change greater than 1.8. Significant changes are highlighted. *Regulation direction is HPA-negative compared to HPA-positive.*

Entrez ID	Gene name	Fold change	p value	Regulation direction*	Reference of involvement of EMT
4811	**NID1**	**5.20**	**0.02**	**UP**	**Pedrola et al., 2015**
3082	HGF	4.35	0.06	UP	Yu et al., 2009
3075	**CFH**	**3.59**	**0.04**	**UP**	**Orr et al., 2012**
2201	**FBN2**	**3.50**	**0.04**	**UP**	**Yang et al., 1999**
6495	**SIX1**	**3.46**	**0.05**	**UP**	**Micalizzi et al., 2010b; Ono et al., 2012**
7431	VIM	3.30	0.18	UP	Mendez et al., 2010
999	CDH1	3.06	0.14	DOWN	Ye et al., 2012
79977	GRHL2	2.86	0.08	DOWN	Werner et al., 2013
7291	TWIST1	2.76	0.11	UP	Lee et al., 2006b
7482	**WNT2B**	**2.69**	**0.03**	**DOWN**	**Kubo et al., 2005**
1290	COL5A2	2.49	0.12	UP	Vittal et al., 2013
6935	ZEB1	2.45	0.07	UP	Burk et al., 2008
4017	LOXL2	2.41	0.12	UP	Moon et al., 2013
6591	SNAI2/SLUG	2.30	0.39	UP	Hajra et al., 2002
1999	ELF3	2.17	0.11	DOWN	Yeung et al., 2017
5157	PDGFRL	2.14	0.15	UP	Guo et al., 2013
655	BMP7	2.09	0.25	DOWN	Duangkumpha et al., 2014

In order to investigate whether the gene expression profiles of HPA-positive and HPA-negative populations have differences in O-glycosylation initiating enzymes the dataset was examined for significantly altered expression of GALNTs and the next most commonly acting transferase C1GalT and its molecular chaperone *COSMC*. As shown in Table 5.3, gene expression of two GALNTs are significantly altered between the MCF7 HPA-positive and HPA-negative populations. GALNT6 was down-regulated in HPA-negative cells ($p<0.05$), with a fold change of 3.10 and GALNT20 (WBSCR17) was also down-regulated in HPA-negative cells ($p<0.05$), with a fold change of 3.22. The remaining 18 GALNTs have negligible altered gene expression between the MCF7 HPA-positive and -negative populations.

Table 5.3 *GALNTs, C1GALT1 and COSMC gene expression level changes of separated MCF7 cells. Significant changes are highlighted. *Regulation direction is negative compared to positive.*

Entrez ID	Gene symbol	Pseudonyms	Fold change	p value	Regulation direction*
2589	GALNT1		1.48	0.20	UP
2590	GALNT2		1.61	0.24	UP
2591	GALNT3		1.05	0.85	DOWN
8593	GALNT4		1.07	0.82	UP
11227	GALNT5		1.19	0.63	DOWN
11226	**GALNT6**		**3.10**	**0.02**	**DOWN**
51809	GALNT7		1.49	0.26	DOWN
26290	GALNT8		1.01	0.99	UP
50614	GALNT9		1.97	0.98	UP
55568	GALNT10		1.97	0.21	DOWN
63917	GALNT11		1.16	0.58	DOWN
79695	GALNT12		1.22	0.59	DOWN
114805	GALNT13		1.00	0.99	DOWN
79623	GALNT14		2.12	0.15	UP
117248	GALNT15	GALNTL2	1.02	0.93	DOWN
57452	GALNT16	GALNTL1	1.09	0.81	DOWN
442117	GALNT17	GALNTL6	1.31	0.32	UP
374378	GALNT18	GALNTL4	1.65	0.12	DOWN
168391	GALNT19	GALNTL5	1.14	0.63	UP
64409	**GALNT20**	**WBSCR17, GALNTL3**	**3.22**	**0.02**	**DOWN**
56913	C1GALT1		1.49	0.34	UP
29071	C1GALT1C1	COSMC	1.50	0.20	UP

The dataset was then assessed for the top 10 largest significant fold changes. As shown in Table 5.4, a number of these genes are involved in basement membrane and extracellular matrix structure and therefore potentially important for cancer cell invasion. The gene with the largest fold change in expression level was NID1 (FC 5.21, $p<0.05$), which was up-regulated in HPA-negative cells. Further genes identified to be significantly up-regulated in the HPA-negative cells included, GAD1 (FC 4.73, $p<0.01$) and SPARC (FC 4.64, $p<0.01$), which have been implicated in cell invasion.

Table 5.4 *Top 10 significant gene expression level fold changes between MCF7 HPA-positive and HPA-negative populations. *Regulation direction is negative compared to positive.*

Entrez ID	Gene name	Fold change	p value	Regulation direction*
4811	Nidogen 1 (NID1)	5.21	0.02	UP
5360	Phospholipid transfer protein (PLTP)	5.08	0.02	UP
28965	Solute carrier family 27 (fatty acid transporter), member 6 (SLC27A6)	4.77	0.02	DOWN
2571	Glutamate decarboxylase 1 (GAD1)	4.73	0.01	UP
55243	Kin of IRRE like (KIRREL)	4.64	0.01	UP
6678	Secreted protein, acidic cysteine-rich (SPARC)	4.64	0.01	UP
285498	Rich finger protein 212 (RNF212)	4.62	0.009	UP
1775	Deoxyribonuclease 1-like 2 (DNASE1L2)	4.48	0.02	DOWN
2192	Fibulin 1 (FBLN1)	4.48	0.03	UP
6445	Sarcoglycan, gamma (34KDa dystrophin-associated glycoprotein) (SGCG)	4.46	0.0004	DOWN

5.3.2 DAVID KEGG pathway analysis

In order to determine links between the differentially expressed genes between the HPA-positive and HPA-negative populations genes which had a fold change of ≥1.8 and a p value of <0.06 (a total of 1119 genes) were used in KEGG pathway analysis. Three pathways were identified, these were leukocyte transendothelial migration (significance level 0.062), Toll-like receptor signalling pathway (significance level 0.058) and the complement and coagulation cascades (significance level 0.006). The leukocyte transendothelial migration pathway (see Figure 5.5) included 11 differentially expressed genes (detailed in Table 5.5). The Toll-like receptor signalling pathway (see Figure 5.6) included 10 differentially expressed genes (detailed in Table 5.6). The complement and coagulation cascades (see Figure 5.7), included 10 differentially expressed genes (detailed in Table 5.7).

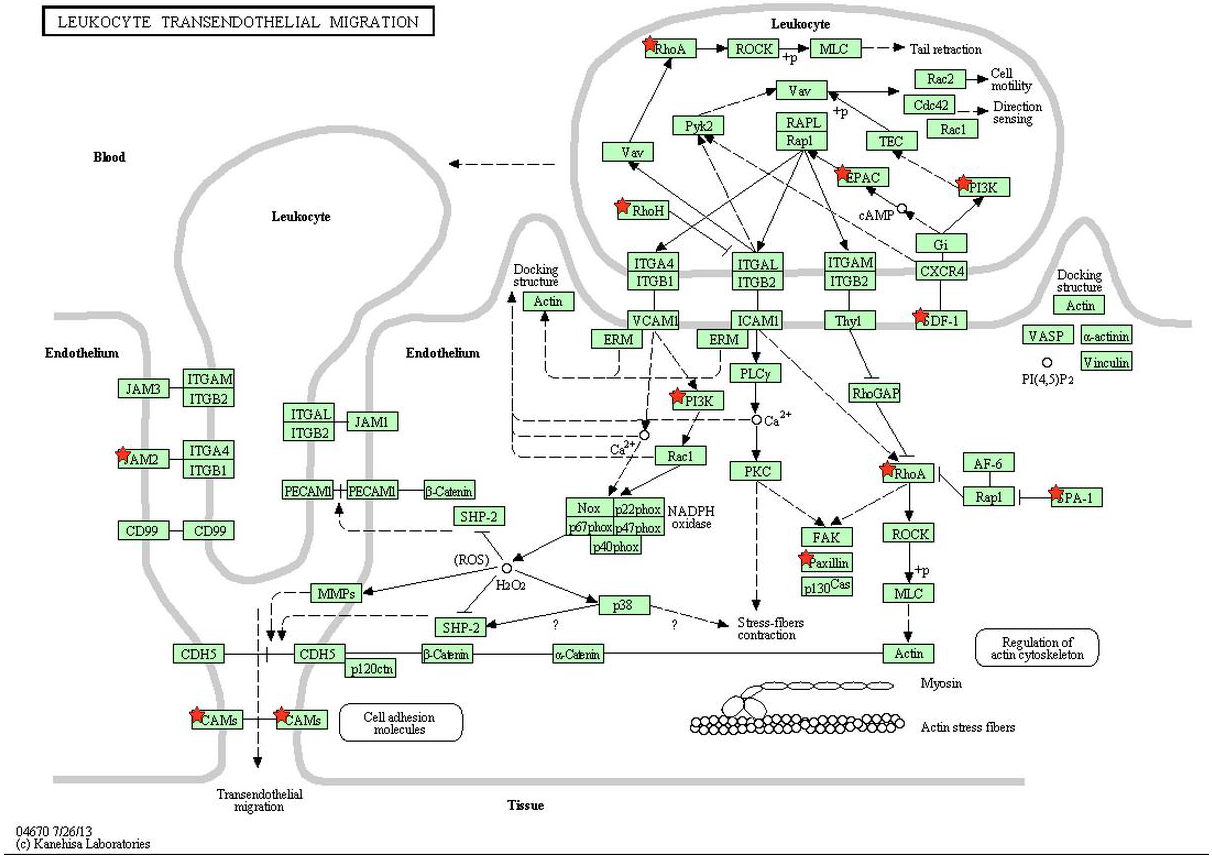

Figure 5.5 *Print screen of leukocyte transendothelial migration KEGG pathway. Red stars denote genes which have significant changes in expression levels between the MCF7 HPA-positive and HPA-negative populations as discerned by the microarray.*

Table 5.5 *Genes highlighted in transendothelial migration pathway (Figure 5.5) which have significant changes in expression levels between MCF7 HPA-positive and HPA-negative populations as discerned by microarray. *Regulation direction is negative compared to positive.*

Entrez ID	Gene symbol	Fold change	p value	Regulation direction*
10411	RAPGEF3	1.96	0.03	UP
6494	SIPA1	1.99	0.05	UP
9073	CLDN8	2.61	0.03	UP
58494	JAM2	2.7	0.01	UP
387	RHOA	2.48	0.03	UP
6387	CXCL12	2.65	0.03	DOWN
9075	CLDN2	1.92	0.05	DOWN
9080	CLDN9	2.44	0.01	DOWN
5829	PXN	2.14	0.03	DOWN
8503	PIK3R3	2.14	0.04	DOWN
399	RHOH	2.09	0.02	DOWN

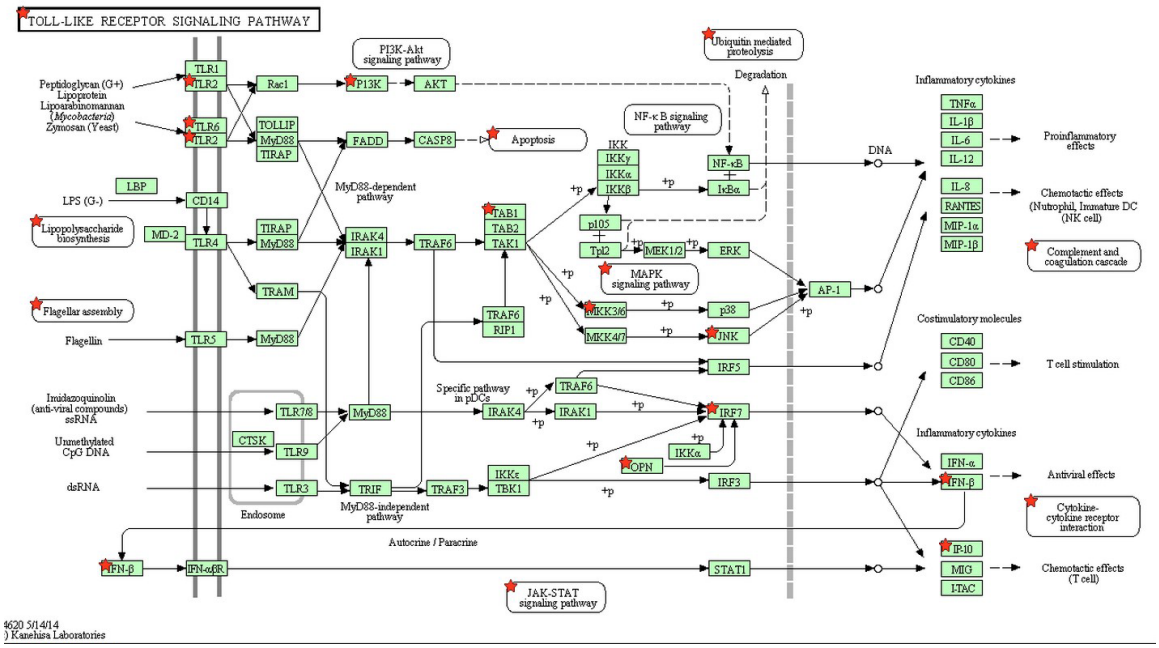

Figure 5.6 *Print screen of Toll-like receptor KEGG pathway. Red stars denote gene which have significant changes in expression levels between the MCF7 HPA-positive and HPA-negative populations as discerned by the microarray.*

Table 5.6 *Genes highlighted in Toll-like receptor signalling pathway (Figure 5.6) which have significant changes in expression levels between MCF7 HPA-positive and HPA-negative populations as discerned by microarray. *Regulation direction is negative compared to positive.*

Entrez ID	Gene symbol	Fold change	p value	Regulation direction*
3456	IFNB1	1.85	0.03	UP
5608	MAPK6	3.74	0.05	UP
6696	SPP1	2.74	0.04	UP
10333	TLR6	2.4	0.02	UP
3627	CXCL10	1.94	0.02	DOWN
3665	IRF7	2.23	0.02	DOWN
5602	MAPK10	2.46	0.04	DOWN
5803	PIK3R3	2.14	0.03	DOWN
7097	TLR2	2.5	0.05	DOWN

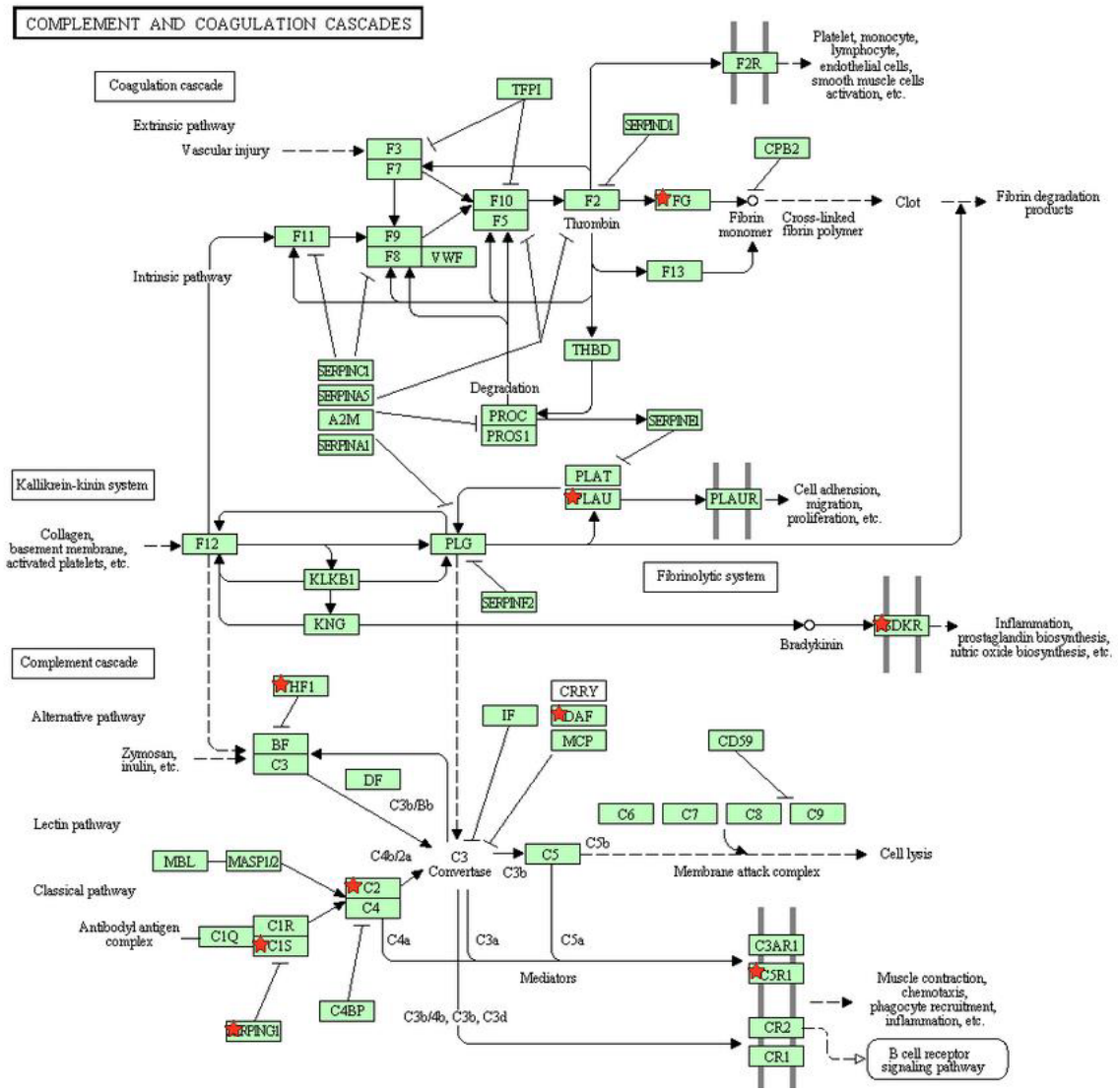

Figure 5.7 *Print screen of complement and coagulation cascades KEGG pathway. Red stars denote gene which have significant changes in expression levels between the MCF7 HPA-positive and HPA-negative populations as discerned by the microarray.*

Table 5.7 *Genes highlighted in complement and coagulation cascades (Figure 5.7) which have significant changes in expression levels between MCF7 HPA-positive and HPA-negative populations as discerned by microarray. *Regulation direction is negative compared to positive.*

Entrez ID	Gene symbol	Fold change	p value	Regulation direction*
716	C1S	2.32	0.04	UP
717	C2	1.97	0.04	UP
3075	CFH	3.59	0.04	UP
2244	FGB	1.89	0.05	UP
2266	FGG	2.42	0.02	UP
5328	PLAU	1.92	0.02	UP
710	SERPING1	2.14	0.05	UP
728	C5AR1	2.16	0.03	DOWN
1604	CD55	2.61	0.04	DOWN
623	BDKRB1	1.95	0.05	DOWN

5.3.3 qPCR to validate microarray data

In order to validate the microarray data, eight genes were chosen (as detailed in Table 5.8) to assess gene expression levels between HPA-positive and HPA-negative cell populations in the MCF7 cell line. MCF7 cells were separated based on their HPA-binding profiles and RNA was extracted, converted to cDNA and qPCRs were performed. As illustrated in Figure 5.8, when the data are normalised to GUSB, the qPCR results, with the exception of SMAD2 agree with those of the microarray. It was observed in the microarray data (see Table 5.8) that CDH1 was down-regulated in MCF7 HPA-negative cells, which is also observed in the qPCR data. The remaining genes, were found to be up-regulated in MCF7 HPA-negative cells in the microarray data and the same is also observed in the qPCR data, although not significantly so and with the exception of SMAD2. In the qPCR results, MCF7 HPA-positive cells expressed significantly more ($p<0.05$) SMAD2, which is contrary to what was observed in the microarray data (see Table 5.8).

Table 5.8 *Regulation direction, fold change and p values for genes chosen from microarray data to validate with qPCR. qPCR results also indicated. *Regulation direction is HPA-negative compared to HPA-positive.*

Gene symbol	Gene description	Gene locus	Fold change	p value	Regulation direction*	
					Microarray	qPCR
CDH1	Cadherin 1	16q22.1	3.06	0.14	DOWN	DOWN
VIM	Vimentin	10p13	2.77	0.08	UP	UP
SMAD2	SMAD family member 2	18q21.1	2.01	0.05	UP	DOWN
GALNT6	Polypeptide N-acetylgalactosaminyltransferase 6	12q13	1.63	0.02	UP	UP
TFPI2	Tissue factor pathway inhibitor 2	7q22	2.38	0.04	UP	UP
SPARC	Secreted protein acidic and cysteine rich	5p33.1	2.21	0.01	UP	UP
FBLN1	Fibulin 1	22q13.31	2.16	0.03	UP	UP
ZEB1	Zinc finger E-box binding homeobox 1	10p11.22	2.45	0.07	UP	UP

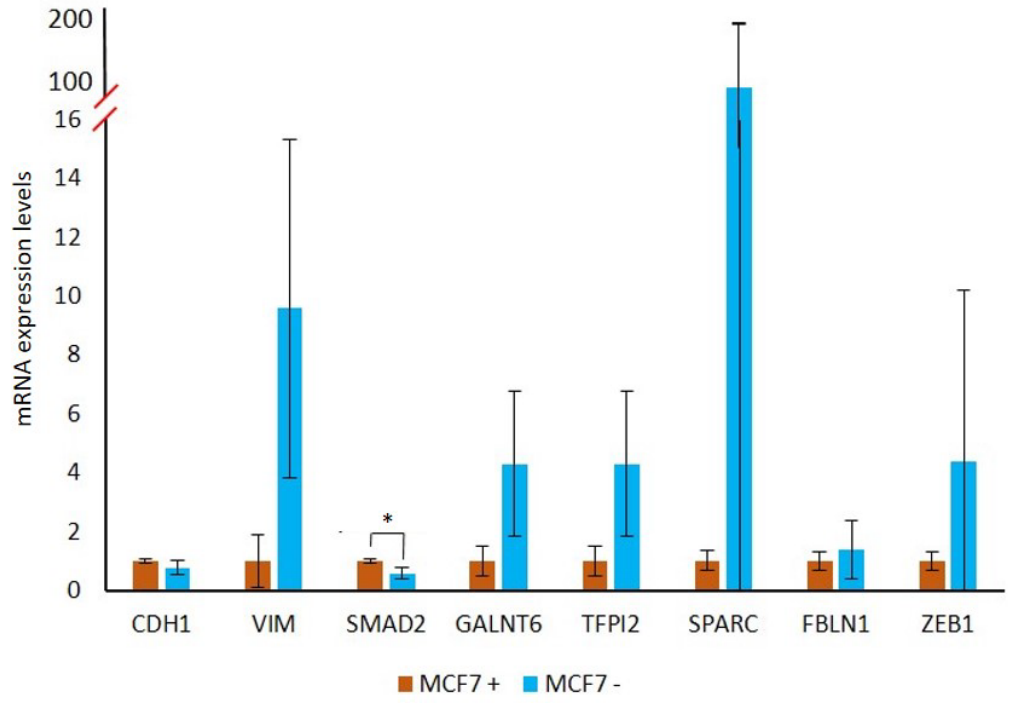

Figure 5.8 *Normalised to GUSB mRNA expression levels of CDH1, VIM, SMAD2, GALNT6, TFPI1, SPARC, FBLN1 and ZEB1 for MCF7 cells normalised using the delta delta Ct method to GUSB and HPA-positive of the same gene. Three biological replicates per cell line used. Error bars are calculated from standard error of the mean. p values calculated from two-tailed t-test. Data is in agreement with what was observed in microarray data except for SMAD2 which is in opposition to what was previously observed.*

Having validated the microarray data for the genes identified (see Table 5.8), expression levels were then assessed in the ZR751 and BT474 cell lines. As illustrated in Figure 5.9 A., ZR751 HPA-positive and HPA-negative cell populations had a different gene expression profile compared to MCF7 cells (see Table 5.9) with GALNT6, TFPI2, SPARC and FBLN1 being down-regulated in HPA-negative cells. BT474 HPA-positive and HPA-negative cell populations (as illustrated in Figure 5.9 B.) also have a different expression profile of the genes tested (see Table 5.9) with all genes being up-regulated in HPA-negative cells.

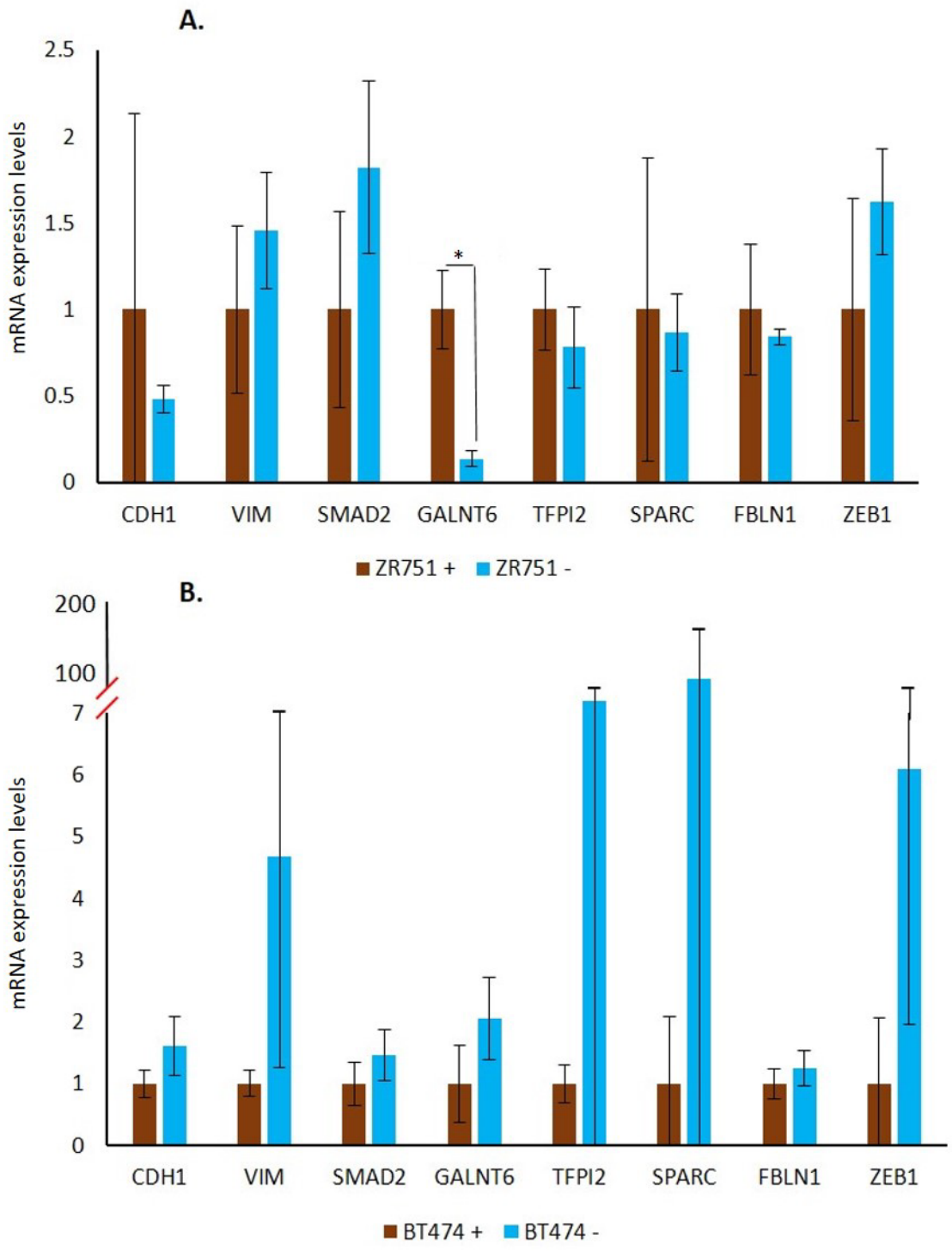

Figure 5.*9 Normalised to ACTB mRNA expression levels of CDH1, VIM, SMAD2, GALNT6, TFPI1, SPACR, FBLN1 and ZEB1 for (A.) ZR751 and (B.) BT474 normalised using the delta delta Ct method to GUSB and HPA-positive of the same gene. Three biological replicates per cell line used. Error bars are calculated from standard error of the mean. p values calculated from two-tailed t-test. Expression levels of the genes of interest were different in P- and N-populations of the ZR751 and BT474 cell than was observed in MCF7 cells.*

Table 5.9 *A comparison of gene regulation direction, *HPA-negative compared to HPA-positive, for the microarray data and all three cell lines (MCF7, ZR751 and BT474).*

Gene symbol	Regulation direction*			
	Microarray	**MCF7**	**ZR751**	**BT474**
CDH1	DOWN	DOWN	DOWN	UP
VIM	UP	UP	UP	UP
SMAD2	UP	DOWN	UP	UP
GALNT6	UP	UP	DOWN	UP
TFPI2	UP	UP	DOWN	UP
SPARC	UP	UP	DOWN	UP
FBLN1	UP	UP	DOWN	UP
ZEB1	UP	UP	UP	UP

5.4 Discussion

In order to investigate transcriptomic differences between the HPA-positive and HPA-negative cell populations, a microarray was performed. This was achieved by cell separating MCF7 cells, extracting their RNA, performing a microarray and then analysing the microarray dataset. The dataset was assessed for significantly differently expressed EMT associated genes between MCF7 HPA-positive and HPA-negative cells. Nidogen 1 (NID1) was most significantly ($p<0.05$) up-regulated in HPA-negative cells. NID1 encodes a BM glycoprotein that is produced predominantly by mesenchymal cells, which mediates BM assembly by connection of laminin and collagen IV networks (Patel et al., 2014). Pedrola et al. (2015) reported that over-expression of the transcription factor ETV5 induces EMT in endometrial cancer cell lines and regulates NID1 expression which modulates cell migration and invasion. This demonstrates that NID1 is involved in cell invasive characteristics. Complement factor H (CFH) was the next most significantly ($p<0.05$) up-regulated gene in HPA-negative cells. Orr et al. (2012) reported that CFH is a novel EMT marker in prostate cancer. Fibrillin 2 (FBN2) is a component of connective tissue microfibrils. Yang et al. (1999) suggested a potential role of EMT in lung development. FBN2 has also been reported to differentially regulate TGFβ during bone formation (Nistala et al., 2010). TGFβ is a key regulator of EMT; Fibrillin 5 (FBLN5) has been reported by Lee et al. (2008) to both initiate and enhance TGFβ-induced EMT in breast cancer cells. Taking this into account, it is reasonable to assume that FBN2 could also modulate EMT through regulation of TGFβ. Sine oculis homeobox 1 (SIX1) was significantly ($p<0.05$) up-regulated in HPA-negative cells. SIX1 is a transcription factor involved in the regulation of cell proliferation, apoptosis and embryonic development. Micalizzi et al. (2010b) reported that SIX1 overexpression up-regulates TGFβ type I receptor (TβRI) and subsequently activates TGFβ signalling, which induces EMT in breast cancer cells. Furthermore, Ono et al. (2012) reported that overexpression of SIX1 represses CDH1 through repression of the miR-200-family and expression of ZEB1, therefore

promoting EMT in colorectal cancer. Wnt family member 2B (WNT2B) was significantly down-regulated in HPA-negative cells. WNT2B is a paralogue of WNT2 and is part of the WNT family of secreted signalling factors which are involved in a number of developmental processes. Kubo et al. (2005) reported that overexpression of WNT2B inhibited cellular differentiation of progenitor cells in marginal retina by down regulating proneural genes, therefore preventing cells from entering the differentiation cascade controlled by Notch. Several of the identified genes induce EMT through repression of E-cadherin (CDH1), including TWIST1, ZEB1, SIX1, LOXL2, SNAI2 and PDGRRL.

The microarray dataset was also assessed for significantly different expression of GALNT genes between MCF7 HPA-positive and HPA-negative cell populations. It was observed that GALNT6 was significantly ($p<0.05$) down-regulated in HPA-negative cells. GALNT6 has been reported as a useful immunohistochemical marker of invasive breast cancer (Berois et al., 2006a), as well as being implicated in EMT through the O-glycosylation of fibronectin (Park et al., 2011; Ding et al., 2012b). GALNT20 was also significantly ($p<0.05$) down-regulated in MCF7 HPA-negative cell populations. GALNT20 is fairly new addition to the GALNT gene family (Nakamura et al., 2005) but has been implicated in regulation of pseudopodia formation (Nakayama et al., 2012), which is linked with invasive characteristics. There have been several reports in the literature demonstrating that GALNTs regulate EMT induction and signalling molecules as well as facilitating epithelial or mesenchymal phenotypes. For example, Herr et al. (2008) demonstrated that GALNT16 (GALNTL1) negatively regulates TGFβ signalling through the modulation of TGFβ receptor ActR-IIB. TGF-β is a key EMT inducer, with GALNT16 acting as a regulator to TGF-β consequently it is also regulating EMT. A further example or GALNT regulation of EMT is reported by Wu et al. (2011) who showed that up-regulation of GALNT2 suppresses EGF-induced cell growth by modifying the response of EGFR binding to EGF. Boskovski et al. (2013) demonstrated that GALNT11 activates Notch signalling cascade, which is also a key EMT inducer. Huanna et al. (2015) reported that overexpression of GALNT14 resulted in enhanced cell migration and invasion, as well as up-regulation of the mesenchymal markers N-cadherin, vimentin, MMP-2, VEGF and TGFβ and the down-regulation of epithelial marker E-cadherin. Taken together, it is clear that GALNTs and therefore glycosylation which is commonly de-regulated in cancers is interconnected and potentially regulating EMT↔MET. Taken together these findings indicate that GALNT6 and GALNT20 may play a role in regulating protein O-glycosylation between HPA-positive and HPA-negative MCF7 cell populations.

The microarray dataset was also assessed for the top 10 genes with the largest significant fold change in expression levels between the MCF7 HPA-positive and HPA-negative cell populations. It was observed that the gene with the largest fold change was NID1 (FC 5.21, $p<0.05$). This gene encodes a glycoprotein which establishes and maintains basement membrane structure as well as interacting with cell receptor molecules and controlling cell polarisation, migration and invasion. It has also been reported that NID1s promoter is aberrantly methylated in colon and gastric cancers, which prevents transcription of nidogen

1, therefore weakening the basement membrane architecture and providing favourable conditions for cell invasion to occur (Ulazzi et al., 2007). A further gene identified was GAD1 (FC 4.73, $p<0.01$), which encodes the enzyme glutamic acid decarboxylase 1 that catalyses the production of γ-aminobutynic acid (GABA) from L-glutamic acid, the principle neurotransmitter in the brain. Kimura et al. (2013) reported that up regulation of GAD1 was characteristic in oral squamous cell carcinoma and that GAD1 correlated with cell invasiveness and migration by regulating β-catenin translocation to the nucleus and subsequent MMP7 activation. SPARC (FC 4.64, $p<0.01$) encodes a secreted extracellular glycoprotein associated with morphogenesis and tissue remodelling and has been reported to modulate the expression of several MMPs including MMP2 in breast cancer cell lines (Gilles et al., 1998).

To further analyse the microarray data KEGG pathway analysis was performed. Genes which were found to have >1.8-fold change with a p value of <0.06 were used within the KEGG pathway analysis to find correlations between the 1119 genes which were significantly changed. Three pathways were identified, these were: transendothelial migration pathway, Toll-like receptor signalling pathway and complement and coagulation cascades. The transendothelial migration is important in cancer cell metastasis as they must leave the circulation to form secondary tumours (see Section 1.2.5). For this pathway to be highlighted here could suggest that there the isolated cell populations have the ability to successfully extravasate. The genes which were involved in the transendothelial migration pathway included several junctional maintenance genes which can be misregulated and lead to a mesenchymal phenotype through loss of cell-cell junctions. Ras homolog family member A (RHOA) was significantly ($p<0.05$) up-regulated in HPA-negative cells. RHOA controls cell adhesion and motility through regulation of the actin cytoskeleton by actomyosin contractility. Yoshioka et al. (1999) reported that over-expression of RHOA increased the invasive ability of tumour cells. Phosphoinositide-3-Kinase Regulatory Subunit 3 (PIK3R3) was significantly ($p<0.05$) down-regulated in HPA-negative cells. Wang et al. (2014) reported that overexpression of PIK3R3 increased cell invasion. The Toll-like receptor signalling pathway is part of the innate immune system and results in inflammation, which is conducive to cancer cell proliferation (Chen et al., 2007). The complement cascade promotes a number of cancer traits (reviewed by Rutkowski et al., 2010) as too does the coagulation cascade (reviewed by Falanga et al., 2003). Taken together, gene expression patterns determined in the work presented in this chapter and through microarray analysis are consistent with results obtained in previous chapters that suggested that both the MCF7 HPA-positive and HPA-negative cell populations possess characteristics that collectively are important for successful metastasis.

Microarrays are reliant on many steps and normalisation processes and so can provide potentially unreliable data (Smyth et al., 2003). To resolve this, several genes were chosen for qPCR analysis in order to validate the microarray data. The genes were: CDH1, VIM, SMAD2, GALNT6, TFPI2, SPACR, FBLN1 and ZEB1. MCF7 cells were separated based on their HPA-binding profile, RNA was extracted and converted

into cDNA and subjected qPCRs. It was found that MCF7 HPA-isolated populations had the same expression profile as determined by microarray, except for SMAD2, therefore largely-validating the microarray data. ZR751 and BT474 cell lines where then assessed for their expression of the same genes. As detailed in Table 5.9, all three cell lines had different expression profiles of the genes tested. BT474 HPA-negative isolated cells expressed both CDH1 and VIM than HPA-positive cells, which suggests that these cells are "metastable" and have features of both epithelial and mesenchymal cells (Lee et al., 2006a). ZR751 HPA-negative cells expressed less GALNT6, TFPI2, SPARC and FBLN1 than HPA-positive cells which was opposite to what was observed in both MCF7 and BT474 cells. Perhaps suggesting that the transcriptomic expression of the genes tested are not directly related to the cells glycosylation profiles.

5.5 Key findings

- A number of EMT associated genes (NID1, CFH, FBN2, SIX1, WNT2B) were significantly differentially regulated between the HPA-positive and HPA-negative cell populations, as determined by microarray and were consistent with their epithelial-like and mesenchymal-like phenotypes, respectively.
- GALNT6 and GALNT20 were significantly down regulated in MCF7 HPA-negative cells, as determined by microarray, possibly suggesting a role of these genes in synthesis of truncated O-glycans in HPA-positive cells.
- DAVID analysis of the microarray data revealed several KEGG pathways that differentially expressed genes were involved in. One of these pathways was transendothelial migration, a key stage in the metastatic cascade.

Chapter 6

Functional differences between HPA-positive and HPA-negative populations

6.0 Functional differences between HPA-positive and HPA-negative populations

6.1 Background

HPA labelling has been reported as being associated with metastatic competence of cancer as reviewed by Brooks (2000) and in Section 1.4 of this thesis. As observed during the work described in Chapter 4, HPA-negative cells have a motile, invasive, mesenchymal-like phenotype and HPA-positive cells have a rounded, epithelial-like phenotype. Furthermore, it was observed in Chapter 4 that when cells were separated based on their HPA binding profiles, they reverted to a mixed population over 72 hours, suggesting that the cells have the ability to transition between HPA-positive (epithelial-like) and HPA-negative (mesenchymal-like) states and *vice versa*. It was observed in the work described in Chapter 5 that a number of EMT↔MET associated genes were dysregulated between the MCF7 HPA-positive and HPA-negative cells. If the cells are able to utilise both the adhesive traits associated with epithelial cells and the motile/invasive characteristics of the mesenchymal cells, related to their glycosylation, then this would hypothetically aid in successful metastasis. In order to investigate the different aspects of the metastatic cascade that HPA-positive and HPA-negative cells may be involved in, cell migration and invasion assays as well as cell adhesion assays will be considered.

6.1.1 Cell migration and invasion assays

Cell migration and cell invasion are terms that are often used interchangeably; however, in experimental cell biology they are distinct terms (Kramer et al., 2013). Migration refers to the directed movement of cells on a substrate occurring on a 2D surface without any obstructive fibre network; whilst invasion is cell movement through, and remodelling of, a 3D matrix (Kramer et al., 2013). The process of cell invasion is composed of adhesion to, and proteolysis of, ECM and also migration (Friedl and Wolf, 2009), therefore making migration a condition of invasion. There are many *in vitro* and *in vivo* assays which measure the invasive or migratory potential of a cell. Only *in vitro* assays will be discussed here, but for a comprehensive review of *in vivo* assays see Wolf et al. (2009) and Zhou et al. (2011). The choice of migration or invasion assay to use depends on cost, technical experience, cell type and depends on what needs to be observed (see Tables 6.1 and 6.2). Firstly, cell migration assays will be considered. Cell migration assays *in vitro* can be categorised as either those which assess filling a space, single-cell tracking or those which use a chemoattractant. Space filling assays include wound-healing or scratch assays, cell exclusion zone assays, fence or ring assays, microcarrier bead assays and spheroid migration assays. Single-cell tracking assays include single cell motility assays and time-lapse cell tracking assays.

Those which use a chemoattractant include transwell migration or Boyden chamber assays and capillary chamber migration or microfluidic chamber assays.

Wound-healing or scratch assays allow for the study of cell migration on a 2D surface. A cell monolayer is artificially "wounded" by removing a line of cells by scratching with an instrument along the monolayer. Cell migration can then be studied from the undamaged area into the scratch and cell movement calculated by measuring the reduction of the scratched area at different time points until the "wound" is "healed". This method of assessing cell migration is inexpensive, requires no specialised equipment and is easy to analyse (Justus et al., 2014). However, discriminating between cell migration and cell proliferation in a wound-healing assay that lasts for longer than 24 hour is dependent upon the cells doubling time, so slow migrating cell types can be difficult to assess in this assay. Furthermore, discrepancies in scratch thickness, folded cells at the edge of the wound that can subsequently re-attach to the wounded site and artefacts induced from mechanical cell damage can all affect the results of the assay (Kam et al., 2008). To avoid these issues, further techniques have been developed such as the cell exclusion zone assay where a silicone stopper or a dissolvable biocompatible gel creates a 2mm diameter cell-free zone. This method is highly reproducible and causes no cell damage. However, care must be taken when setting up the assay as cells can migrate into the exclusion zone if the silicone stopper is not secured properly. Alternatively, fence or ring assays are the reverse of an exclusion zone assay where-by cells are seeded into an artificial "fence" until a monolayer is achieved and then the "fence" is removed and cells can migrate radially outwards (Ashby and Zijlstra, 2012).

Microcarrier bead assay uses cells grown on the surface of microcarrier beads, which are then placed on a 2D cell culture surface which they migrate on to. The microcarrier is removed after a set period of time and the number of cell migrated onto the culture surface is assessed. By culturing cells on the microbead, cell-cell contacts are established, which mimic tight contacts of cells *in vivo* (Rosen et al., 1990). However, this technique requires technical experience and is expensive. To better mimic *in vivo* tumour structure, an improvement on the microcarrier bead assay is the spheroid migration assay which combines the 3D structure of a spheroid with 2D migration across cell culture plates. The cell spheroid much more closely mimics micro-metastases than the microcarrier bead assay as different cellular states, nutrient and oxygen supplies are modelled depending on cell location in the spheroid. Again, this technique requires technical expertise and is only possible if cells can form spheroids (Pedersen et al., 1994).

A single-cell motility assay is used to observe the undirected migration of single cells. One method to do this uses cell culture plates coated with colloidal gold particles which, when observed using a light microscope, appear as a layer of dark dots. Alternatively, quantum dots can be used. Cells seeded onto this layer migrate through by phagocytosing the gold particle thereby leaving a white trail, which can be imaged and quantified (Niinaka et al., 2001). Absolute cell speed can be determined via this method,

although analysis is labour intensive as only one track can be analysed at a time. An improvement on this method is time lapse cell tracking which uses video-microscopy to track multiple cell tracks at once and can be automated (Debeir et al., 2005).

The transwell migration assay was first reported by Stephen Boyden (1962) for the study of leukocyte chemotaxis, so is also referred to as a Boyden chamber assay. The transwell assay system is comprised of two chambers separated by a permeable membrane. Cells are added to the top chamber in serum-free (SF) or reduced serum medium and vertically transmigrate through the membrane towards the chemoattractant (serum-containing medium or higher serum concentration medium) contained in the bottom chamber. The size of the pores in the membrane vary from 3µm to 12µm, and which pore size to choose depends on the size of the cells used in the assay. The pore size should be smaller than the cell size to prevent non-specific passage. Incubation time for the assay is cell-specific so should be optimised for each cell type used. Removal of non-invaded cells which remain on the upper surface of the membrane is performed by wiping with a cotton swab. Quantification of the number of migrated cells can be performed two ways. Firstly, migrated cells can be fixed and stained with cytological dyes such as haematoxylin and the number of cell counted. Alternatively, cells can be fluorescently stained, and removed from the membrane by trypsinisation, and subsequently quantified using a fluorescent reader. This is less time consuming and can be more sensitive than counting cells manually but all non-invaded cells must be removed for accuracy (Harisi et al., 2009). Alternatively, NeuroProbe have developed a system that uses “bubble entrapment” and the use of dark coloured porous membranes which block light transmission, therefore removing the need for two chambers and allowing the process to be reduced in size so that experiments can be carried out on 96-well plates and accurately quantified using a fluorescent plate reader (Frevert et al., 1998). The transwell method of measuring cell migration is inexpensive, easy to set up with no special equipment other than the transwell plate and is readily available commercially. However, optimisation can be time consuming and choice of quantification method can affect reliability of results.

The capillary chamber migration assay uses two parallel chambers connected by a narrow bridge (capillary tube). On one side, a chemoattractant is added, and cells are added to the other. The number of cells in the capillary tube is a measure of the migratory ability of the cells. This approach uses small assay volumes making it a suitable choice for rare cell types or expensive reagents, although the small reagent volumes mean frequent medium changes are required (Kramer et al., 2013).

Table 6.1 *Assessment of types of in vitro cell migration assays. See text for source material.*

Assay	Type	Pros	Cons
Wound-healing	Space-fill assessing 2D migration	Inexpensive, no specialised equipment needed, easy analysis	Can only be observed ≤24hr, not consistently reproducible, can damage cells
Exclusion zone migration	Space-fill assessing 2D migration	Reproducible, no cell damage, readily available commercially	Needs to be set-up correctly, can only be used to assess adherent cells
Fence	Space-fill assessing 2D migration	Reproducible, no cell damage, readily available commercially	Needs to be set-up correctly, can only be used to assess adherent cells
Microcarrier bead	Space-fill assessing 2D migration	Mimics cell-cell contact of a tumour	Expensive, requires technical experience, kits not readily commercially available
Spheroid migration	3D to 2D space-fill	Mimics micro-metastases	Expensive, requires technical knowledge, no kits commercially available
Single-cell motility	Single-cell tracking of 2D migration	Can calculate absolute cell speed, undirected cell movement	Analysis is time consuming
Time lapse cell tracking	Single-cell tracking of 2D migration	Can be automated, can track several cells at once, can calculate absolute cell speed	Equipment and software can be expensive
Transwell (Boyden chamber)	Vertical chemotaxis assessing 2D migration	Inexpensive, easy to set up, readily available commercially	Optimisation needed, quantification method affects reliability of results
Capillary chamber migration	Horizontal chemotaxis assessing 2D migration	Good for rare cells or expensive reagents as only small volumes needed	High maintenance, difficult to automate

Cell invasion assays are similar to migration assays except they assess 3D cell movement, so all assays include a matrix component for cells to invade through. Cell invasion assays *in vitro*, like cell migration assays, can be categorised as either those which assess filling a space, single-cell tracking, those which use a chemoattractant and those that use spheroids.

Exclusion zone invasion assay, sometimes called Platypus invasion assay, after the first company to manufacture them, is similar to the exclusion zone migration assay as invasion of cells into the exclusion zone is monitored over time and quantified. However, the setup of the assay is slightly different: a thin layer of basement membrane extracts (BME) which is ECM found at the base of lumen-lining epithelial

and endothelial cells is added to the bottom of a 96-well plate and a silicone stopper is added to create an exclusion zone. Cells are seeded and allowed to adhere to the ECM. The stopper is removed and a second thicker layer of BME is added, sandwiching cells between two sheets of ECM and leaving the exclusion zone to be all ECM (Lim et al., 2010). A simpler version of this assay is also used where cells are added on top of a column of ECM or collagen I and are observed as they invade vertically (Burgstaller et al., 2013). This assay is a standardised technique and is commercially available and easy to set up. However no chemokine gradient is used, so migration is undirected and cells are suspended singularly in the ECM and no cell-cell contacts are made. This makes the assay limited in modelling *in vivo* processes (Kramer et al., 2013).

3D cell tracking uses time-lapse video-microscopy and computer-aided analysis to follow the invasion patterns of cells in a 3D ECM allowing for assessment of cell conformational changes and proteolysis of ECM (Zaman et al., 2003). It is challenging to track cells in a 3D environment over time and microscopy techniques such as wide field, confocal and multiphoton can be used (Rabut and Ellenberg, 2004). Only a limited number of cells can be analysed at one time as the process is time consuming. Furthermore, specialised equipment and technical knowledge is required.

Spheroid single-cell invasion assays measure the invasive property of a cell type A (invasive cell suspension) into a spheroid of cell type B (non-invasive) (Kramer et al., 2013). Cell type A adheres to the spheroid and invades inwards. Spheroid confrontation assays measure the invasion of cell type A (invasive spheroid) into a spheroid of cell type B. If invasive, the two spheroids will join and spheroid type A will invade into the spheroid type B. However, if non-invasive, then a distinct border will form between the two spheroids (Hatterman et al., 2011). Spheroid gel invasion assays measure the astral outward invasion of a single spheroid suspended in ECM (Del Duca et al., 2004). If the cells are non-invasive then the spheroid remains as a compact ball with a distinct border with the ECM (Vinci et al., 2015). Quantification of invasion in the spheroid techniques is achieved by either confocal microscopy or by paraffin wax embedding and sectioning for immunocytochemical analysis. Spheroid assays most closely mimic *in vivo* tumour cell clusters and are therefore considered preferable to other cell invasion assays (Vinci et al., 2015). However, these assays are limited to cells that can form spheroids, quantification of invasion is difficult, the techniques are not standardised or readily available commercially and some technical expertise is required. Therefore, spheroid invasion assays are uncommonly used even though they most closely reflect *in vivo* circumstances.

Transwell invasion assay uses the same technique as transwell migration assay except that a thin layer of ECM overlays the permeable membrane. The ECM is usually composed of either BME or collagen I. The ECM blocks the pores of the membrane, therefore preventing non-invasive cells from migrating through, whilst invasive cells can degrade matrix and invade through the ECM layer (Justus et al., 2014).

Transwell invasion assays are commonly used as the protocol is standardised, although analysis of invaded cells by cytological staining and cell counting can be unreliable (Albini et al., 2004).

Table 6.2 *Assessment of types of in vitro cell invasion assays. See text for source material.*

Assay	Type	Pros	Cons
Exclusion zone invasion	Space-fill assessing 3D invasion	Commercially available, standardised technique, easy to setup	No chemokine gradient, single cell suspension no cell-cell contact
3D cell tracking	Single-cell tracking of 3D invasion	Monitoring of 3D cell movement in real-time	Specialised equipment and technical knowledge, limited analysis, expensive
Transwell invasion	Vertical chemotaxis assessing 3D invasion	Commercially available, standardises technique, easy to setup	Can be difficult to analyse
Spheroid single-cell invasion	3D invasion of non-invasive spheroid	Closely mimics *in vivo* architecture	Non-standardised, not commercially available, technical knowledge needed, cells must be able to form spheroids
Spheroid confrontation	3D invasion of invasive spheroid and non-invasive spheroid	Closely mimics *in vivo* architecture	Non-standardised, not commercially available, technical knowledge needed, cells must be able to form spheroids
Spheroid gel invasion	3D invasion of spheroid into ECM	Closely mimics *in vivo* architecture	Non-standardised, not commercially available, technical knowledge needed, cells must be able to form spheroids

6.1.2 Endothelial cell adhesion assays

Endothelial cell adhesion assays are used to model cancer cells adhesion to, and subsequent extravasation from, blood vessels into tissues (as discussed in Section 1.2.5). *In vivo* mouse models of extravasation are often performed with intravital video microscopy as reviewed in Xu et al. (2011). However, here *in vitro* assays only will be discussed (see Table 6.3). Assays which mimic vascular adhesion and extravasation *in vitro* fall into two categories: those which are performed under static conditions and those which are performed under flow conditions. Static assays are performed by growing a monolayer of endothelial cells, which prior to the experiment are activated by pro-

inflammatory cytokines such as TNF-α to increase expression of cell surface proteins which facilitate attachment of cancer cells to endothelial cell surface (Lowe and Raj, 2015). Before being added to endothelial cell monolayer, cancer cells are labelled with an amphiphilic fluorescent probe so that they can be differentiated from the endothelial cells once bound. Labelled cancer cells are removed from culture flask with a non-enzymatic dissociation reagent and incubated with the endothelial cell monolayer for a period of time. Non-bound cells are removed and the bound cells counted (Glinsky et al., 2000; Wilhelmsen et al., 2013). Static assays are easy to perform and require no special equipment or specialist technical expertise; however this assay does lack the physiological variable of fluid shear stress (Lawrence and Springer, 1991). Alternatively, it could be argued that static assay better represents vascular adhesion of cells which have arrested in small capillaries (as discussed in Section 1.2.5). Certain adhesive interactions can only occur under shear flow and cannot be studied under static conditions (Lawrence et al., 1997). Flow adhesion assays are generally performed using a parallel plate flow chamber which simulates physiological flow rates (Lane et al., 2012). The equipment consists of a transparent chamber which is mounted on an inverted microscope. A heater is placed in the chamber to maintain a temperature of 37^{o}C. Endothelial cell monolayers are established on a microslide, which consists of separate wells supplied by a single inlet and a single outlet, and placed into the chamber. The chamber connects to a syringe pump which is set to a specific with-drawal rate depending on shear stress required. Cells can be introduced at the microslide inlet (Shetty et al., 2014). Video microscopy is used to capture cells adhering to endothelial cells under flow.

Alternatively, Bapu et al. (2014) reported a simpler flow adhesion assay which allowed for the study of vascular adhesion under sweeping flow, termed the rocking adhesion assay. This assay allows for the study of adhesion under flow but does not need the expensive specialised equipment that for example the parallel plate flow chamber requires. The assay setup is the same as detailed for the static assay where endothelial cells are grown on glass bottomed cell culture plates to confluence. Prior to the assay, the endothelial monolayer is activated with cytokine stimulation. Cancer cells are labelled with an amphiphilic fluorescent probe so that they can be differentiated from the endothelial cells once bound and removed from their cell culture flask with a non-enzymatic dissociation reagent. Labelled cells are introduced to the activated endothelium and placed on a rocking platform which instigates the sweeping flow for a period of time. Non-bound cells are removed and the bound cells quantified using fluorescence microscopy. Flow adhesion assays mimic physiological shear flow conditions, however require specialised equipment and technical knowledge, however the rocking adhesion assay provides a simpler experimental setup to study adhesion under sweeping flow (Bapu et al., 2014).

Table 6.3 *Assessment of types of in vitro endothelial adhesion assays. See text for source material.*

Assay	Type	Pros	Cons
Static	Mimics cancer cell adhesion to vascular endothelium under static conditions	Easy to setup, requires no specialised equipment. Mimics static flow for example stasis in small capillaries	Does not mimic physiological flow conditions
Flow	Mimics cancer cell adhesion to vascular endothelium under flow conditions	Better mimics physiological shear flow conditions	Specialised equipment and technical knowledge required. Weakly adherent cells cannot be studied
Sweeping flow (rocking assay)	Mimics cancer cell adhesion to vascular endothelium under sweeping flow conditions	Easier to setup than flow assays. Doesn't remove weakly adherent cells	Some specialised equipment required. Does not mimic physiological flow conditions

After considering the different *in vitro* assays available to investigate cell invasion and migration as well as cell adhesion, it was decided that a Matrigel (transwell) cell invasion assay and a static adhesion assay would be employed. When cells were separated based on their HPA binding profile morphological differences were observed between the HPA-positive and HPA-negative isolated populations as detailed in Chapter 4. HPA-negative cells were observed to have an elongated morphology with multiple pseudopodia suggesting a more mesenchymal-like phenotype. The presence of pseudopodia on the HPA-negative cells suggested an invasive phenotype (Weaver, 2006). To test the invasiveness of the HPA-negative cells the Matrigel invasion assay offered a readily available standardised technique. The HPA-positive cells were observed as having a rounded morphology reminiscent of epithelial cells, and HPA positivity has also been reported to be associated with metastatic competence of tumours (see Section 1.4). Previously in our laboratory, a rocking adhesion assay has been optimised and employed, and has been used to model cancer cell adhesion to endothelium of blood vessels under conditions of sweeping flow (Bapu et al., 2014). Using this system it was demonstrated for whole cell lines (MCF7, ZR751, BT474) that HPA-binding glycans are functionally involved in cancer cell adhesion to endothelial cells under sweeping flow conditions (Bapu et al., 2016). However, adhesion under static conditions had not been trialled and the static assay is much simpler to perform than the rocking adhesion assay.

In the work described here therefore, a static adhesion assay was used as this it is a simple technique that requires no specialist equipment and mimics adhesion to vascular endothelium under static conditions, for example, during stasis in capillaries (as discussed in Section 1.2.5).

Aims and Objectives

The work described in this chapter aimed to assess the behaviour of the HPA-positive and HPA-negative cell populations in models of different aspects of the metastatic cascade. This was achieved by:

I. The use of a Matrigel invasion assay to assess invasive abilities such as motility and degradation of Matrigel matrix.
II. The use of a static adhesion assay to assess the cell adhesion to activated endothelial cells.

6.2 Methods

6.2.1 Matrigel® invasion assay

See Figure 6.1 for protocol overview.

Preparation of Corning® BioCoat™ Matrigel® plate

A Corning® BioCoat™ Matrigel® plate was removed from storage at -20°C and allowed to equilibrate to room temperature (~30min). After this time, the Matrigel® matrix was rehydrated by adding 500µl of warmed (37°C) serum free (SF) tissue culture medium to the insert and 500µl to the well and both were incubated for 2hr in a humidified tissue culture incubator at 37°C with 5% CO_2 atmosphere. Once rehydrated, the SF-medium was aspirated from both the well and the inserts and 750µl of complete culture medium (detailed in Section 2.1.2) was added to the well only.

Preparation of cell suspensions

24hr before the assay, several T75 cell culture flasks of MCF7, ZR751 and BT474 cells were fed with SF-medium. On the day of the assay, cells from half of the prepared flasks were separated according to their HPA-binding characteristics and magnetic beads removed as detailed in Section 2.3. A cell suspension of 200,000 cells/ml in SF-medium was prepared of each of the HPA-positive, HPA-negative isolated populations and a mixed population as detailed in Section 2.3. 250µl of each cell suspension was added per insert and gently swirled once to ensure an equal distribution of cells. The plate was then incubated for 24hr in a humidified tissue culture incubator at 37°C with 5% CO_2 atmosphere.

Preparation of lectin labelling controls

To ensure that the glycosylation profiles of the unseparated ZR751 and HPA-positive and HPA-negative populations were consistent with what was previously described (see Section 3.0), HPA lectin labelling controls were set up alongside the Matrigel® plates. 13mm diameter glass coverslips were briefly sterilised in 70% v/v IMS in tap water and gently placed into the wells of 24-well cell culture plates. The

culture plate lids were left off and the coverslips allowed to air dry in a class II cell culture hood. 250µl of either unseparated ZR751, HPA-positive or HPA-negative cell suspension (prepared above in "Preparation of cell suspensions") were added per well, then 750µl of complete culture medium was added per well. 3 biological replicates of each were performed. The plate was incubated for 24hr in a humidified tissue culture incubator at 37°C with 5% CO_2 atmosphere. After which time the cells were fixed and HPA labelled as detailed in Section 2.2.

Fixation, staining and mounting of membranes

The inserts were removed from the wells. Matrigel® matrix and non-invaded cells were removed from the inserts by lightly scrubbing the upper surface of the insert with a cotton-tipped swab and then repeating the process with a cotton-tipped swab lightly moistened in SF-medium. The upper surface of the insert was then washed twice with SF-medium. The inserts were then placed into a 24-well cell culture plate prepared with 1ml/well of ice cold methanol and fixed for 30min at 4°C. The inserts were washed twice in phosphate buffered saline (PBS), pH 7.4, and then permeabilised in 0.1% Triton X-100 in PBS for 10min at room temperature. The inserts were washed twice in PBS and then stained in Harris' haematoxylin for 3min at room temperature. The inserts were "blued" in running tap water and then dehydrated though an alcohol series (70%, 90%, 100%, 100%), cleared in xylene and mounted using Depex.

Imaging and invasion analysis

The membranes were observed using a Zeiss Axioplan microscope fitted with a JENOPTIK ProgResC3 colour camera. Images at low power resolution of the complete membrane were captured so that all of the invaded cells could be counted. This was achieved by imaging the membrane in a grid formation starting on the top left hand corner and working left-to-right across the membrane, then down a row and across again. If a cell appeared in a previous image, then it was not counted in the next. See Figure 6.2.

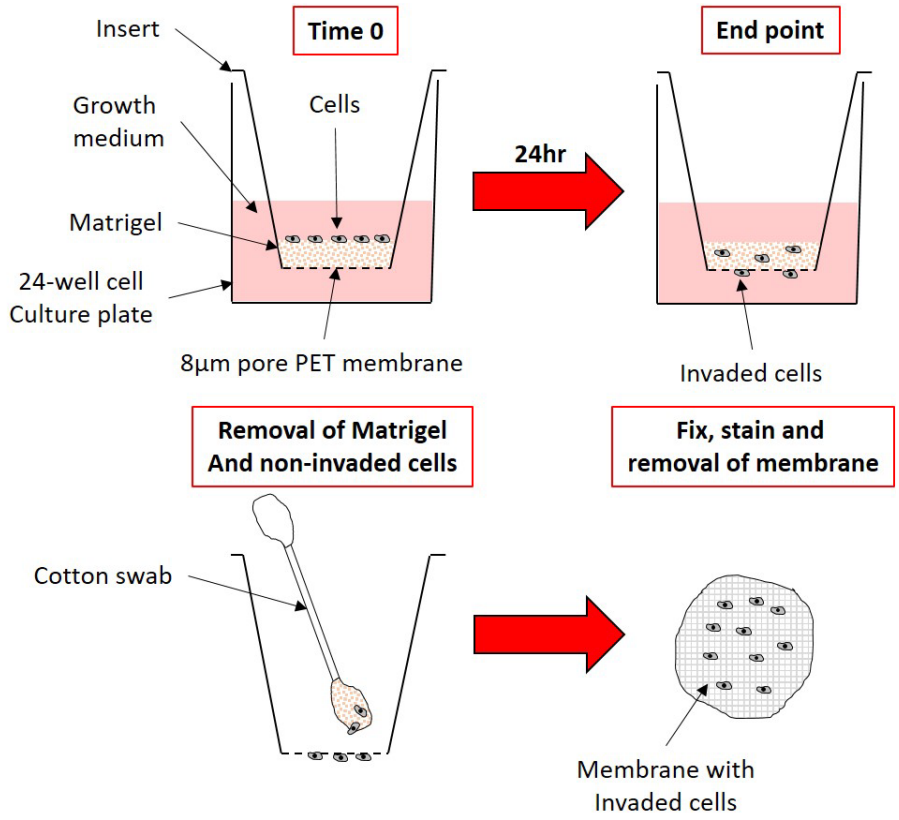

Figure 6.1 *Corning® BioCoat™ Matrigel® invasion assay protocol. The matrigel membrane is rehydrated and then 750µl of complete growth medium added to the well and 250µl of cell suspension added to the insert. The plate is incubated for 24hr and then the medium, matrigel and non-invaded cells are removed and the membrane fixed and stained.*

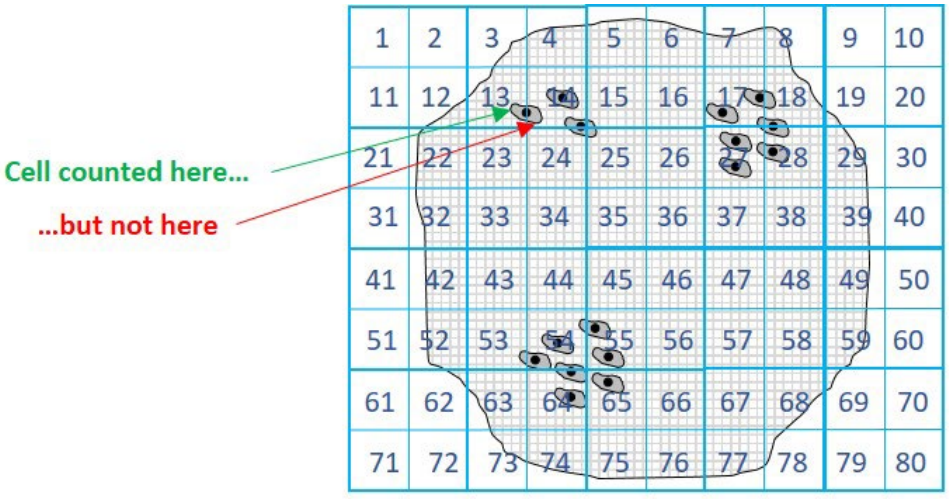

Figure 6.2 *Matrigel® membrane counting technique. All of the invaded cells per membrane were counted. This was achieved by imaging the membrane in a grid formation starting on the top left hand corner and working left-to-right across the membrane, then down a row and across again. If a cell appeared in a previous image, then it was not counted in the next.*

6.2.2 Static endothelial adhesion assay

See Figure 6.3 for protocol overview.

Preparation of endothelial layer

13mm diameter glass coverslips were briefly sterilised in 70% v/v IMS in tap water and gently placed into the wells of 24-well cell culture plates. The culture plate lids were left off and the coverslips allowed to air dry in a class II cell culture hood. After this time, 500µl of 0.2% w/v bovine gelatine in PBS, pH 7.4, was added per well and then allowed to adhere for 30min. Excess gelatine was aspirated and 100,000 HUVEC cells (see Section 2.1.1) were seeded per well. The culture medium was changed daily (see Section 2.1.2) until the cells had achieved a confluent monolayer. Prior to the assay, the endothelial cells were pre-stimulated with 10ng/ml of TNF-α (Sigma) in EBM-2 cell culture medium for 2hr in a humidified tissue culture incubator at 37°C with 5% CO_2 atmosphere.

Preparation of cancer cells

T75 flasks of MCF7, ZR751 and BT474 cancer cells were incubated for 2hr in a humidified tissue culture incubator at 37°C with 5% CO_2 atmosphere with a warmed (37°C) solution of the fluorescent dye 8-hydroxypyrenetrisulphonic acid (PTS) (Sigma) at a concentration of 10mg/ml in preferred cell culture medium (see Table 2.2). After this time, the PTS solution was aspirated and the cells washed 5x with warmed (37°C) PBS, pH 7.4 to removed excess PTS. 10ml of preferred cell culture medium (see Table 2.2) was dispensed into the culture flask and the cells were scraped from the plastic using a rubber cell scraper. The cell suspension was aspirated and pelleted by centrifugation at 1,100 x g for 3min, the supernatant discarded and the cell pellet either used for: 1. Cell separation (as detailed in Section 2.3), 2. A “mock cell separation” control (as detailed in Section 2.3) or 3. A “mixed population” control (as detailed in section 2.3).

Static adhesion assay

The TNF-α solution was aspirated from the endothelial cells and 200,000 cancer cells in 1ml of preferred growth medium were introduced per well. The plate was gently swirled to distribute cancer cells and then placed in a humidified tissue culture incubator at 37°C with 5% CO_2 atmosphere. Cancer cells were allowed to adhere for a range of times (1min, 5min, 10min, 20min, 40min and 1hr) before the non-adherent cell suspension was gently aspirated and the well washed gently 3x with warmed (37°C) PBS.

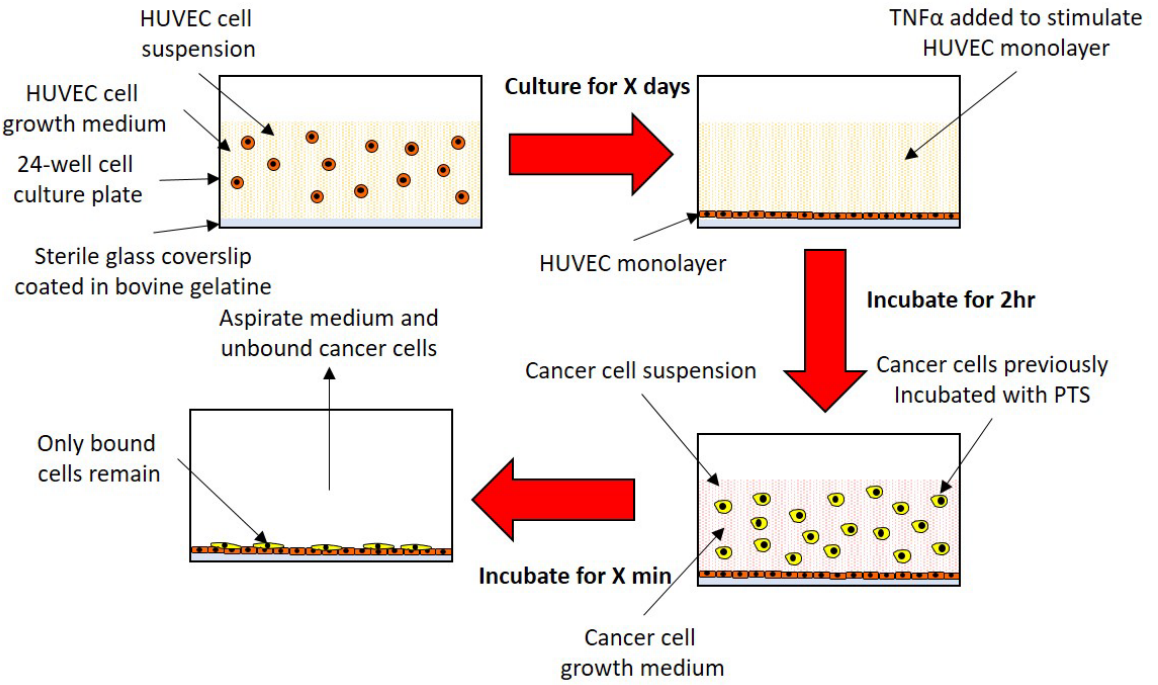

Figure 6.3 *Static adhesion assay protocol. HUVEC monolayer cultured and then activated by the addition of TNF-α. Cancer cell suspension added to the monolayer and allowed to attach for a range of incubation periods, after which time the medium and unbound cells are aspirated and only cells bound to the monolayer remain.*

Preparation of labelling controls

As well as separated populations, unseparated and artificially unseparated populations were seeded alongside (see Section 2.3). To ensure that the separation was performed correctly, separated populations were seeded into 24-well plates with sterilised 13mm diameter glass coverslips allowed to adhere for 24hr and then fixed and lectin labelled as detailed in Section 2.2.

Preparation of binding controls

In order to control for the potential effect of steric hindrance created by the relatively large HPA molecule and to test the effect of masking GalNAc-glycans specifically, binding controls were performed. Here, unseparated cells were incubated with either 10µg/ml HPA (Sigma) or Con A (Sigma) in preferred growth medium on an end-over-end mixer for 10min prior to addition to endothelium. Con A (Concanavalin A), a lectin isolated from Jack beans (*Canavalia ensiformis*), has a sugar binding specificity for terminal α-D-mannosyl and α-D-glucosyl residues (Naismith and Field, 1996) and has been demonstrated to bind breast cancer cells (Yu et al., 1995). By incubating the cancer cells with Con A prior to incubation with the endothelial cell monolayer, irrelevant, as far as these experiments are concerned,

terminal α-D-mannosyl and α-D-glucosyl residues were masked, thus controlling for non-specific inhibition of adhesion mediated simply by the presence of a lectin binding. Incubating cancer cells with HPA prior to incubation with the endothelial cells masks GalNAc-glycans therefore preventing GalNAc-glycan mediated binding to endothelial cells.

Treatment with HPA-negative conditioned media

See Figure 6.4 for protocol overview. A cell separation was performed using MCF7 cells as detailed in Section 2.3. The HPA-negative population was cultured, and after 4 hours conditioned media was collected and filtered through a 0.2µm filter and kept warm (37°C). A new cell separation was performed using MCF7 cells as detailed in Section 2.3, yielding a 2x HPA-positive populations, 2x HPA-negative populations, 2x mixed populations (90:10) and 2x unseparated populations. All populations were PTS treated as described previously. To one flask of each population, regular medium was added, whilst HPA-negative conditioned medium was added to the other. The populations were incubated with the media (regular and HPA-negative conditioned) for 10min in an end-over-end mixer prior to a 10min incubation with endothelial cells.

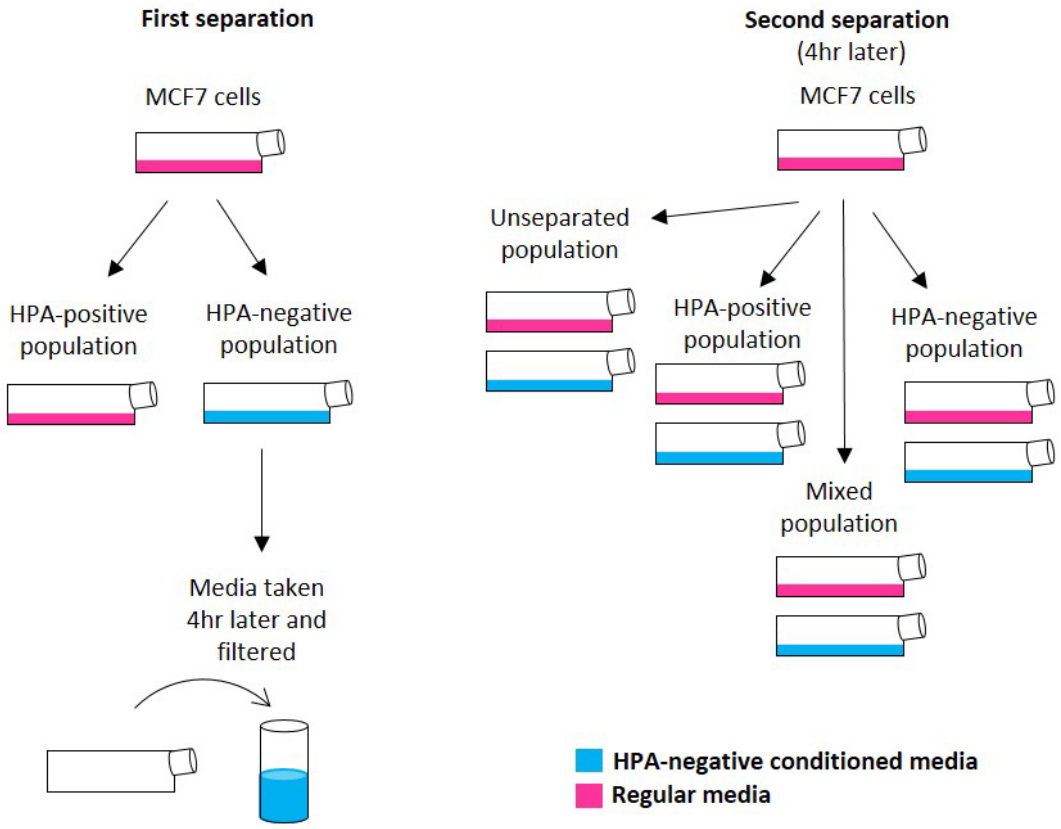

Figure 6.4 *Conditioned media assay. An initial separation with MCF7 cells was performed and the separated populations cultured for 4hr. After this time, the conditioned medium from the HPA-negative cell populations was aspirated from the flask and filtered through a 0.2µm cell culture filter to remove any debris. A second cell separation was performed with MCF7 cells that had been treated with PTS yielding a PTS-labelled HPA-positive population, a HPA-negative population, a mixed population and an unseparated population to which each was treated with either HPA-negative conditioned medium or regular medium in an end-over-end mixer for 10min before being added to activated endothelial cell monolayer for 10min.*

Fixation, imaging and analysis

Cancer cells bound to endothelial cell monolayers were fixed by adding 1ml/well of ice cold 25% v/v acetic acid in methanol for 10min at 4°C. After this time, the coverslips were carefully removed from the 24-well cell culture plate and mounted onto glass slides with a small amount of fluoromount anti-fade mountant (Sigma). Slides were observed within 48hr and stored at 4°C in the dark to preserve fluorescence. An inverted fluorescence microscope (Zeiss Primvert fitted with AxioCamICM1) was used to observe slides. All adherent cancer cells were counted per coverslip. Counting was performed in a checkerboard formation as shown in Figure 6.2. Counts were normalised to unseparated populations within each assay and averaged to give fold change.

6.3 Results

6.3.1 HPA-negative population are more invasive than HPA-positive and unseparated populations

In order to assess whether cells which were isolated based on their HPA-binding profiles had different invasive capabilities, MCF7, ZR751 and BT474 cancer cells were separated based on their HPA-binding status into HPA-positive and HPA-negative populations. Along with unseparated cells, HPA-positive and HPA-negative populations were subjected to Matrigel invasion assays to assess invasive ability (example of cells invaded through Matrigel membrane are illustrated in Figure 6.5). To check that the separation of the cells on the basis of their HPA-binding profiles was successful, HPA lectin labelling was performed parallel to the Matrigel assays. As illustrated in Figure 6.6, (A) unseparated ZR751 cells labelled 70% with HPA at an intensity of ++, (B) HPA-positive ZR751 cells labelled 100% with HPA at an intensity of +++ and (C) HPA-negative ZR751 cells labelled 0% with HPA at an intensity of -. These findings demonstrate that the cell separation was successful. To ensure that the lectin labelling, and hence the separations, was specific, lectin labelling controls were performed as illustrated in Figure 6.7, all negative controls were negative and therefore HPA labelling was deemed specific.

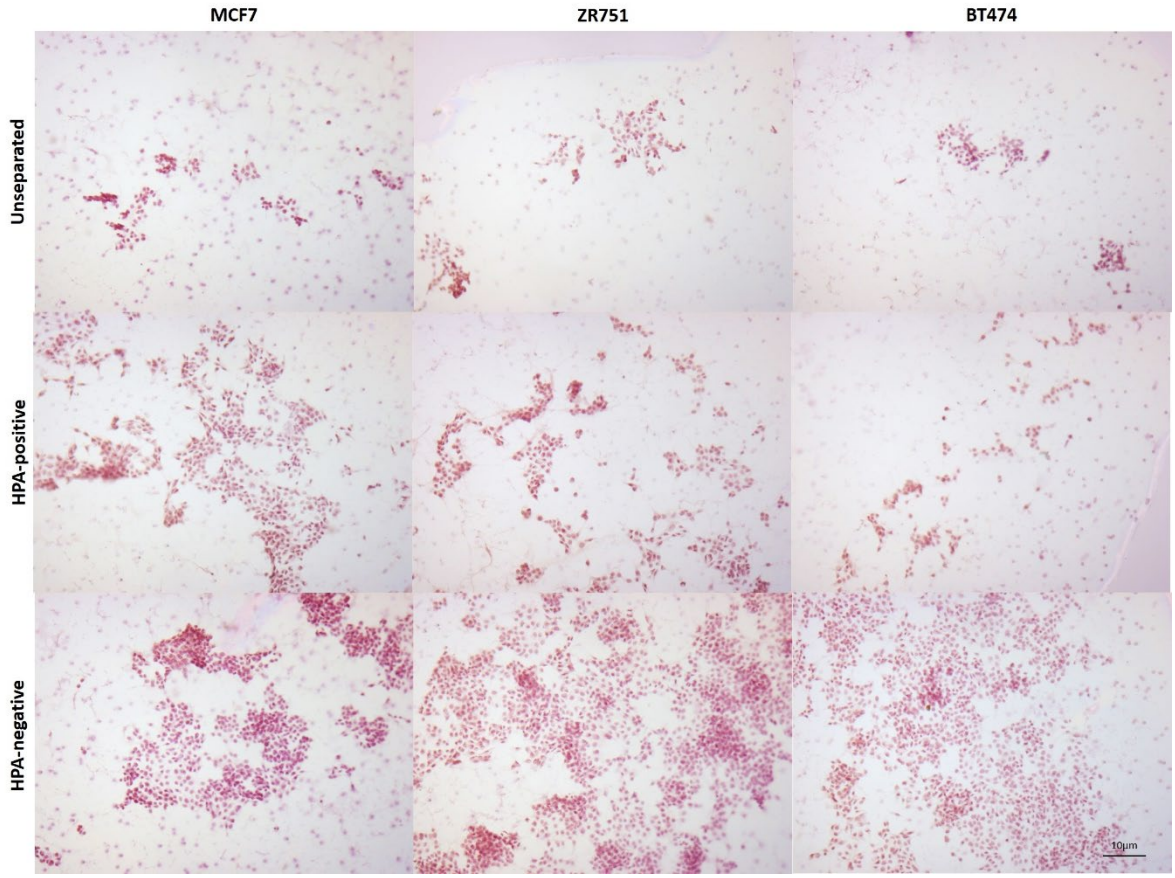

Figure 6.5 *Cells invaded through Matrigel® membrane 24hr post seeding. 50,000 cells seeded per membrane. Images representative of 3 biological replicates per cell line with around 50 images per replicate. Images captured with a Zeiss, Axioplan microscope fitted with a JENOPTIK ProgResC3 camera. Scale bar = 10µm.*

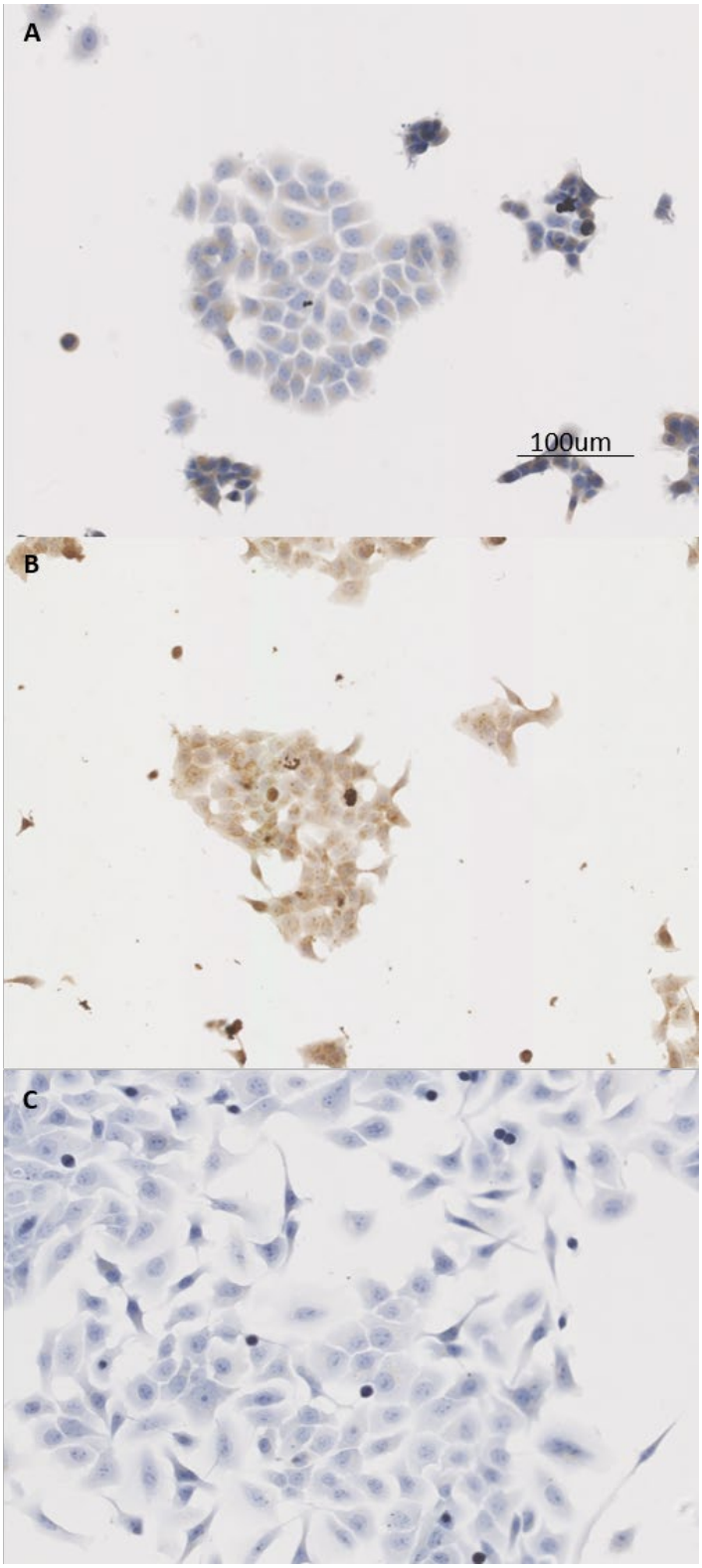

Figure 6.6 *HPA lectin labelling of ZR751 cells labelled parallel to the Matrigel assay. 50,000 cells seeded per well. A. Unseparated ZR751 cells. B. HPA-positive ZR751 cells. C. HPA-negative ZR751 cells. HPA labelling of was consistent with what was previously observed. Images representative of 3 biological replicates with 10 images captured per replicate. Images captured with a Zeiss, Axioplan microscope fitted with a JENOPTIK ProgResC3 camera. Scale bar = 100µm.*

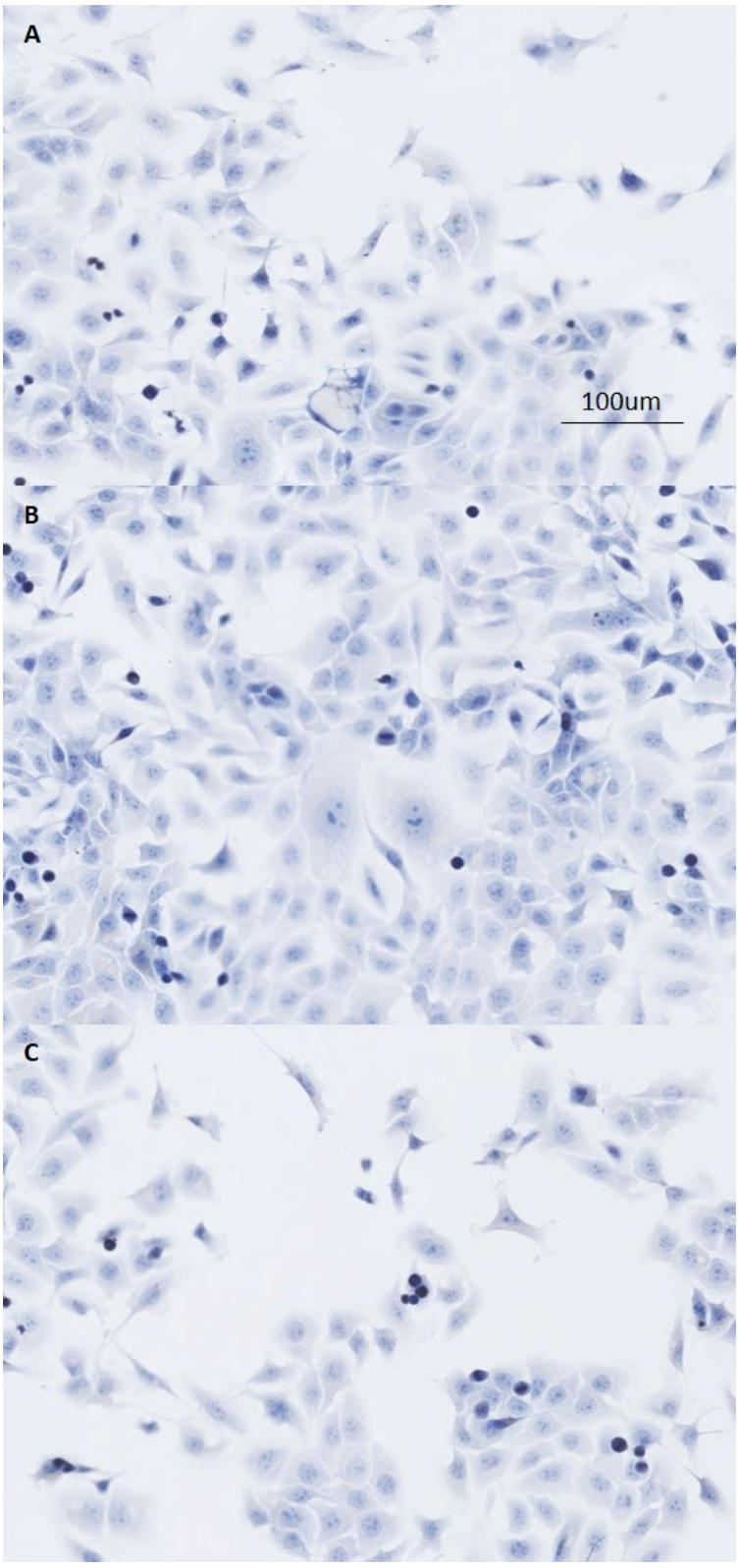

Figure 6.7 *Lectin labelling negative controls of ZR751 cells labelled parallel to the Matrigel assay. 50,000 cells seeded per well. All unseparated ZR751 cells. A. GalNAc inhibition control. B. No HPA control. C. DAB only control. For all negative controls abolished HPA labelling was observed. Images representative of 3 biological replicates with 10 images captured per replicate. Images captured with a Zeiss, Axioplan microscope fitted with a JENOPTIK ProgResC3 camera. Scale bar = 100µm.*

As illustrated in Figure 6.8 (also see Tables A2.1-A2.3), HPA-negative populations of MCF7, ZR751 and BT474 were significantly more invasive than both the HPA-positive ($p<0.05$, $p<0.001$, $p<0.01$, respectively) and unseparated ($p<0.01$, $p<0.001$, $p<0.01$, respectively) populations. This demonstrates that HPA-negative cells are more invasive and that HPA-binding glycans are not apparently involved in cell invasion as assessed in Matrigel invasion assays. In order to ensure that the high levels of invasion observed in the HPA-negative cells is not artificially induced by the cell separation procedure, an additional control was performed. The cells were separated and then mixed back together again in the original proportions of HPA-positive cells and HPA-negative cells, and the invasiveness of this "mixed" population was then compared with that of the original (unseparated) ZR751 cells. As illustrated in Figure 6.9 (also see A2.4), there are no significant differences between unseparated ZR751 cells and "mixed" ZR751 cells, so demonstrating that the cell separation procedure itself does not impart invasive properties and that HPA-negative cells are more invasive than both HPA-positive and unseparated populations.

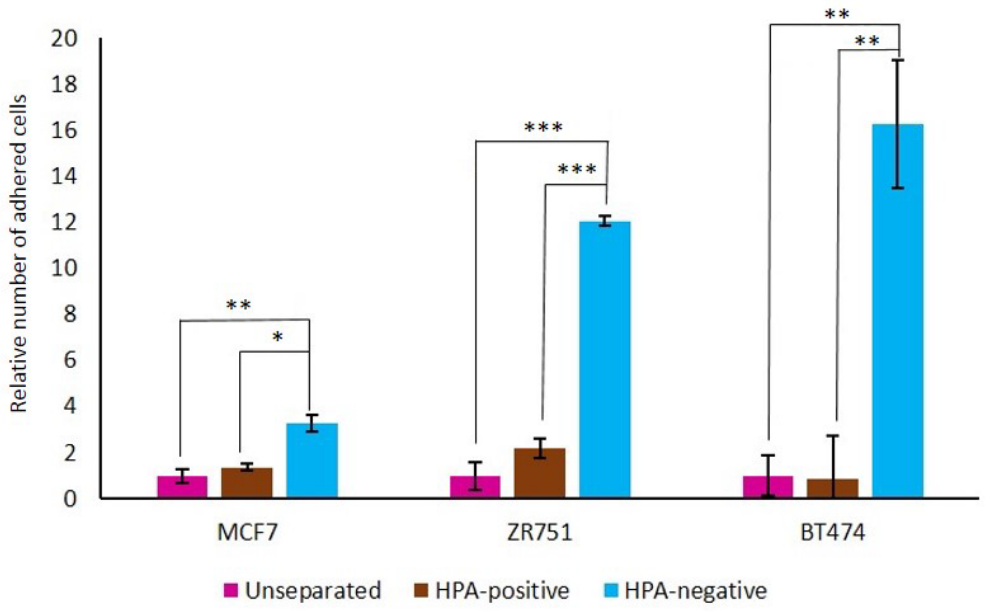

Figure 6.8 *A comparison of invasive ability as determined by the Corning® BioCoat™ Matrigel® invasion assay between unseparated cells, HPA-positive cells and HPA-negative MCF7, ZR751 and BT474 cells. For all cell lines HPA-negative cells were significantly more invasive than either HPA-positive or unseparated cells. Data compiled from 3 biological replicates per cell line. Error bars indicate standard error of the mean, and the p values are calculated from a 2-tailed t-test.*

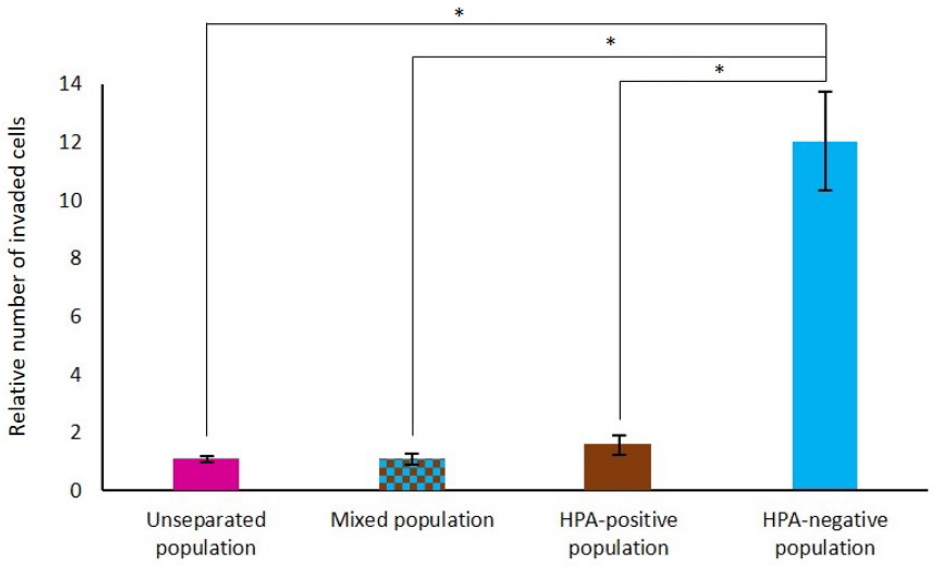

Figure 6.9 *A comparison of invasive ability as determined by the Corning® BioCoat™ Matrigel® invasion assay of unseparated, "mixed", HPA-positive and HPA-negative ZR751 cells. HPA-negative cells were significantly more invasive than either HPA-positive, "mixed" or unseparated cells. Data compiled from 3 biological replicates per cell line. Error bars indicate standard error of the mean, and the p values are calculated from a 2-tailed t-test.*

6.3.2 HPA-positive populations are more adhesive to endothelial cell monolayers than HPA-negative and unseparated populations

In order to assess the adhesive ability of HPA-binding glycans, cancer cells were isolated based on their HPA-binding glycans into HPA-positive and HPA-negative populations, and their ability to adhere to an endothelial cell monolayer was assessed. Alongside unseparated populations, HPA-positive and HPA-negative populations were tested in a static adhesion assay which mimics cell adhesion to vascular endothelium under conditions of slowed blood flow or stasis during the process of extravasation. To ensure that the separation on the basis of HPA-binding profiles was successful, HPA lectin labelling was performed alongside the static assays (see Figure A2.1-A2.2). Separation of HPA-positive and HPA-negative populations was successful. HPA-positive cells were shown to be considerably more able to adhere to endothelial cell monolayers than either HPA-negative or unseparated populations, as illustrated in Figure 6.10 (also see Table A2.5). After 30 seconds incubation on the endothelial cell monolayer, MCF7 HPA-positive populations were significantly more adhesive than HPA-negative ($p<0.01$) and unseparated ($p<0.05$) populations. At all other time points, the HPA-positive cells were considerably more adhesive than HPA-negative or unseparated populations but not significantly so. ZR751 (Figure 6.10) HPA-positive populations across all time points tested consistently show a trend of being more adhesive to endothelial cell monolayers than HPA-negative and unseparated populations, and are significantly more adhesive than HPA-negative populations at 10 minutes ($p<0.01$) and 20 minutes ($p<0.05$) incubation on endothelial cell monolayers. Again, BT474 (Figure 6.10) HPA-positive populations at all time points show a trend of being more adhesive to endothelial cell monolayers than both HPA-negative and unseparated populations. At 5 and 20 minutes incubation points, HPA-positive BT474 cells are significantly more adhesive than HPA-negative ($p<0.05$, $p<0.05$, respectively) and unseparated ($p<0.05$) populations. Taken together, these results demonstrate that HPA-positive cells are better able to adhere to endothelial monolayers than HPA-negative cells.

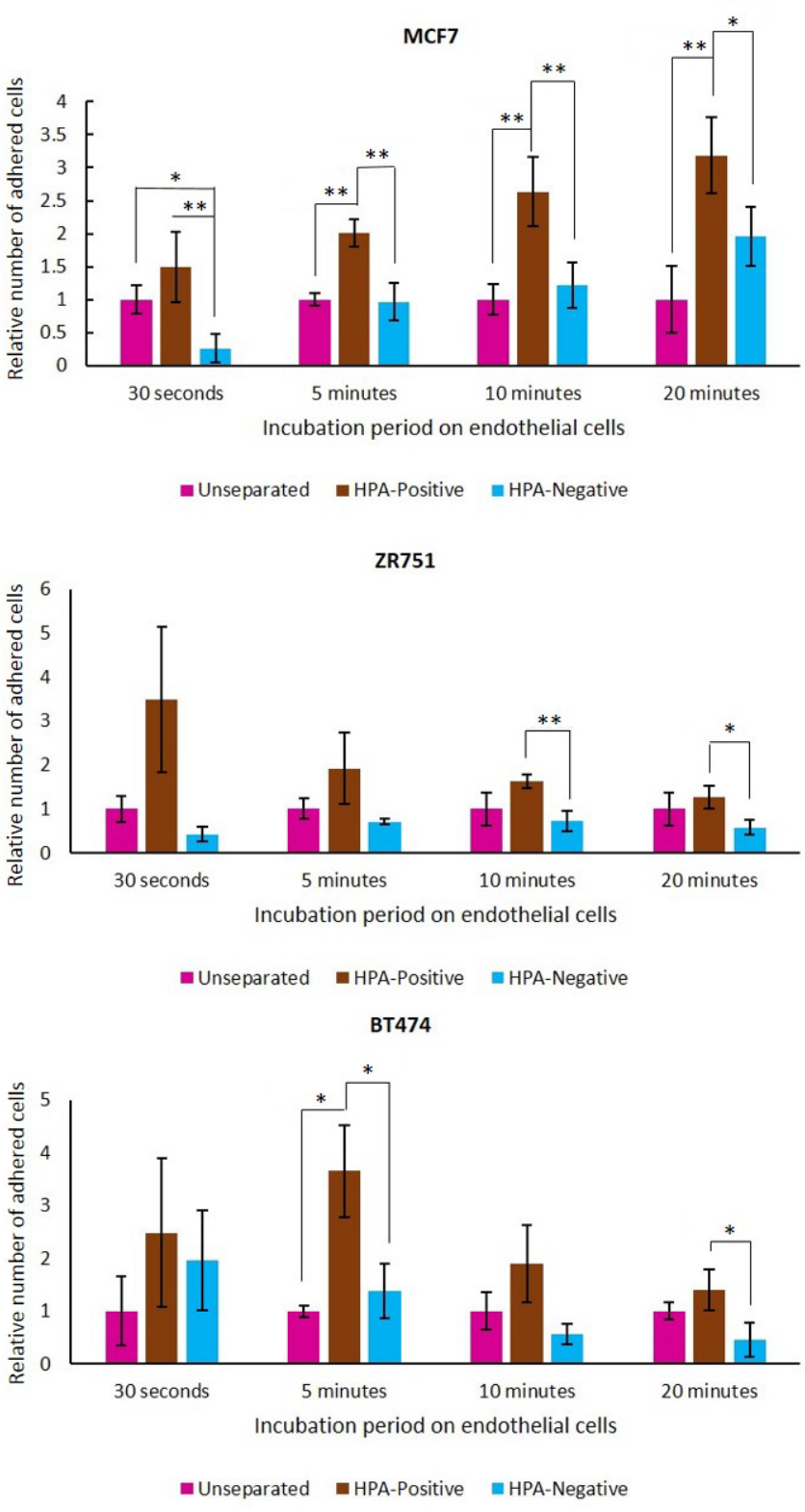

Figure 6.10 *A comparison of adhesion of MCF7, ZR751 and BT474 cell to endothelial cell monolayers over-time as determined by static adhesion assay. At all time points for all cell lines HPA-positive cells were more adhesive to endothelial cell monolayers than either HPA-negative or unseparated cells. Data compiled from 3 biological replicates per cell line. Error bars indicate standard error of the mean, and the p values are calculated from a 2-tailed t-test.*

In order to control for the potential effect of steric hindrance from the relatively large HPA molecule and for the effects of blocking HPA-binding glycans specifically, unseparated MCF7, ZR751 and BT474 cells were incubated with either Con A or HPA or regular medium prior to a 10 minute incubation with the endothelial cell monolayer. As illustrated in Figure 6.11 (also see Table A2.6), masking of HPA-binding glycans significantly reduced cancer cell binding to endothelial cells in MCF7 ($p<0.001$), ZR751 ($p<0.001$) and BT474 ($p<0.01$). Binding to endothelial cells was also significantly reduced by masking of HPA-binding glycans compared to masking of Con A-binding glycans (terminal α-D-mannosyl and α-D-glucosyl residues) in MCF7 ($p<0.01$), ZR751 ($p<0.05$) and BT474 ($p<0.01$). Masking Con A-binding glycans also significantly reduced binding of ZR751 cells ($p<0.05$), to endothelial cell monolayer compared to unseparated cells, indicating that some steric hindrance may be resulting in reduced binding to endothelial cell monolayers in these cell lines. However, the effect of masking HPA-glycans remains much more pronounced and no significant effect of masking using Con A is seen in adhesion of MCF7 and BT474 cells.

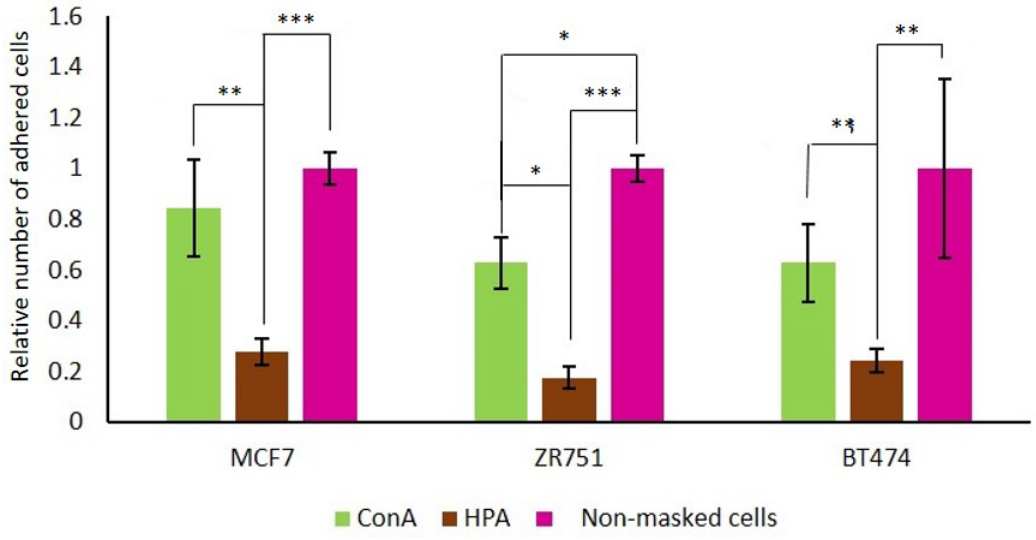

Figure 6.11 *A comparison of adhesion of MCF7, ZR751 and BT474 cells to endothelial cell monolayers at 10min incubation as determined by static adhesion assay after masking of glycans with either Con A (green bar) or HPA (brown bar). Non-masked cells compared alongside (pink bar). Masking HPA-binding glycans significantly reduced cell adhesion to endothelial cell monolayers when compared to both non-masked cells and Con A masked cells. Masking Con A-binding glycans also significantly reduced cell adhesion to endothelial cell monolayers compared to non-masked cells but not to the extent of masking with HPA. Data compiled from 3 biological replicates per cell line. Error bars indicate standard error of the mean, and the p values are calculated from a 2-tailed t-test.*

It was observed (as illustrated in Figure 6.10) that HPA-positive MCF7 cells are more adhesive (at time points 30 sec $p<0.01$, 5min $p<0.01$, 10min $p<0.01$, 20min $p<0.01$) to endothelial cell monolayers than unseparated, parental MCF7 cells. As approximately 90% of the parental, unseparated MCF7 cells are HPA-positive, such a large difference in the ability of the separated HPA-positive cells to adhere to endothelial monolayers is unexpected and suggested that the presence of HPA-negative cells in the unseparated population may be having a modulating effect on the HPA-positive cells' behaviour. In order to address the possibility of cell-cell signalling, HPA-negative cell conditioned medium was collected from an MCF7 cell separation. HPA-positive, HPA-negative, unseparated and mixed (90% HPA-positive:10% HPA-negative) cells were then incubated with either regular medium or the HPA-negative conditioned medium prior to their introduction to the static adhesion assay. As illustrated in Figure 6.12 (also see Table A2.7), there was no significant difference in adhesion to endothelial cell monolayers between unseparated and mixed cells incubated in either HPA-negative cell conditioned medium or regular medium. However, the HPA-positive population incubated with HPA-negative cell conditioned medium was significantly more adhesive ($p<0.05$) than HPA-positive cells incubated with regular medium. This is consistent with the HPA-negative cell conditioned medium contained signalling molecules which acted to increase the adhesive ability of HPA-positive cells. Furthermore, although it did not reach statistical significance ($p=0.1$), there was a trend for the HPA-negative population to become less able to adhere to endothelial cell monolayers when incubated with HPA-negative conditioned medium compared to regular medium. This, again, is consistent with cell signalling, mediated through elements secreted into the culture medium, regulating adhesive capabilities.

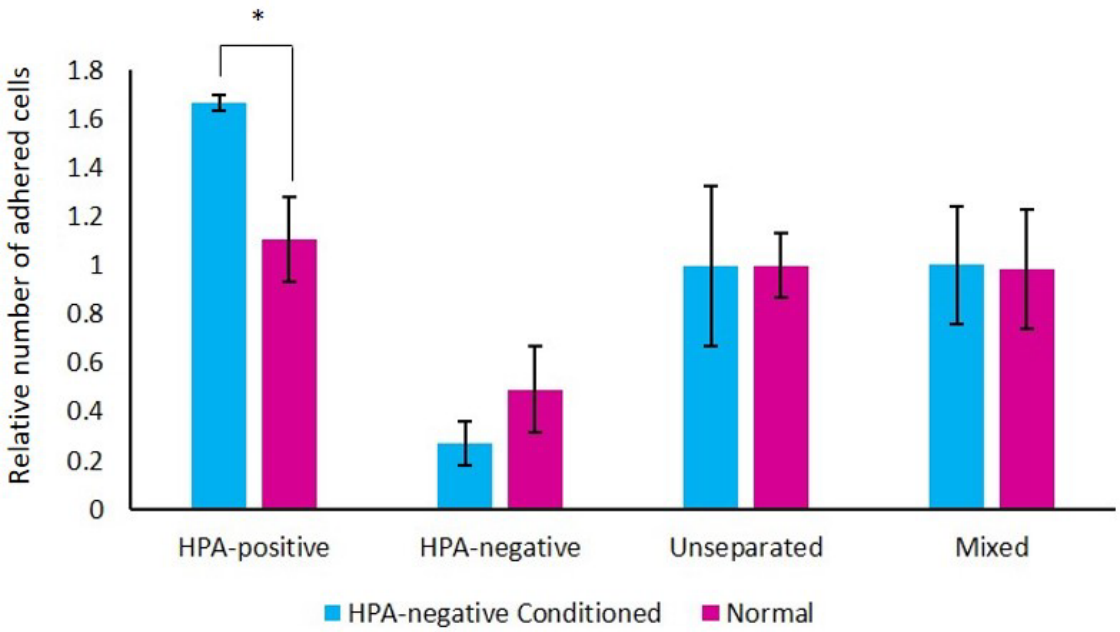

Figure 6.12 *Static adhesion assay of MCF7 cells and HPA-negative conditioned-medium. A comparison of adhesion of MCF7 cells to endothelial cell monolayer between populations incubated with HPA-negative conditioned medium or normal medium at 10min incubation. Incubating with HPA-negative conditioned medium did not significantly affect unseparated or "mixed" cells adhering to endothelial cell monolayer. However, when HPA-positive isolated cells were incubated with HPA-negative conditioned medium adhesion to endothelial cell monolayer was significantly increased. HPA-negative cells treated with HPA-negative conditioned medium demonstrated a trend of reducing adhesion to endothelial cell monolayer however not significantly so. Data compiled from 3 biological replicates. Error bars indicate standard error of the mean, and the p values are calculated from a 2-tailed t-test.*

6.4 Discussion

It was observed that separated HPA-negative cell populations were significantly more invasive than both HPA-positive and unseparated cell populations when tested in a Matrigel invasion assay. These results demonstrate that the HPA-negative cells have an invasive phenotype. Discovering that HPA-negative cells are invasive is consistent with what was reported previously in Chapter 4, where HPA-negative cells had morphological features associated with motility and invasive characteristics. To ensure that the cell separation process itself did not influence invasiveness, an artificially unseparated population termed "mixed" was prepared from equal proportions of separated HPA-positive and HPA-negative cells. When compared against unseparated, HPA-positive and HPA-negative ZR751 cell populations in Matrigel invasion assays, no significant difference in invasion was observed between the "mixed" and unseparated populations confirming that the separation procedure itself did not influence invasive

ability. Interestingly, using whole, unseparated cell lines, Brooks and Hall (2002) reported that HPA-binding glycans had no effect on cancer cell adhesion to, and invasion through, Matrigel® membrane. Brooks and Hall (2002) used a range of breast cancer cell lines which stably synthesis varying levels of HPA-binding glycans, including MCF7, ZR751 and BT474. Adhesion to, and invasion through, Matrigel was investigated with whole cell lines and with and without masking HPA-binding glycans. No significant difference was observed between the masked and un-masked samples, therefore demonstrating that HPA-binding glycans had no functional effect on cell invasion as tested in this assay system. These findings are consistent with the work that is reported here, where it is the HPA-negative cells that are able to adhere to, and invade the Matrigel.

Separated HPA-positive cell populations were significantly more adhesive to endothelial cell monolayers in the static adhesion assay, and were found to adhere after only 30 seconds of incubation with the endothelial cell monolayer. This is consistent with what is reported *in* vivo where under physiological conditions where a metastatic cancer cell may arrest in the capillaries (Chambers et al., 2002) and, adhesion to the vascular endothelium would occur almost instantaneously (Weiss et al., 1985; Weiss and Dimitrov, 1986). To ensure that the cell separation process itself did not influence cell adhesiveness, a "mixed" MCF7 population was prepared from 90% separated HPA-positive cell and 10% separated HPA-negative cells. No significant difference was observed in the adhesive ability between unseparated parental MCF7 cell populations and "mixed" MCF7 cell populations when assessed in a 10 minute incubation with the static adhesion assay. This demonstrates that the cell separation process did not influence cell adhesion. Osborne (2004) and Lomax-Browne (2009) reported in unpublished work presented in there PhD theses that DU 4475, T47D and MCF7 (unseparated, parental) cell lines which label highly with HPA were considerably more adhesive to endothelial cell monolayers under flow and sweeping flow conditions compared to weakly HPA labelling BT474 cells. Bapu et al. (2016) reported that GalNAc-glycan rich cell lines MCF7 and ZR751 adhered greatly to endothelial cells in a sweeping flow assay, and that masking GalNAc-glycans inhibited such adhesion, which is in agreement with findings reported here that HPA-positive cells are more adhesive to endothelial cell monolayers and that GalNAc-glycans are functional in this adhesion. If more time was afforded to this project, it would be informative to assess separated HPA-positive and HPA-negative populations in a more complex adhesion assay such as the rocking adhesion assay employed by Bapu et al. (2016), which takes into account shear flow and better mimics *in vivo* physiology or in an assay under physiological flow conditions such as that described by Glinsky et al. (2003), or in a flow assay similar to that used previously in our group by Osborne, (2004).

MCF7 separated HPA-positive cell populations were consistently observed to be significantly more adhesive (at time points 30sec $p<0.01$, 5min $p<0.01$, 10min $p<0.01$, 20min $p<0.01$) to endothelial cell monolayers than unseparated, parental cell lines at all incubation times tested. As many as 90% of

unseparated, parental MCF7 cells are HPA-positive with only around 10% HPA-negative (as described in Chapter 3), yet the isolated HPA-positive population of cells are significantly more adhesive in the static adhesion assay. This suggests that the presence of a relatively small proportion of HPA-negative cells in the unseparated, parental cell line has a regulatory or inhibitory effect on cell adhesiveness. For example, as 200,000 cells of the MCF7 unseparated, parental cell line were seeded into the assay of these 180,000 would be HPA-positive and 20,000 would be HPA-negative cells. Thus, the MCF7 HPA-positive isolated population only has 20,000 more HPA-positive cells than the unseparated, parental sample, yet adheres to endothelial cell monolayers by 0.5-2 fold more than the unseparated MCF7 cells. In order to investigate whether the presence of HPA-negative cells influences the adhesive capabilities of their neighbours through some form of cell-cell signalling an HPA-negative cell conditioned medium experiment was devised. An MCF7 cell separation was performed yielding two populations of each of the following: HPA-positive, HPA-negative, unseparated and "mixed". To these, either HPA-negative cell conditioned medium or normal medium was given prior to assessment of the cells adhesive behaviour in the static adhesion assay. Treatment with HPA-negative conditioned medium did not affect unseparated or "mixed" MCF7 cells and significantly increased adhesion in HPA-positive MCF7 cell populations. In contrast, HPA-negative cell populations treated with HPA-negative conditioned medium showed reduced adhesion. This suggests that the HPA-positive and HPA-negative isolated cell populations respond differently to signalling molecules in the HPA-negative cell conditioned medium. It is evident that both separated HPA-positive and HPA-negative cell populations are responding to a signal in the HPA-negative conditioned medium, but the nature and identity of the signal was not explored during the limited experiments performed here. To better understand the mechanisms at play, further experiments are required, for example, investigating the effects of HPA-positive conditioned medium on HPA-positive, HPA-negative, unseparated and "mixed" populations, as well as investigating ZR751 and BT474 cell lines. It would also be informative to investigate what the potential signals could be, for example cytokines (Partridge et al., 2004) or exosomes (Melo et al., 2014).

The data reported here suggest that HPA-binding glycans are functionally involved in the HPA-positive cells' adhesion to endothelial cell monolayers. To confirm this, a masking experiment was performed where the HPA-binding GalNAc-glycans on MCF7, ZR751 and BT474 cells were masked with HPA or irrelevant (as far as these experiments are concerned) glycans masked with Con A (which has a sugar binding specificity for terminal α-D-mannosyl and α-D-glucosyl residues) prior to incubation with the endothelial cell monolayer. Adhesion was compared with that of untreated cells. HPA masking significantly reduced the adhesion of all cell lines tested to the endothelial cell monolayers, therefore demonstrating that HPA-binding glycans are functionally involved in adhesion of cancer cells to an endothelial cell monolayer. Masking cell surface glycans by Con A also significantly reduced adhesion of ZR751 cells but not MCF7 and BT474 cells to endothelial cell monolayers, although not as significantly as HPA masking. This may indicate that some level of steric hindrance is occurring due to the presence

of a large lectin molecule at the surface, or potentially that Con A-binding glycans (terminal α-D-mannosyl and α-D-glucosyl residues) are also functionally involved in cancer adhesion, although to a lesser extent than HPA-binding GalNAc-glycans. This finding is in agreement with what was reported by Bapu et al. (2016) under conditions of sweeping flow.

The post-transformational modification of proteins by the addition of complex glycans affects protein structure and function and bestows a further level of information (Cummings, 2009; Moremen et al.,2013). Oligosaccharide functions fall into two categories: they either mediate specific recognition events or provide modulation of biological processes (Varki, 1993). There is no distinct universal function for oligosaccharides, they can modify the fundamental properties of proteins by changing their stability, protease resistance or structure (Dwek, 1994). Therefore, it is reasonable to assume that the differential glycosylation observed between the separated HPA-positive and HPA-negative cells is resulting in altered protein function which is demonstrated in the invasive and adhesive differences observed in the experiments performed here. The differential glycosylation of the cell surface proteins may also explain why the separated HPA-positive and HPA-negative cell populations reacted in different ways to the signalling in the HPA-negative cell conditioned medium. Furthermore, the GalNAc-glycans on the HPA-positive cells are presumably being recognised by a receptor on the cell surface of the endothelial cells which mediates the adhesion observed in these assays. Selectins are known to mediate cancer cell binding to vascular endothelium, as discussed in Section 1.2.5. E-selectin has been demonstrated by Brodt et al. (1997) and Kanngi et al. (2005) to mediate the adhesion of cancer cells to vascular endothelium and be functionally implicated in metastatic dissemination (reviewed by Witz, 2006). Furthermore, inhibition of E-selectin has been reported by Kobayashi et al. (2000) and Khatib et al. (2002) to correlate with inhibition of cancer metastasis. If more time and resources were available to the project, identification of the putative endothelial GalNAc-glycan binding receptor would be indicated.

6.5 Key findings

- HPA-negative cells were significantly more invasive than HPA-positive cells, when tested in a Matrigel invasion assay.
- HPA-positive cells were significantly more adhesive to endothelial cell monolayers than HPA-negative cells when tested in a static adhesion assay.
- There is potentially cross-talk between the HPA-positive and HPA-negative cells which regulates invasive and adhesive abilities of the cell population.

Chapter 7

Final discussion

7.0 Final discussion

7.1 Overview of experimental work and implications for cancer metastasis

In order to ensure that HPA-labelling produced identical results to those reported previously (Schumacher et al., 1995; Schumacher and Adam, 1997; Brooks et al., 2001) for the cell lines used within this study, lectin labelling optimisation was performed. In the optimised HPA lectin labelling procedure, HPA incubation time was reduced from 1 hour to 5 minutes, demonstrating that HPA binds much more quickly than previously realised. Using the optimised procedure, three different quantification methods for assessing HPA-labelling were performed. It was observed that the HPA labelling of the cell lines was much more complex than previously reported and showed a marked heterogeneity of glycosylation between cells within the cell lines. This suggests subtle control of glycosylation is occurring to maintain the different glycosylation profiles observed. The heterogeneity of glycosylation observed here is consistent with that reported in clinical tumours (Leathem and Brooks, 1987; Brooks and Leathem, 1991; Brooks et al., 2001). Initiation of O-glycosylation is regulated by GALNTs (reviewed by Gill et al., 2011). In the work reported here, no clear indication was found that aberrant GALNT expression is responsible for the synthesis of HPA-binding glycans in all three cell lines. However, MCF7 cells exhibited a reduction in C1GalT and its molecular chaperone *COSMC*, which build core 1, which is consistent with failure of normal chain extension (Fenlon et al., 1987; Ju et al., 2014). Gill et al. (2010) reported that relocation of GALNTs from the Golgi apparatus to the ER, increased O-glycan density and the occurrence of truncated O-glycans. This may suggest a mechanism for the heterogeneity of HPA-binding glycans reported here.

Morphological analysis was also performed on the cell lines and it was observed that HPA-positive cells, irrespective of the HPA-labelling intensity, had a rounded morphology, whilst HPA-negative cells were elongated. This further demonstrated the heterogeneity of cells within the cell lines. The rounded morphology of the HPA-positive cells was reminiscent of epithelial cells whilst the elongated morphology of the HPA-negative cells was reminiscent of mesenchymal cells (reviewed by Yang and Weinberg, 2008). This was an unexpected finding, as HPA-positive tumours are associated with metastatic ability, but the HPA-negative cells have a mesenchymal-like morphology and so would presumably be more motile and hence better equipped to metastasise. In a SCID mouse model, Schumacher et al. (1992) demonstrated that HPA-positive tumours give rise to both HPA-positive and HPA-negative metastases, and this finding was confirmed by Brooks et al. (1995) in clinical tumour samples. Taken together these findings suggest that HPA-positive cells are epithelial-like and HPA-negative cells are mesenchymal-like and begin to suggest a putative relationship between GalNAc-glycosylation revealed by HPA-labelling and EMT (reviewed by Tam and Weinberg, 2013).

The rapid binding time of HPA revealed during the optimisation of the lectin labelling procedure enabled a method of cell isolation based on the glycosylation profiles of cells to be developed and this was subsequently published (Beaman et al., 2017, see Appendix 3). The shortened procedure meant that cells were subjected to minimum stress and could be cultured post-separation. MCF7, ZR751 and BT474 cell lines, when separated based on their HPA-binding profiles, yield a HPA-positive population which, consistent with what was observed in the unseparated parental cell lines, has a rounded morphology. The HPA-negative population has an elongated morphology, which, again, is consistent with what was observed in unseparated cells (as detailed in Figure 7.1). When these isolated populations were cultured post-separation, they reverted to a mixed population over a time frame of 72 hours, resembling the glycosylation profile of the original, unseparated parental cell line. This finding is consistent with the theory developed from the unseparated cells, that the glycosylation profiles of the cells are highly regulated. It was observed that as the isolated populations revert to a mixed HPA-labelling population over time, the corresponding morphological traits also revert. For example, the HPA-positive cells that emerge from a HPA-negative population are rounded, whilst the HPA-negative cells are always elongated. This morphological plasticity, again suggested also by observations of the morphologies of cells in the unseparated parental cell lines, is reminiscent of the developmental program EMT and its reverse program MET.

To ensure that the HPA-positive and HPA-negative cells separated from the original parent populations were genuinely of the same cell type and not, for example, a result of contamination with another cell line, CODIS STR analysis was performed. This confirmed that the HPA-positive and HPA-negative cells derived from each cell line were indistinguishable from the parental cell line, but exhibited different glycosylation. These findings are consistent with reports of consistent proportions of HPA-positive and HPA-negative cells within several cancer cell lines (Schumacher et al., 1995; Schumacher and Adam, 1997; Brooks et al., 2001), as well as heterogeneity of HPA-labelling within clinical tumours (Leathem and Brooks, 1987; Fukutomi et al., 1989; Brooks and Leathem, 1991; Thomas et al., 1993; Noguchi et al., 1993a; Noguchi et al., 1993b; Ikeda et al., 1994; Noguchi et al., 1994a; Noguchi et al., 1994b; Laack et al., 2002).

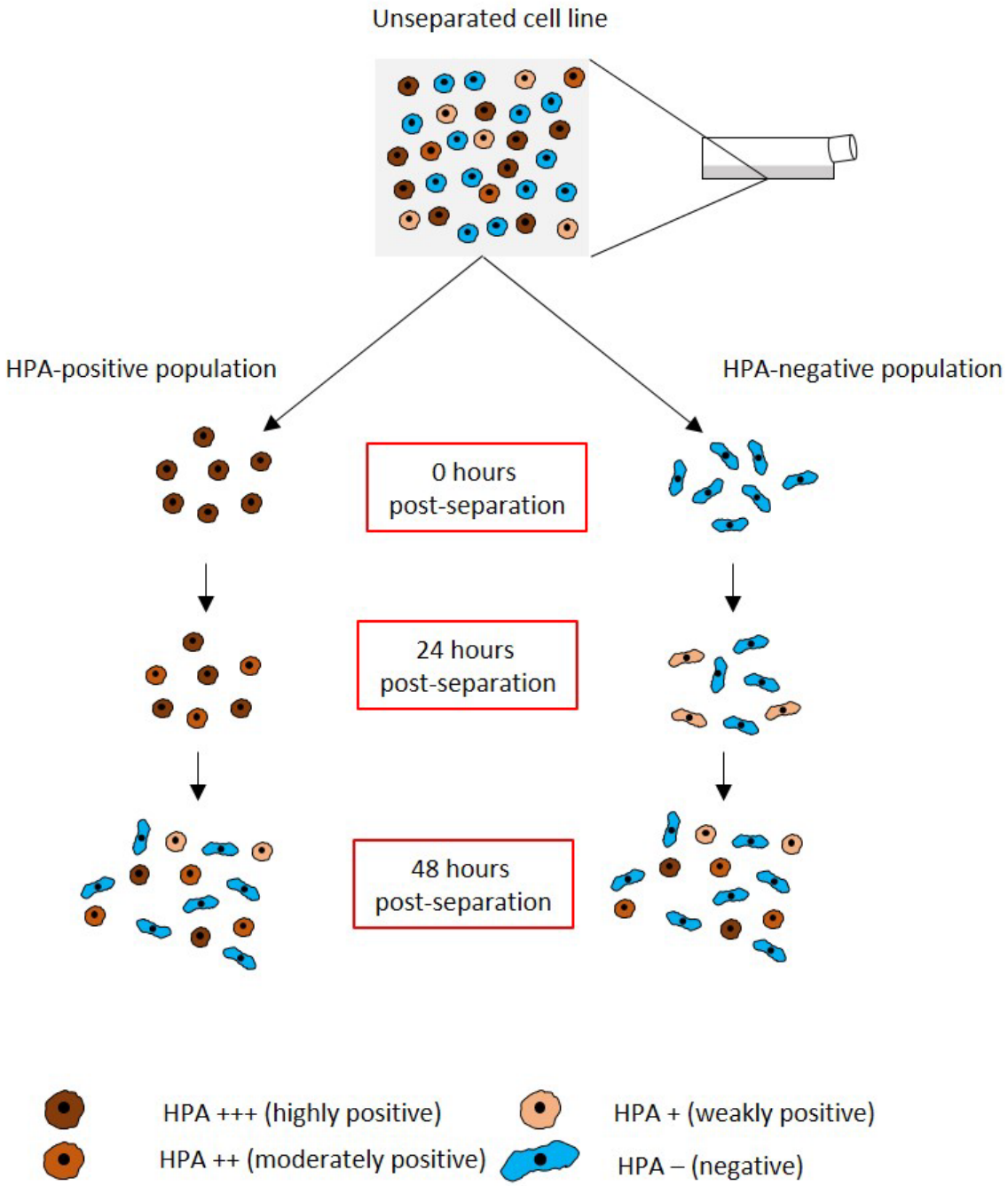

Figure 7.1 *Cells isolated based on their HPA-binging profiles via the use of lectin coated magnetic beads yields a HPA-positive population which has a rounded morphology and a HPA-negative population which has an elongated morphology. Over 24 hours post-separation the HPA-positive and HPA-negative isolated populations start to revert to mixed populations. By 48 hours post-separation both HPA-positive and HPA-negative populations are comprised of a mixed proportion of HPA labelling intensities which resembled the unseparated parental HPA labelling proportions.*

To investigate potential transcriptomic differences between the HPA-positive and HPA-negative isolated cell sub-populations, a microarray was performed to analyse separated MCF7 cells. This revealed that several EMT-associated genes were differentially expressed between the HPA-positive and HPA-negative cells. For example, vimentin (VIM) was up-regulated in HPA-negative cells. VIM is a commonly reported mesenchymal marker (Kokkinos et al., 2007). As reported by Mendez et al. (2010), transfection of vimentin cDNA into epithelial cells results in a change of cell shape from rounded to spindle-shaped and an increase in invasive potential. Conversely, the knock-down of vimentin in mesenchymal cells results in a change in shape from spindle-shaped to round (Mendez et al., 2010). That VIM is up-regulated in HPA-negative cells is consistent with their elongated morphology and suggests that they have mesenchymal traits. In the microarray analysis, E-cadherin (CDH1) was down-regulated in HPA-negative cells. CDH1 is a commonly reported epithelial marker (Gravdal et al., 2007). That CDH1 is down-regulated in HPA-negative cells and therefore up-regulated in HPA-positive cells is consistent with their rounded morphology and suggests that they have epithelial traits. Interestingly, snail family transcriptional repressor 2 (SLUG) and zinc finger E-box binding homeobox 1 (ZEB1) were up-regulated in HPA-negative cells. SLUG and ZEB1 are transcriptional repressors of CDH1 and induce mesenchymal phenotypes through targeting CDH1 (Hajra et al., 2002; Sánchez-Tilló et al., 2010). Furthermore, several genes associated with invasion were up-regulated in HPA-negative cells. For example, secreted protein acidic and cysteine rich (SPARC) was significantly up-regulated in HPA-negative cells. Briggs et al. (2002) reported that suppression of SPARC in MCF7 cells inhibited cell motility and invasion. TWIST1 was also up-regulated in HPA-negative cells and it was reported by Mikheeva et al. (2010) that up-regulation of TWIST1 increased invasion in xenotransplants. These findings support that there is a relationship between EMT and glycosylation with HPA-positive cells exhibiting epithelial-like characteristics, and HPA-negative cells exhibiting mesenchymal-like characteristics.

In order to investigate the potential functional significance of GalNAc-glycosylation of cancer cells in metastasis, an invasion and an adhesion assay were performed. The Matrigel cell invasion assay modelled cell invasion through ECM and BM components, whilst the adhesion assay modelled cancer cell adhesion to endothelium during slowed blood flow or stasis in small capillaries during metastasis. As illustrated in Figure 7.2, HPA-negative cells were highly invasive in the Matrigel cell invasion assay, whilst the HPA-positive cells were not. Again, this is consistent with HPA-negative cells having a mesenchymal-like and invasive phenotype and HPA-positive cells being more epithelial, adhesive and non-invasive.

To further confirm and investigate the functional involvement of HPA-binding GalNAc-glycans in metastatic mechanisms, static adhesion assays were performed. HPA-positive cells were able to adhere to endothelial cell monolayers in high numbers, whilst HPA-negative cells were not. This is consistent with earlier observations that HPA-negative cells have a mesenchymal-like non-adhesive phenotype.

That HPA-binding glycans were functionally involved in cancer cell adhesion to endothelial cell monolayers was confirmed by masking the HPA-binding glycans prior to their introduction onto the endothelial cell monolayer. This resulted in a significant reduction (MCF7 $p<0.001$, ZR751 $p<0.001$, BT474 $p<0.01$) in cancer cell adhesion. This finding demonstrates that HPA-binding glycans are functionally involved in cancer cell binding to endothelial cell monolayers under static conditions. This finding is consistent with what has been previously reported about unseparated whole cell lines which label highly for HPA being more adhesive in a sweeping flow adhesion assay (Osborne, 2004; Lomax-Browne, 2009; Brooks et al., 2009; Bapu et al., 2016). Bapu et al. (2016), for example, demonstrated that MCF7 and ZR751 cells, which label highly with HPA, bound greatly to endothelial cell monolayers under conditions of sweeping flow and masking the HPA-binding glycans significantly reduced adhesion.

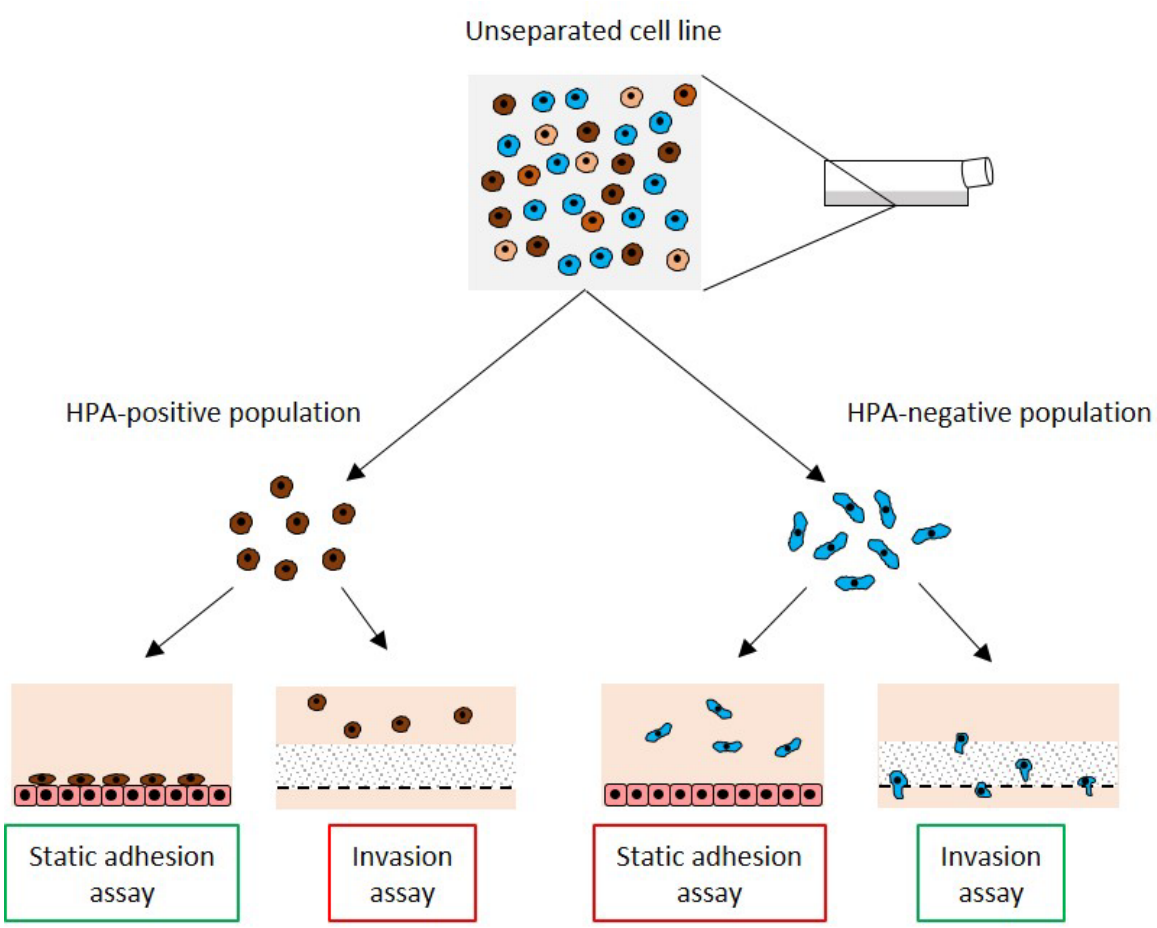

Figure 7.2 *Cells were separated based on their HPA-binding profiles and were tested in a static adhesion assay to endothelial cell monolayers and a Matrigel invasion assay. HPA-positive cells were found to be highly adhesive to endothelial cell monolayers, whilst HPA-negative cells were not. HPA-negative cells were highly invasive in the Matrigel invasion assay, while the HPA-positive cells were not.*

It was observed that over all time periods tested, the MCF7 HPA-positive population were consistently significantly more adhesive to the endothelial cell monolayer than the unseparated parental cell line. This unexpected finding may indicate that the small proportion (10%) of HPA-negative cells within the unseparated parental cell lines are in some way modulating the behaviour of the majority (90%) HPA-positive cells. This modulating effect could be the result of cell signalling. To investigate this, a cell separation was performed and conditioned medium from HPA-negative cells was collected. Regular medium and conditioned medium was then applied to an unseparated population, an HPA-positive population, an HPA-negative population and an artificially "mixed" population. The behaviour of the cells was then observed in the adhesion assay. It was observed that HPA-positive cells treated with the HPA-negative cell conditioned medium were significantly more adhesive than those treated with regular medium. Conversely, it was observed that HPA-negative cells treated with HPA-negative cell conditioned medium became slightly less adhesive, although not significantly so. The conditioned medium resulted in no effect on both the unseparated and "mixed" populations. These finding confirm that there is some form of cell-cell signalling between HPA-positive and HPA-negative cells occurring. Currently there is much interest in the involvement of exosomes in cell signalling. For example, Senfter et al. (2015) demonstrated that by treating colon cancer cells with exosomes containing miR-200, EMT was repressed, as the miR-200 family transcriptionally repress EMT transcription factors ZEB1 and SLUG. Bigagli et al. (2016) reported that exosomes containing miR-210 released from colon cancer cells resulted in the regulation of EMT and MET characteristics in neighbouring cells. Alternatively, cytokines such as TNF-α may be implicated in the cell-cell signalling observed in the work reported here. For example, Julien et al. (2007) demonstrated that Snail expression and subsequent E-cadherin repression is mediated by TNF-α-induced Akt kinase activation of nuclear factor-κB. Wu et al. (2009) reported that TNF-α also induces Snail stabilisation and EMT induction through repression of E-cadherin.

The work reported here demonstrates the ability of the HPA-positive and HPA-negative cell populations to transition from HPA-positive, rounded, epithelial and adhesive cells to HPA-negative, elongated, mesenchymal and invasive cells and vice versa. Whether there may be a causal relationship between glycosylation and morphological characteristics is not known. However, several studies reported in the literature demonstrate an association between deregulation of the enzymes of glycosylation and changes in cell behaviour. For example, Wu et al. (2011) reported that knock-down of GALNT2 in hepatocytes increased cell invasion and migration. Peng et al. (2012) reported that miR-124 suppresses invasiveness of cervical cancer cells by directly targeting GALNT7. Freire-de-Lima et al. (2011) demonstrated that knock-down of GALNT3 and GLANT6 in human prostate epithelial cell lines inhibited TGF-β induced EMT through failure to O-glycosylate the type III homology connective segment of oncofoetal fibronectin, a common mesenchymal marker. These findings taken together all suggest a possible link between EMT and glycosylation, and a potential role of GALNTs regulating cell plasticity through altered expression.

Other lines of evidence also suggest that glycosylation and EMT↔MET may be interrelated. For example, Lange-Consiglio et al. (2014) reported that equine amnion epithelial cells transformed into mesenchymal cells during cell culture and that the epithelial and mesenchymal cells had different glycosylation profiles as determined by labelling using a panel of 12 lectins. Shao et al. (2016) demonstrated that posttranslational modification of E-cadherin by less core fucosylation activated Src kinase thereby promoting EMT in lung cancer cells. Maupin et al. (2010) used micro array analysis of 22 pancreatic cancer cell lines and subsequent qPCR validation to demonstrate that alterations in glycogene expression is a key factor of EMT. Taken together these reports, as well as the data reported in the study presented here, suggest a role of glycosylation in cancer cell plasticity.

The intriguing observation, that HPA-positive, highly adhesive cell populations are able to transition to HPA-negative, highly invasive cell populations, and vice versa, may have significant functional consequences in metastatic mechanisms. Hypothetically, HPA-negative cells would be able to detach from the primary tumour and invade local basement membrane and tumour vasculature. Then, HPA-positive cells would be able to adhere to vascular endothelium and extravasate (illustrated in Figure 7.3). HPA-negative cells would then migrate into tissues at a secondary site and HPA-positive cells form cohesive secondary tumours.

HPA-positivity of clinical tumours is well reported to be associated with metastatic competence (Leathem and Brooks, 1987; Fenlon et al., 1987; Fukutomi et al., 1989; Alam et al., 1990; Brooks and Leathem, 1991; Fukutomi et al., 1991; Thomas et al., 1993; Noguchi et al., 1993; Brooks et al., 1993; Brookes et al., 1996; Brooks and Wilkison, 2003); however, it is also reported that tumours possess both HPA-positive and HPA-negative cell populations. Furthermore, HPA-positive tumours give rise to both HPA-positive and HPA-negative metastases (Schumacher et al., 1992; Brooks and Leathem, 1999), therefore suggesting that either HPA-positivity is lost through the natural progression of the cancer or that HPA-positivity is plastic. From the data reported here, it was shown that cells isolated based on their HPA-binding profiles revert to a mixed population, and are plastic. Taken together, this suggests that co-operation of HPA-positive and HPA-negative cell populations, or perhaps transition from HPA-positive cells to HPA-negative cells or the inverse, is necessary to achieve successful metastasis.

The cell separation procedure devised in the work reported here (which is described in Section 2.3 and published Beaman et al., 2017, see Appendix 3) has numerous applications for the wider cancer research field. The ability to be able to isolate cells based on their cell surface carbohydrates, which are commonly irregular on cancer cells, and be able to culture both positive and negative isolated populations post-separation allows for subsequent independent analysis, which has not been previously reported

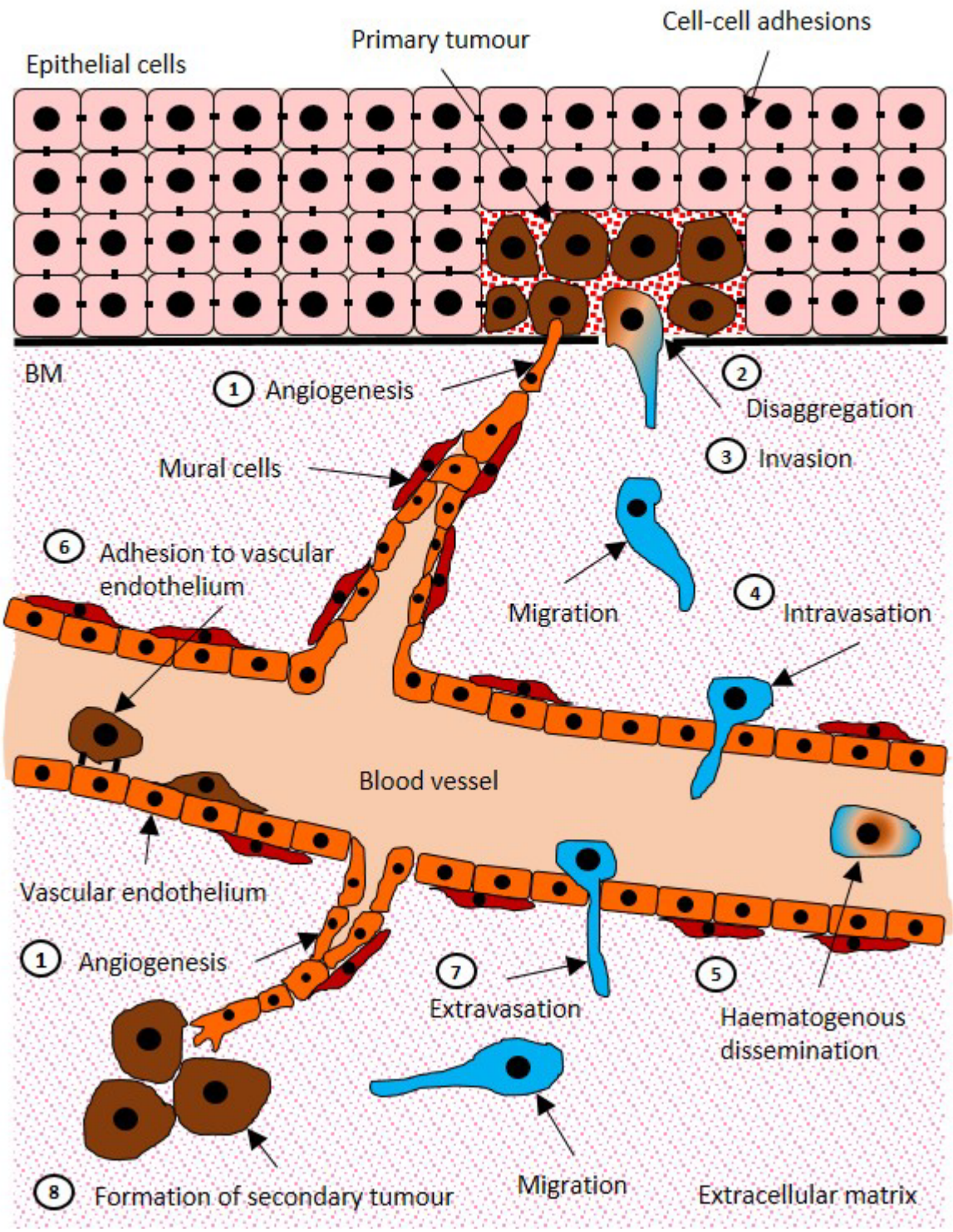

Figure 7.3 *Hypothesised transition of HPA-positive and HPA-negative cells in metastatic mechanisms. 1 HPA-negative cells can detach from the primary tumour and (2) invade local basement membrane, (3) migrate to and invade (4) tumour vasculature. During haematogenous dissemination (5) HPA-negative cells transition to HPA-positive cells and then, HPA-positive cells would be able to adhere to vascular endothelium (6). HPA-negative cells would be able to extravasate (6) and then migrate into tissues at a secondary site and HPA-positive cells form cohesive secondary tumours (8).*

7.2 Novel contributions

The novel contributions of the work presented here are:

- Demonstration that within both parental cell lines and in populations isolated based on their glycosylation profiles, HPA-negative cells have an elongated, mesenchymal-like morphology whilst HPA-positive cells have a rounded, epithelial-like morphology.
- Demonstration that cells isolated based on their HPA-binding profiles revert to a mixed population, with similar glycosylation profiles as unseparated parental cell lines, and that glycosylation is therefore dynamic, plastic and tightly regulated.
- Demonstration that a number of EMT-associated genes are differentially regulated between HPA-positive (epithelial, rounded) and HPA-negative (mesenchymal, elongated) isolated cell populations. Also, that a number of invasion-associated genes are up-regulated in HPA-negative (mesenchymal, elongated) isolated cell populations.
- Demonstration that HPA-negative (mesenchymal, elongated) isolated cell populations are more invasive through BM and ECM components and that HPA-positive (epithelial, rounded) isolated cell populations are more adhesive to endothelial cell monolayers. Also, that there is some form of cell signalling between the HPA-positive and HPA-negative cells which modulates their adhesive abilities.

7.3 Future work

The work reported here demonstrates that when cells are isolated based on their HPA-binding profiles and are cultured post-separation they revert to pre-separation HPA labelling profiles. HPA-positive isolated cell populations have a rounded morphology, are highly adhesive to an endothelial cell monolayer and have epithelial-like characteristics. HPA-negative isolated cell populations have an elongated morphology, are highly invasive and have mesenchymal-like characteristics. The HPA-positive and HPA-negative cells characteristics are consistent, yet plastic, transitioning from one state to another over time. This process is reminiscent of EMT↔MET. These aspects of the work reported here forms the basis of a patent (UK patent application number: 1702582.6, date of filing: 17 February 2016, title: screening method). That these findings might be of commercial interest lies in their potential for use as an anti-metastasis drug screening tool.

Currently the method of isolating cells based on their HPA-binding glycans and subsequent quantification, as reported in this thesis (see Section 3.2.3) is lengthy, taking several days. Further development would initially require the process to be refined and automated. Initially, fluorescent HPA

labelling would need to be optimised to yield HPA-labelling proportions consistent with what is reported here. Once this is achieved, fluorescently labelled cells could be rapidly separated and quantified using a fluorescence activated cell sorter (FACS). Using such a refined assay, rapid screening of agents could be performed which might block the transition between HPA-positive (epithelial, adhesive) and HPA-negative (mesenchymal, invasive) cell populations. If plasticity is required for successful metastasis, as proposed in this thesis, then agents preventing the switch may be effective halting metastatic mechanisms. Such agents might include small molecules such as proteins, peptides, lectins, small molecule drugs, aptamers, oligos, shRNAs, RNAis or siRNAs.

That HPA-binding glycans have been shown in the work reported here to function in adhesion of cancer cells to endothelial monolayers also raises the question as to the identity of the epithelial GalNAc-glycan binding receptor. Identification could be achieved through extraction of the cell surface proteins from HUVECs and isolation of the receptor using α-GalNAc bound to a molecule such as BSA. The receptor could then be analysed using western blot and sequenced. Potentially, its identification might open pathways to discover means to block GalNAc-glycosylated cells from adhering to endothelium.

References

A

Abulí A., Fernández-Rozadilla C., Alonso-Espinaco V., Muñoz J., Gonzalo V., Bessa X., Gonzálex D., Clofent J., Cubiella J., Morillas J.D., Rigau J., Latorre M., Fernández-Bañares F., Peña E., Riestra S., Payá A., Jover R., Xicola R.M., Llor X., Carvajal-Carmona L., Villanueva C.M., Moreno V., Piqué J.M., Carracedo A., Castells A., Andreu M., Ruiz-Ponte C. and Castellví-Bel S. (2011) Case-study for colorectal cancer genetic susceptibility in EPICOLON: previously identified variants and mucins. BMC Cancer, 11: 339.

Ackland M.L., Newgreen D.F., Fridman M., Waltham M.C., Arvanitis A., Minichiello J., Price J.T. and Thompson E.W. (2003) Epidermal growth factor-induced epithelia-mesenchymal transition in human breast carcinoma cells. Laboratory Investigation, 88(3): 435-448.

Adams J.M. and Cory S. (2007) The Bcl-2 apoptotic switch in cancer development and therapy. Oncogene, 26: 1324-1337.

Adams R.H. and Alitalo K. (2007) Molecular regulation of angiogenesis and lymphangiogenesis. Nature Reviews Molecular Cell Biology, 8: 464-478.

Adams A.A., Okagbare P.I., Feng J., Hupert M.L., Patterson D., Göttert J., McCarley R.L., Nikitopoulos D., Murphy M.C. and Soper S.A. (2008) Highly efficient circulating tumour cell isolation from whole blood and label-free enumeration using polymer-based microfluidics with an integrated conductivity sensor. Journal of the American Chemical Society, 130(27): 8633-8641.

Aebi M. (2013) N-linked protein glycosylation in the ER. Biochemica et Biophysica Acta, 1833(11): 2430-2437.

Alam S. M., Whitford P., Cushley W., George W. D. and Campbell A. M. (1990) Flow cytometric analysis of cell surface carbohydrates in metastatic human breast cancer. British Journal of Cancer, 62(2): 238-242.

Albini A., Benelli R., Noonan D.M. and Brigati C. (2004) The “chemoinvasion assay”: as a tool to study tumour and endothelial cell invasion of basement membranes. International Journal of Developmental Biology, 48: 563-571.

Alblazi K. M. and Siar C. H. (2015) Cellular protrusions--lamellipodia, filopodia, invadopodia and podosomes--and their roles in progression of orofacial tumours: current understanding. Asia Pacific Journal of Cancer Prevention, (6)2: 2187-2191.

Almog N. (2010) Molecular mechanisms underlying tumour dormancy. Cancer Letters, 294(2): 139-146.

Ambrosi M., Cameron N.R. and Davis B.G. (2005) Lectins: tools for the molecular understanding of the glycocode. Organic and Biomolecular Chemistry, 3: 1593-1608.

Appeddu P.A. and Shur B.D. (1994) Control of stable lamellipodia formation by expression of cytoplasmic domains. Journal of Cell Science, 107: 2535-2545.

Apweiler R., Hermjakob H. and Sharon N. (1999) On the frequency of protein glycosylation, as deduced from analysis of the SWISS-PROT database. Biochemica et Biophysica Acta, 1773(1): 4-8.

Armstrong A.J., Marengo M.S., Oltean S., Kemeny G., Bitting R.L., Turnbull J.D., Herold C.I., Marcom P.K., George D.J. and Garcia-Blanco M.A. (2011) Circulating tumour cells from patients with advanced prostate and breast cancer display both epithelial and mesenchymal markers. Molecular Cancer Research, 9(8): 997-1007.

Arya M., Shergill I.S., Williamson M., Gommersall L., Arya N. and Patel H.R.H. (2005) Basic principles of real-time quantitative PCR. Expert Reviews in Molecular Diagnostics, 5(2): 209-219.

Ashby W.J. and Zijlstra A. (2012) Established and novel methods of interrogating two-dimensional cell migration. Integrative Biology, 4(11): 1338-1350.

Auerbach R., Lu W.C., Pardon E., Gumkowski F., Kaminska G. and Kaminski M. (1987) Specificity of adhesion between murine tumour cells and capillary endothelium: an *in vitro* correlate of preferential metastasis *in vivo*. Cancer Research, 47: 1492-1496.

Azari S., Ahmedi N., Tehrani M.J. and Shokri F. (2007) Profiling and authentication of human cell lines for using short tandem repeat (STR) loci: report from the National Cell Bank of Iran. Biologicals, 35(3): 195-202.

B

Baccelli I., Schneeweis A., Riethdorf S., Stenzinger A., Schillert A., Vogel V., Klein C., Saini M., Bäverle T., Wallwiener M., Holland-Letz T., Höfner T., Sprick M., Scharpff M., Marmé F., Sinn H.P., Pantel K., Weichert W. and Trumpp A. (2013) Identification of a population of blood circulating tumour cells from breast cancer patients that initiates metastasis in xenograft assay. Nature Biotechnology, 31(6): 539-545.

Baguley B.C. and Leung E. (2010) Heterogeneity of phenotype in breast cancer cell lines. In: Breast Cancer – Carcinogenesis, Cell Growth and Signalling Pathways. Gunduz M. (ed) InTech doi: 10.5772/21984.

Baker D.A., Sugii S., Kabat E.A., Ratcliffe R.M., Hermentin P. and Lemieux R.U. (1983) Immunochemical studies on the combining sites of Forssman hepten reactive hemagglutinins from *Dolichocbiflorus*, *Helix pomatia* and *Wistaria floribunda*. Biochemistry, 22(11): 2741-2750.

Balkwill F. and Matovani A. (2001) Inflammation and Cancer: back to Virchow? The Lancet, 357(9255): 539-545.

Bapu D., Khadim M. and Brooks S.A. (2014) Rocking adhesion assay system to study adhesion and transendothelial migration of cancer cells. Methods in Molecular Biology, 1070: 37-45.

Bapu D., Runions J., Kadhim M. and Brooks S.A. (2016) N-acetylgalactosamine glycans function in cancer cell adhesion to endothelial cells: A role for truncated O-glycans in metastatic mechanisms. Cancer Letters, 375(2): 367-374.

Bard C. and Chia J. (2016) Cracking the glycome encoder: signaling trafficking, and glycosylation. Trends in Cell Biology, 26(5): 379-388.

Barrow H., Tam B., Duckworth C.A., Rhodes J.M. and Yu L.G. (2013) Suppression of core 1 Gal-transferase is associated with reduction of TF and reciprocal increase of Tn, sialyl-Tn and Core 3 glycans in human colon cancer cells. PLoS One, 8(3): e59792. doi:10.1371/journal.pone.0059792.

Bartel D.P. (2004) MicroRNAs: genomics, biogenesis, mechanism, and function. Cell, 116(2): 281-297.

Beaman, E.-M. and Brooks, S.A. (2014) The extended ppGalNAc-T family and their functional involvement in the metastatic cascade. Histology and Histopathology, 29: 293-304.

Beaman E.-M., Carter D.R.F. and Brooks S.A. (2017) Isolation of viable glycosylation-specific cell populations for further *in vitro* or *in vivo* analysis using lectin-coated magnetic beads. In: Pellicciari C. and Biggiogera M. (eds) *Histochemistry of Single Molecules. Methods in Molecular Biology 1560*. New York: Humana Press. 109-119.

Beatson R., Maurstad G., Picco G., Arulappu A., Coleman J., Wandell H.H., Clausen H., Mandel U., Taylor-Papadimitriou J., Sletmoen M. and Burchell J.M. (2015) The Breast Cancer-Associated Glycoforms of MUC1, MUC1-Tn and sialyl-Tn, Are Expressed in COSMC Wild-Type Cells and Bind the C-Type Lectin MGL. PLoS One, 10(5): e0125994.

Bendas G. and Borsig L. (2012) Cancer cell adhesion and metastasis: selectins, integrins, and the inhibitory potential of heparins. International Journal of Cell Biology, Article ID 676731, 10 pages, doi:10.1155/2012/676731.

Bennett E.P., Hassan H. and Clausen H. (1996) cDNA cloning and expression of a novel human UDP-N-acetyl-alpha-D-galactosamine:polypeptide N-acetylgalactosaminyltransferase, GalNAc-T3. The Journal of Biological Chemistry, 271(29): 17006-17012.

Bennett E.P., Hassan H., Mandel U., Mirgorodskaya E., Roepstorff P., Burchell J., Taylor-Papadimitriou J., Hollingsworth M.A., Merkx G., van Kessel A.G., Eiberg H., Steffensen R. and Clausen H. (1998) Cloning of a human UDP-N-acetyl-alpha-D-galactosamine:polypeptide N-acetylgalactosaminyltransferase that complements other GalNAc-transferases in complete O-glycosylation of the MUC1 tandem repeat. The Journal of Biological Chemistry, 273(46): 30472-30481.

Bennett E.P., Hassan H., Mandel U., Hollingsworth M.A., Akisawa N., Ikematsu Y., Merkx G., van Kessel A.G., Olofsson S. and Clausen H. (1999a) Cloning and characterization of a close homologue of human UDP-N-acetyl-alpha-D-galactosamine:polypeptide N-acetylgalactosaminyltransferase-T3, designated GalNAc-T6. Evidence for genetic but not functional redundancy. The Journal of Biological Chemistry, 274(36): 25362-25370.

Bennett E.P., Hassan H., Hollingsworth M.A. and Clausen H. (1999b) A novel human UDP-N-acetyl-D-galactosamine:polypeptide N-acetylgalactosaminyltransferase, GalNAc-T7, with specificity for partial GalNAc-glycosylated acceptor substrates. FEBS Letters, 460(2): 226-30.

Bennett E.P., Mandell U., Clausen H., Gerken T.A., Fritz T.A. and Tabak L.A. (2012) Control of mucin-type O-glycosylation: a classification of the polypeptide GalNAc-transferase gene family. Glycobiology, 22(6): 736-756.

Berdasco M. and Esteller M. (2010) Aberrant epigenetic landscape in cancer. How cellular identities go awry. Development Cell Biology, 1a: 698-711.

Bergers G. and Benjamin L.E. (2003) Tumorigenesis and the angiogenic switch. Nature Reviews Cancer, 3: 401-410.

Berois N., Mazal D., Ubillos L., Trajtenberg F., Nicolas A., Sastre-Garau X., Magdelenat H. and Osinaga E. (2006a) UDP-*N*-acetyl-d-galactosamine: polypeptide *N*-acetylgalactosaminyltranferase-6 as a new immunhistochemical breast cancer marker. Journal of Histochemistry and Cytochemistry, 54(3): 317-328.

Berois N., Blanc E., Ripoche H., Mergui X., Trajtenberg F., Cantais S., Barrois M., Dessen P., Kågedal B., Bénard J., Osinaga E. and Raguénez G. (2006b) ppGalNAc-T13: a new molecular marker of marrow involvement in neuroblastoma. Clinical Chemistry, 52(9): 1701-1712.

Berois N., Gattolliat C., Barrios E., Capandeguy L., Douc-Rasy S., Valteau-Couanet D., Bénard J. and Osinaga E. (2013) *GALNT9* gene expression is a prognostic marker in neuroblastoma patients. Clinical Chemistry, 59(1): 225-233.

Beyers S., Sommers S., Hoxter B., Mercurio A. and Tozeren A. (1995) Role of E-cadherin in the response of tumour cell aggregates to lymphatic venous and arterial flow: measurement of cell-cell adhesion strength. Journal of Cell Science, 108: 2053-2064.

Bigagli E., Luceri C., Guasti D. and Cinci L. (2016) Exosomes secreted from human colon cancer cells influence the adhesion of neighbouring metastatic cells: role of microRNA-120. Cancer Biology and Therapy, 17(10): 1062-1069.

Blasco M.A. (2005) Telomeres and human disease: aging, cancer and beyond. Nature Reviews Genetics, 6: 611-622.

Blood C. H. and Zetter B. R. (1990) Tumour interactions with the vasculature: angiogenesis and tumour metastasis. Biochemica et Biophysica Acta, 1032: 89-118.

Bockhorn M., Jain R.K. and Munn L.L. (2007) Active versus passive mechanisms in metastasis: do cancer cells crawl into vessels or are they pushed? The Lancet. Oncology, 8(5): 444-448.

Bolós V., Peinado H., Pérez-Moreno M.A., Fraga M.F., Esteller M. and Cano A. (2003) The transcription factor Slug represses E-cadherin and induces epithelial to mesenchymal transitions: a comparison with Snail and E47 repressors. Journal of Cell Science, 116(Pt3): 499-511.

Boskovski M.T., Yuan S., Perdersen N.B., Gath C.K., Makova S., Clausen H., Brueckner M. and Khokha M.K. (2013) The heterotaxy gene, GALNT11, glycosylates Notch to orchestrate cilia type and laterality. Nature, 504(7480): 456-459.

Boyden S. (1962) The chemotactic effects of mixtures of antibody and antigen on polymorphonuclear leukocytes. The Journal of Experimental Medicine, 1(115): 435-466.

Boyer B., Tucker G., Valles A., Franke W. and Thiery J. (1989) Rearrangements of desmosomal and cytoskeletal proteins during the transition from epithelial to fibroblastoid organization in cultured rat bladder carcinoma cells. Journal of Cell Biology, 109: 1495-1509.

Brabletz S. and Brabletz T. (2010) The ZEB/miR-200 feedback loop – a motor of cellular plasticity in development and cancer. EMBO Reports, 11(9): 670-677.

Brabletz T. (2012) miR-34 and Snail: another double-negative feedback loop controlling cellular plasticity/EMT governed by p53. Cell Cycle, 11(2): 215-216.

Breier G. (2000) Angiogenesis in embryonic development – a review. Placenta, 21(Sa): 11-15.

Breitling J. and Aebi M. (2013) N-linked protein glycosylation in the endoplasmic reticulum. Cold Spring Harbour Perspectives in Biology, 5(8): a013359.

Briggs J., Chamboredon S., Castellazzi M., Kerry J.A. and Bos T.J. (2002) Transcriptional upregulation of SPARC, in response to c-Jun overexpression, contributes to increased motility and invasion of MCF7 breast cancer cells. Oncogene, 21(46): 7077-7091.

Brodt P., Fallavollita L., Bresalier R.S., Meterissian S., Norton C.R. and Wolitzky B.A. (1997) Liver endothelial E-selectin mediates carcinoma cell adhesion and promotes liver metastasis. International Journal of Cancer, 71(4): 612-619.

Brooks S.C., Locke E.R. and Soule H.D. (1973) Estrogen receptor in a human cell line (MCF-7) from breast carcinoma. The Journal of Biological Chemistry, 248(17): 6251-6253.

Brooks S.A. and Leathem A.J. (1989) *Helix pomatia* lectin binding to metastases arising from primary carcinoma of the breast. The Journal of Pathology, 157: 164A.

Brooks S. and Leathem A. (1991) Prediction of lymph node involvement in breast cancer by detection of altered glycosylation in the primary tumour. The Lancet, 338: 71-74.

Brooks S., Leathem A., Camplejohn R. and Gregory W. (1993) Markers of prognosis – the relationship between binding of the lectin HPA and histological grade, SPF, and ploidy. Breast Cancer Research and Treatment, 25: 247-256.

Brooks S., Leathem A. and Dwek M. (1994) Altered expression of N-acetyl galactosamine glycoproteins by breast cancers. Biochemical Society Transactions, 22: 95S.

Brooks S.A., Lymboura M., Schumacher U. and Leathem A.J. (1996) Histochemistry to detect *Helix pomatia* binding in breast cancer: methodology makes a difference. The Journal of Histochemistry and Cytochemistry, 44(5): 519-524.

Brooks S. and Leathem A. (1999) Expression of N-acetyl galactosaminylated and sialylated glycans by metastases arising from primary breast cancer. Invasion and Metastasis, 18: 115-121.

Brooks S.A. (2000) The involvement of *Helix pomatia* lectin (HPA) binding N-acetylgalactosamine glycans in cancer progression. Histology and Histopathology, 15(1): 143-158.

Brooks S. and Carter, T. (2001) N-acetylgalactosamine, N-acetylglucosamine and sialic acid expression in primary breast cancers. Acta Histochamistry, 103: 37-51.

Brooks S.A., Hall D.M. and Buley I. (2001) GalNAc glycoprotein expression by breast cell lines, primary breast cancer and normal breast epithelial membrane. British Journal of Cancer, 85(7): 1014-1022.

Brooks S.A. and Hall D.M. (2002) Investigations into the potential role of aberrant N-acetylgalactosamine glycans in tumour cell interactions with basement membrane components. Clinical and Experimental Metastases, 19(6): 487-493.

Brooks S.A., Dwek M.V. and Schumacher U. (2002) *Functional and Molecular Glycobiology.* Oxford: BIOS Scientific Publishers.

Brooks S.A. and Wilkinson D. (2003) Validation of a simple avidin-biotin detection method for *Helix pomatia* lectin (HPA) binding as a prognostic marker in cancer. Acta Histochemica, 105(3): 205-212.

Brooks S., Carter T., Bennett E., Clausen H. and Mandel U. (2007) Immunolocalisation of members of the polypeptide N-acetylgalactosaminyl transferase (ppGalNAc-T) family is consistent with biologically relevant altered cell surface glycosylation in breast cancer. Acta Histochemica, 109: 273-284.

Brooks S.A., Lomax-Browne H., Kinch C., Nash G. and Kieda C. (2009) Altered cell surface glycosylation functions in mechanisms of cancer cell metastasis. Anadolu University Journal of Science and Technology, 10(1): 91-101.

Brooks S.A., Lomax-Browne H.J., Carter T.M., Kinch C.E. and Hall D.M.S. (2010) Molecular interactions in cancer cell metastasis. Acta Histochemica, 112: 3-25.

Brooks S.A. and Hall D.M.S. (2012) Lectin histochemistry to detect altered glycosylation in cells and tissues. In: Dwek M., Brooks S.A. and Schumacher U. eds. Metastasis Research Protocols, Second Edition. London: Humana Press, pp 31-50.

Buckner D., Graw R.G. Jr, Eisel R.J., Henderson E.S. and Perry S. (1969) Leukapheresis by continuous flow centrifugation (CFC) in patients with chronic myelocytic leukaemia (CML). Blood, 33: 353-369.

Bullock M.D., Sayar A.E., Packham G.K. and Mirnezami A.H. (2012) MicroRNAs: critical regulators of epithelial to mesenchymal transition (EMT) and mesenchymal to epithelial transition (MET) in cancer progression. Biology of the Cell, 104: 3-12.

Burgstaller G., Oehrle B., Koch I., Linder M. and Eickelberg O. (2013) Multiplex profiling of cellular invasion in 3D cell culture models. PLOS One, 8(5): e63121.

Burk U., Schubert J., Wellner U, Schmalhofer O., Vincan E., Spaderna S. and Brabletz T. (2008) A reciprocal repression between ZEB1 and members of the miR-200 family promotes EMT and invasion in cancer cells. EMBO Reports, 9(6): 582-589.

Burkhart D.L. and Sage J. (2008) Cellular mechanisms of tumour suppression by the retinoblastoma gene. Nature Reviews Cancer, 8(9): 671-682.

Bustin S. (2004) A-Z of quantitative PCR. IUL Biotechnology Series, International university Line, La Jolla, California.

Bustin S.A. and Mueller R. (2005) Real-time reverse transcription PCR (qRT-PCR) and its potential use in clinical diagnosis. Clinical Science, 109: 365-379.

Bustin S.A., Benes V., Garson J.A., Hellemans J., Huggett J., Kubista M., Mueller R., Nolan T., Pfaffl M.W., Shipley G.L., Vandesampele J. and Wittwer C.T. (2009) The MIQE guidelines: minimum information for publications of quantitative real-time PCR experiments. Clinical Chemistry, 55(4): 1-12.

Butkinaree C., Park K. and Hart G.W. (2010) O-linked β-N-acetylglucosamine (O-GlcNAc): extensive cross talk with phosphorylation to regulate signalling and transcription in response to nutrients and stress. Biochemica et Biophysica Acta, 1800(2): 96-106.

Butte A.J., Ye J., Niederfellner G., Rett K., Häring H.U., White M.F. and Kohane I.S. (2001) Determining significant fold differences in gene expression analysis. Pacific Symposium on Biocomputing, 6: 6-17.

C

Campbell B.J., Finnie I.A., Hainsell E.F. and Rhodes J.M. (1995) Direct demonstration of increased expression of Thomsen-Friedenreich (TF) antigen in colonic adenocarcinoma and ulcerative colitis mucin and its concealment in normal mucin. The Journal of Clinical Investigations, 95(2): 571-576.

Cancer Research UK, http://info.cancerresearchuk.org accessed on: 03.02.2016.

Cano A., Pérez-Moreno M.A., Rodrigo I., Locascio A., Blanco M.J., del Barrio M.G., Portillo F. and Nieto M.A. (2000) The transcription factor Snail controls epithelial-mesenchymal transitions by repressing E-cadherin expression. Nature Cell Biology, 2(2): 76-83.

Carmeliet P. (2005) VEGF as a key mediator of angiogenesis in cancer. Oncology, 69(53): 4-10.

Casas E., Kim J., Bendesky A., Ohno-Machado L., Wolfe C.J. and Yang J. (2011) Snail2 is an essential mediator of Twist1-induced epithelial-mesenchymal transition and metastasis. Cancer Research, 71(1): 245-254.

Cavallo F., Astolfi A., Iezzi M., Cordero F., Lollini P., Forni G. and Calogero R. (2005) An integrated approach of immunogenomics and bioinformatics to identify new tumor associated antigens (TAA) for mammary cancer immunological prevention. BMC Bioinformatics, 6: S7.

Cerio R. and MacDonald D.M. (1986) Effect of routine paraffin wax processing on cell membrane immunoreactivity in cutaneous tissue. Journal of Clinical and Laboratory Immunology, 20(2): 97-100.

Chambers A.F., Groom A.C. and MacDonald I.C. (2002) Metastasis: dissemination and growth of cancer cells at metastatic sites. Nature Reviews Cancer, 2: 563-572.

Chao Y.L., Shepard C.R. and Wells A. (2010) Breast carcinoma cells re-express E-cadherin during mesenchymal to epithelial reverting transition. Molecular Cancer, 7(9): 179 doi: 10.1186/1476-4598-9-179.

Chen R., Alvero A.B., Silasi D.A. and Mor G. (2007) Inflammation, cancer and chemoresistance: taking advantage of the toll-like receptor signalling pathway. American Journal of Reproductive Immunology, 57(2): 93-107.

Cheng L., Tachibana K., Zhang Y., Guo J.M., Kahori Tachibana K., Kameyama A., Wang H., Hiruma T., Iwasaki H., Togayama A., Kudo T. and Narimatsu H. (2002) Characterisation of a novel human UDP-GalNAc transferase, pp-GalNAc-T10. FEBS Letters, 531(2): 115-121.

Cheng L., Tachibana K., Iwasaki H., Kameyama A., Zhang Y., Kubota T., Hinima T., Tachibana K., Kudo T., Guo J.M. and Narimatsu H. (2004) Characterisation of a novel human UDP-GalNAc transferase, PP-GalNAc-T15. FEBS Letters, 566(1-3): 17-24.

Chia J., Goh G. and Bard F. (2016) Short O-GalNAc glycans: regulation and roles in tumour development and clinical perspectives. Biochemica et Biophysica Acta, 1860(8): 1623-1639.

Chomczynski P. and Sacchi N. (1987) Single-step method of RNA isolation by acid guanidinum thiocynate-phenol-chloroform extraction. Analytical Biochemistry, 162(1): 156-159.

Chomczynski P. (1993) A reagent for the single-step simultaneous isolation of RNA, DNA and proteins from cell and tissue samples. Biotechniques, 15(3): 532-534.

Clarke E., Green R.C., Green J.S., Mahoney K., Parfrey P.S., Younghusband H.B. and Woods M.O. (2012) Inherited deleterious variant in *GALNT12* are associated with CRC susceptibility. Human Mutations, 33(7): 1056-1058.

Comijn J., Berx G., Vermassen P., Verschueren K., van Grunsven L., Bruyneel E., Mereel M., Huylebroeck D. and van Roy F. (2001) The two-handed E box binding zinc finger protein SIP1 downregulates E-cadherin and induces invasion. Molecular Cell, 7(6): 1267-1278.

Cordero D.R., Brugmann S., Chu Y., Bajpai R., Jame M. and Helms J.A. (2011) Cranial neural crest cells on the move: their roles in craniofacial development. American Journal of Medical Genetics. Part A, 155A(2): 270-279.

Cummings R.D. (2009) The repertoire of glycan determinants in the human glycome. Molecular Biosystems, 5(10): 1087-1104.

D

DAVID Nature Protocols 2009; 4(1):44 & Nucleic Acids Res. 2009;37(1):1.

Davies J.A. (1996) Mesenchyme to epithelium transition during development of the mammalian kidney tubule. Acta Anatomica, 156(3): 187-201.

De Craene B. and Berx G. (2013) Regulatory networks defining EMT during cancer initiation and progression. Nature Reviews Cancer, 13(2): 97-110.

Debeir O., Van Ham P., Kiss R. and Decaestecker C. (2005) Tracking of migrating cells under phase-contrast video microscopy with combined mean-shift processes. IEEE Transactions on Medical Imaging, 24(6): 697-711.

Del Duca D., Werbowetski T. and Del Maestro R.F. (2004) Spheroid preparation from hanging drops: characterisation of a model of brain tumour invasion. Journal of Neuro-Oncology, 67(3): 295-303.

Deng C.-X. (2006) BRCA1: cell cycle checkpoint, genetic instability, DNA damage response and cancer evolution. Nucleic Acids Research, 34(5): 1416-1426.

Dennis G. Jr., Sherman B.T., Harack D.A., Yang J., Gao W., Lane H.C. and Lempicki R.A. (2003) DAVID: database for annotation, visualisation, and integrated discovery. Genome Biology, 4(9): R60.

Dewald J.H., Colomb F., Bobowski-Gerard M., Groux-Degroote S. and Delannoy P. (2016) Role of cytokine-induced glycosylation changes in regulating cell interactions and cell signalling in inflammatory diseases and cancer cells. Cells, 5(43): doi: 10.3390/cells5040043.

Diepenbruck M. and Christofori G. (2016) Epithelial-mesenchymal transition (EMT) and metastasis: yes, no, maybe? Current Opinions in Cell Biology, 43: 7-13 doi: 10.1016/j.ceb.2016.06.002.

Dimri G., Band H. and Bard V. (2005) Mammary epithelial cell transformation: insights from cell culture and mouse models. Breast Cancer Research, 7: 171-179.

Ding M., Wang H., Wang J., Zhan H., Zuo Y., Yang D., Liu J., Wang W., Ke C. and Yan R. (2012a) ppGalNAc T1 as a potential novel marker for human bladder cancer. Asian Pacific Journal of Cancer Prevention, 13: 5653-5657.

Ding Y., Gelfenbeyn K., Freire-de-Lima L., Handa K. and Hakomori S.-I. (2012b) Induction of epithelial-mesenchymal transition with O-glycosylated oncofoetal fibronectin. FEBS Letters, 586(13): 1813-1820.

DiPietro L.A. (2016) Angiogenesis and wound repair: when enough is enough. Journal of Leukocyte Biology, 100(5): 979-984.

Dodla M.C., Young A., Venable A., Hasneen K., Rao R.R., Machacek D.W. and Stice S.L. (2011) Differing lectin binding profiles among human embryonic stem cells and derivations aid in the isolation of neuronal progenitor cells. PLOS one, 6-8: e23266.

Duangkumpha K., Techasen A., Loilome W., Namwat N., Thanan R., Khuntikeo N. and Yongvanit P. (2014) BMP-7 blocks the effects of TGF-β-induced EMT in cholangio carcinoma. Tumour Biology, 35(10): 9667-9676.

Duband J.L., Monier F., Delannet M. and Newgreen D. (1995) Epithelium-mesenchyme transition during neural crest development. Acta Anatomica, 154(1): 63-78.

Duffy M. J. (1996) The biochemistry of metastasis. Advanced Clinical Chemistry, 32:135-160.

Dwek R.A. (1994) Glycobiolgy: “towards understanding the function of sugars”. Biochemical Society Transactions, 23(1): 1-25.

Dwek, M. V., Ross, H. A., Streets, A. J., Brooks, S. A., Adam, E., Titcomb, A., Woodside, J. V., Schumacher, U. and Leathem, A. J. (2001) *Helix pomatia* agglutinin lectin-binding oligosaccharides of aggressive breast cancer. International Journal of Cancer, 95(2): 79-85.

E

Eger A., Aigner K., Sonderegger S., Dampier B., Oehler S., Schreiber M., Berx G., Cano A., Beug H. and Foisner R. (2005) DeltaEF1 is a transcriptional repressor of E-cadherin and regulates epithelial plasticity in breast cancer cells. Oncogene, 24(14): 2375-2385.

Eilken H.M. and Adams R.H. (2010) Dynamics of endothelial cell behaviour in sprouting angiogenesis. Current Opinions in Cell Biology, 22: 617-625.

Engel L.W. and Young N.A. (1978) Human breast cancer cells in continuous culture: a review. Cancer Research, 38: 4327-4339.

Engel L., Young N., Tralka T., Lippman M., O’Brien S. and Jo Joyce M. (1978) Establishment and characterisation of three new continuous cell lines derived from human breast carcinomas. Cancer Research, 38: 3352-3364.

Engelhardt B. and Wolburg H. (2004) Transendothelial migration of leukocytes: through the front door or around the side of the house? European Journal of Immunology, 34: 2955-2963.

F

Falanga A., Marchetti M., Vignoli A. and Balducci D. (2003) Clotting mechanisms and cancer: implications in thrombus formation and tumour progression. Clinical Advances in Haematology and Oncology, 1(11): 673-678.

Fang X., Cai Y., Liu J., Wang Z., Wu Q., Zhang Z., Yang C.J., Yuan L. and Ouyang G. (2011) Twist2 contributes to breast cancer progression by promoting an epithelial-mesenchymal transition and cancer stem-like cell self-renewal. Oncogene, 30(47): 4707-4720.

Fardini Y., Dehennaut V., Lefebvre T. and Issad T. (2013) O-GlcNAcylation: a new cancer hallmark? Frontiers in Endocrinology, 4(99): doi: 10.3389/fendo.2013.00099.

Fedi P., Tronick S.R. and Aaronson S.A. (1997) Growth factors. In Cancer Medicine. Holland J.F., Bast R.C., Morton D.L., Frei E., Kufe D.W. and Weichselbaum R.R. (eds) Baltimore, MD: Williams and Wilkins, pp 41-64.

Fenlon, S., Ellis, I., Bell, J., Todd, J., Elston, C. and Blamey, R. (1987) *Helix pomatia* and *Ulex europeus* lectin binding in human breast carcinoma. Journal of Pathology, 52:169-176.

Fidler I.J. (2003) The pathogenesis of cancer metastasis: the “seed and soil” hypothesis revisited. Nature Reviews Cancer, 3: 1-6.

Fitchett J.E. and Hay E.D. (1989) Medial edge epithelium transforms to mesenchymal after embryonic palatal shelves fuse. Developmental Biology, 131(2): 445-474.

Folberg R., Hendrix M.J. and Maniotis A.J. (2000) Vasculogenic mimicry and tumour angiogenesis. The American Journal of Pathology, 156(2): 361-381.

Francavilla C., Maddeluno L. and Cavallaro U. (2009) The functional role of the cell adhesion molecules in tumour angiogenesis. Seminars in Cancer Biology, 19: 298-309.

Freire T. and Osinaga E. (2003) Immunological and biomedical relevance of the Tn antigen. Inmunología, 22(1): 27-38.

Freire T., Berois N., Sóñora C., Varangot M., Barrios E. and Osinaga E. (2006) UDP-*N*-acetyl-D-galactosamine:polypeptide *N*-acetylgalactosaminyltransferase 6 (ppGalNAc-T6) mRNA as a potential new marker for detection of bone marrow-disseminated breast cancer cells. International Journal of Cancer, 119: 1383-1388.

Freire-de-Lima L., Gelfenbeyn K., Ding Y., Mandel U., Clausen H., Handa K. and Hakomori S.-I. (2011) Involvement of O-glycosylation defining oncofoetal fibronectin in epithelial-mesenchymal transition process. PNAS, 108(43): 17690-17695.

Frevert C.W., Wong V.A., Goodman R.B., Goodwin R. and Martin T.R. (1998) Rapid fluorescence-based measurements of neutrophil migration *in vitro*. Journal of Immunological Methods, 213: 41-52.

Friedl P. and Wolf K. (2003) Tumour cell invasion and migration: diversity and escape mechanisms. Nature Reviews Cancer, 3: 362-374.

Friedl P. (2004) Prespecification and plasticity: shifting mechanisms of cell migration. Current Opinions in Cell Biology, 16: 14-23.

Friedl P. and Gilmour D. (2009) Collective cell migration in morphogenesis, regeneration and cancer. Nature Reviews Molecular Cell Biology, 10: 445-457.

Friedl, P. and Wolf, K. (2009) Plasticity of cell migration: a multiscale tuning model. Journal of Cell Biology, 188(1): 11-19.

Frisch S.M., Schaller M. and Cieply B. (2013) Mechanisms that link the oncogenic epithelial-mesenchymal transition to suppression of anoikis. The Journal of Cell Science, 126(1): 21-29.

Fritz T.A., Hurley J.H., Trinh L.B., Shiloach J. and Tabak L.A. (2004) The beginnings of mucin biosynthesis: the crystal structure of UDP-GalNAc: polypeptide alpha N-acetylgalactosaminyltransferase-T1. Proceeding of the National Academy of Sciences of the United States of America, 101(43): 15307-15312.

Fritz T.A., Raman J. and Tabak L.A. (2006) Dynamic association between the catalytic and lectin domains of human UDP-GalNAc: polypeptide alpha-N-acetylgalactosaminyltransferase-2. The Journal of Biological Chemistry, 281(13): 8613-8619.

Fry S.A., Sinclair J., Timms J.F., Leathem A.J. and Dwek M.V. (2013) A targeted glycoproteomics approach identifies cadherin-5 as a novel biomarker of metastatic breast cancer. Cancer Letters, 328(2): 335-344.

Fry S.A., Robertson C.E., Swann R. and Dwek M.V. (2016) Cadherin-5: a biomarker for metastatic breast cancer with optimum efficacy in oestrogen receptor-positive breast cancers with vascular invasion. British Journal of Cancer, 114(9): 1019-1026.

Fukutomi T., Itsabashi M., Tsuane S., Yamamoto H., Nanasawa T. and Hiroto T. (1989) Prognostic contributions of *Helix pomatia* and carcinoembryonic antigen staining using histochemical techniques in breast carcinomas. Japanese Journal for Clinical Oncology, 19: 127-134.

Fukutomi T., Hiohashi S., Tsuda H., Nanasawa T., Yamamoto H., Itabashi M. and Shimosato Y. (1991) The prognostic value of tumour-associated carbohydrate structures correlated with gene amplifications in human breast carcinomas. The Japanese Journal of Surgery, 21(5): 499-507.

Functional Glycomics Gateway: http://www.functionalglycomics.org/.

G

Gao Y., Wells L., Comer F.I., Parker G.J. and Hart G.W. (2001) Dynamic O-glycosylation of nuclear and cytosolic proteins: cloning and characterisation of a neutral, cytosolic β-N-acetylglucosaminidase from human brain. The Journal of Biological Chemistry, 276(13): 9838-9845.

Gao Y., Liu Z., Feng J., Sun Q., Zhang B., Zheng W. and Ma W. (2013) Expression pattern of polypeptide N-acetylgalactosaminyltransferase-10 in gastric carcinoma. Oncology Letters, 5: 113-116.

Gaziel-Sovran A., Segura M.F., Di Micco R., Collins M.K., Hanniford D., Vega-Saenz de Miera M.K., Rakus J.F., Dankert J.F., Shang S., Kerbel R.S., Bhardwaj N., Shao Y., Darvishian F., Zavadil J., Erlebacher A., Mahal L.K., Osmann I. and Hernando E. (2011) miR-30b/30d regulation of GalNAc transferases enhances invasion and immunosuppression during metastasis. Cancer Cell, 20(1): 104-118.

Geraghty R.J., Capes-Davis J.M., Downward J., Freshney R.I., Knezevic I., Loveu-Badge R., Masters J.R., Meredith J., Stacey G.N., Thraves P., Vias M. and Cancer Research U.K. (2014) Guidelines for the use of cell lines in biomedical research. British Journal of Cancer, 111(6): 1021-1046.

Gerhardt H., Golding M., Fruttiger M., Ruhrberg C., Lundkvist A., Abramsson A., Jeltsch M., Mitchell C., Alitalo K., Shima D. and Betsholtz C. (2003) VEGF guides angiogenic sprouting utilising endothelial tip cell filopodia. The Journal of Cell Biology, 161(6): 1163-1177.

Germanov E., Berman J. and Guernsey D. (2006) Current and future approaches for the therapeutic targeting of metastasis. International Journal of Molecular Medicine, 18: 2025-2036.

Ghazarian H., Idoni B. and Oppenheimer S.B. (2011) A glycobiology review: carbohydrates, lectins and implications in cancer therapeutics. Acta Histochemica, 113: 236-247.

Gianni L., Eiermann W., Semiglazov V., Manikhas A., Luich A., Tjulandin S., Zambetti M., Vazguez F., Byakhow M., Climent M.A., Ciruelos E., Ojeda B., Mansutti M., Bozhok A., Baronio R., Feyereislova A., Barton C., Valegussa P. and Baselga J. (2010) Neoadjuvent chemotherapy with trastuzumab followed by adjuvant trastuzumab versus neoadjuvant chemotherapy alone, in patients with HER-2 positive locally advanced breast cancer (the NOAH trial): a randomized controlled superiority trial with parallel HER-2 negative cohort. Lancet, 375(9712): 377-384.

Gianni-Barrera R., Bartolomeo M., Vollmar B., Djonov V. and Banfi A. (2014) Split for the cure: VEGF, PDGF-BB and intussusception in therapeutic angiogenesis. Biochemical Society Transactions, 42(6): 1637-1642.

Gibson T.M., Wang S.S., Cerhan J.R., Maurer M.J., Hartge P., Habermann T.M., Davis S., Cozen W., Lynch C.F., Severson R.K., Rothman N., Chanock S.J. and Morton L.M. (2012) Inherited genetic variation and overall survival following follicular lymphoma. American Journal of Hematology, 1: 724-726.

Gill D.J., Chia J., Senewiratne J. and Bard J. (2010) Regulation of O-glycosylation through Golgi-to-ER relocation of initiation enzymes. The Journal of Cell Biology, 189(5): 843-858.

Gill D.J., Clausen H. and Bard F. (2011) Location, location, location: new insights into O-GalNAc protein glycosylation. Trends in Cell Biology, 21(3): 149-158.

Gilles C., Bassuk J.A., Pulyaeva H., Sage E.H., Foidart J.-M. and Thompson E.W. (1998) SPARC/osteonectin induces matrix metalloproteinase 2 activation in human breast cancer cell lines. Cancer Research, 58(23): 5529-5536.

Glinskii O.V., Huxley V.H., Glinsky G.V., Pienta K.J., Ras A. and Glinsky V. (2005) Mechanical entrapment is insufficient and intracellular adhesion is essential for metastatic cell arrest in distant organs. Neoplasia, 7(5): 522-527.

Glinsky V.V., Huflejt M.E., Glinsky G.V., Deutscher S.L. and Quinn T.P. (2000) Effects of Thomsen-Friedenreich antigen-specific peptide P-30 on β-galactoside-mediated homotypic aggregation and adhesion to the endothelium of MDA-MB-435 human breast carcinoma cells. Cancer Research, 60: 2584-2588.

Glinsky V.V., Glinsky G.V., Rittenhouse-Olson K., Huflejt M.E., Glinskii O.V., Deutscher S.L. and Quinn T.P. (2001) The role of Thomson-Friedenreich antigen in adhesion of human breast and prostate cancer cells to the endothelium. Cancer Research, 61: 4851-4857.

Gnemmi V., Bouillez A., Gaudelot K., Hémon B., Ringot B., Pottier N., Glowacki F., Villers A., Vindrieux D., Cauffiez C., Van Seuningen I., Bernard D., Leroy X., Aubert S. and Perrais M. (2014) MUC1 drives epithelial-mesenchymal transition in renal carcinoma through Wnt/β-catenin pathway and interaction with Snail promoter. Cancer Letters, 346: 225-236.

Goldstein I.J., Hughes R.C., Monsigny M., Osawa T. and Sharon N. (1980) What should be called a lectin? Nature, 285: 66.

Goldstein I.J. and Poretz R.D. (1986) Isolation, physicochemical characterisation, and carbohydrate-binding specificity of lectin. In: Liener I.E., Sharon N. and Goldstein I.J. eds. The Lectins: properties, functions, and applications in biology and medicine. London: Academic Press Inc, pp 35-209.

Gray-McGuire C., Guda K., Adrianto I., Lin C.P., Natale L., Potter J.D., Newcomb P., Poole E.M., Ulrich C.M., Lindor N., Goode E.L., Fridley B.L., Jenkins R., Le Marchand L., Casey G., Haile R., Hopper J., Jenkins M., Young J., Buchanan D., Gallinger S., Adams M., Lewis S., Willis J., Elston R., Markowitz S.D. and Wiesner G.L. (2010) Cancer Research, 70(13): 5409-5418.

Gravdal K., Halvorsen O.J., Haukas S.A. and Akslen L.A. (2007) A switch from E-cadherin to N-cadherin expression indicates epithelial to mesenchymal transition and is of strong and independent importance for the progress of prostate cancer. Clinical Cancer Research, 13(23): 7003-7011.

Greene H.S.N. and Harvey E.K. (1964) The relationship between the dissemination of tumor cells and the distribution of metastases. Cancer Research, 24: 799-811.

Greenburg G. and Hay E.D. (1982) Epithelia suspended in collagen gels can lose polarity and express characteristics of migrating mesenchymal cells. The Journal of Cell Biology, 95: 333-339.

Grivennikov S.I., Greten F.R. and Karin M. (2010) Immunity, inflammation, and cancer. Cell, 140: 883-899.

Gronthos S., Mankani M., Brahim J., Robey G. and Shi S. (2000) Postnatal human dental pulp stem cells (DPSCs) *in vitro* and *in vivo*. PNAS, 97(25): 13625-13630.

Gu C., Oyama T., Osaki T., Li J., Takenoyama M., Izumi H., Sugio K., Kohno K and Yasumoto K. (2004) Low expression of polypeptide GalNAc *N*-acetylgalactosaminyl transferase-3 in lung adenocarcinoma: impact on poor prognosis and early recurrence. British Journal of Cancer, 90: 436-442.

Guda K, Moinova H., He J., Jamison O., Ravi L., Natale L., Lutterbaugh J., Lawrence E., Lewis S., Willson J.K.V., Lowe J.B., Wiesner G.L., Parmigiani G., Barnholtz-Sloan J., Dawson D.W., Velculescu V.E., Kinzler K.W., Papadopoulos N., Vogelstein B., Willis J., Gerken T.A. and Markowitz S.D. (2009) Inactivating germ-line and somatic mutations in polypeptide *N*-acetylgalactosaminyltransferase 12 in human colon cancers. PNAS, 106(31): 12921-12925.

Gunasinghe N.P., Wells A., Thompson E.W. and Hugo H.J. (2012) Mesenchymal-epithelial transition (MET) as a mechanism for metastatic colonisation in breast cancer. Cancer Metastasis Reviews, 31(2-4): 469-478.

Guo J.M., Zhang Y., Cheng L., Iwasaki H., Wang H., Kubota T., Tachibana K. and Narimatsu H. (2002) Molecular cloning and characterisation of a novel member of the UDP-GalNAc:polypeptide N-acetylgalactosaminyltransferase family, pp-GalNAc-T12. FEBS Letters, 524(1-3): 211-218.

Guo J., Chen H., Wang G., Zhang Y. and Narimatsu H. (2004) Expression of UDP-GalNAc:polypeptide N-acetylgalactosaminyltrnasferase-12 in gastric and colonic cancer cell lines and in human colorectal cancer. Oncology, 67: 271-276.

Guo Y., Yin J., Zha L. and Wang Z. (2013) Clinicopathological significance of platelet-derived growth factor B, platelet-derived growth factor receptor-β, and E-cadherin expression in gastric carcinoma. Contemporary Oncology, 17(2): 150-155.

Guo G., Gong K., Wohlfeld B., Hatanpaa K.J., Zhao D. and Habib A.A. (2015) Ligand-independent EGFR signalling. Cancer Research, 75(17): 3436-3441.

Gur-Dedeoglu B., Konu O., Bozkurt B., Ergul G., Seckin S. and Yulug I.G. (2009) Identification of endogenous reference genes for qRT-PCR analysis in normal match beast tumour tissues. Oncology Research, 17(8): 353-365.

Gusterson B.A. and the International (Ludwig) Breast Cancer Study Group. (1993) Prognostic value of *Helix pomatia* in breast cancer. British Journal of Cancer, 68(1): 146-150.

H

Hajra K.M., Chen D.Y.-S. and Fearon E.R. (2002) The SLUG zinc-finger protein represses E-cadherin in breast cancer. Cancer Research, 62(6): 1613-1618.

Haltiwanger R.S., Holt G.D. and Hart G.W. (1990) Enzymatic addition of O-GlcNAc to nuclear and cytoplasmic proteins: identification of a uridine diphospho-N-acetylglucosamine: polypeptide β-N-acetylglucosaminyl transferase. The Journal of Biological Chemistry, 265(5): 2563-2568.

Hang H. and Bertozzi C. (2005) The chemistry and biology of mucin-type O-linked glycosylation. Bioorganic and Molecular Chemistry, 13: 5021-5034.

Hanover J.A., Krause M.W. and Love D.C. (2010) The hexosamine signalling pathway: O-GlcNAc cycling in feast or famine. Biochemica et Biophysica Acta, 1800(20): 80-95.

Hansen R.K. and Bissel M.J. (2000) Tissue architecture and breast cancer: the role of extracellular matrix and steroid hormones. Endocrine-Related Cancers, 7: 95-113.

Harisi R., Kenessey I., Olah J.N., Timar F., Babo I., Pogany G., Paku S. and Jeney A. (2009) Differential inhibition of single and cluster type tumour migration. Anticancer Research, 29(8): 2981-2985.

Hart G.W., Housley M.P. and Slawson C. (2007) Cycling of O-linked β-N-acetylglucosamine on nucleocytoplasmic proteins. Nature, 446: 1017-1022.

Hatterman K., Held-Feindt J. and Mentlein R. (2011) Spheroid confrontation assay: a simple method to mimic the three-dimensional migration of different cell types *in vitro*. Annals of Anatomy, 193(3): 181-184.

Hay E.D. (1995) An overview of epithelial-mesenchymal transformation. Acta Anatomica, 154(1): 8-20.

Hazes B. (1996) The (QxW)3 domain: a flexible lectin scaffold. Protein Science, 5(8): 1490-1501.

Heerboth S., Housman G., Leary M., Longacre M., Byler S., Lapinska K., Willbanks A. and Sarkar S. (2015) EMT and tumour metastasis. Clinical and Translational Medicine, 4(6) doi: 10.1186/540169-015-0048-3.

Hendrix M.J., Seftor E.A., Hess A.R. and Seftor R.E. (2003) Vasculogenic mimicry and tumour-cell plasticity: lessons from melanoma. Nature Reviews Cancer, 3(6): 411-421.

Herr P., Korniychuk G., Yamamoto Y., Grubisic K. and Oelgeschläger M. (2008) Regulation of TGF-β signalling by N-acetylgalactosaminyltransferase-like 1. Development, 135(10): 1813-1822.

Herzenberg L.A., Parks P., Sahaf B., Perez O., Roederer M. and Herzenberg L.A. (2002) The history and future of the fluorescence activated cell sorter and flow cytometry: a view from Stanford. Clinical Chemistry, 48(10): 1819-1827.

Hess K.R., Varadhadary G.R., Taylor S.H., Wei W., Raber M.N., Lenzi R. and Abbruzzese J.L. (2006) Metastatic patterns in adenocarcinoma. Cancer, 106(7): 1624-1633.

Hidaka C. and Mitsui S (2015) N-glycosylation modulates filopodia-like protrusions induced by sez-6 through regulating the distribution of this protein on the cell surface. Biochemical and Biophysical Research Communication, 462(4): 346-351.

Hillen F. and Griffioen A.W. (2007) Tumour vascularisation: sprouting angiogenesis and beyond. Cancer Metastasis Reviews, 26: 489-502.

Hofmann, B. T., Schlüter, L., Lange, P., Mercanoglu, B., Ewald, F., Fölster, A., Picksak, A. S., Harder, S., El Gammal, A. T., Grupp, K., Güngör, C., Drenckhan, A., Schlüter, H., Wagener, C., Izbicki, J. R., Jücker, M., Bockhorn, M. and Wolters-Eisfeld, G. (2015) *COSMC* knockdown mediated aberrant O-glycosylation promotes oncogenic properties in pancreatic cancer. Molecular Cancer, 14: 109. doi: 10.1186/s12943-015-0386-1.

Holt G.D. and Hart G.W. (1986) The subcellular distribution of terminal N-acetylglucosamine moieties: location of a novel protein-saccharide linkage, O-linked GlcNAc. The Journal of Biological Chemistry, 261(17): 8049-8057.

Homa F.L., Hollander T., Lehman D.J., Thomsen D.R. and Elhammer A.P. (1993) Isolation and expression of a cDNA clone encoding a bovine UDP-GalNAc: polypeptide N-acetylgalactosaminyltransferase. The Journal of Biological Chemistry, 268(17): 12609-12616.

Howell A. and Wardley A.M. (2005) Overview of the impact of conventional systemic therapies on breast cancer. Endocrine-related Cancer, 12 (Suppl 1): S9-S16.

Huang Z., Fasco M.J. and Kaminsky L.S. (1996) Optimisation of Dnase I for removal of contaminating DNA from RNA for use in quantitative RNA-PCR. Biotechniques, 20(6): 1012-1014.

Huanna T., Tao Z., Xiangfei W., Longfei A., Yuanyuan X., Jianhua W., Cuifang Z., Manjing J., Wenjing C., Shaochuan Q., Feifei X., Naikang L., Jinchao Z. and Chen W. (2015) GALNT14 mediates tumour invasion and metastasis in breast cancer cell line MCF7. Molecular Carcinogenesis, 54(10): 1159-1171.

I

Ikeda Y., Mori M., Adachi Y., Matsushima T. and Sugimachi K. (1994) Prognostic value of the histochemical expression of *Helix pomatia* agglutinin in advanced colorectal cancer: a univariate and multivariate analysis. Diseases of the Colon and Rectum, 37(2): 181-184.

Imberty A., Piller V., Piller F. and Breton C. (1997) Fold recognition and molecular modelling of a lectin-like domain in UDP-GalNAc:polypeptide N-acetylgalactosaminyltransferases. Protein Engineering, 10(12): 1353-1356.

Iorns E., Drews-Elger K., Ward T.M., Dean S., Clarke J., Berry D., El Ashy D and Lippman M. (2012) A new mouse model for the study of human breast cancer metastasis. Plos On, 7(10): e47995.

Ishikawa M., Kitayama J., Kohno K. and Nagawa H. (2005) The expression pattern of UDP-N-acetyl-α-D-galactosamine-polypeptide N-acetyl-galactosaminyl transferase-3 in squamous cell carcinoma of the oesophagus. Pathobiology, 72: 139-145.

Iyer S.P.N., Akimoto Y. and Hart G.W. (2003) Identification and cloning of a novel family of coiled-coil domain proteins that interact with O-GlcNAc transferase. The Journal of Biological Chemistry, 287(7): 5399-5409.

J

Jiang J., Tang Y.L. and Liang X.H. (2011) EMT: a new vision of hypoxia promoting cancer progression. Cancer Biology and Therapy, 11(8): 714-723.

Jing Y., Han Z., Zhang S., Liu Y. and Wei L. (2011) Epithelial-mesenchymal transition in tumour microenvironment. Cell and Bioscience, 1: 29 doi: 10.1186/2045-3701-1-29.

Jones R.G. and Thompson C.B. (2009) Tumour suppressors and cell metabolism: a recipe for cancer growth. Genes and Development, 23: 537-548.

Ju T., Aryal R.P., Stowell C.J. and Cummings R.D. (2008a) Regulation of protein O-glycosylation by the endoplasmic reticulum-localised molecular chaperone Cosmc. The Journal of Cell Biology, 182(3): 531-542.

Ju, T., Lanneau, G. S., Gautam, T., Wang, Y., Xia, B., Stowell, S. R., Willard, M. T., Wang, W., Xia, J. Y., Zuna, R. E., Laszik, Z., Benbrook, D. M., Hanigan, M. H. and Cummings, R. D. (2008b) Human tumor antigens Tn and Sialyl Tn arise from mutations in *Cosmc*. Cancer Research, 68(6): 1636-1646.

Ju T., Otto V.I. and Cummings R.D. (2011) The Tn antigen-structural simplicity and biological complexity. Angewandte Chemie International Edition, 50(8): 1770-1791.

Ju T., Aryal R.P., Kudelka M.R., Wang Y. and Cummings R.D. (2014) The *Cosmc* connection to the Tn antigen in cancer. Cancer Biomarkers, 14(1): 63-81.

Julien S., Puig I., Caretti E., Bonaventure J., Nelles L., van Roy F., Dargemont C., de Herreros A.G., Bellacosa A. and Larue L. (2007) Activation of NF-κB by Akt upregulates Snail expression and induces epithelium mesenchyme transition. Oncogene, 26(53): 7445-7456.

Julien S., Videira P.A. and Delannoy P. (2012) Sialyl-Tn in cancer: (how) did we miss the target? Biomolecules, 2(4): 435-466.

Juntilla M.R. and Evan G.I. (2009) p53 – a Jack of all trades but master of none. Nature Reviews Cancer, 9: 821-829.

Justus C.R., Leffler N., Ruiz-Echevarria M. and Yang C.V. (2014) *In vitro* cell migration and invasion assays. Journal of Visualised Experiments, 88: e51046.

K

Kakeji Y., Tsujitani S., Mori M., Maehara Y. and Sugimachi K. (1991) *Helix pomatia* agglutinin binding activity is a predictor of survival time for patients with gastric carcinoma. Cancer, 68(11): 2438-2442.

Kakeji Y., Maehara Y., Tsujitani S., Baba H., Ohno S., Watanabe A. and Sugimachi K. (1994) *Helix pomatia* agglutinin binding activity and lymph node metastasis in patients with gastric cancer. Seminars in Surgical Oncology, 10(2): 130-134.

Kalluri R. and Neilson E.G. (2003) Epithelial-mesenchymal transition and its implications for fibrosis. The Journal of Clinical Investigation, 112(12): 1776-1784.

Kalluri R. and Weinberg R.A. (2009) The basics of epithelial-mesenchymal transition. The Journal of Clinical Investigation, 119(6): 1420-1428.

Kam Y., Guess C., Estrada L., Weidau B. and Quaranta V. (2005) A novel circular invasion assay mimics *in vivo* invasive behaviour of cancer cell lines and distinguishes single-cell motility *in vitro*. BMC Cancer, 8(198): doi: 10.1186/1471-2407-8-198.

Kanada M., Zhang J., Yan L., Sakurai T. and Terakawa S. (2014) Endothelial cell-initiated extravasation of cancer cells visualized in zebrafish. PeerJ 2: e688, https://dx.doi.org/10.7717/peerj.688.

Kannagi R., Izawa M., Koike T., Miyazaki K. and Kimura N. (2004) Carbohydrate-mediated cell adhesion in cancer metastasis and angiogenesis. Cancer Science, 95(5): 377-384.

Kannagi R., Izawa M., Koike T., Miyazaki K. and Kimura N. (2005) Carbohydrate-mediated cell adhesion in cancer metastasis and angiogenesis. Cancer Science, 95(5): 377-384.

Karnoub A.E. and Weinberg R.A. (2006-2007) Chemokine networks and breast cancer metastasis. Breast Disease, 26: 75-85.

Kato K. and Radbruch A. (1992) Isolation and characterisation of $CD34^{+}$ hematopoietic stem cells from human peripheral blood by high-gradient magnetic cell sorting. Cytometry, 14(4): 384-392.

Katsuno Y., Lamouille S. and Derynck R. (2013) TGF-β signalling and epithelial-mesenchymal transition in cancer progression. Current Opinions in Oncology, 25(1): 76-84.

Kawai T., Suzuki M., Torikata C. and Suzuki Y. (1991) Expression of blood group-related antigens and *Helix pomatia* agglutinin in malignant pleural mesothelioma and pulmonary adenocarcinoma. Human Pathology, 22(2): 118-124.

Kelly W.G., Dahmus M.E. and Hart G.W. (1993) RNA polymerase II is a glycoprotein: modification of the COOH- terminal domain by O-GlcNAc. The Journal of Biological Chemistry, 268(14): 10416-10424.

Khatib A.M., Fallavollita L., Wancewicz E.V., Monia B.P. and Brodt P. (2002) Inhibition of hepatic endothelial E-selectin expression by c-raf antisense oligonucleotides blocks colorectal carcinoma liver metastasis. Cancer Research, 62(19): 5393-5398.

Kimelman D. (2006) Mesoderm induction: from caps to chips. Nature Reviews Genetics, 7(5): 360-372.

Kimura R., Kasamatsu A., Koyama T., Fukumoto C., Shiiba M., Tanzawa H. and Uzawa K. (2013) Glutamate acid decarboxylase 1 promotes metastasis of human oral cancer by β-catenin translocation and MMP7 activation. BMC Cancer, 13(555): DOI: 10.1186/1471-2407-13.

Klonowski K.D., Williams K.J., Marzo A.L., Blair D.A., Lingenheld E.G. and Lefrançois L. (2004) Dynamics of blood-borne CD8 memory T cell migration *in vivo*. Immunity, 20(5): 551-562.

Kobayashi K., Matsumoto S., Morishima T., Kawabe T. and Okamoto T. (2000) Cimetidine inhibits cancer cell adhesion to endothelial cells and prevents metastasis by blocking E-selectin expression. Cancer Research, 60(14): 3978-3984.

Kohsaki T., Nishimori I., Nakayama H., Miyazaki E., Enzan H., Nomoto M., Hollingsworth M.A. and Onishi S. (2000) Expression of UDP-GalNAc: polypeptide *N*-acetylgalactosaminyltransferase isozymes T1 and T2 in human colorectal cancer. Journal of Gastroenterology, 35: 840-848.

Kokkinos M.I., Wafai R., Wong M.K., Newgreen D.F., Thompson E.W. and Waltham M. (2007) Vimentin and epithelial-mesenchymal transition in human breast cancer-observations *in vitro* and *in vivo*. Cells, Tissues, Organs, 185(1-3): 191-203.

Kong D., Wang Z., Sarkar S.H., Li Y., Banerjee S., Saliganan A., Kim H.R., Cher M.L. and Sarkar F.H. (2008) Platelet-derived growth factor-D overexpression contributes to epithelial-mesenchymal transition of PC3 prostate cancer cells. Stem Cells, 26(6): 1425-1435.

Korpal M., Lee E.S., Hu G. and Kang Y. (2008) The miR-200 family inhibits epithelial-mesenchymal transition and cancer cell migration by direct targeting of E-cadherin transcriptional repressors ZEB1 and ZEB2. The Journal of Biological Chemistry, 283: 14910-14914.

Kopparapu P.K., Boorjian S.A., Robinson B.D., Downer M., Gudas L.J., Mongan N.P. and Persson J.L. (2013) Expression of VEGF and its receptors VEGFR1/VEGFR2 is associated with invasiveness of bladder cancer. Anticancer Research, 33(6): 2381-2390.

Koyanagi K., Bilchik A.J., Saha S., Turner R.R., Wiese D., McCarter M., Shen P., Deacon L., Elashoff D. and Hoon D.S.B. (2008) Prognostic relevance of occult nodal micrometastases and circulating tumour cells in colorectal cancer in a prospective multicenter trial. Clinical Cancer Research., 14(22): 7391-7396.

Kramer N., Walzl A., Unger C., Rosner M., Krupitza G., Hengstschläger M and Dolznig H. (2013) *In vitro* cell migration and invasion assays. Mutation Research, 752: 10-24.

Kubo F., Takeichi M. and Nakagawa S. (2005) WNT2B inhibits differentiation of retinal progenitor cells in the absence of Notch activity by down regulating the expression of proneural genes. Development, 132(12): 2759-2770.

Kubota T., Shiba T., Sugioka S., Furukawa S., Sawaki H., Kato R., Wakatsuki S. and Narimatsu H. (2006) Structural basis of carbohydrate transfer activity by human UDP-GalNAc:polypeptide alpha-N-acetylgalactosaminyltransferase (pp-GalNAc-T10). Journal of Molecular Biology, 359(3): 708-727.

Kumar A. and Srivastava A. (2010) Cell separation using cryogel-based affinity chromatography. Nature Protocols, 5(11): 1737-1747.

Kurella M., Hsiao L.-L., Yoshida T., Randell J.D., Chow G., Sarang S.S., Jensen R.V. and Gullans S.R. (2001) DNA microarray analysis of complex biological processes. Journal of the American Society of Nephrology, 12(5): 1072-1078.

Kurkon T., Liu Z., Paradkar A.V., Vaiana C.A., Koppolu S., Agrawar P. and Mahal L.K. (2015) miRNA proxy approach reveals hidden functions of glycosylation. PNAS, 112(23): 7327-7332.

L

Laack E., Nikbakht H., Peters A., Kugler C., Jasiewicz Y., Edler L., Hossfeld D.K. and Schumacher U. (2002) Lectin histochemistry of resected adenocarcinoma of the lung: Helix pomatia agglutinin binding is an independent prognostic factor. American Journal of Pathology, 160(3): 1001-1008.

Lacroix M. (2007) Persistent use of “false” cell lines. International Journal of Cancer, 122(1): 1-4.

Laczy B., Hiu B.G., Wang K., Paterson A.J., White C.R., Xing D., Chen Y.F., Darley-Usmar V., Oparil S. and Chatham J.C. (2009) Protein O-GlcNAcylation: a new signalling paradigm for the cardiovascular system. American Journal of Physiology, 296(1): H13-28.

Lamouille S., Xu J. and Derynck R. (2014) Molecular Mechanisms of epithelial-mesenchymal transition. Nature Reviews Molecular Cell Biology, 15(3): 178-196.

Landers K.A., Burger M.J., Tebay M.A., Purdie D.M., Scells B., Samaratunga H., Lavin M.F. and Gardiner R.A. (2005) Use of multiple biomarkers for a molecular diagnosis of prostate cancer. International Journal of Cancer, 114: 950-956.

Lane W.O., Jantzen A.E., Carlon T.A., Jamlo I., Kowski R.M., Grenet J.E., Ley M.M., Haseltine J.M., Galinat L.J., Lin F.-H., Allen J.D., Truskey G.A. and Achneck H.E. (2012) Parallel-plate flow chamber and continuous flow circuit to evaluate endothelial progenitor cells under laminar flow shear stress. Journal of Visualised Experiments, 59: e3349.

Lange-Consiglio A., Accogli G., Gremonesi F. and Desantis S. (2014) Cell surface glycan changes in the spontaneous epithelial-mesenchymal transition of equine amniotic multipotent progenitor cells. Cells, Tissues, Organs, 200(3-4): 212-226.

Langkilde N.C., Wolf H., Clausen H. and Orntoft T.F. (1992) Human urinary bladder carcinoma glycoconjugates expressing T- (Gal beta(1-3)GalNAc alpha 1-O-R) and T-like antigens: a comparative study using peanut agglutinin and poly- and monoclonal antibodies. Cancer Research, 52(18): 5030-5036.

Lasfargues E., Coutinho W. and Redfield E. (1978) Isolation of two human tumour epithelial cell lines from solid breast carcinomas. Journal of the National Cancer Institute, 61(4): 967-978.

Lauffenburger D.A. and Horwitz A.F. (1996) Cell migration: a physically integrated molecular process. Cell, 84: 359-369.

Lawrence M.B. and Springer T.A. (1991) Leukocytes roll on a selectin at physiologic flow rates: distinction from and prerequisite for adhesion through integrins. Cell, 65: 859-873.

Lawrence M.B., Kansas G.S., Kunkel E.J. and Ley K. (1997) Threshold levels of fluid shear promote leukocyte adhesion through selectins (CD63L,P,E). The Journal of Cell Biology, 136(3): 717-727.

Lazarus B.D., Love D.C. and Hanover J.A. (2009) O-GlcNAc cycling: implications for neurodegenerative disorders. The International Journal of Biochemistry and Cell Biology, 41(11): 2134-2146.

Leathem, A. and Brooks, S. (1987) Predictive value of lectin binding on breast-cancer recurrence and survival. The Lancet, 1(8541): 1054-1056.

Lee J.M., Dedhar S., Kalluri R. and Thompson E.W. (2006a) The epithelial-mesenchymal transition: new insights in signalling, development, and disease. Journal of Cell Biology, 172(7): 973-981.

Lee T.K., Poon R.T., Yuan A.P., Ling M.T., Kwok W.K., Wang X.H., Wong Y.C., Guan X.Y., Man K., Chau K.L. and Fan S.T. (2006b) TWIST overexpression correlates with hepatocellular carcinoma metastasis through induction of epithelial-mesenchymal transition. Clinical Cancer Research, 12(18): 5369-5376.

Lee Y.-H., Albig A.R., Regner M.-A., Schiemann B.J. and Schiemann W.P. (2008) Fibulin-5 initiates epithelial-mesenchymal transition (EMT) and enhances EMT induced by TGF-β in mammary epithelial cells via a MMP-dependant mechanism. Carcinogenesis, 29(12): 2243-2251.

Lee E.Y.H.P. and Muller W.J. (2010) Oncogenes and tumour suppressor genes. Cold Spring Harbour Perspectives in Biology, 2: a003236.

Lehnus K.S., Donovan L., Huang X., Zhao N., Warr T.J., Pilkington G.J. and An Q. (2013) CD133 glycosylation is enhanced by hypoxia in cultured glioma stem cells. International Journal of Oncology, 42: 1011-1017.

Leong H.S., Robertson A.E., Stoletov K., Leith S.J., Chin C.A., Chien A.E., Hague M.N., Ablack A., Carmine-Simmen K., McIherson V.A., Postenka C.O., Turley E.A., Courtreidge S.A., Chambers A.F. and Lewis J.D. (2014) Invadopodia are required for cancer cell extravasation and are a therapeutic target for metastasis. Cell Reports, 8: 1558-1570.

Lescar J., Sanchez J.-F., Audfray A., Coll J.-L., Breton C., Mitchel E.P. and Imberty A. (2007) Structural basis for recognition of breast and colon cancer epitopes Tn antigen and Forssman disaccharide by *Helix pomatia* lectin. Glycobiology, 17(10): 1077-1083.

Li G., Satyamoorthy K. and Herlyn M. (2001) N-cadherin-mediated intracellular interactions promotes survival and migration of melanoma cells. Cancer Research, 61: 3819-3825.

Li Z., Yamada S., Inenaga S., Imamura T., Wu Y., Wang K-Y., Shimajiri S., Nakano R., Izumi H., Kohno K. and Sasaguri Y. (2011) Polypeptide *N*-acetylgalactosaminyltransferase 6 expression in pancreatic cancer is an independent prognostic factor indicating better overall survival. British Cancer Journal, 104: 1882-18.

Li X., Wang J., Li W., Xu Y., Shao D., Xie Y., Xie W., Kubota T., Narimatsu H. and Zhang Y. (2012) Characterisation of ppGalNAc-T18, a member of the vertebrate-specific Y subfamily of UDP-*N*-acetyl-α-D-galactosamine:polypeptide *N*-acetylgalactosaminyltransferases. Glycobiology, 22(5): 602-615.

Liao D. and Johnson R.S. (2007) Hypoxia: a key regulator of angiogenesis in cancer. Cancer and Metastasis Reviews, 26: 281-290.

Lim S.O., Kim H. and Jung G. (2010) p53 inhibits tumour cell invasion via the degradation of Snail protein in hepatocellular carcinoma. FEBS Letters, 584(11): 2231-2236.

Linder S. (2009) Invadosomes at a glance. Journal of Cell Science, 122(17): 3009-3013.

Liotta L.A. (1984) Tumour invasion and metastasis: role of the basement membrane. Warner-Lambert Parke-Davis award lecture. The American Journal of Pathology, 117(3): 339-348.

Liotta L. (1986) Tumor invasion and metastasis – role of the extracellular matrix: Rhodes memorial award lecture. Cancer Research, 46: 1-7.

Liotta L. and Stetler-Stevenson W. (1991) Tumour invasion and metastasis: an imbalance of positive and negative regulation. Cancer Research, 51: 5054s-5059s.

Liscovitch M. and Ravid D. (2007) A case study in misidentification of cancer cell lines: MCF7/AdrR (re-designated NCI/ADR-RES) are derived from OVCAR-8 human ovarian carcinoma cells. Cancer Letters, 245(1-2): 350-352.

Lis J.G. and Osgood E.E. (1949) A method for the rapid separation of leukocytes and nucleated erythrocytes from blood or marrow with a phytohemagglutinin for red beans (*Phaseolus vulgaris*).Blood, 4(5): 670-675.

Lo H.W., Hsu S.C., Xia W., Cao X., Shin J.Y., Wei Y., Abbruzzese J.L., Hortobagyi G.N. and Hung M.C. (2007) Epidermal growth factor receptor cooperates with signal transducer and activator of transcription 3 to induce epithelial-mesenchymal transition in cancer cells via up-regulation of TWIST gene expression. Cancer Research, 67(19): 9066-9076.

Lomax-Browne H.J. (2009) Interactions between cancer cell glycans and endothelial cells during adhesion and transmigration events in metastasis. PhD thesis, Oxford Brookes University.

López-Novoa J.M. and Nieto M.A. (2009) Inflammation and EMT: an alliance towards organ fibrosis and cancer progression. EMBO Molecular Medicine, 1 (6-7): 305-314.

Lowe D.J. and Ray K. (2015) Quantitation of endothelial cell adhesiveness *in vitro*. Journal of Visualised Experiments, 100: e52924.

Lu M., Jolly M.K., Levine H., Onuchic J.N., Ben-Jacob E. (2013) MicroRNA-based regulation of epithelial-hybrid-mesenchymal fate determination. PNAS, 110(45): 18144-18149.

Lynch T.P., Ferrer C.M., RaElle Jackson S., Shahriari K.S., Vosseller K. and Reginato M.J. (2012) Critical role of O-linked β-N-acetylglucosamine transferase in prostate cancer invasion, angiogenesis, and metastasis. The Journal of Biological Chemistry, 287: 11070-11081.

M

Ma J. and Hart G.W. (2013) Protein O-GlcNAcylation in diabetes and diabetic complications. Expert Review of Proteomics, 10(4): 365-380.

MacCallum R.M., Martin A.C.R. and Thornton J.M. (1996) Antibody-antigen interactions: contact analysis and binding site topography. Journal of Molecular Biology, 5(11): 732-745.

Mahara A. and Yamaoka T. (2010) Continuous separation of cells of high osteoblastic differentiation potential from mesenchymal stem cells on an antibody-immobilised column. Biomaterials, 31(14): 4231-4237.

Maini P.K., McElwain D.L. and Leavesley D.I. (2004) Travelling wave model to interpret a wound-healing cell migration assay for human peritoneal mesothelial cells. Tissue Engineering, 10(3-4): 475-482.

Manalo D.J., Rowan A., Lavoie T., Natarajan L., Kelly B.D., Ye S.Q., Garcia J.G. Semenza G.L. (2005) Transcriptional regulation of vascular endothelial cell responses to hypoxia by HIF-1. Blood, 105(2): 659-669.

Maniotis A.J., Folberg R., Hess A., Seftor E.A., Gardner L.M., Pe'er J., Trent J.M., Meltzer P.S. and Hendrix M.J. (1999) Vascular channel formation by human melanoma cells in vivo and in vitro: vasculogenic mimicry. The American Journal of Pathology, 155(3): 739-752.

Markiv A., Peiris D., Curley G.P., Odel M. and Dwek M.V. (2010) Identification, cloning, and characterisation of two N-acetylgalactosamine-binding lectins from the albumin gland of *Helix pomatia*. The Journal of Biological Chemistry, 286(23): 20260-20266.

Marmot M.G., Altman D.G., Cameron D.A., Dewar J.A., Thompson S.G. and Wilcox M. (2012) The benefits and harms of breast cancer screening: an independent review. The Lancet, 380(9855): 1778-1786.

Martin F.T. Dwyer R.M., Kelly J., Khan S., Murphy J.M., Curran C., Miller N., Hennessy E., Dockery P., Barry F.P., O'Brien T. and Kenn M.J. (2010) Potential role of mesenchymal stem cells (MSCs) in the breast tumour microenvironment: stimulation of epithelial to mesenchymal transition (EMT). Breast Cancer Research and Treatment, 124(2): 317-326.

Mason J.C., Yarwood H., Sugars K. and Haskard D.O. (1997) Human umbilical vein and dermal microvascular endothelial cells show heterogeneity in response to PKC activation. The American Journal of Physiology, 273(4pt1): c1233-1240.

Matsubayashi Y., Ebisuya M., Honjoh S. and Nishida E. (2004) ERK activation propagates in epithelial cell sheets and regulates their migration during wound healing. Current Biology, 14(8): 731-735.

Matsui T., Hamako J., Ozaki Y. and Titani K. (2001) Comparative study of blood group-recognising lectins towards ABO blood group antigens on neoglycoproteins, glycoproteins and complex-type oligosaccharides. Biochemica et Biophysica Acta, 1525: 50-57.

Maupin K.A., Sinha A., Eugster E., Miller J., Ross J., Paulino V., Keshamouni V.G., Tran N., Berens M., Webb C. and Haab B.B. (2010) Glycogene expression alterations associated with pancreatic cancer epithelial-mesenchymal transition in complimentary model systems. Plos One, 5(9): e13002.

Méhes G., Witt A., Kubista E. and Ambros P.F. (2001) Circulating breast cancer cells are frequently apoptotic. The American Journal of Pathology, 159(1): 17-20.

Melo S.A., Sugimoto H., O'Connel J.T., Kato N., Villanueva A., Vidal A., Qiu L., Vitkin E., Perelman L.T., Melo C.A., Lucci A., Ivan C. and Calin G.A. (2014) Cancer exosomes perform cell independent microRNA biogenesis and promote tumorigenesis. Cancer Cell, 26: 707-721.

Mendez M.G., Kojima S.-I. and Goldmen R.D. (2010) Vimentin induces changes in cell shape, motility, and adhesion during epithelial to mesenchymal transition. FASEB Journal, 24(6): 1838-1851.

Meng F. and Wu G. (2012) The rejuvenated scenario of epithelial-mesenchymal transition (EMT) and cancer metastasis. Cancer Metastasis Reviews, 31(3-4): 455-467.

Mi W., Gu Y., Han C., Liu H., Fan Q., Zhang X., Cong Q. and Yu W. (2011) O-GlcNAcylation is a novel regulator of lung and colon cancer malignancy. Biochemica et Biophysica Acta, 1812(4): 514-511.

Micalizzi D.S., Farabaugh S.M. and Ford H.L. (2010a) Epithelial-mesenchymal transition in cancer: parallels between normal development and tumor progression. Journal of Mammary Gland Biology and Neoplasia, 15(2): 117–134.

Micalizzi D.S., Wang C.-A., Farabough S.M., Schiemann W.P. and Ford H.L. (2010b) Homeoprotein SIX1 increases TGF-β type I receptor and converts TGF-β signaling from suppressive to supportive for tumour growth. Cancer Research, 70(24): 10371-10380.

Mikheeva S.A., Mikheev A.M., Petit A., Beyer R., Oxford R.G., Khorasani L., Maxwell J.P., Glackin C.A., Wakimoto H., González-Herrero I., Sánchez-García I., Silber J.R., Horner P.J. and Rostomily R.C. (2010) TWIST1 promotes invasion through mesenchymal change in human glioblastoma. Molecular Cancer, 9(194): doi: 10.1186/1476-4590-9-194.

Miles F.L., Pruitt F.L., van Golen K.L. and Cooper C.R. (2008) Stepping out of the flow: capillary extravasation in cancer metastasis. Clinical and Experimental Metastasis, 25: 305-324.

Mina L.A. and Sledge G.W. Jr. (2011) Rethinking the metastatic cascade as a therapeutic target. Nature Reviews Clinical Oncology, 8(6): 325-332.

Mitchell B.S., Vernon K., Schumacher U. and Habil M. (1995) Ultrastructural localization of *Helix pomatia* agglutinin (HPA) -binding sites in human breast cancer cell lines and characterization of HPA-binding glycans by western blotting. Ultrastructural Pathology, 19(1): 51-59.

Mitchell, B.S. and Schumacher, U. (1999) The use of the lectin *Helix pomatia* agglutinin (HPA) as a prognostic indicator and as a tool in cancer research. Histology and Histopathology, 14(1): 217-226.

Miyahara N., Shoda J., Kawamoto T., Furukawa M., Ueda T., Todoroki T., Tanaka N., Matsuo K., Yamada Y., Kohno K. and Irimura T. (2004) Expression of UDP-*N*-acetyl-α-D-galactosaminyltranferase isozyme 3

in the subserosal layer correlates with postsurgical survival of pathological tumor stage 2 carcinoma of the gallbladder. Clinical Cancer Research, 10: 2090-2099.

Moon H.-J., Finney J., Xu L., Moore D., Welch D.R. and Mure M. (2013) MCF-7 cells expressing nuclear associated lysyl oxidase-like 2 (LOXL2) exhibit an epithelial-to-mesenchymal transition (EMT) phenotype and are highly invasive *in vitro*. The Journal of Biological Chemistry, 288(42): 30000-30008.

Moremen K.W., Tiemeijer M. and Nairn A.V. (2012) Vertebrate protein glycosylation: diversity, synthesis and function. Nature Reviews Molecular Cell Biology, 13: 448-462.

Mougiakakas D., Choudhury A., Lladser A., Klessling R. and Johansson C.C. (2010) Regulator T cells in cancer. Advances in Cancer Research, 107: 57-117.

Mourali N., Muenz L.R., Tabbane F., Belhassen S., Bahi J. and Levine P.H. (1980) Epidemiologic features of rapidly progressing breast cancer in Tunisia. Cancer, 46(12): 2741-2746.

Müller A., Homey B., Soto H., Ge N., Carton D., Buchanan M.E., McClanahan T., Murphy E., Yaun W., Wagner S.N., Barrera J.L., Mohar A., Verástegui E. and Zlotnik A. (2001) Involvement of chemokine receptors in breast cancer metastasis. Nature, 410(6824): 50-56.

N

Nagai T., Arao T., Furuta K., Sakai K., Kudo K., Kaneda H., Tumura D., Aomatsu K., Kimura H., Fujita Y., Matsumoto K., Saijo N., Kudo M. and Nishio K. (2011) Sorafenib inherits the hepatocyte growth factor-mediated epithelial mesenchymal transition in hepatocellular carcinoma. Molecular Cancer Therapeutics, 10(1): 169-177.

Naismith J.H. and Field R.A. (1996) Structural basis of trimannoside recognition by concanavalin A. The Journal of Biological Chemistry, 271(2): 972-976.

Nakajima S., Doi R., Toyoda E., Tsuji S., Wada M., Koizumi M., Tulachan S.S., Ito D., Kami K., Mori T., Kawaguchi Y., Fujimoto K., Hosotani R. and Imamura M. (2004) N-cadherin expression and epithelial-mesenchymal transition in pancreatic carcinoma. Clinical Cancer Research, 10(12 Pt 1): 4125-4133.

Nakamura N., Toba S., Hirai M., Morishita S., Mikami T., Konishi M., Itoh N. and Kurasaka A. (2005) Cloning and expression of a brain-specific putative UDP-GalNAc: polypeptide N-acetylgalactosaminyltransferase gene. Biological and Pharmaceutical Bulletin, 28(3): 429-433.

Nakayama Y., Nakamura N., Oki S., Wakabayashi M., Ishihama Y., Miyake A., Itoh N. and Kurosaka A. (2012) A putative polypeptide N-acetylgalactosaminyltransferase/Williams-Beuren syndrome chromosome region 17 (WBSCR17) regulates lamellipodium formation and micropinocytosis. The Journal of Biological Chemistry, 287(38): 32222-32235.

Narimatsu Y., Kubota T., Furukawa S., Shimojima M., Iwasaki H., Tozawa Y., Tachibana K. and Narimatsu H. (2011) Co-translational function of *Cosmc*, core 1 synthase specific molecular chaperone, revealed by a cell-free translation system. FEBS Letters, 585: 1276-1280.

Nash, G. F., Turner, L. F., Scully, M. F. and Kakkar, A. K. (2002) Platelets and Cancer. The Lancet Oncology, 3: 425-430.

Naumov G.N., MacDonald I.C., Chambers A.F. and Groom A.C. (2001) Solitary cancer cells as a possible source of tumour dormancy. Seminars in Cancer Biology, 11(4): 271-276.

Nelson-Rees W.A. and Flandermeyer R.R. (1976) HeLa cultures defined. Science, 191(4222): 96-98.

Nieto M.A., Huang R.Y.-J., Jackson R.A. and Thiery J.P. (2016) EMT: 2016. Cell, 166: 21-45.

Niinaka Y., Haga A. and Raz A. (2001) Quantification of cell motility: gold colloidal phagokinetic track assay and wound healing assay. In: Brooks S.A. and Schumacher U. (eds) *Metastasis Research Protocols. Volume 58 of the Series Methods in Molecular Medicine*. New York: Humana Press. 55-60

Nistala H., Lee-Arteaga S., Smaldone S., Siciliano G., Carta L., Ono R.N., Sengle G., Arteaga-Solis E., Levasseur R., Ducy P., Sakai L.Y., Karsenty G. and Ramirez F. (2010) Fibrillin-1 and -2 differentially modulate endogenous TGF-β and BMP bioavailability during bone formation. The Journal of Cell Biology, 190(6): 1107-1121.

Noguchi M., Thomas M., Kitagawa H., Kinishita K., Kinami S., Takamura H., Miyazaki I. and Mizukami Y. (1993a) DNA ploidy and *Helix pomatia* lectin binding as predictors of regional lymph node metastasis and prognostic factors in breast cancer. Breast Cancer Research and Treatment, 26(1): 67-75.

Noguchi M., Thomas M., Kitagawa H., Kinoshita K., Ohta N., Nagamori M. and Miyazaki I. (1993b) Further analysis of predictive value of *Helix pomatia* lectin binding to primary breast cancer for axillary and internal mammary lymph node metastasis. British Journal of Cancer, 67(6): 1368-1371.

Noguchi M., Earashi M., Ohnishi I., Kinashita K., Thomas M., Fusida S., Miyazaki I. and Mizukami K. (1994a) NM23 expression versus *Helix pomatia* lectin binding in human breast cancer metastasis. International Journal of Oncology, 4(6): 1353-1358.

Noguchi M., Thomas M., Kitagawa K., Earashi M., Kinam S.-I., Takamura H., Miyazaki I. and Mizukami Y. (1994b) *Helix pomatia* lectin and c-erbB2 expression versus axillary and internal mammary lymph node metastasis in prognostic assessment of breast cancer. International Journal of Oncology, 2(6): 985-989.

Naumov G. N., Akslen L. A. and Folkman J. (2006) Role of angiogenesis in human tumour dormancy: animal models of the angiogenic switch. Cell Cycle, 5(16): 1779-1787.

O

Offner F.A., Wirtz H.C., Schiefer J., Bigalke I., Klosterhalfen J., Bittinger F., Mittermayer C. and Kirkpatrick C.J. (1992) Interaction of human malignant melanoma (ST-ML-12) tumour spheroids with endothelial cell monolayers. The American Journal of Pathology, 141(3): 601-610.

Olsvik O., Popovik T., Skjerve E., Cudjoe K.S., Hornes E., Ugelstad J. and Uhlen M. (1994) Magnetic separation techniques in diagnostic microbiology. Clinical Microbiology Reviews, 7(1): 43-54.

Onitsuka K., Shibao K., Nakayama Y., Minagawa N., Hirata K., Izumi H., Matsuo K., Nagata N., Kitazato K., Kohno K. and Itoh H. (2003) Prognostic significance of UDP-*N*-acetyl-α-D-galactosamine:polypeptide *N*-acetylgalactosaminyltransferase-3 (GalNAc-T3) expression in patients with gastric carcinoma. Cancer Science, 94(1): 32-36.

Ono H., Imoto I., Kozaki K., Tsuda H., Matsui T., Kurasawa Y., Muramatsu T., Sugihara I. and Inazawa J. (2012) SIX1 promotes epithelial-mesenchymal transition in colorectal cancer through ZEB1 activation. Oncogene, 31(47): 4923-4934.

Orr B., Riddick A.C., Hayward S.W., Stewart G.O., Anderson R.A., Franco O.E., Hayward S.W. and Thomson A.A. (2012) Identification of stromally expressed molecules in the prostate by tag-profiling of cancer associated fibroblasts, normal fibroblasts and foetal prostate. Oncogene, 31(9): 1130-1142.

Osborne C.E. (2004) Functional role of *Helix pomatia* binding glycans in breast cancer metastasis. PhD thesis, Oxford Brookes University.

P

Pantel K. and Brakenhoff R. (2004) Dissecting the metastatic cascade. Nature Reviews, 4: 448-456.

Parameswaran R., Sadler G. and Brooks S. (2011) *Helix pomatia* agglutinin binding glycoproteins in thyroid tumours. World Journal of Surgery, 35(10): 2219-2227.

Park S.-M., Gaur A.B., Lengyel E. and Peter M.E. (2008) The miR-200 family determines the epithelial phenotype of cancer cells by targeting the E-cadherin repressors ZEB1 and ZEB2. Genes and Development, 22(7): 894-907.

Park J.-H., Nishidate T., Kijima K., Ohashi T., Takegawa K., Fujikane T., Hirata K., Nakamura Y. and Katagiri T. (2010) Critical roles of mucin 1 glycosylation by transactivated polypeptide N-acetylgalactosaminyltransferase 6 in mammary carcinogenesis. Molecular and Cellular Pathobiology, 7(70): 2759-2769.

Park J.-H., Katagiri T., Chung S., Kijima K. and Nakamura Y. (2011) Polypeptide N-acetylgalactosaminyltransferase 6 disrupts mammary acinar morphogenesis through O-glycosylation of fibronectin. Neoplasia, 13(4): 320-326.

Partridge E.A., Le Roy C., Di Guglielmo G.M., Pawling J., Cheung P., Granovsky M., Nabi I.R., Wrana J.L. and Dennis J.W. (2004) Regulation of cytokine receptors by Golgi N-glycans processing and endocytosis. Science, 306: 120-124.

Paulson J.C. and Colley K.J. (1989) Glycosyltransferases. Structure, localisation, and control of cell type-specific glycosylation. The Journal of Biological Chemistry, 264(30): 17615-17618.

Patani N., Jiang W. and Mokbel K. (2008) Prognostic utility of glycosyltransferase expression in breast cancer. Cancer Genomics and Proteomics, 5: 333-340.

Patel T.R., Bernards C., Meier M., McEleney K., Winzor D.J., Manuel K. and Stretefeld J. (2014) Structural eludation of full-length nidogen and the laminin-nidogen complex in solution. Matrix Biology, 33: 60-67.

Pederson P.H., Ness G.O., Engebraaten O., Bjerkvig R., Lillehaug J.R. and Laerum O.D. (1994) Heterogeneous response to the growth factors [EGF, PDGF(bb), TGF-alpha, bFGF, IL-2] on glioma spheroid growth, migration and invasion. International Journal of Cancer, 56(2): 255-261.

Pedrola N., Devis L., Llauradó M., Campoy I., Martinez-Garcia E., Garcia M., Muinelo-Romay L., Alonso-Alconada L., Abal M., Alameda F., Mancebo G., Carreras R., Castellví J., Cabrera S., Gil-Moreno A., Matias-Guiu X., Iovanna J.L., Colas E., Reuentós J. and Ruiz A. (2015) Nidogen I and nuclear protein I: novel targets of ETV5 transcription factors involved in endometrial cancer invasion. Clinical and Experimental Metastasis, 32(5): 467-478.

Peiris D., Ossondo M., Fry S., Loizidou M., Smith-Ravin J. and Dwek M.V. (2015) Identification of O-linked glycoproteins binding to the lectin Helix pomatia agglutinin as marked of metastatic colorectal cancer. Plos One, 10(10): e0138345.

Peng C., Togayachi A., Kwon Y.D., Xie C., Wu G., Zou X., Sato T., Ito H., Tachibana K., Kubota T., Noce T., Narimatsu H. and Zhang Y. (2010) Identification of a novel human UDP-GalNAc transferase with unique catalytic activity and expression profile. Biochemical and Biophysical Research Communications, 402(4): 680-686.

Peng R.-Q., Wan H.-Y., Li H.-F., Liu M., Li X. and Tang H. (2012) MicroRNA-214 suppresses growth and invasiveness of cervical cancer cells by targeting UDP-N-α-D-galactosamine: polypeptide N-acetylgalactosaminyltransferase 7. The Journal of Biological Chemistry, 287(17): 14301-14309.

Person A.D., Klewer S.E. and Runyan R.B. (2005) Cell biology of cardiac cushion development. International Review of Cytology, 243: 287-335.

Piller V., Piller F. and Cartron J.-P. (1990) Comparisons of the carbohydrate-binding specificities of seven N-acetyl-D-galactosamine-recognising lectins. European Journal of Biochemistry, 191(2): 461-466.

Polyak K and Weinberg R.A. (2009) Transitions between epithelial and mesenchymal states: acquisition of malignant and stem cell traits. Nature Reviews Cancer, 9: 265-273.

R

Rabut G. and Ellenberg J. (2004) Automatic real-time three-dimensional cell tracking by fluorescence microscopy. Journal of Microscopy, 216(2): 131-137.

Raman J., Fritz T.A., Gerken T.A., Jamison O., Live D., Liu M. and Tabak L.A. (2008) The catalytic and lectin domains of UDP-GalNAc:polypeptide alpha-N-acetylgalactosaminyltransferase function in concert to direct glycosylation site selection. The Journal of Biological Chemistry, 283(34): 22942-22951.

Raman J., Guan Y., Perrine C.L., Gerken T.A. and Tabak L.A. (2012) UDP-N-acetyl-a-D-galactosamine:polypeptide N-acetylgalactosaminyltransferases: completion of the family tree. Glycobiology, 22(6): 768-777.

Rambaruth N.D.S., Greenwall P. and Dwek M.V. (2012) The lectin *Helix pomatia* agglutinin recognises O-GlcNAc containing glycoproteins in human breast cancer. Glycobiology, 22(6): 839-848.

Ribatti, D. (2006) Genetic and epigenetic mechanisms in the early development of the vascular system. Journal of Anatomy, 208(2): 139-152.

Ribatti D. and Crivellato E. (2012) “Sprouting angiogenesis”, vasculogenic mimicry and tumour angiogenesis. The American Journal of Pathology, 156(2): 361-381.

Rosen E.M., Meromsky L., Setter E., Vinter D.W. and Goldberg I.D. (1990) Quantitation of cytokine-stimulated migration of endothelium and epithelium by a new assay using microcarrier beads. Experimental Cell Research, 186(1): 22-31.

Roth J. (1984) Cytoplasmic localization of terminal N-acetyl-D-galactosamine residues in cellular compartments of intestinal goblet cells: implications for topology of O-glycosylation. The Journal of Cell Biology, 98: 399-406.

Röttger S., White J., Wandall H.H., Olivo J.C., Stark A., Bennett E.P., Whitehouse C., Berger E.G., Clausen H. and Nilsson T. (1998) Localisation of three human polypeptide GalNAc-transferases in HeLa cell

suggests initiation of O-linked glycosylation throughout the Golgi apparatus. Journal of Cell Science, 111(Pt 1): 45-60.

Rudd P.M. and Dwek R.A. (1997) Glycosylation: heterogeneity and the 3D structure of proteins. Critical Reviews in Biochemistry and Molecular Biology, 32(1): 1-100.

Ruitberg C. M., Reeder D. J. and Butler J. M. (2001) STRBase: a short tandem repeat DNA database for the human identity testing community. Nucleic Acids Research, 29(1): 320-322.

Russo J. and Russo I.H. (2004) Development of the human breast. Maturitas, 49: 2-15.

Rutkowski M.J., Sughrue M.E., Kane A.J., Mills S.A. and Parsa A.T. (2010) Cancer and the complement cascade. Molecular Cancer Research, 8(11): 1453-1465.

S

Sabeh F., Shimizu-Hirota R. and Weiss S.J. (2009) Protease-dependent versus -independent cancer cell invasion programs: three-dimensional amoeboid movement revisited. The Journal of Cell Biology, 185(1): 11-19.

Šafařík I. and Šafaříková M. (1999) Use of magnetic techniques for the isolation of cells. Journal of Chromatography B, 722: 33-35.

Saint-Guirons J., Zeqiraj E., Schumacher U., Greenwall P. and Dwek M. (2007) Proteome analysis of metastatic colorectal cancer cells recognised by the lectin *Helix pomatia* agglutinin (HPA). Proteomics, 7(22): 4082-4089.

Sanchez J-F., Lescar J., Chazalet V., Audfray A., Gagnon J., Alvarez R., Breton C., Imberty A. and Mitchell E.P. (2006) Biochemical and structural analysis *of Helix pomatia* agglutinin (HPA): a hexameric lectin with a novel fold. The Journal of Biological Chemistry, 281(29): 20171-20180.

Sánchez-Tilló E., Lázaro A., Torrent R., Cuatrecasas M., Vaguero E.C., Castells A., Engel P. and Postigo A. (2010) ZEB1 represses E-cadherin and induces an EMT by recruiting the SW1/SNF chromatin-remodelling protein BRG1. Oncogene, 29(24): 3490-3500.

Sánchez-Tilló E., Liu Y., de Barrios O., Siles L., Fanio L., Cuatrecasas M., Darling D.S., Castells A. and Postigo A. (2012) EMT-activating transcription factors in cancer: beyond EMT and tumour invasiveness. Cellular and Molecular Life Sciences, 69(20): 3429-3456.

Sanyal A., O'Driscoll S.W., Bolander M.E. and Sarkar G. (1997) An effective method of completely removing contaminating genomic DNA from a RNA sample to be used for PCR. Molecular Biotechnology, 8(2): 135-137.

Savagner P., Yamada K.M. and Thiery J.P. (1997) The zinc-finger protein Slug causes desmosome dissociation, an initial and necessary step for growth factor-induced epithelial-mesenchymal transition. The Journal of Cell Biology, 137(6): 1403-19.

Savagner, P. (2001) Leaving the neighbourhood: molecular mechanisms involved during epithelial-mesenchymal transition. Bioessays, 23: 912-923.

Schumacher U., Kretzschmar H., Brooks S. and Leathem A. (1992) *Helix pomatia* lectin binding pattern of brain metastases originating from breast cancers. Pathology, Research and Practice, 188(3): 284-286.

Schumacher U., Higgs D., Loizidou M., Pickering R., Leathem A. and Taylor I. (1994a) *Helix pomatia* agglutinin binding is a useful prognostic indicator in colorectal carcinoma. Cancer, 74(12): 3104-3107.

Schumacher U., Adam E., Favell D., Boehm D., Brooks S. and Leathem A. (1994b) Glycosylation patterns of the human colon cancer cell line HT-29 detected by *Helix pomatia* agglutinin and other lectins in culture, in primary tumours and in metastases in SCID mice. Clinical and Experimental Metastasis, 12: 398-404.

Schumacher U., Adam E., Brooks S.A. and Leathem A.J. (1995) Lectin-binding properties of human breast cancer cell lines and human milk with particular reference to *Helix pomatia* agglutinin. Journal of Histochemistry and Cytochemistry, 43(3): 275-281.

Schumacher U. and Adam E. (1997) Lectin histochemical HPA-binding pattern of human breast and colon cancers is associated with metastases formation in severe combined immunodeficient mice. Histochemical Journal, 29(9): 677-684.

Schwientek T., Bennett E.P., Flores C., Thacker J., Hollmann M., Reis C.A., Behrens J., Mandel U., Keck B., Schäfer M.A., Haselmann K., Zubarew B., Roepstorff P., Burchell J.M., Taylor-Papadimitriou J., Hollingsworth M.A. and Clausen H. (2002) Functional conservation of subfamilies of putative UDP-N-acetylgalactosamine:polypeptide N-acetylgalactosaminyltransferases in Drosophila, Caenorhabditis elegans, and mammals. One subfamily composed of I(2)35Aa is essential in Drosophila. The Journal of Biological Chemistry, 277(25): 22623-22638.

Semenza G.L. (2001) HIF-1: mediator of physiological and pathophysiological responses to hypoxia. Journal of Applied Physiology, 88(4): 1474-1480.

Senfter D., Holzner S., Kalipayan M., Staribacher A., Walzl A., Huttary N., Krieger S., Brenner S., Jäger W., Krupitza G., Polznig H. and Mader R.M. (2015) Loss of miR-200 family in 5-fluorouracil resistant colon cancer drives lymphendothelial invasiveness *in vitro*. Human Molecular Genetics, 24(13): 3689-3698.

Shankar J., Messenberg A., Chan J., Underhill T.M., Foster J.J. and Nabi I.R. (2010) Pseudopodia actin dynamics control epithelial-mesenchymal transformation in metastatic cancer cells. Cancer Research, 70(9): 3780-3790.

Shao K., Chen Z.Y., Gautam S., Deng N.H., Zhou Y. and Wu X.Z. (2016) Posttranslational modification of E-cadherin by core fucosylation regulates Src activation and induces epithelial-mesenchymal transition-like process in lung cancer cells. Glycobiology, 26(2): 142-154.

Sharon N. and Lis H. (1989) Lectins. Thomson Press: India.

Sharpe P.T. (1988) Methods of cell separation. Amsterdam: Elsevier Science Publishers.

Shay J.W. and Wright W.E. (2000) Hayflick, his limit, and cellular ageing. Nature Reviews Molecular Cell Biology, 1: 72-76.

Shetty S., Weston C.J., Adams D.H. and Lalor P.F. (2014) A flow adhesion assay to study leukocyte recruitment to human hepatic sinusoidal endothelium under conditions of shear stress. Journal of Visualised Experiments, 85: e51330.

Shibao K., Izumi H., Nakayama Y., Ohta R., Nagata N., Nomoto M., Matsuo K., Yamada Y., Kitazato K., Itoh H. and Kohno K. (2002) Expression of UDP-N-acetyl-α-D-galactosamine-polypeptide GalNAc N-acetylgalactosaminyl transferase-3 in relation to differentiation and prognosis in patients with colorectal carcinoma. Cancer, 94(7): 1939-1946.

Shiraishi T., Atsumi S. and Yatani R. (1992) Comparative study of prostatic carcinoma bone metastasis amongst Japanese in Japan and Japanese, Americans and Whites in Hawaii. Advances in Experimental Medicine and Biology, 324: 7-16.

Shrimal S., Cherepanova N.A. and Gilmore R. (2015) Cotranslational and posttranslational N-glycosylation of proteins in the endoplasmic reticulum. Seminars in Cell and Developmental Biology, 41: 71-78.

Shtutman M., Levina E., Ohouo P., Baig M. and Rninson I.B. (2006) Cell adhesion molecule L1 disrupts E-cadherin-containing adherens junctions and increases scattering and motility of MCF7 breast carcinoma cells. Cancer Research, 66(23): 11370-11380.

Siemens H., Jackstadt R., Hünten S., Kaller M., Menssen A., Götz U. and Hermeking H. (2011) miR-34 and Snail form a double-negative feedback loop to regulate epithelial-mesenchymal transitions. Cell Cycle, 10(24): 4256-4271.

Singletary S.E., Aured C., Ashley P., Bassett L.W., Berry D., Bland K.I., Borgen P.I., Clark G., Edge S.B., Hayes D.F., Hughes L.L., Hutter R.V.P., Morrow M., Page D.L., Recht A., Theriault R.L., Thor A., Weaver

D.L., Wieand H.S. and Greene F.L. (2002) Revision of the American joint committee on cancer staging system for breast cancer. Journal of Clinical Oncology, 20(17): 3628-3636.

Skobe M. and Fusenig N.E. (1998) Tumorigenic conversion of immortal human keratinocytes through stromal cell activation. PNAS, 95(3): 1050-1055.

Slawson C., Pidala J. and Potter R. (2001) Increased N-acetyl-β-glucosaminidase activity in primary breast carcinomas corresponding to a decrease in N-acetylglucosamine containing proteins. Biochemica et Biophysica Acta, 1537(2): 147-157.

Slawson C. and Hart G.W. (2011) O-GlcNAc signalling: implications for cancer cell biology. Nature Reviews Cancer, 11(9): 678-684.

Smith R.D. and Lupashin V.V. (2008) Role of the conserved oligomeric Golgi (COG) complex in protein glycosylation. Carbohydrate Research, 343(12): 2024-2031.

Smyth G.K., Yang Y.-H. and Speed T.P. (2003) Statistical issues in cDNA microarray data analysis. Methods in Molecular Biology, 224: 111-136.

Soule H., Vazquez J., Long A., Albert A. and Brennan M. (1973) A human cell line from a pleural effusion derived from a breast carcinoma. Journal of the National Cancer Institute, 51(5): 1409-14-16.

Sousa A.F., Andrade P.Z., Pirzgalska R.M., Galhoz T.M., Azevedo A.M., da Silva C.L., Aires-Barros M.R. and Cabral J.M. (2011) A novel method for human hematopoietic stem/progenitor cell isolation from umbilical cord blood based on immunoaffinity aqueous two-phase portioning. Biotechnology Letters, 33(12): 2373-2377.

Sporn M.B. (1996) The war on cancer. Lancet, 347: 1377-1381.

Springer G.F., Chandrasekaran E.V., Desai P.R. and Tegtmeyer H. (1988) Blood group Tn-active macromolecules from human carcinomas and erythrocytes: characterisation of and specific reactivity with mono- and poly-clonal anti-Tn antibodies induced by various immunogens. Carbohydrate Research, 178(1): 271-292.

Stamenkovic I. (2003) Extracellular matrix remodelling: the role of matrix metalloproteinases. The Journal of Pathology, 200(4): 448-464.

Stone R.C., Pastar I., Ojeh N., Chen V., Liu S., Garzan K.I. and Tomic-Canic M. (2016) Epithelial-mesenchymal transition in tissue repair and fibrosis. Cell and tissue research, 365(3): 495-506.

STRbase http://www.cstl.nist.gov/div831/strbase/str_fact.htm.

Strell C., Lang K., Niggemann B., Zaenker K.S. and Entschladen F. (2007) Surface molecules regulating rolling and adhesion to endothelium of neutrophils, granulocytes and MDA-MB-468 breast carcinoma cells and their interaction. Cellular and Molecular Life Sciences, 64(24): 3306-3316.

Strell C. and Entschladen F. (2008) Extravasation of leukocytes in comparison to tumor cells. Cell Communication and Signaling, 6(10): 1-13.

Sun Y. F., Yang X.R., Zhou J., Qiu S.J., Fan J. and Xu Y. (2011) Circulating tumour cells; advances in detection methods, biological issues and clinical relevance. Journal of Cancer Research and Clinical Oncology, 137(8): 1151-1173.

T

Takahashi H., Oyaizu T., Fujita Y. and Tsubura A. (1994) Lectin-binding profiles of MNNG-induced shrew oesophageal carcinomas. Anticancer Research, 14(4A): 1569-1572.

Takasaki N., Tachibana K., Ogasawara S., Matsuzaki H., Hagiuda J., Ishikawa H., Mochida K., Inoue K., Ogonuki N., Ogura A., Noce T., Ito C., Toshimori I.C. and Narimatsu H. (2014) A heterozygous mutation of GALNTL5 affects male sperm motility. Proceedings of the National Academy of Sciences of the United States of America, 111(3): 1120-1125.

Tam W.L. and Weinberg R.A. (2013) The epigenetics of epithelial-mesenchymal plasticity in cancer. Nature Medicine, 19(11): 1438-1449.

Tan S.C. and Yiap B.C. (2009) DNA, RNA and protein extraction: the past and the present. Journal of Biomedicine and Biotechnology, doi:10.1155/2009/574398.

Tang N., Wang L., Esko J., Giordano F.J., Huang Y., Gerber H.P., Ferrera N. and Johnson R.S. (2004) Loss of HIF-1 alpha in endothelial cells disrupts a hypoxia-driven VEGF autocrine loop necessary for tumourigenesis. Cancer Cell, 6(5): 485-495.

Thiery J.P. (2002) Epithelial-mesenchymal transitions in tumour progression. Nature Reviews Cancer, 2: 442-454.

Thiery J.P. and Sleeman P. (2006) Complex networks orchestrate epithelial-mesenchymal transitions. Nature Reviews Molecular Cell Biology, 7: 131-142.

Thomas M., Noguchi M., Fonseca L., Kitagawa H., Kinoshita K. and Miyazaki I. (1993) Prognostic significance of *Helix pomatia* lectin and c-erbB-2 oncoprotein in human breast cancer. British Journal of Cancer, 68(3): 621-626.

Toba S., Tenno M., Konishi M., Mikami T., Itoh N. and Kurosaka A. (2000) Brain-specific expression of a novel human UDP-GalNAc: polypeptide N-acetylgalactosaminyltransferase (GalNAc-T9). Biochemica et Biophysica Acta, 1493(1-2): 264-268.

Tomlinson M.J., Tomlinson S., Yang X.B. and Kirkham J. (2012) Cell separation: terminology and practical considerations. Journal of Tissue Engineering, 3(1): doi: 10.117/2041731412472690.

Torres C.-R. and Hart G.W. (1984) Topography and polypeptide distribution of terminal N-acetylglucosamine residues on the surfaces of intact lymphocytes. The Journal of Biological Chemistry, 259(5): 3308-3317.

Tsai J.H. and Yang J. (2013) Epithelial-mesenchymal plasticity in carcinoma metastasis. Genes and Development, 27: 2192-2206.

Tse J.C. and Kalluri R. (2007) Mechanisms of metastasis: epithelial-to-mesenchymal transition and contribution to tumour microenvironment. Journal of Cellular Biochemistry, 101(4): 816-829.

Tremblay P.L., Huot J. and Auger F.A. (2008) Mechanisms by which E-selectin regulates diapedesis of colon cancer cell under flow conditions. Cancer Research, 68(13): 5167-5176.

U

Ulazzi L., Sabbioni S., Miotto E., Farinati F., Sasaki T., Lanza G. and Negrini M. (2007) Nidogen 1 and 2 gene promoters are aberrantly methylated in human gastrointestinal cancer. Molecular Cancer, 6(17): DOI: 10.1186/1447-4598-6-17.

V

Valentiner U., Hall D.M.S., Brooks S.A. and Schumacher U. (2005) HPA binding and metastasis formation of human breast cancer cell lines transplanted into severe combined immunodeficient (SCID) mice. Cancer Letters, 219(2): 233-242.

Van der Steen P., Rudd P.M., Dwek R.A., Opdenakker G. (1998) Concepts and principles of O-linked glycosylation. Critical Reviews in Biochemistry and Molecular Biology, 33(3): 151-208.

Vander Heiden M.G., Cantley L.C. and Thompson C.B. (2009) Understanding the Warburg effect: the metabolic requirements of cell proliferation. Science, 324: 1029-1033.

Varki A. (1993) Biological roles of oligosaccharides: all of the theories are correct. Glycobiology, 3(2): 97-130.

Varki A., Cummings R.D., Esko J.D., Freeze H.H., Stanley P., Marth J.D., Bertozzi C.R., Hart G.W. and Etzler M.E. (2009) Symbol nomenclature for glycan representation. Proteomics, 9(24): 5398-5399.

Vesuna F., van Diest P., Chen J.-H. and Raman V. (2008) Twist is a transcriptional repressor of E-cadherin gene expression in breast cancer. Biochemical and Biophysical Research Communications, 367(2): 235-241.

Vinci M., Box C. and Eccles S.A. (2015) Three-dimensional (3D) tumour spheroid invasion assay. Journal of Visualised Experiments. 99: e52686.

Vittal R., Fan L., Greenspan D.S., Mickler E.A., Gopalakrishnan B., Cru H., Benson H.L., Zhang C., Burlingham W., Cummings O.W. and Wilkes D.S. (2013) IL-17 induces type V collagen overexpression and EMT via TGF-β-dependant pathways in obliterative bronchiolitis. American Journal of Physiology, 304(6): L401-L414.

Vonderhaar B.K. (1988) Regulation of development of the normal mammary gland by hormones and growth factors. Cancer Treatment and Research, 40: 251-266.

W

Wandall H.H., Irazoqui F., Tarp M.A., Bennett E.P., Mandel U., Takeuchi H., Kato K., Irimura T., Suryanarayanan G., Hollingsworth M.A. and Clausen H. (2007) The lectin domains of polypeptide GalNAc-transferases exhibits carbohydrate-binding specificity for GalNAc: lectin binding to GalNAc-glycoprotein substrates is required for high density GalNAc-O-glycosylation. Glycobiology, 17(4): 374-387.

Wang H., Tachibana K., Zhang Y., Iwasaki H., Kameyama A., Cheng L., Guo J.M., Hiruma T., Togayachi A., Kudo T., Kikuchi N. and Narimatsu T. (2003) Cloning and characterisation of a novel UDP-GalNAc:polypeptide N-acetylgalactosaminyltransferase, pp-GalNAc-T14. Biochemical and Biophysical Research Communications, 300(3): 738-744.

Wang Z., Li Y., Kong D. and Sakar F.H. (2010a) The role of Notch signalling pathway in epithelial-mesenchymal transition (EMT) during development and tumour aggressiveness. Current Drug Targets, 11(6): 745-751.

Wang Z., Udeshi N.D., Slawson C., Compton P.D., Sakabe K., Cheung W.D., Shabanowitz J., Hunk D.F. and Hart G.W. (2010b) Extensive crosstalk between O-GlcNAcylation and phosphorylation regulates cytokinesis. Science Signalling, 3(144): ra2 doi: 10.1126/scisignal.2000526.

Wang Y.-C., Nakagawa M., Garitaonandia I., Slavin I., Altun G., Lacharite R.M., Nazor K.L., Tran H.T., Lynch C.L., Leonardo T.R., Liu Y., Peterson S.E., Laurent L.C., Yamanaka S. and Loring J.F. (2011) Specific lectin biomarkers for isolation of human pluripotent stem cells identified through array-based glycomic analysis. Cell Research, 21: 1551-1563.

Wang R., Yu C., Zhao D., Wu M. and Yang Z. (2013) The mucin-type glycosylating enzyme polypeptide N-acetylgalactosaminyltransferase 14 promotes the migration of ovarian cancer by modifying mucin 13. Oncology Reports, 30(2): 667-676.

Wang G., Yang X., Li C., Cao X., Luo X. and Hu J. (2014) PIK3R3 induces epithelial-to-mesenchymal transition and promotes metastasis in colorectal cancer. Molecular Cancer Therapeutics, 13(7): 1837-1847.

Warburg O.H. (1930) The metabolism of tumours: investigations from the Kaiser Wilhelm Institute for Biology, Berlin-Dahlem (London, UK: Arnold Constable).

Warburg O. (1956a) On the origin of cancer cells. Science, 123: 309-314.

Warburg O. (1956b) On respiratory impairment in cancer cells. Science, 124: 269-270.

Weaver A.M. (2006) Invadopodia: specialised cell structures for cancer invasion. Clinical and Experimental Metastasis, 23(2): 95-105.

Weinberg R.A. (2014) *The Biology of Cancer* 2nd edition. Garland Science: Abingdon.

Weis L., Dimitrov D.S. and Angelova M. (1985) The hemodynamic destruction of intravascular cancer cells in relation to myocardial metastasis. Proceedings of the National Academy of Sciences of the United States of America, 82(17): 5737-5741.

Weis L. and Dimitrov D.S. (1986) Mechanical aspects of the lungs as cancer cell-killing organs during hematogenous metastasis. Journal of Theoretical Biology, 121(3): 307-321.

Wells L., Gao Y., Mahoney J.A., Vosseller K., Chen C., Rosen A. and Hart G.W. (2002) Dynamic O-glycosylation of nuclear and cytosolic proteins: further characterisation of the nucleocytoplasmic β-N-acetylglucosaminidase, O-GlcNAcase. The Journal of Biological Chemistry, 277(3): 1755-1761.

Wells L., Whelan S.A. and Hart G.W. (2003) O-GlcNAc: a regulatory post-translational modification. Biochemical and Biophysical Research Communications, 302: 435-441.

Werner S., Frey S., Riethdorf S., Schulze C., Alawi M., Kling L., Vafaizadeh V., Sauter G., Terracciano L., Schumacher U., Pantel K. and Assmann V. (2013) Dual roles of the transcription factor grainyhead-like 2 (GRHL2) in breast cancer. The Journal of Biological Chemistry, 288(32): 22993-23008.

White T., Bennett E.P., Takio K., Sørensen T., Bonding N. and Clausen H. (1995) Purification and cDNA cloning of a human UDP-N-acetyl-alpha-D-galactosamine: polypeptide N-acetylgalactosaminyltransferase. The Journal of Biological Chemistry, 270(41): 24156-24165.

White K.E., Lorenz B., Evans W.E., Meitinger T., Strom T.M. and Econs M.J. (2000) Molecular cloning of a novel human UDP-GalNAc:polypeptide N-acetylgalactosaminyltransferase, GalNAc-T8, and analysis as a candidate autosomal dominant hypophosphatemic rickets (ADHR) gene. Gene, 246(1-2): 347-356.

Wilhelmsen K., Farrar K. and Hellman J. (2013) Quantitative *in vitro* assay to measure neutrophil adhesion to activated primary human micro-vasculature endothelial cells under static conditions. Journal of Visualised Experiments, 78: e50677.

Willis B.C., Liebler J.M., Luby-Phelps K., Nicholson A.G., Crandell E.D., du Bois R.M. and Borok Z. (2005) Induction of epithelial-mesenchymal transition in alveolar epithelial cells by transforming growth factor beta 1: potential role in idiopathic pulmonary fibrosis. The American Journal of Pathology, 166(5) 1321-1232.

Witz I.P. (2006) The involvement of selectins and their ligands in tumour-progression. Immunology Letters, 104(1-2): 89-93.

Wolf K., Alexander S., Schacht V., Coussens L.M., Von Andrian U., Van Rheenen J., Deryugina E. and Friedl P. (2009) Collagen-based cell migration models *in vitro* and *in vivo*. Seminars in Cell Developmental Biology, 20(8): 931-941.

Wu A.M. and Suggi S. (1991) Coding and classification of D-galactose, N-acetyl-D-galactosamine and Beta-D-Galp-[1-]3(4)]-Beta-D-Glcpnac, specificities of applied lectins. Carbohydrate Research, 213:127-143.

Wu Y., Deng J., Rychahou P.G., Qiu S., Evers B.M. and Zhou B.P. (2009) Stabilisation of Snail by NF-κB is required for inflammation-induced cell migration and invasion. Cancer Cell 15(5): 416-428.

Wu C., Guo X., Wang W., Wang Y., Shan Y., Zhang B., Song W., Ma S., Ge J., Deng H. and Zhu M. (2010) N-acetylgalactosaminyltransferase-14 as a potential biomarker for breast cancer by immunohistochemistry. BMC Cancer, 10: 123.

Wu Y.-M., Liu C.-H., Hu R.-H., Huang M.-J., Lee J.-J., Chen C.-H., Huang J., Lai H.-S., Lee P.-H., Hsu W.-W., Huang H.-C. and Huang M.-C. (2011) Mucin glycosylating enzyme GALNT2 regulates the malignant character of hepatocellular carcinoma by modifying the EGF receptor. Cancer Research, 71(23): 7270-7279.

Wu S., Liu S., Liu Z., Huang J., Pu X., Li J., Yang D., Deng H., Yang N., and Xu J. (2015) Classification of circulating tumour cells by epithelial-mesenchymal transition markers. Plos One, 10(4): e0123976.

Wyckoff J.B., Jones J.G., Condeelis J.S. and Segall J.E. (2000) A critical step in metastasis: *in vivo* analysis of intravasation at the primary tumour. Cancer Research, 60(9): 2504-2511.

Wyckoff J., Wang Y., Lin E., Li J., Goswami S., Stanley E., Segall J., Pollard J. and Condeelis J. (2007) Direct visualization of macrophage-assisted tumor cell intravasation in mammary tumors. Cancer Research, 67(6): 2649-2656.

X

Xiong H., Hong J., Du W., Lin Y.W., Ren L.L., Wang Y.C., Su W.Y., Wang J.L., Cui Y., Wang Z.H. and Fang J.Y. (2012) Roles of STAT3 and ZEB1 proteins in E-cadherin down-regulation and human colorectal cancer epithelial-mesenchymal transition. The Journal of Biological Chemistry, 287(8): 5819-5832.

Xu N., Xi L. and Liu L. (2011) Tracking neutrophil intraluminal crawling, transendothelial migration and chemotaxis in tissue by intravital vide microscopy. Journal of Visualised Experiments, 55: e3296.

Y

Yao D., Dai C. and Peng S. (2011) Mechanism of the mesenchymal–epithelial transition and its relationship with metastatic tumour formation. Molecular Cancer Research, 9(12): 1608-1620.

Yang Q., Ota K., Tian Y., Kumar A., Wada J., Kashihara N., Wallner E. and Kanwar Y.S. (1999) Cloning of rat fibrillin-2 cDNA and its role in branching morphogenesis of embryonic lung. Developmental Biology, 212: 229-242.

Yang J. and Weinberg R.A (2008) Epithelial-mesenchymal transition: at the crossroads of development and tumour metastasis. Developmental Cell, 14: 818-829.

Yang L., Pang Y. and Moses H.L. (2010) TGF-beta and immune cells: an important regulatory axis in the tumour microenvironment and progression. Trends in Immunology, 31: 220-227.

Ye J., Wu D., Shen J., Wu P., Chen J., Zhao J., Zhang T., Wang X. and Huang J. (2012) Enrichment of colorectal cancer stem cells through epithelial-mesenchymal transition via CDH1 knockdown. Molecular Medicine Reports, 6(3): 507-512.

Yeung T.-L., Leung C.S., Wong K.-K., Gutierrez-Hartmann A., Kwong J., Gershenson D.M. and Mok S.C. (2017) ELF3 is a negative regulator of epithelial-mesenchymal transition in ovarian cancer cells. Oncotarget, [Epub ahead of print]: doi: 10.18632/oncotarget.15208.

Yin J.J., Mohammad K.S., Käkönen S.M., Harris S., Wu-Wong J.R., Wessale J.L., Padley R.J., Garrett I.R., Chirgwin J.M. and Guise T.A. (2003) A causal role for the endothelin-1 in the pathogenesis of osteoblastic bone metastases. Proceedings of the National Academy of Sciences of the United States of America, 100(19): 10954-10959.

Yonezawa S., Tachikawa T., Shin S. and Sato E. (1992) Sialosyl-Tn antigen. Its distribution in normal human tissues and expression in adenocarcinoma. American Journal of Clinical Pathology, 98(2): 167-174.

Yook J.I., Li X.-Y., Ora I., Fearson E.R. and Weiss S.J. (2005) Wnt-dependant regulation of the E-cadherin repressor Snail. The Journal of Biological Chemistry, 280(12): 11740-11748.

Yoshida Y., Okamura T. and Shirakusa T. (1993) An immunohistochemical study of *Helix pomatia* agglutinin binding on carcinomas of the oesophagus. Surgery, Gynaecology and Obstetrics, 177(3): 299-302.

Yoshika K., Nakamori S. and Itoh K. (1999) Overexpression of small GTP-binding protein RhoA promotes invasion of tumour cells. Cancer Research, 59(8): 2004-2010.

Young H.M., Bergner A.J., Anderson R.B., Enomoto H., Milbrandt J., Newgreen D.F. and Whitington P.M. (2004) Dynamics of neural crest-driven cell migration in the embryonic mouse gut. Developmental Biology, 270(2): 455-473.

Yu M., Sato H., Seiki M. and Thompson W. (1995) Complex regulation of membrane-type matrix metalloproteinase expression and matrix metalloproteinase-2 activation by concanavalin A in MDA-MB-231 human breast cancer cells. Cancer Research, 55: 3272-3277.

Yu M.-A., Shin K.-S., Kim J.H., Kim Y.-I., Chung S.S., Park S.-H., Kim Y.-L. and Kang D.-H. (2009) HGF and BMP-7 ameliorate high glucose-induced epithelial-to-mesenchymal transition of peritoneal mesothelium. Journal of the American Society of Nephrology, 20(3): 567-581.

Yu J., Xie F., Bao X., Chen W. and Xu Q. (2014) miR-300 inhibits epithelial to mesenchymal transition and metastasis by targeting Twist in human epithelial cancer. Molecular Cancer, 13(12): doi: 10.1186/1476-4598-13-121.

Z

Zachara N.E. and Hart G.W. (2004) O-GlcNAc a sensor of cellular state: the role of nucleocytoplasmic glycosylation in modulating cellular function in response to nutrient and stress. Biochemica et Biophysica Acta, 1673: 13-28.

Zaman M.H., Trapani L.M., Sieminski A.L., MacKellar D., Gong H., Kamm R.D., Wells A., Lauffenburger D.A. and Matsudaira P. (2006) Migration of tumor cells in 3D matrices is governed by matrix stiffness along with cell-matrix adhesion and proteolysis. PNAS, 103(37): 2231-2236.

Zavadil J. and Böttinger E.P. (2005) TGFβ and epithelial-to-mesenchymal transitions. Oncogene, 24(37): 5764-5774.

Zhang Y., Guo L. and Wu C. (2002) A critical role of the PINCH-integrin-linked kinase interaction in the regulation of cell shape change and migration. The Journal of Biological Chemistry, 277(1): 318-326.

Zhang L., Yang N., Mohamed-Hadley A., Rubin S.C. and Coukos G. (2003a) Vector-based RNAi, a novel tool for isoform-specific knock-down of VEGF and anti-angiogenesis gene therapy of cancer. Biochemical and Biophysical Research Communications, 303(4): 1169-1178.

Zhang Y., Iwasaki H., Wang H., Kudo T., Kalka T.B., Hennet T., Kubota T., Cheng L., Inaba N., Gotoh M., Togayachi A., Guo J., Hisatomi H., Nakajima K., Nishihara S., Nakamura M., Marth J.D. and Narimatsu H. (2003b) Cloning and characterisation of a new human UDP-N-acetyl-D-galactosamine:polypeptide N-acetylgalactosaminyltransferase, designated pp-GalNAc-T13, that is specifically expressed in neurons and synthesises GalNAc alpha-serine/threonine antigen. The Journal of Biological Chemistry, 278(1): 573-584.

Zhao, Y-Y., Takahashi, M., Gu, J-G., Miyoshi, E., Matsumoto, A., Kitazume, S. and Taniguchi, N. (2008) Functional roles of N-glycans in cell signaling and cell adhesion in cancer. Cancer Science, 99(7): 1304-1310.

Zheng H. and Kang Y. (2014) Multilayer control of the EMT master regulators. Oncogene, 33(14): 1755-1763.

Zhou Z.N., Boimel P.J. and Segall J.E. (2011) Tumour-stroma: *in vivo* assays and intravital imaging to study cell migration and metastasis. Drug discovery today. Disease Models, 8(2-3): 95-112.

Zhou C., Liu J., Tang Y. and Liang X. (2012) Inflammation linking EMT and cancer stem cells. Oral Oncology, 48(11): 1068-1075.

Zhu Q., Zhai L., Yang Z., Lai M., Xie H., Wu L., Xing C., Zhang F. and Zheng S. (2012) O-GlcNAcylation plays a role in tumour recurrence of hepatocellular carcinoma following liver transplantation. Medical Oncology, 29(2): 985-993.

Appendices

Appendix 1

Data tables from Chapter 3

Table A1.1 *Counts of HPA labelled (+) versus non-labelled (-) MCF7 cells across 6 slides (biological replicates) and 10 fields of view (technical replicates).*

Field of view	**Slide**											
	1		2		3		4		5		6	
	+	**-**	**+**	**-**	**+**	**-**	**+**	**-**	**+**	**-**	**+**	**-**
1	41	6	94	0	51	1	74	0	105	10	121	6
2	107	14	36	5	170	1	332	26	43	5	54	0
3	89	0	118	3	45	0	159	6	52	12	90	0
4	42	0	95	0	117	0	163	1	52	4	146	0
5	17	12	10	3	57	0	80	3	63	3	85	4
6	66	5	30	0	79	1	85	7	63	2	90	12
7	229	0	12	5	94	6	122	0	34	0	32	10
8	74	33	41	31	151	6	158	1	57	3	52	8
9	179	55	69	0	93	14	78	0	79	1	14	9
10	235	3	75	9	133	0	81	0	67	0	58	1
Totals	1079	128	580	56	990	29	1332	44	615	40	742	50
Overall total	5338	347										

Table A1.2 *Counts of HPA labelled (+) versus non-labelled (-) ZR751 cells across 6 slides (biological replicates) and 10 fields of view (technical replicates).*

Field of view	**Slide**											
	1		2		3		4		5		6	
	+	**-**	**+**	**-**	**+**	**-**	**+**	**-**	**+**	**-**	**+**	**-**
1	232	173	90	44	99	93	103	66	174	26	89	201
2	111	139	22	39	41	140	49	55	114	111	121	109
3	177	154	38	13	70	98	101	115	103	105	46	70
4	85	151	71	80	118	65	8	117	33	43	28	59
5	148	137	35	162	131	98	31	104	72	66	56	152
6	78	147	48	89	68	100	18	36	49	25	78	50
7	121	91	94	108	54	60	107	110	89	44	48	58
8	239	65	0	67	134	144	77	106	38	49	53	73
9	29	90	36	123	179	61	1	65	96	92	40	96
10	125	97	15	77	139	112	25	74	34	18	56	68
Totals	1345	1244	449	802	1033	971	520	848	802	579	615	936
Overall total	4764	5380										

Table A1.3 *Counts of HPA labelled (+) versus non-labelled (-) MCF7 cells across 6 slides (biological replicates) and 10 fields of view (technical replicates).*

Field of view	**Slide**											
	1		2		3		4		5		6	
	+	**-**	**+**	**-**	**+**	**-**	**+**	**-**	**+**	**-**	**+**	**-**
1	8	91	0	76	2	171	11	37	0	82	0	58
2	2	125	0	81	7	195	51	30	4	61	3	134
3	8	142	5	135	7	129	9	85	8	103	0	85
4	13	214	2	89	9	114	0	5	4	66	3	59
5	12	132	0	160	0	73	0	48	0	106	20	68
6	16	102	19	76	0	41	8	41	0	39	4	133
7	23	32	0	62	1	103	15	70	0	145	0	56
8	28	123	16	77	0	44	0	60	3	94	0	101
9	0	80	14	111	6	29	10	33	2	67	0	107
10	3	105	0	71	1	43	8	74	0	95	1	145
Totals	113	1146	56	938	33	942	112	483	21	858	31	946
Overall total	366	5313										

Appendix 2

Data tables and figures from Chapter 6

Table A2.1 *Matrigel invasion assay; Fold changes of unseparated, HPA-positive and HPA-negative MCF7 cell populations normalised to unseparated within each experiment.*

Experiment Nº	Biological replicate Nº	Unseparated population	HPA-positive population	HPA-negative population
1	1	2.81	5.46	0.58
	2	0.13	1.54	6.35
	3	0.47	0.61	6.25
	4	0.59	1.22	5.68
Average		**1.00**	**2.21**	**4.72**
2	1	1.15	0.65	1.10
	2	1.71	0.14	1.53
	3	0.56	1.03	2.76
	4	0.58	0.18	2.07
Average		**1.00**	**0.50**	**1.87**

Table A2.2 *Matrigel invasion assay; fold changes of unseparated, HPA-positive and HPA-negative ZR751 cell populations normalised to unseparated within each experiment.*

Experiment Nº	Biological replicate Nº	Unseparated population	HPA-positive population	HPA-negative population
1	1	1.34	5.12	22.83
	2	0.90	2.77	15.36
	3	0.53	5.79	22.69
	4	1.23	2.94	18.85
Average		**1.00**	**4.15**	**19.93**
2	1	1.19	0.90	5.23
	2	1.28	1.17	2.22
	3	0.29	1.20	4.27
	4	1.23	2.00	2.91
Average		**1.00**	**1.31**	**3.66**
3	1	0.31	1.86	11.39
	2	0.18	0.74	3.60
	3	2.71	3.69	13.26
	4	0.79	3.80	15.7
Average		**1.00**	**2.52**	**11.00**
4	1	0.45	0.18	14.37
	2	1.64	1.13	24.33
	3	0.91	1.01	10.53
	4	1.00	0.38	5.40
Average		**1.00**	**0.70**	**8.00**

Table A2.3 *Matrigel invasion assay; fold changes of unseparated, HPA-positive and HPA-negative BT474 cell populations normalised to unseparated within each experiment.*

Experiment Nº	Biological Replicate Nº	Unseparated population	HPA-positive population	HPA-negative population
1	1	0.76	1.41	9.71
	2	0.53	0.61	21.75
	3	0.61	0.65	13.64
	4	2.10	0.72	19.85
Average		**1.00**	**0.85**	**16.24**

Table A2.4 *Matrigel invasion assay; fold changes of unseparated, "mixed", HPA-positive and HPA-negative ZR751 cell populations normalised to unseparated within each experiment.*

Experiment Nº	Biological Replicate Nº	Unseparated population	Mixed population	HPA-positive population	HPA-negative population
1	1	1.16	1.20	1.84	15.21
	2	0.92	1.02	1.43	9.93
	3	0.92	0.60	0.77	10.45
Average		**1.00**	**0.94**	**1.35**	**11.86**

Table A2.5 *Static adhesion assay; fold changes of unseparated, HPA-positive and HPA-negative MCF7, ZR751 and BT474 cell populations over time normalised to unseparated within each experiment.*

	Incubation time	HPA-positive				HPA-negative				Unseparated			
		1	2	3	Avg	1	2	3	Avg	1	2	3	Avg
MCF7	30 sec	1.16	1.22	2.11	**1.50**	2.19	2.04	1.78	**2.00**	0.96	0.93	1.11	**1.00**
	5 min	2.19	2.04	1.78	**200**	1.27	0.91	0.71	**0.96**	0.96	0.93	1.11	**1.00**
	10 min	2.79	2.06	3.07	**2.64**	1.00	1.04	1.62	**1.22**	0.83	0.91	1.23	**1.00**
	20 min	3.39	2.53	3.63	**3.18**	1.68	2.47	1.73	**1.96**	0.69	0.73	1.58	**1.00**
ZR751	30 sec	3.17	5.28	2.03	**3.51**	0.46	0.24	0.57	**0.42**	0.78	0.87	1.35	**1.00**
	5 min	2.65	2.01	1.03	**1.92**	0.72	0.64	0.77	**0.71**	1.08	0.74	1.19	**1.00**
	10 min	1.47	1.63	1.79	**1.63**	0.97	0.55	0.66	**0.73**	1.40	0.67	0.92	**1.00**
	20 min	1.10	1.57	1.15	**1.27**	0.59	0.41	0.73	**0.57**	0.63	1.38	0.98	**1.00**
BT474	30 sec	3.56	3.00	0.89	**2.48**	2.37	2.63	0.89	**1.96**	0.52	0.74	1.74	**1.00**
	5 min	2.97	4.64	3.34	**3.65**	1.64	0.77	1.72	**1.38**	0.99	1.11	0.91	**1.00**
	10 min	1.32	2.73	1.63	**1.89**	0.48	0.79	0.42	**0.56**	0.66	1.38	0.96	**1.00**
	20 min	0.10	1.43	1.76	**1.41**	0.18	0.80	0.37	**0.45**	0.92	1.18	0.89	**1.00**

Table A2.6 *Static adhesion assay; fold changes of unseparated, parental cell lines (MCF7, ZR751 and BT474) after 10min incubation and masking with either Con A or HPA compared to untreated. Normalised to unseparated populations within each experiment.*

Cell line	Masking with Con A				Masking with HPA				Unseparated			
	1	2	3	**Avg**	1	2	3	**Avg**	1	2	3	**Avg**
MCF7	0.96	0.76	0.82	**0.84**	0.34	0.25	0.25	**0.28**	1.10	1.01	0.93	**1.00**
ZR751	0.48	0.84	0.89	**0.74**	0.24	0.30	0.21	**0.25**	0.97	0.60	1.43	**1.00**
BT474	0.45	0.69	0.75	**0.63**	0.18	0.21	0.13	**0.17**	1.02	0.94	1.04	**1.00**

Table A2.7 *Static adhesion assay; fold changes of HPA-positive, HPA-negative, unseparated and "mixed" MCF7 cell populations when incubated with either HPA-negative conditioned-medium or regular medium. Normalised to unseparated cells within each experiment.*

	HPA-negative conditioned media				Regular media			
	1	2	3	**Average**	1	2	3	**Average**
HPA-positive	1.63	1.71	1.67	**1.67**	1.22	1.19	0.91	**1.10**
HPA-negative	0.29	0.35	0.17	**0.27**	0.43	0.35	0.69	**0.49**
Unseparated	1.38	0.85	0.78	**1.00**	0.91	1.15	0.95	**1.00**
Mixed	1.04	0.74	1.22	**1.00**	0.93	1.25	0.77	**0.99**

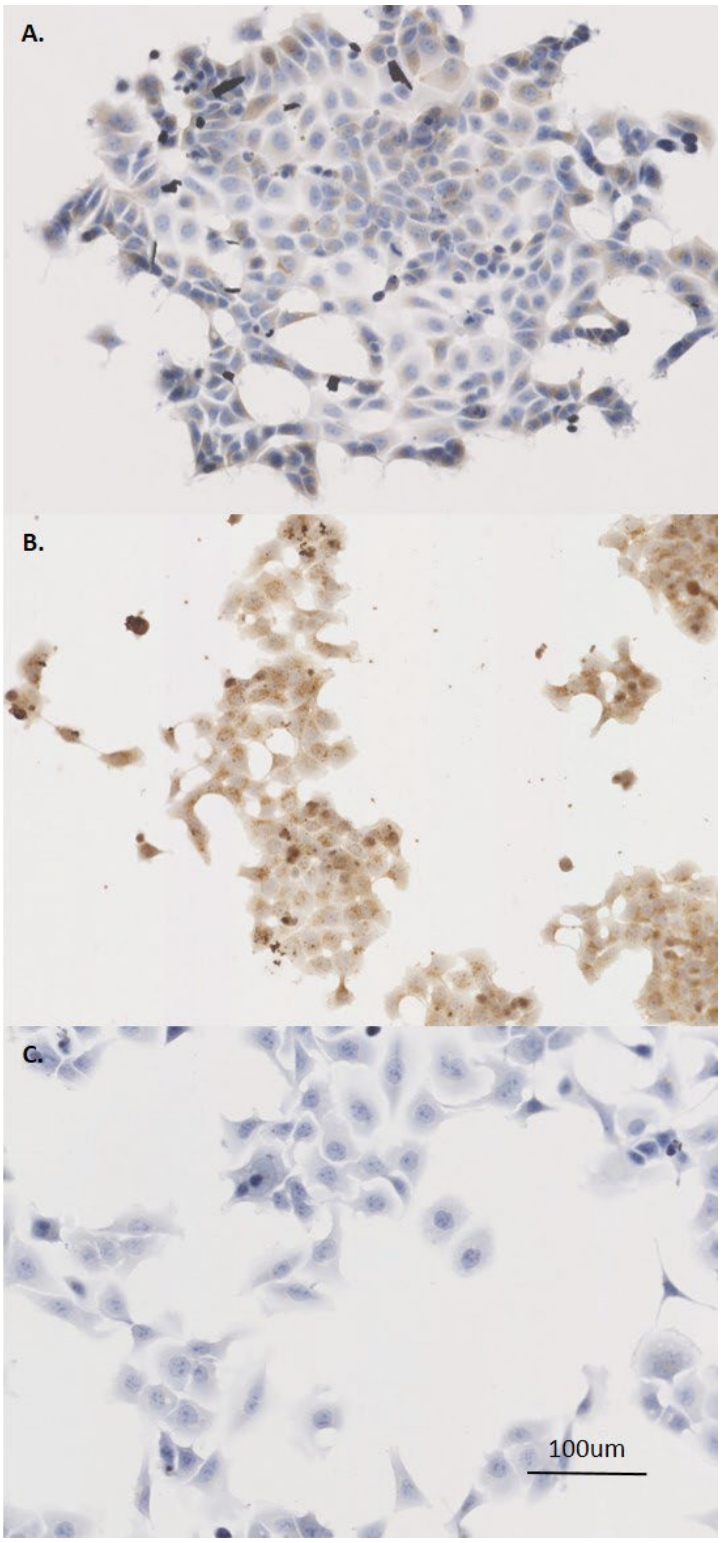

Figure A2.1 *HPA lectin labelling of ZR751 cells HPA labelled parallel to the static adhesion assay. 20,000 cells seeded per well. A. Unseparated ZR751 cells. B. HPA-positive ZR751 cells. C. HPA-negative ZR751 cells. Images captured with a Zeiss, Axioplan microscope fitted with a JENOPTIK ProgResC3 camera. Scale bar = 100µm.*

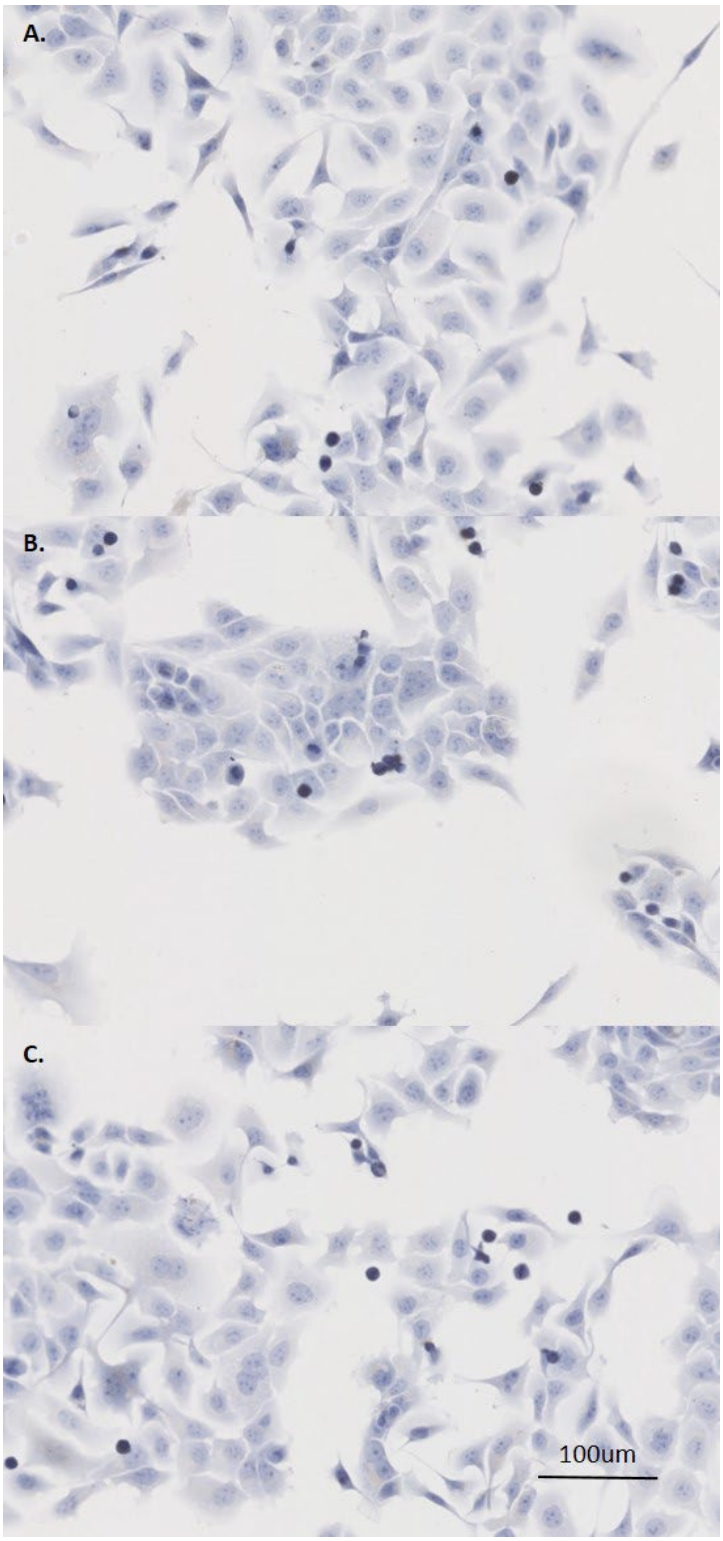

Figure A2.2 *Lectin labelling negative controls of ZR751 cells labelled parallel to the static adhesion assay. 20,000 cells seeded per well. A. Unseparated ZR751 cells. B. HPA-positive ZR751 cells. C. HPA-negative ZR751 cells. Images captured with a Zeiss, Axioplan microscope fitted with a JENOPTIK ProgResC3 camera. Scale bar = 100µm.*

Appendix 3

Publications arising from work presented in this thesis

Beaman E.-M. and Brooks S. A. (2014) The extended ppGalNAc-T family and their functional involvement in the metastatic cascade. Histology and Histopathology, 29: 293-304.

Beaman E.-M., Carter D.R.F. and Brooks S.A. (2017) Isolation of viable glycosylation-specific cell populations for further *in vitro* or *in vivo* analysis using lectin-coated magnetic beads. In: Pellicciari C. and Biggiogera M. (eds) *Histochemistry of Single Molecules. Methods in Molecular Biology 1560*. New York: Humana Press. 109-119.